SPECTROSCOPICALLY EVALUATED RATES AND ENERGIES

FOR PROTON TRANSFER AND BJERRUM DEFECT

MIGRATION IN CUBIC ICE

By

WILLIAM BRIDGMAN COLLIER

Bachelor of Science
Oral Roberts University
Tulsa, Oklahoma
1977

Master of Science
Oklahoma State University
Stillwater, Oklahoma
1981

Submitted to the Faculty of the Graduate College
of the Oklahoma State University
in partial fulfillment of the requirements
for the Degree of
DOCTOR OF PHILOSOPHY
December, 1983

SPECTROSCOPICALLY EVALUATED RATES AND ENERGIES

FOR PROTON TRANSFER AND BJERRUM DEFECT

MIGRATION IN CUBIC ICE

Thesis Approved:

J. Paul Devlin
Thesis Adviser

M. G. Rockley

N. V. V. J. Swamy

Lionel M. Raff

Norman N. Durham
Dean of the Graduate College

ACKNOWLEDGMENTS

Science and its advancement depends heavily on the support of
fellow researchers and the labors of scientists long past. Truly no
research work is the product of one individual, but rather a team.
I would like to take this opportunity to acknowledge a small part of
that team.

To my parents, John R. and Carrie M. Collier, goes a debt of gratitude for love, patience, and help, above and beyond all call of duty. Without their support this work would never have materialized.

And lastly goes honor and gratitude to Almighty God, the author of all original thought, and creator of ice in the first place.

TABLE OF CONTENTS

LIST OF TABLES

LIST OF FIGURES

CHAPTER I

LITERATURE REVIEW

Introduction

Ice is a peculiar solid. Its unique properties have fascinated

scientists for decades but surprisingly its behavior and structure is

still often ambiguous. The importance of ice to chemistry, physics,

geophysics, atmospheric science, hydrology, cryobiology, molecular

biology, and other fields has grown and with it an immense volume of

published research. Any review of ice must be necessarily selective

and the present work is no exception. The main focus will be the

areas of ice research related to the spectroscopy of ice with

special emphasis on proton transfer.

Ice can exist in several solid phases. The low pressure forms

are amorphous or vitreous ice (ice Ia or Iv), cubic ice (ice Ic), and

the naturally occurring hexagonal ice (ice Ih). Sometimes cubic and

hexagonal ice mixtures or hexagonal ice alone is referred to as

polycrystalline ice I. The presently known high pressure polymorphs

are ice II-VII and are accessible at pressures in the kilobar range.

As early as 1917 (1) x-ray diffraction studies on ice were

pursued. In 1922 Bragg (2) deduced that each oxygen atom is located

at the center of gravity of its four neighboring oxygen atoms for

hexagonal ice. Since then modern x-ray and electron diffraction data

(3) have confirmed that hexagonal ice is composed of tetrahedrally

1

coordinated oxygen atoms stacked such that it gives a hexagonal crystal structure. Figure 1 gives the oxygen lattice structure of hexagonal ice with its dimensions. Notice that the oxygen atoms can be grouped into a series of rough planes called basal planes that are normal to the crystal c-axis. By looking parallel to the c-axis the hexagonal holes of ice Ih are readily seen. This open structure gives hexagonal ice its lower than liquid water density.

Since each oxygen atom has two bonded hydrogen atoms, the oxygen lattice must somehow accommodate these hydrogens. One early suggestion by Barnes (4) was to put the hydrogens midway between each oxygen-oxygen link. This would preserve the symmetry and stoichiometry of the crystal. However this arrangement was ruled out since the water molecule would be ionized into H^+ and O^{2-} ions, and water is a poor electrical conductor. Bernal and Fowler (5) suggests that the hydrogens were distributed between the oxygen-oxygen bonds but displaced such that a given hydrogen atom was about 1 angstrom from one oxygen atom and 1.76 angstroms from the other with the arrangement of hydrogen atoms in the complete lattice such that each oxygen atom has two hydrogens chemically bonded at 1 angstrom and two hydrogen bonds to two adjacent water molecules with the hydrogen at 1.76 angstroms. Figure 2 illustrates Bernal and Fowler's suggestion. A closer examination of this model reveals a water subunit with a HOH angle of approximately 109° compared with the gas phase value of approximately 105°. The OH bond length is 1 angstrom compared with .97 angstrom for the gas phase. Thus the distortion of a water molecule transcending the gas to ice transition is slight. Some researchers have even suggested that the H_2O subunit retains its gas phase angle in the hexagonal phase ice such that the
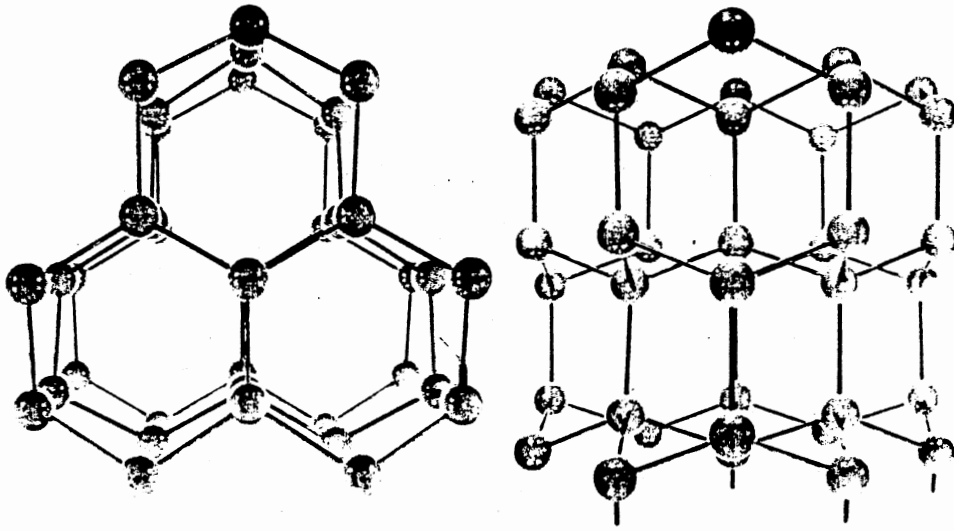
Figure 1. Oxygen Lattice Structure of Hexagonal Ice
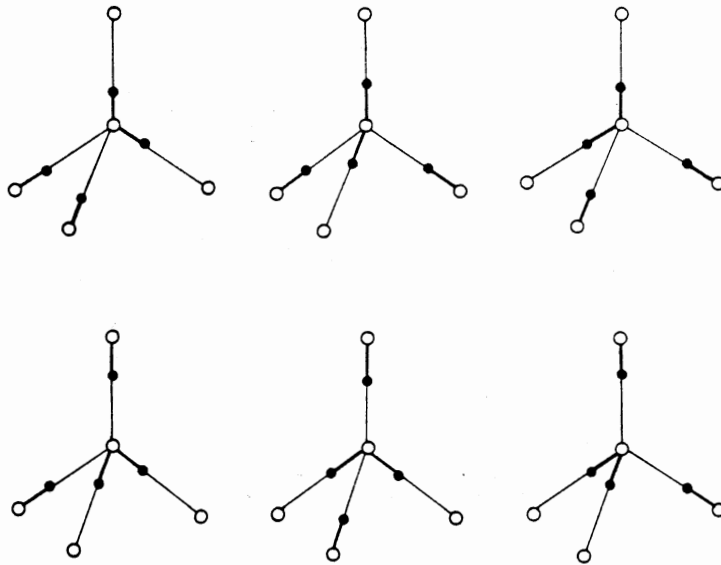
Figure 2. Possible Hydrogen Configuration in
Ice Ih

hydrogens lie slightly off center of the O-O lines.

One interesting implication of the Bernal and Fowler model is that around any given oxygen atom there are six possible configurations of hydrogens as Figure 2 illustrates. Thus even at 0 K ice Ih may freeze into a number of different possible hydrogen configurations leaving ice with a nonzero thermodynamic probability and hence a nonzero residual entropy at 0 K. This led Pauling (6) to propose a statistical model for ice Ih with the following assumptions.

    (1) Each oxygen atom has two hydrogen atoms attached at distances of about 0.95 angstroms, thus forming a water molecule.

    (2) Each water molecule is oriented so that its two hydrogen atoms are directed approximately towards two of the four oxygen atoms which surround it tetrahedrally.

    (3) The orientations of neighboring water molecules are such that one hydrogen atom normally lies between each pair of oxygen atoms.

    (4) Under normal conditions ice Ih can exist in any one of a large number of configurations, each of which corresponds to a particular hydrogen atom distribution among the oxygen lattice (p. 2680).

These four assumptions are often called the Bernal and Fowler rules and ice crystals which follow them are called ideal crystals.

Bjerrum (7) in 1951 proposed ice crystal defects that could facilitate proton transfer. These defects named Bjerrum defects are created when the third Bernal and Fowler rule is violated. A D defect is formed when two hydrogen atoms occupy an O-O bond and an L defect is formed when an O-O bond is left vacant. In conjunction with ionization defects, these could allow positive and negative ionic charges to migrate through the ice crystal. If a hydrogen ion in an ideal hexagonal ice crystal shifts from one OH bonded position to the OH

bonded position of the adjacent oxygen, i.e. a movement of approximately
.24 angstroms of a hydrogen to the adjacent hydrogen bonded oxygen, then
two ion defects will be formed. One will be the H_3O^+ ion about the
oxygen the defect moved toward, the other a hydroxyl -OH ion left
behind. Figure 3 illustrates these defects.

As mentioned earlier, there are presently two other known low
pressure phases of ice, amorphous ice (ice Ia or Iv) and cubic ice
(ice Ic). If water vapor is condensed on a substrate below 130 K ice
Ia is formed. If the temperature is above 130 K and below approxi-
mately 170 K - 190 K then cubic ice is formed. Above 190 K hexagonal
ice tends to form, though it should be noted that the exact temperatures
are disputed.

Amorphous ice has a disordered structure associated with it
since the energy of the substrate is not sufficient to allow a
deposited water molecule to reorient itself to a more energetically
favorable position. Because of the lack of structural order amorphous
ice has been studied as a possible model for liquid water structure.

Cubic ice can be made in situ by direct vapor deposition, or by
warming amorphous ice to above the cubic ice transition temperatures
as noted by Honjo et al. (8). The oxygen lattice of cubic ice is
almost identical to the hexagonal lattice except that every alternate
basal plane is rotated 60° about the crystal c-axis relative to the
adjacent nonrotated basal planes. This preserves the tetrahedral
oxygen lattice but removes the hexagonal holes along the c-axis.
Honjo and Shimaoko (9) investigated the possible hydrogen atom
positions of cubic ice using electron diffraction and found that the
cubic equivalent of Pauling's statistical model of ice Ih still holds.
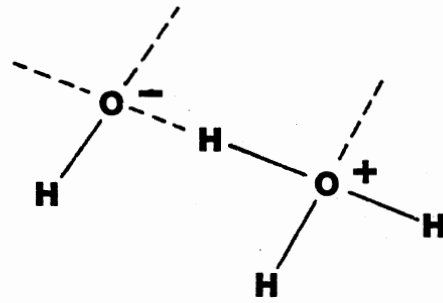
ION PAIR DEFECT
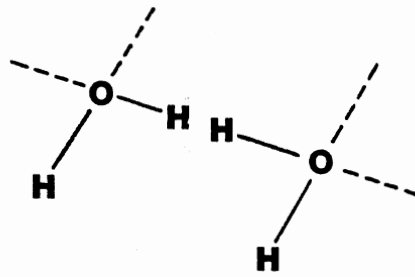
D ROTATIONAL DEFECT
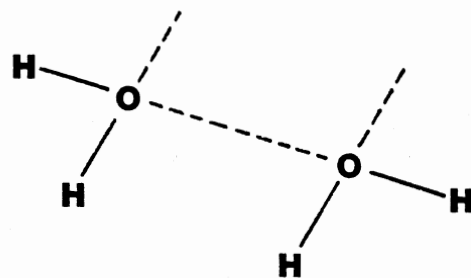
L ROTATIONAL DEFECT

Figure 3.   Ice Crystal Lattice
Defects

Further evidence of the cubic hydrogen atom positions comes from infrared spectroscopy where, to date, no definite difference has been detected between the cubic and hexagonal ice IR spectra. Likewise it appears that the Bjerrum and ionization defects of hexagonal ice also apply to cubic ice. The oxygen lattice structure of cubic ice is shown in Figure 4.

The H_2O molecule possesses a C_{2v} symmetry with three normal modes of vibration as shown in Figure 5. The ν_3 vibration is the asymmetric stretch belonging to the B_1 irreducible representation and occurs in the 3000 - 3500 cm^{-1} region for H_2O and 2200 - 2600 cm^{-1} for D_2O. The ν_1 vibration is the symmetric stretching mode belonging to the A_1 irreducible representation, and has a wavenumber range similar to ν_3. The ν_2 bending vibration also belongs to the A_1 irreducible representation and usually is found around 1500 - 1800 cm^{-1} for H_2O and 1100 - 1300 cm^{-1} for D_2O.

In ice and liquid water ν_3 and ν_1 are found in the OH stretching region as a very broad almost featureless band whose width has traditionally been attributed to hydrogen bonding. Certain lattice modes are found below ν_2 and their combinations with other modes are often interspersed among the fundamentals.

Pure Ice Spectra

The spectra of pure ice has been studied for many years. Bertie and Whalley have figured significantly in the early characterizations of the ice IR spectra.

In 1968 Bertie, Labbe', and Whalley (10) examined the absorptivity of ice I in the 4000 to 30 cm^{-1} range. True absorptivity profiles of
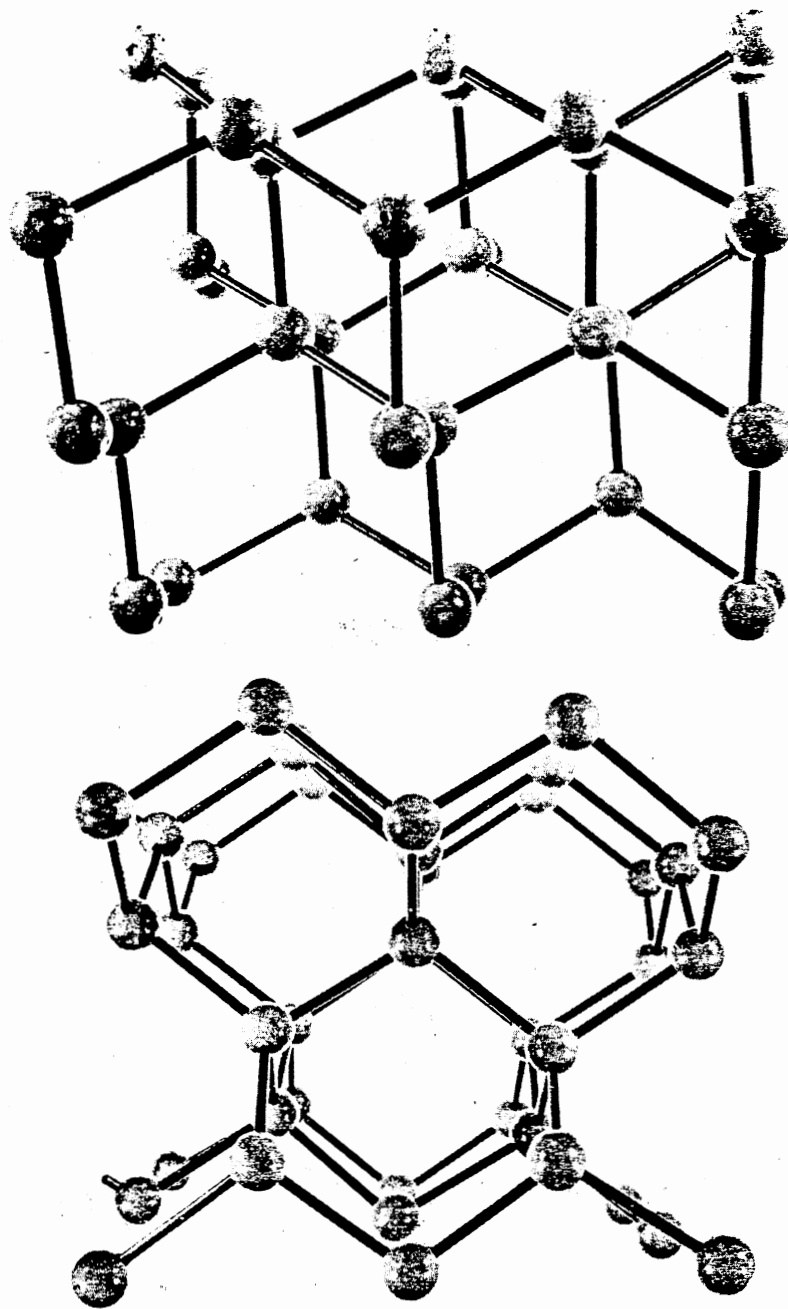
Figure 4.   Oxygen Lattice Structure of Cubic Ice

ν_1 Symmetric Stretching Mode
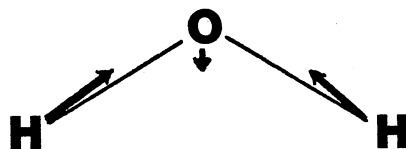
ν_2 Bending Mode
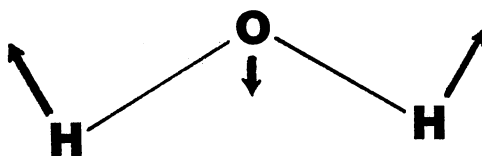
ν_3 Asymmetric Stretching Mode
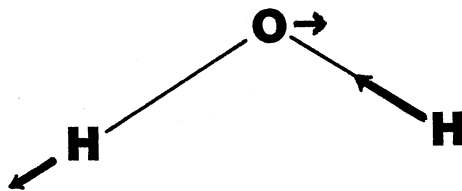
Figure 5. Free H_2O Normal Modes of
Vibration

solid state ice can be difficult to obtain, especially near large
absorptivities where the infrared index of refraction changes
dramatically. Therefore a true absorptivity profile that accounted
for reflection and scattering losses would facilitate interpretation
of ice spectra.

The vitreous to cubic ice I phase transition was studied by
Hardin and Harvey (11) by monitoring the bandshape changes of several
bands over a 92 to 210 K temperature range. They reported the well
known sharpening of the vitreous ice bands upon transformation to
the cubic phase. One exception noted was the vitreous ice ν_2 bending
mode whose half-height bandwidth was reported as 350 ± 10 cm^{-1} in
the amorphous phase but 365 ± 10 cm^{-1} in the cubic phase. The
transition for this band was between 123 ± 5 K and 137 ± 5 K. However
the 800 cm^{-1} ν_r showed a -25 cm^{-1} decrease in bandwidth at 92 K as
expected. Ice Iv transformed over a 120 ± 5 to 135 ± 5 K temperature
range. They concluded that vitreous (or ice Iv or Ia) ice is stable
up to 120 ± 5 K and undergoes an irreversible transformation to cubic
ice between 120 and 140 K. Hardin and Harvey felt confident that
their spectra represented cubic ice and did contain some small
discernable differences from the spectra of hexagonal ice.

In 1973 Li and Devlin reported the glassy water Raman spectra
from a trapped laser beam. Both polarized and depolarized spectra
in the 3570 to 2950 cm^{-1} region were reported where ν_1 was located
at 3110 cm^{-1} and $2\nu_2$ at approximately 3250 cm^{-1}. In 1975 Narten,
Venkatesh, and Rice (13) obtained x-ray diffraction data on amorphous
H_2O and compared it with neutron diffraction data. They suggested a
high density 10 K ice and a low density 77 K ice amorphous ice phase

to explain their data. Their model predicted a randomized ice I structure, with interstitial molecules, having a density of 1.1 grams/cm^3. Their model was also consistent with the predictions of supercooled water; with no structural changes other than a contraction of the O-O separations. Thus Narten et al. suggested that the low temperature phase of amorphous ice may serve as a model for liquid water.

Whalley (14) studied the spectra of ice Ic and Ih and presented a detailed assignment based on the spectrum of ice VIII. Whalley noted that assignments can be difficult because the vibrations can not be treated as arising from a single molecule, but due to the strong intermolecular coupling that exists in ice, the coupled crystalline lattice. He split the ice I ν_1 mode into in-phase and out-of-phase components at 3083 cm^{-1} and 3420 cm^{-1}, respectively and the ν_3 band into the TO and LO components of 3209 cm^{-1} and 3323 cm^{-1}, respectively. Whalley contended that there should be strong similarities between the spectra of ordered and disordered ice Ic, and that the spectra of ice Ic and Ih are identical.

Scherer and Snyder (15) measured the Raman intensities of a single crystal of ice Ih at various crystallographic orientations. Their analysis suggested that the hydrogen bonds parallel to the crystallographic c-axis are more linear than the equatorial ones. They disagreed with Whalley's (14) 3209 cm^{-1} TO ν_3, and 3420 out-of-phase ν_1 assignments, but instead preferred assignments using various combinations of ν_1, ν_3, and ν_t.

The reduced vibration (RVM) model for describing the amorphous and polycrystalline ice Ih spectra was introduced by Bergren, Schuh,

Sceats, and Rice (16). They claimed that the inter and intramolecular coupling of OH oscillators is almost equal, thus any vibration of the condensed phase does not necessarily have a one-to-one parentage with vibrations of the free molecule. From their data Bergren et al. determined the optical constants of H_2O and D_2O polycrystalline ice Ih and amorphous ice.

Sivakunar, Rice, and Sceats (17) examined the Raman spectra of the OH stretching region of low density amorphous water and poly-crystalline ice Ih. They found that the low temperature amorphous phase is stable at 10 K for at least two months. The spectra support a structure derived from ice Ih which is created by introducing a distribution of O-O-O angles. This angle and separation dispersion is partly responsible for the observed spectral width of the bands.

Scherer (18) published an extensive review on the vibrational spectroscopy of water. Early in the review, Scherer discussed the importance of Fermi resonance and the formation of Evans holes. Much controversy has resulted from whether or not there is Fermi resonance between ν_1 and $2\nu_2$ in the liquid and condensed phases of ice. Scherer pointed out that Fermi resonance between two vibrational states is not as simple as a frequency displacement between two interacting states. Often the magnitude of the interaction constant and the bandshapes of the interacting states can combine to give unusual bandshapes. When a broad band Fermi interacts with a narrow band, the resultant is often a broad band with a spike or hole (Evans hole) that is not a simple sum of the two component bands. This can complicate the inter-pretation of the possible ν_1 and $2\nu_2$ Fermi interaction.

He pointed out that many liquid water bandshape analyses and

bandfitting attempts are based on false assumptions because the ice data and widths of infrared bands do not support a spectral breadth arising from a small number of molecular species, but from a broad distribution of OH bonds strengths, a disorder in the hydrogen bonding environment, and intermolecular coupling.

Scherer stated that the ice Ic to Ih transition seems to be dependent on the thermal history of the particular sample, and lies between $-120^{\circ}C$ and $-63^{\circ}C$. He also raised the question over how much does the disorder from true oxygen tetrahedral coordination widens the OH stretch band versus intermolecular coupling. Ice II which has an ordered proton structure yields four sharp crystallographically distinct ν_{OD} bands. Scherer explained the wide OH stretch region of ice as follows: an uncoupled OH or OD ice oscillator is split under the intramolecular coupling into two vibrations that would be equivalent to ν_3 or ν_1 in the gas phase in their in-phase and out-of-phase character. Strong intermolecular coupling present in the ice lattice would further split each of these into two more components yielding a total of four or more components that could be further broadened by the proton disorder induced broadening effect of hexagonal, cubic, or amorphous ice; and complicated by Fermi resonance between $2\nu_2$ and a smeared ν_1 vibrational state. Since intermolecular coupling increases with decreasing temperature, and the ice OH and OD bandwidths remain essentially unchanged with temperature, Scherer claimed that disorder must play a role in the OH or OD stretch width at higher temperatures. In conclusion Scherer (18) stated:

(1) Fermi resonance between OH stretching and $2\nu_2$ states has been observed.

(2) Band fitting procedures that approximate the Evans
hole with two bands are invalid.

(3) Intermolecular coupling between adjacent water
molecules is important in ice, amorphous ice, and
liquid water.

(4) Isobestic regions in the Raman spectra of water can
not be interpreted as evidence for different
molecular species.

(5) Disorder is responsible for the bandwidth in liquid
water and amorphous ice.

(6) Liquid water at low temperatures is similar to ice
near the melting point or amorphous ice at -180°C.

(7) There is evidence for non-tetrahedral HOH valence
angles in ice, with some orientational preference
for the c-axis hydrogen atoms to form more linear
hydrogen bonds (p. 211).

Rhim, Burum, and Elleman (19) studied the proton anisotropic

shift in single crystal hexagonal ice and confirmed the Pauling model

of ice but could not confirm or reject any possible proton ordering

of ice. No hydrogen motion was observed at the liquid nitrogen

temperatures used.

Recently Hagen, Tielens, and Greenberg (20) performed an exten-

sive temperature study on the ice Ia to Ic transition between 10 and

140 K. They found the transition to occur between 130 and 140 K;

with a 45 minute duration at 140 K, and 90 minute duration at 135 K.

By monitoring the interference of a laser beam through the deposit

Hagen et al. were able to measure the thickness of the sample. They

calculated a $d\nu/dR_{o-o} = 6700 \text{ cm}^{-1}$ (where R_{o-o} is the oxygen-oxygen

lattice separation) and noted that the amorphous to cubic ice

transformation was dependent on the thermal history of the sample.

Matrix Isolated Decoupled Ice Spectra

One of the first matrix isolated systems to be studied was water isolated in solid nitrogen by Thiel, Becker, and Pimentel (21). By obtaining infrared spectra at various water to nitrogen ratios (M/A = 1000 to 10; where M = moles matrix gas and A = moles water) Pimentel et al. distinguished between monomer, dimer, and possibly trimer bands of water. The bands at 3725 cm^{-1} and 3627 cm^{-1} were assigned to the ν_3 and ν_1 stretch of monomeric water and the 3691 cm^{-1} and 3546 cm^{-1} OH stretches to the dimer species. Because of the low number of dimer bands observed Pimental et al. claimed the water dimer had a cyclic structure. They also noted a tenfold increase in the absorption coefficient of polymeric water relative to monomeric water.

In 1960 Haas and Hornig (22) published a benchmark paper in the study of ice. The spectra of HOD mixed with either a H_2O or D_2O matrix at $-80^{\circ}C$ or $-190^{\circ}C$ were recorded. The coupled H_2O and D_2O fundamentals and combinations were assigned, and interestingly, they were able to observe and assign the corresponding isotopically decoupled HOD modes. The HOD OD stretch was observed at 2416 cm^{-1} in a predominately H_2O matrix, and the HOD OH stretch at 3275 cm^{-1} in a predominately D_2O matrix. An unusual facet of the HOD OD stretch was the appearance of two distinct sidebands at 2393 cm^{-1} and 2442 cm^{-1} symmetrically placed about the 2416 cm^{-1} OD stretch. The bands start appearing at HOD concentrations above 10 percent HOD in the ice matrix. Haas and Hornig attributed these sidebands to the coupling of adjacent or near neighbor OD oscillators producing an in and out-of-phase OD coupling at 2393 cm^{-1} and 2442 cm^{-1} respectively. The

narrow bandwidth of the HOD stretches in the presence of strong hydrogen bonding suggested that the large breadth of OH and OD stretches in ice spectra were due not to hydrogen bond variation but intermolecular coupling. The overtone $2\nu_{OH}$ was assigned to 6300 cm^{-1} with a remarkably wide 60 cm^{-1} bandwidth even at low HOD concentrations where intermolecular coupling is absent. The large $2\nu_{OH}$ width along with the greater ν_{OH} width compared with ν_{OD} suggested that a mass dependent phenomena such as tunneling was responsible for the 2ν width. They postulated that since the hydrogen can occupy two symmetric sites on a given oxygen-oxygen bond that a given proton could tunnel from one side of the oxygen-oxygen double well potential to the other. The presence of the $2\nu_{OH}$ band also suggested that the thermal activation energy must be above 18 kcal but below 27.5 kcal if the brief Haas and Hornig calculations are accepted.

Tursi and Nixon (23) studied the water dimer in solid nitrogen. The H_2O, D_2O, and HDO isotopes were isolated in N_2 matrices at 20 K and 4 K. The sample to matrix ratios were varied and M/A plots as in Pimentel's paper were constructed. They observed a lack of the OH stretch in the HOD dimer implying that the deuterium hydrogen bond was stronger than the H hydrogen bond; thus producing a lack of these species in the matrix. Murby and Pullin (28), Bentwood, Barnes, and Orville-Thomas (29), and Barnes and Suzuki (30) have recently reinvestigated the self-association of matrix isolated water and concurred with Tursi and Nixon (23) that there seemed to be a preference for HOD to form OD hydrogen bonds rather than OH hydrogen bonds.

The decoupled frequencies of OH_2 and OD_2 oscillators in ice were

highly desired as appropriate starting points from which to build a coupled model of ice vibrations. In a series of papers (24, 25, 26) Devlin et al. elucidated these frequencies and assigned the vibrational frequency pattern of the isotopic ices. Ritzhaupt and Devlin (24) published the $\nu_3-\nu_1$ OD stretch region of D_2O isolated and decoupled in a glassy H_2O matrix at 90 K. By simultaneously depositing a small amount of D_2O vapor with a large quantity of H_2O vapor they were able to obtain the sample with virtually no HOD contamination in the OD stretch region of isolated D_2O and with little isotopic scrambling at 90 K.

In a latter paper Ritzhaupt, Thornton, and Devlin (25) developed the simultaneous deposition technique so that D_2O spectra decoupled and isolated in cubic H_2O could be realized. They deposited a 0.1 micron film of H_2O (Ic) at 180 K, prior to the codeposition of dense H_2O and dilute D_2O vapors on a substrate held at 135 K. The expitaxial layer insured the ice deposit would be cubic, and the 135 K temperature that no deuteron or proton exchange occurred in the sample preparation period. The ice Ic D_2O stretching frequencies were identified as $\nu_1 = 2367$ cm^{-1} and $\nu_3 = 2444$ cm^{-1} for D_2O in H_2O. The bending modes (ν_2) were 1220 cm^{-1} for D_2O in cubic ice and 1230 cm^{-1} for amorphous or glassy ice. Both of these bending mode frequencies were high enough to discount any significant Fermi resonance interaction between $2\nu_2$ and ν_1 in D_2O decoupled ice spectra. By raising the sample temperature to 140 to 160 K they were able to initiate proton-deuteron exchange as evidenced by the growth of the HOD band and decay of the D_2O bands. The ability to measure the exchange rates at different temperatures presented the opportunity of measuring the activation energy of the

exchange process. This they found to be approximately 10 kcal; well within the range suggested by Haas and Hornig (22).

By 1980 Ritzhaupt, Collier, Thornton, and Devlin (26) were using the expitaxial method of cubic ice deposition to unravel the uncoupled H_2O ice Ic frequencies. About 5 percent H_2O was codeposited with a D_2O matrix at 135 K. By allowing the sample to warm to 155 K the growth and decay of the appropriate isotopic exchange bands were observed. Both Raman spectra with polarization measurements and FTIR spectra were obtained. The use of digitilized FTIR spectra allowed for the subtraction and scaling of different isotopic exchange spectra such that the change and identification of fundamental H_2O modes was enhanced. Ritzhaupt et al. placed the decoupled H_2O cubic ice ν_3 at 3270 cm^{-1}, ν_1 at 3200 cm^{-1}, and ν_2 at 1732 cm^{-1}. Likewise the HOD ν_{OH} was assigned to 3270 cm^{-1}, ν_{OD} to 2418 cm^{-1}, and ν_2 to 1510 cm^{-1} for a D_2O matrix and 1465 cm^{-1} for a H_2O matrix. Sceats, Stavola, and Rice (27) from their theoretical calculations suggested that Fermi resonance of $2\nu_2$ with ν_1 actually pushed ν_1 and ν_3 bands into coincidence with the ν_{OH} band yielding a single absorption. Ritzhaupt et al. showed that the coincidence of the cubic ice ν_3 and ν_{OH} was correct but the Fermi resonance of $2\nu_2$ with ν_1 actually increased the $\nu_{OH}-\nu_1$ separation. With all the observed decoupled isotopic cubic ice frequencies available, Ritzhaupt et al. were able to perform overlay normal mode calculations for the calculated decoupled frequencies and quadratic force constants.

Theory of Ice Spectra

Much of the recent theoretical work done on coupled and decoupled

ice spectra has been done by Rice and Sceats who developed a method for predicting vibrational modes in highly intermolecularly coupled systems that is called the reduced vibrational model or RVM that greatly simplifies calculations.

McGraw, Madden, Bergren, Rice, and Sceats (31) used the RVM model to build a 64 molecule ice Ih cell in which the symmetry, ice rules, and zero net dipole moment were met. Like Whalley et al. (10) and Haas and Hornig (22), they contended that strong intermolecular coupling had to be accounted for before any realistic assignments could be made about the ice I stretching region. In examining their results they found that long range coupling between molecules not directly hydrogen bonded served to make features more diffuse but not to greatly affect the spectral distribution. In addition, the intermolecular coupling was predicted to be of the same magnitude as the intramolecular coupling. Rice et al. found that the modes predicted by the 64 molecule cell were complex mixtures of molecular motions such that identification of regions of the ice Ih stretching IR and Raman spectra with isolated molecular modes was not useful, but the predicted spectra agreed well with the observed spectra.

In a follow-up paper Madden, Bergren, McGraw, Rice, and Sceats (32) extended the theory and model to the OH stretching region of amorphous ice. Interestingly they found that the random orientation required of the new model cell had little affect on the predicted spectra but changes in the oxygen-oxygen lattice distances had a sizable one. They concluded that a distribution of force constants such as would result for oxygen-oxygen lattice changes rather than a change from the regular crystalline topology of ice Ih was

responsible for the infrared spectral changes between hexagonal and amorphous ice. This could lead to some interesting conclusions regarding the spectra of liquid water.

Sceats and Rice (33) utilized the overtone spectrum of ice I to develop an intramolecular potential. They assumed the intramolecular potential could be accurately described by a hydrogen bond dependence of the diagonal harmonic stretching force constant and the stretch-stretch interaction force constant. All other harmonic and diagonal anharmonic force constants were presumed to remain independent of hydrogen bond perturbations and hence could be derived from gas phase values or other sources. The results of their potential analysis of the ice overtone region indicated that the breadth of the $2\nu_{OH}$ overtone may be due to intermolecular coupling rather than tunneling as suggested by Haas and Hornig (22).

The experimental work of Ritzhaupt et al. (24, 25) prompted Sceats, Stavola, and Rice (34) to extend their models to reproduce the stretching spectrum of D_2O in H_2O and H_2O in D_2O in both amorphous and crystalline ice I. They interpreted the amorphous D_2O decoupled in H_2O such that Fermi resonance of a near coincident $2\nu_2$ with ν_1 pushes ν_1 further away from ν_3 thus increasing what should have been a smaller $\nu_1-\nu_2$ splitting and increasing the width of ν_1 with the shifted $2\nu_2$ state.

In cubic ice the situation is similar but the coincidence of $2\nu_2$ and ν_1 is not as great and hence the resultant Fermi splitting gives a component on the high frequency side of ν_3. For H_2O decoupled in D_2O they calculated a spectra with a very small $\nu_1-\nu_3$ splitting such that Fermi resonance of $2\nu_2$ with ν_1 produces a single peak centered

around the HDO OH decoupled stretching frequency. In a later paper
by Ritzhaupt et al. (26) this was confirmed except that the ν_1 frequency
was assigned to a much lower frequency rather than coincident with ν_3
and ν_{OH} as predicted by Sceats, Stavola, and Rice.

Morse and Rice (35) compared different pair potentials suggested
by researchers for computer simulations of ice and water. Since the
structures of ice I, II, III, IV, V, VI, and VII are known, the
accuracy with which these structures could be predicted by the pair
potentials would be a sensitive test of their validity. They tested
several potentials in predicting a proton ordered ice Ih structure
and found the ab initio pair potential calculated by Matsuoka, Clementi,
and Yoshimine (36) succeeded best.

Proton Transfer in Ice

Proton transfer has been studied in many systems by widely varying
techniques. Much of the earlier work on proton transfer in ice and
liquid water was accomplished through conductance studies. One note-
worthy theoretical and experimental study was that of Conway, Bockris,
and Linton (37). They developed a theory of proton conduction in
liquid water that broke the conduction into two processes, one quantum
mechanical tunneling of a hydrogen from one molecule to another and
then, two, rotation of the molecule breaking the surrounding solvent
cage bonds to transfer the hydrogen or proton to the other side of the
cage. By such a series of transfers and rotations a proton could be
transported through the liquid. Conway et al. claimed that the
tunneling transfers occurred rapidly and the classical rotations much
slower and thus the rotational step was rate determining. They

predicted from Morse potential curves that the classical proton transfer activation energy in liquid water was 3.85 kcal for hydrogen and 5.81 kcal for deuterium and the predicted proton to deuterium transfer rate ratio was 6:1. The rotational activation energy was found to be quite costly energetically and dependent on the mode of rotation. They calculated that the proton spends 1 percent of its time undergoing quantum mechanical tunneling transfers. In a note Conway and Bockris (38) suggested that if their theory was applied to ice the concentration of defect formed protons might be low enough that water molecule rotation may no longer be the rate determining step and hence the tunneling process could become rate determining and hence the mobility of the proton would increase until it was limited by the now faster rate determining tunneling transfer step.

Kim and Schmidt (39) developed a theory of proton transport in ice that suggested the mobility is limited not by barrier hopping but lattice scattering. One of the implications of this particular theory is that the mobility is predicted to increase with decreasing temperature.

Conductivity measurements of ice have been studied over several decades with widely varying results and much controversy. However by the mid 1960's much of the discrepancy was resolved and the problem traced to the use of two terminal conductivity cells which gave conductivities and resulting activation energies that were a mixture of bulk and surface ice conductivities. The use of guarded or three terminal conductivity cells or holders lead to more consistent measurements among researchers. Durand, Deleplanque, and Kahane (40) utilized ion exchange membranes for electrodes in conductivity measurements. The

temperature of the ice was kept between $-20^{\circ}C$ and $-100^{\circ}C$ to prevent

surface conductivity effects thus negating the need for a third guard

electrode. They measured a conductivity thermal activation energy of

about 9 kcal/mole between $-30^{\circ}C$ and $-70^{\circ}C$ and a 13 kcal/mole activation

energy between $-90^{\circ}C$ and $-100^{\circ}C$.

In another similar conductivity measurement Bullemer, Eisel,

Engelhardt, Riehl, and Seige (41) determined the bulk and surface

conductivity of ice at $-10^{\circ}C$. They found an activation energy of

8.5 ± 0.5 kcal/mole for the bulk conductivity and 26-30 kcal/mole

for surface conductivity using a three terminal guarded potential

probe method.

An alternate theoretical view of proton conduction in ice has

been advanced by A. von Hippel et al. (42) in a series of papers

describing their experimental and theoretical technique. A. von

Hippel postulated that the Bjerrum D and L defects were formed in a

single asymmetric stretch and bend combination photon excitation

that did not require a molecular rotation that broke three hydrogen

bonds. The calculated activation energy was about 13 kcal. Further-

more he predicted that Bjerrum defects would be the current carriers in

the free volume of the crystal with ionic defects only playing a role

near the electrodes. The movement of defects in the free volume was

expected to be in polaronic fashion, and in rapidly expanding drift

ellipsoids when under the influence of an externally applied electrical

field. This is in contrast to the theory of Jaccard (43) who claimed

that D, L Bjerrum defects were the majority current carriers but ionic

defects also played a role and had a 400 times higher mobility which

was explained by proton tunneling. Experimentally A. von Hippel et al.

measured a surface conduction activation energy of about 33 kcal/mole between 0°C and 30 $^\circ$C which could be reduced to 20 kcal/mole by enclosing the sample in a vacuum. The bulk conductivity activation energy was about 12 kcal/mole with a three terminal holder. Below -35°C both two and three terminal holders gave consistent results of about 12 kcal/mole. Previously measured zero activation energies were claimed to result from measurements made in the initial millisecond time range where a stable conductive state had not yet been reached. Ice crystal age was also found to affect conductivity emasurements. A. von Hippel did not feel the need to invoke proton tunneling to explain proton mobility in ice.

Hubmann (44) extended Jaccard's theory to accept the complementary action of ionic defects and Bjerrum D, L defects in proton migration in ice.

Evidence for proton tunneling and c-axis order in ice Ih was found by Lumpkin and Dixon (45). They measured the ^{17}O quadrupole resonance of ice Ih at 4.2 and 1.3 K using a double resonance technique and found only two resonances consistent with the explanation offered.

Ritzhaupt and Devlin (46) took the thin layer techniques developed in references 25 and 26 and isolated D_2O in cubic H_2O at 130 K. Two bands at 2444 cm^{-1} and 2367 cm^{-1} were assigned to the D_2O ν_3 and ν_1 respectively. Upon warming the sample to 165-180 K the D_2O ν_3 and ν_1 bands lost intensity while a band at 2418 cm^{-1} attributed to the OD stretch of HOD grew in and gained intensity representative of the following exchange reaction.

$$D_2O + H_2O \longrightarrow 2HOD$$
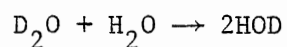
Ritzhaupt and Devlin obtained FTIR spectra at several time

intervals during the exchange reaction at elevated temperatures. By
subtracting the appropriate scaled pure HOD 2418 cm^{-1} component band
from the D_2O-HOD exchange band complex the time dependence of D_2O loss
could be followed by the D_2O band intensities after HOD subtraction or
by the scaling factors used to scale the original 2418 cm^{-1} HOD band
used in the subtraction. Figure 6 illustrates the spectral changes
accompanying deuterium-hydrogen exchange. Over the temperature range
of 165 K to 181 K the activation energy was found to be 9.3 kcal. They
noted that this value was close to half the formation energy of ion
pair defects (18.6 kcal) found by Bullemer et al. (41). This was con-
sidered indicative of the thermally activated proton tunneling mechanism
suggested by Haas and Hornig (22) where a thermally activated H_3O^+ ion
defect is mobilized by proton tunneling. Such a process should reflect
an Arrhenius type behavior. It was also suggested that such thermal
activation would involve a ground to excited state stretching mode
vibration whose energy of about 9.2 kcal/mode is amazingly close to
the measured activation energy.

In a subsequent paper Ritzhaupt and Devlin (47) discovered that
the previous samples of D_2O isolated in cubic H_2O discussed in reference
46 had been contaminated with minute quantities of aromatic compounds
desorbing from the cell walls. As the contamination was slowly cleared
up in subsequent experimental runs it was found that the rate of
exchange reaction increased considerably with a new transitory peak at
2396 cm^{-1} slowly appearing as the reaction proceeded and then losing
intensity as the exchange neared completion. Figure 7 shows the D_2O
2444 ν_3 cm^{-1}, 2367 ν_1 cm^{-1}, and 2396 cm^{-1} intermediary band spectral
changes with time after interfering H_2O and HOD bands have been
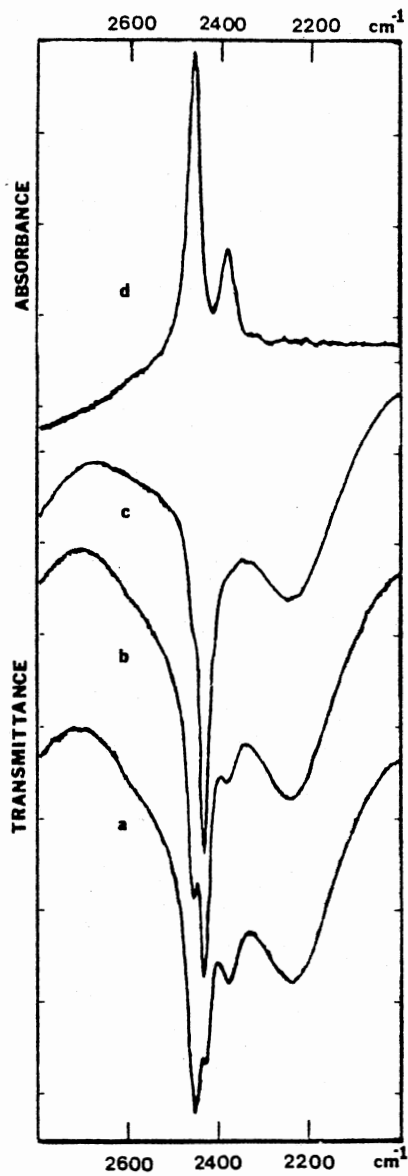
Infrared curves for ≈ 2% D_2O in H_2O ice I_c: (a) original deposit warmed to 165 K; (b) same sample after two hours at 165 K; (c) same sample (165 K) after seven hours at 165 K and following brief annealing at 185 K and (d) D_2O absorbance spectrum from curve (b) using curve (c) to remove HOD absorbance.

Figure 6. D_2O Spectral Changes with Isotopic Exchange
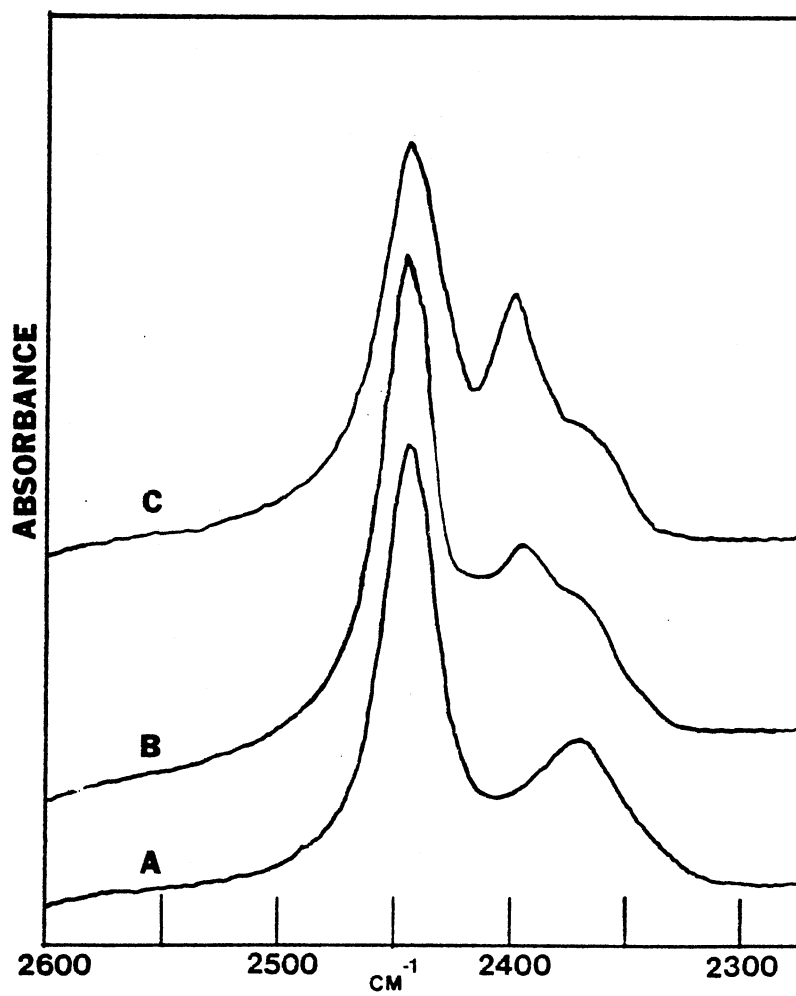
Figure 7. (HOD)$_2$ Spectral Changes with Isotopic Exchange

digitally subtracted. The 2396 cm^{-1} band could clearly be identified
with the 2393 cm^{-1} dimer HOD coupled in-phase OD stretch assigned by
Haas and Hornig (22). The 2442 cm^{-1} out-of-phase coupled OD oscillator
stretch should be obscured beneath the more intense D_2O ν_3 vibration
at 2444 cm^{-1}. This suggested the following exchange reactions.

$$D_2O \text{ (isolated)} + H_2O \xrightarrow{k_1} (HOD)_2 \text{ (coupled)}$$
$$(HOD)_2 \text{ (coupled)} \xrightarrow{k_2} 2HOD \text{ (isolated)}$$
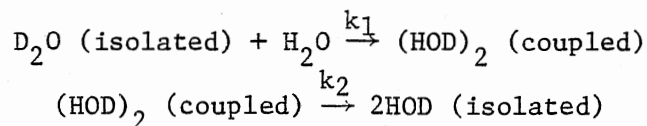
Devlin et al. attributed the first step to a proton transfer
which would produce a coupled HOD unit and the second step to a
Bjerrum defect migration by a molecular rotation which decouples or
destroys the coupled HOD producing two isolated HOD subunits. They
explained the behavior of the doped and pure ice systems as follows.
The doped system inhibited the transfer process enough that $k_2 \gg k_1$
and hence the $(HOD)_2$ concentration was a very small steady state value
and not spectrally observed. Hence the overall rate was slower and
higher temperatures were needed to initiate the exchange. As the
dopant was removed and $k_1 \approx k_2$ the steady state situation was removed
with a corresponding increase in $(HOD)_2$ concentration and greater
overall exchange rates. The dopant appeared to have no effect on the
rotational step. Rough calculations on the k_1 rate or proton transfer
process indicated an activation energy of 8.5 to 10.5 kcal. This
suggested the dopants affected the proton transfer rate by trapping
ion pair defects rather than altering the activation energy for defect
formation. Devlin et al. suggested the possibility existed for eluci-
dating the activation energy for both the ion pair defect formation
and Bjerrum rotational defect migration.

In a recent note Kunst and Warman (48) used a microwave conduc-

tivity pulse radiolysis technique to find the mobility of protons and deuterons in ice. The proton virtual mobility in H_2O ice was determined to be .0064 $cm^2/V \cdot s$ at $-5^{o}C$ and the deuteron virtual mobility in D_2O ice to be .0024 $cm^2/V \cdot s$ at $-5^{o}C$ with a deuteron mobility to proton mobility ratio of .375.

Presentation of Problem

Ritzhaupt and Devlin (47) presented their analysis of the infrared D_2O stretching region of D_2O isolated and decoupled in cubic H_2O ice at 130-180 K. From the spectral changes observed it was concluded that proton or deuteron migration in ice followed a two fold process. The first step involved an ionic defect formation which mobilized a proton via a tunneling mechanism that allowed the defect to migrate throughout the crystal once formed. This proton transfer encountering a D_2O molecular subunit in an H_2O ice crystal would initiate isotopic scrambling by proton transfer; i.e. exchanging and transferring a proton for a deuteron leaving a vibrationally coupled $(HOD)_2$ dimer. The $(HOD)_2$ dimer would further scramble to two vibrationally decoupled and more spatially removed HOD molecular subunits in the H_2O ice crystal lattice by a molecular rotation or Bjerrum D, L defect migration.

The goal of this study is to find the best quantitative estimate of the ionic defect formation and Bjerrum D, L defect migration activation energies and examine their possible implications for proton transport in hydrogen bonded molecular networks. The study of these energies could yield possible insights into the role proton transport could have in alternate electrical control devices, and energy conversion and storage in biological systems.

Accomplishing this study will involve developing experimental techniques to implement the following procedures.

(1) Collection time resolved IR spectra of D_2O-H_2O exchange processes over a suitable range of sampling times, time durations, samples, and experimental temperatures to perform kinetic analyses of the data obtained.

(2) Assure sample purity such that the rates obtained reflect a reasonably pure ice situation.

(3) Resolve the D_2O-HOD band complex obtained in each sample collection into its individual spectral components.

(4) Relate the spectral intensity of the spectral components to each component concentration.

(5) Develop a kinetic model for obtaining the proton transfer rate via ionic defect migration and Bjerrum D, L defect rotation rate from the spectral component concentrations.

(6) Find the proton transfer and rotational rates over as wide a temperature range as experimentally feasible and find their respective activation energies.

(7) Analyse the results for implications.

CHAPTER II

EXPERIMENTAL PROCEDURES AND RESULTS

Matrix Isolation Methods

Matrix isolation techniques are usually used to isolate a particular molecular specie in an inert matrix. This is accomplished by directing the gaseous mixture of the molecular specie and an inert gas matrix onto a cryogenic surface where the frozen gas mixture may be examined by optical spectroscopy or other means.

For this work matrix isolation techniques were used but the matrix gas of H_2O interacted significantly with the guest molecule D_2O. Though the electronic interaction between the matrix and guest were large, the different isotopic masses caused a decoupling of specific normal modes of vibration between the matrix and guest molecules. So the present work is better described as matrix decoupled spectroscopy.

All of the experimental work was accomplished by depositing vapors of H_2O and D_2O on a nitrogen gas cooled or mechanically cooled cesium iodide substrate. Two types of vapor deposition cells were used.

Metal Cell Technique

The first phase of the experimental work consisted of creating crystalline deposits of ice Ih with a 5% to 95% ratio of D_2O to H_2O. Figures 8 and 9 show the experimental apparatus used for this. The heart of the cryostat is an Air Products and Chemicals,

31

E – Cu sampling block

F – Cu heat shield

G – Thermocouple leads
(gold-chromel 0.7% Fe)

H – Model CS-202 Displex^{TM}
displacer/expander

I – Self-sealing coupling
(low pressure return)

J – Self-sealing coupling
(surge line)

K – Self-sealing coupling
(high pressure supply)

L – Electrical connector

M – Flexible metal lines
to compressor

Front View

A – Electrical leads to in-
ternal resistance heater
located at the cryotip

B – Cryotip

C – CsI inner window

D – Removable Cu plate

Side View

Figure 8. Air Products CS-202 Displacer/Expander Module with Tip and
Sample Deposition Window
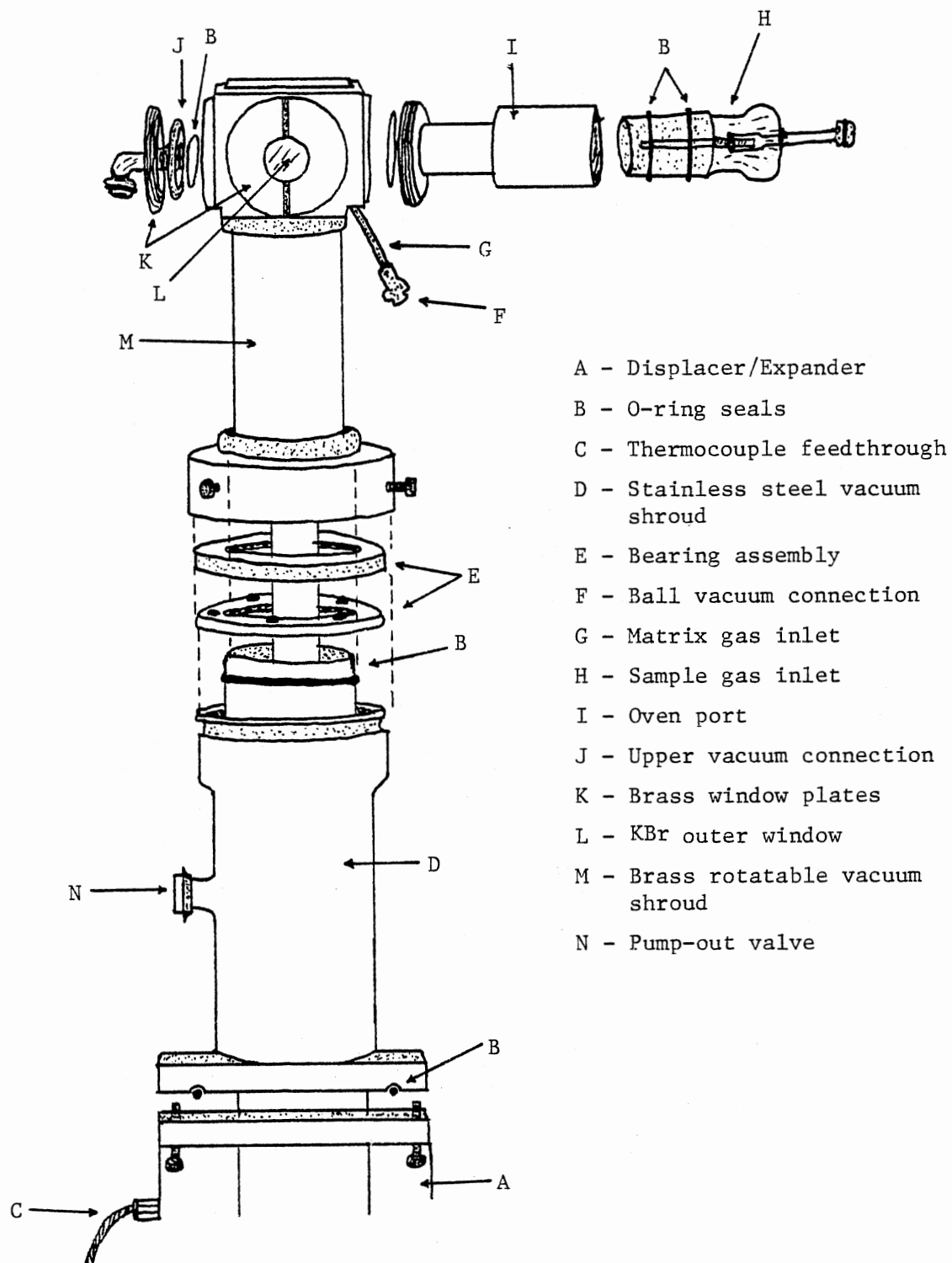
Figure 9. Brass Vacuum Shroud for Displacer/Expander Module

A - Displacer/Expander

B - O-ring seals

C - Thermocouple feedthrough

D - Stainless steel vacuum shroud

E - Bearing assembly

F - Ball vacuum connection

G - Matrix gas inlet

H - Sample gas inlet

I - Oven port

J - Upper vacuum connection

K - Brass window plates

L - KBr outer window

M - Brass rotatable vacuum shroud

N - Pump-out valve

Inc. Model CS-202 Displex closed cycle helium refrigerator. Included in the system is a displacer/expander module connected by flexible lines to a compressor and control panel. The displacer/expander module has a refrigerated tip on which the cesium iodide substrate window is mounted. The module may assume any orientation and has a capability of temperature to 10 K. A small resistance heater mounted on the refrigerator tip allows temperature control from $10^{o}K$ to $300^{o}K$ with an accuracy of $\pm$ .5°K. If an insulating vacuum of 10^{-4} torr is maintained around the cryotip, the cool-down time from room temperature to $10^{o}K$ is approximately one hour. On the end of the cryotip is a copper block for mounting a cesium iodide substrate window for infrared transmission studies. Four screws and a copper backing plate holds the window to the salt plate holder. Thermal contact is assured by indium wire gaskets between the window and backing plate and copper block. Two gold (0.7% Fe) chromel thermocoupler measure the cryotip and CsI window temperature. One is attached directly to the refrigerator tip with indium solder for the internal heater control; and the other is sandwiched between the CsI and copper block in the indium gasket to monitor the CsI window surface temperature on the deposition side.

To maintain the necessary vacuum for vapor deposition and cryogenic temperatures a brass vacuum shroud was available that would cover and seal the displacer/expander module allowing vacuum operation and injection of sample and matrix gasses through two injection ports (Figure 9). Also as shown in Figure 9 the shroud has the opposing potassium bromide windows and a vacuum connection. The shroud was mounted on bearings to allow rotation of the shroud while under vacuum and was

equipped with vacuum valves so that once a good vacuum was reached, the displacer/expander module could be sealed off and removed from the vacuum pumps and removed to a FTIR infrared spectrophotometer for infrared studies of the deposit made on the cryotip cesium iodide window. The brass shroud could be rotated to bring the two shroud potassium bromide windows in line with the inner cesium iodide window for easy optical examination.

The matrix gas H_2O is introduced through G and the sample gas D_2O through H. D_2O vapors are sent to the cryostat from a vacuum valve sealed glass reservoir connected to a micro-flow needle valve that is connected to the sample line at C. The vapor pressure of D_2O at $0^{\circ}C$ provided the necessary D_2O gas for deposition. H_2O vapors were likewise introduced into the cryostat. The H_2O vapor flow rate is controlled by a teflon needle valve above the H_2O water reservoir and monitored by a Fisher-Porter 1/16 glass flowmeter inserted into the H_2O sample line.

All vacuum selas in the system are made with lightly greased viton 0-rings except for the D_2O and H_2O sample and matrix gas lines where the vacuum grease was omitted to prevent any possible grease contaminations in the deposits.

Glass Cell Apparatus

During the course of the investigation it was found necessary to make D_2O-H_2O deposits doped with 7-azaindole. Rather than risk con-tamination of the metal cell where pure D_2O-H_2O deposits were being made, these samples were prepared in an all glass vapor deposition cell as shown in Figure 10. This cell being very similar in function
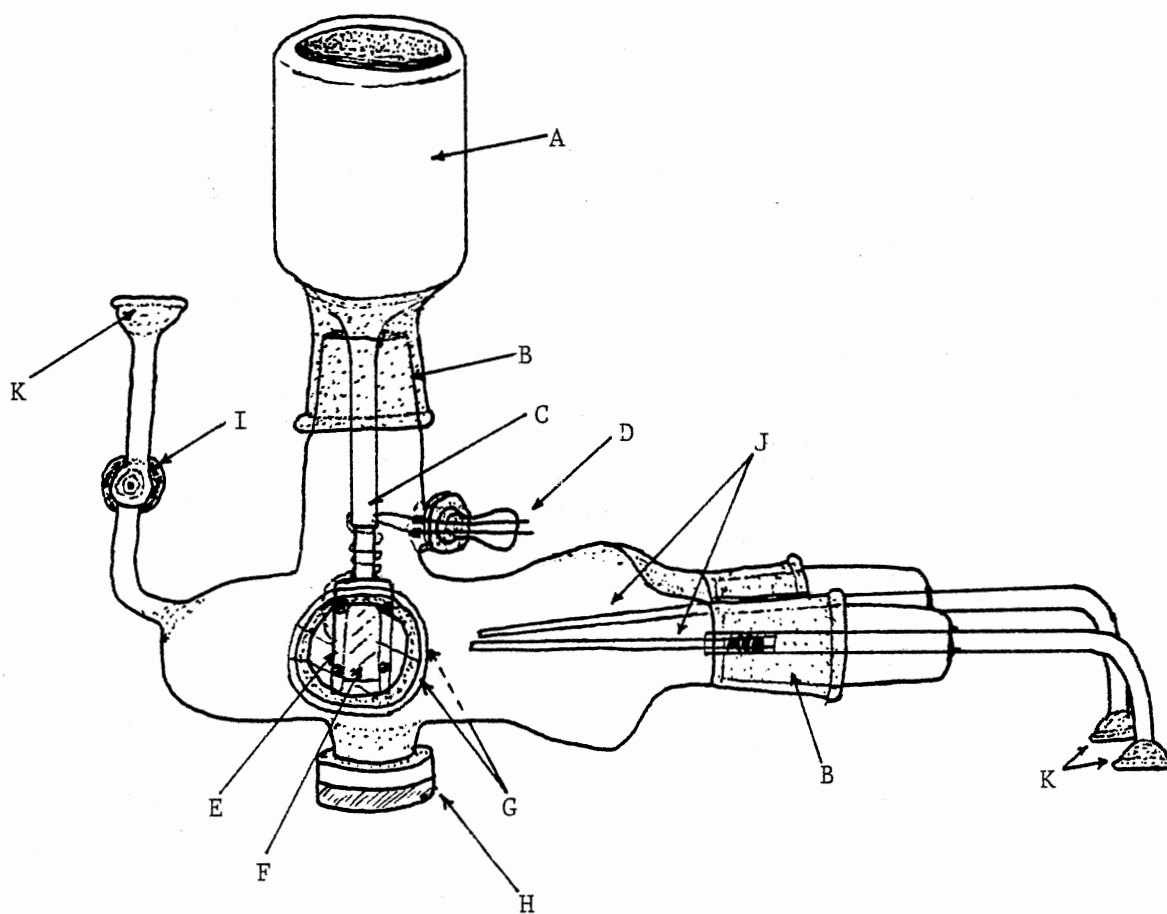
A - Liquid nitrogen dewar

B - Vacuum greased taper joint

C - Dewar stem glass—metal connection

D - Thermocouple wire vacuum seal

E - Cu sample block

F - CsI window

G - Outer KBr windows

H - Glass window

I - Teflon vacuum valve

J - Sample and matrix gas inlet

K - Female ball vacuum connections

Figure 10.   Glass Cryostat Cell for Vapor Deposition

to the closed-cycle helium refrigerator apparatus is comprised of a

glass container with provisions for introducing the matrix and sample

gasses through two sample lines terminating in nozzles aimed at a

cesium iodide substrate window. The cesium iodide substrate window

is attached to a copper holder with indium gaskets for thermal

contact. The copper substrate holder is connected by a Kovar glass

to metal seal to the bottom of a liquid nitrogen dewar for cooling.

The dewar is attached to the glass cell by a greased glass taper

joint so that the cesium iodide substrate window may be turned facing

the sample gas inlet nozzles for deposition and then rotated 90° for

optical spectroscopy through two potassium bromide windows fastened

on opposing sides of the glass vapor deposition cell. The temperature

was monitored by an iron-constanton thermocouple inserted into the

indium wire gasket between the copper holder and deposition side of

the inner cesium window. To obtain reproducible and consistent

temperature measurements and correspondence between the metal cell

and glass cell deposit temperature it was found necessary to temper

the glass cell thermocouple leads by stripping off the outer insulation

jacket of the thermocouple wire and wrapping the two individually

insulated leads at least twenty times around the dewar stem attached

to the copper holder before running the thermocouple leads outside

the cell for voltage measurement. A Honeywell model no. 2745 potentio-

meter was used for all thermocouple temperature measurements. To check

the temperature correspondence between the metal and glass cell

measurements a series of spectra of D_2O decoupled in H_2O at various

temperatures were made. The ν_3 asymmetric stretch bond of D_2O was

expanded so that $2^{\circ}K$ temperature shift effects could be detected in

the bandshapes as shown in Figure 11. By comparing spectra collected in the metal or glass cells with these spectra plots any temperature measurement inaccuracies could readily be detected. Both cells with different composition thermocouples were found to yield identical temperature shifted D_2O ν_3 bands at a given temperature setting over the 135 to 160 K range to at least a ± 1 K accuracy.

The matrix and sample gasses were introduced from D_2O and H_2O liquid reservoirs as in the metal cell apparatus. The 7-azaindole dopant was introduced by lightly dusting a glass wool plug with small crystals of 7-azaindole and placing it in the H_2O vapor sample line so that small quantities of sublimed 7-azaindole would be swept by the H_2O matrix vapors into the deposit. Temperature control with the glass cell was considerably more difficult. To circumvent the invariability of the liquid nitrogen boiling point for temperature control, a pressurized cool nitrogen gas cooler was designed as shown in Figure 12. A 50 liter liquid nitrogen dewar was mounted on a movable cart with a small glassware rack. The dewar was sealed off and a needle-valve controlled insulated tygon tubing line was used to direct the vented nitrogen gas to the glass cell dewar stem for cooling. Pressurization of the 50 liter dewar was provided by inserting a nichrome wire resistance heater into the liquid nitrogen of the 50 liter dewar and running the heater leads through a pressure seal in the 50 liter dewar top to a 110 AC variac. By controlling the heater voltage and adjusting the needle valve controlling the cool nitrogen gas flow, sufficient liquid nitrogen could be vaporized and blown into the glass cell dewar stem so that temperatures between 100 K and room temperature could be maintained with an accuracy of ± .5 K. By mounting
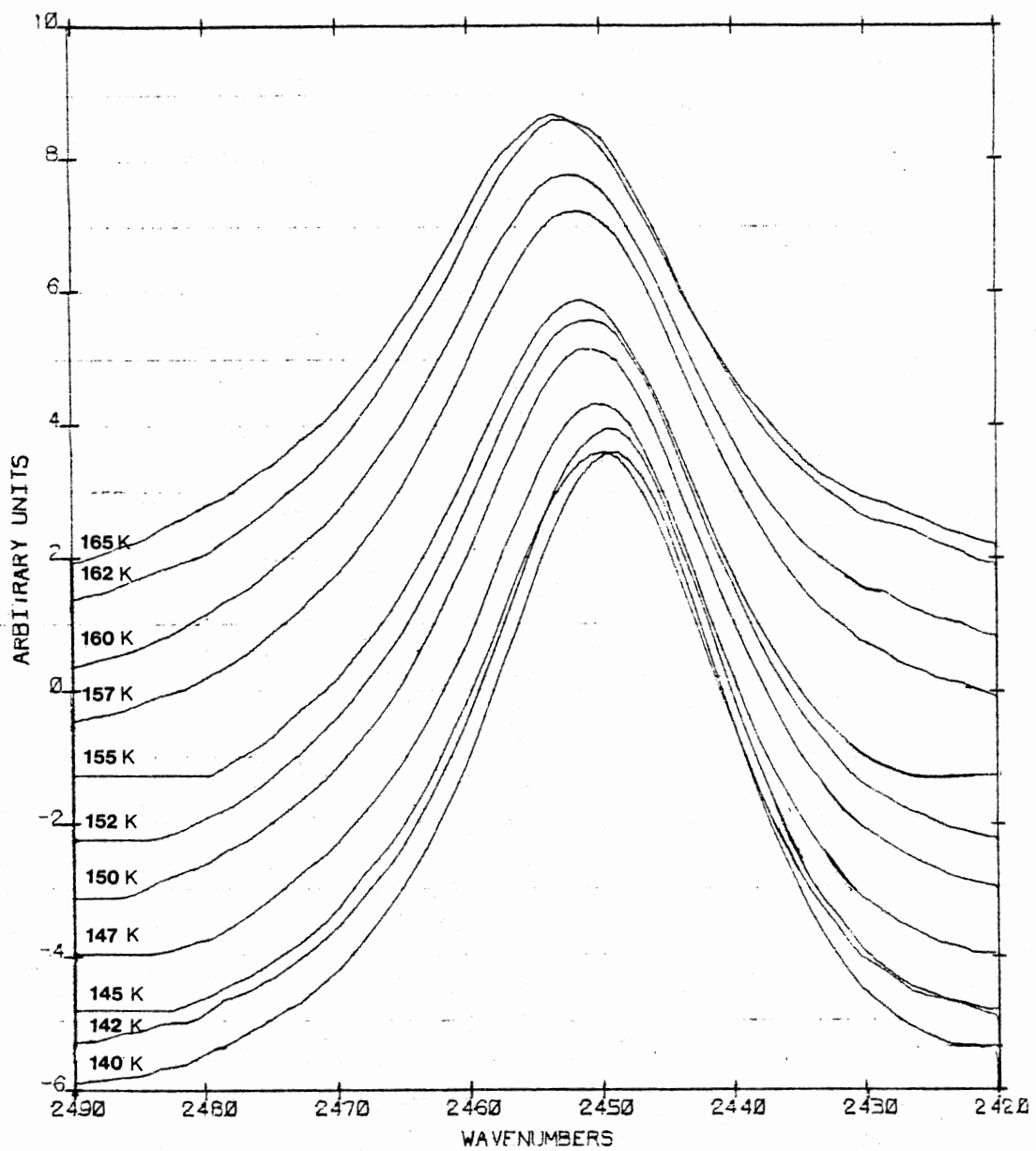
Figure 11. Expanded D_2O Decoupled in H_2O Ice ν_3 Bandshapes
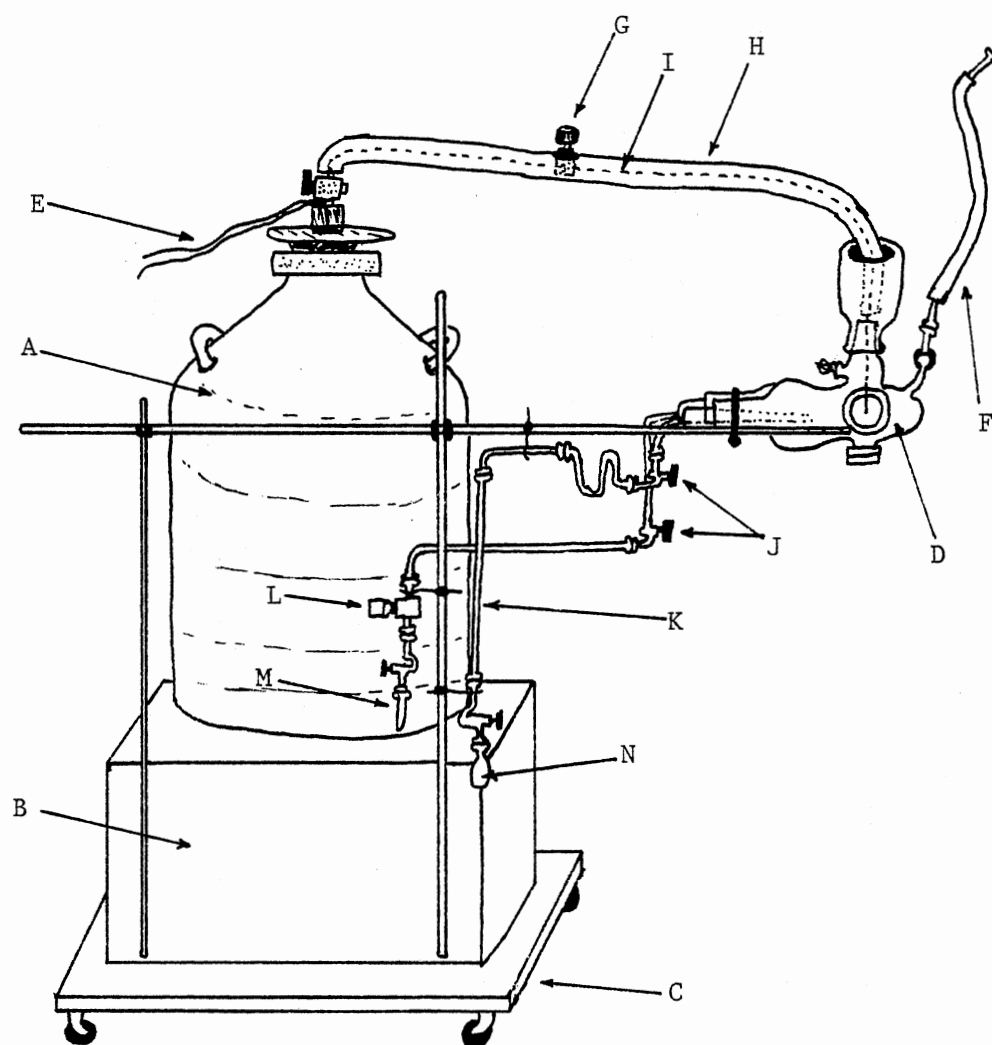
A – Liquid N_2 dewar

B – Dewar and rack support

C – Rollable cart

D – Glass cryostat

E – Resistance heater leads

F – Flexible vacuum line

G – N_2 gas needle valve

H – Foam insulation

I – Tygon tubing

J – Vacuum valves

K – Fisher-Porter flowmeter

L – Micro-needle valve

M – D_2O reservoir

N – H_2O reservoir

Figure 12. Nitrogen Gas Cooler System for Glass Cryostat Cell

the glass dewar cell onto the 50 liter glassware rack the whole unit could be rolled to the vacuum rack for evacuation and deposition, then sealed off and disconnected from the vacuum rack to be moved to the FTIR for infrared transmission studies.

All infrared spectra were collected on a Digilab FTS-20C Fourier transform infrared spectrophotometer. This is a single beam instrument which collects digitalized interferograms via a Michelson interferometer for storage or immediate computer transform analysis to a real-time frequency infrared spectrum. All spectra can be ratioed against an earlier or later run reference spectra for background correction. The digitalized nature of the collected interferograms or computed spectra, dedicated mini-computer, and additional disk storage, allow for easy manipulation, expansion, addition and subtraction of infrared spectra. The faster collection speed, much improved accuracy, and superior quantitative features of FTIR spectroscopy were essential requirements for the completion of this work.

All spectra were collected with a triangular apodization function, a gain ranging factor (FTS-20C parameter GRR) of 40, a zero filling factor (ZFF) of 2, and detector signal sensitivities of 1 to 4 depending on the samples used and the particular experimental situation. The triangular apodization function weighs the interferogram to minimize tail fringes that may accompany Fourier transforms of infrared bands. The gain ranging factor determines the detector signal amplification changes over different parts of the interferogram to obtain the best signal to noise ratio. The zero filling factor adds additional zeroes to the end of the collected interferogram so that additional space filling points are integrated into the computed spectra. While not providing

additional resolution it smoothes out the digitalized nature of FTIR spectra. The overall detector sensitivity was adjusted to provide maximum signal gain without overflowing the analog to digital signal converter. The number of scans that were coadded to form the final interferogram varied from 10 to 500 scans depending on the time available for the scans, and signal to noise requirements.

Procedure

A typical D_2O/H_2O deposit and experimental kinetic analysis for the mechanically cooled metal deposition cell proceeded as follows.

If the cryostat's optical windows needed cleaning the cell assembly was partially dismantled, cleaned, and oven-dried to remove moisture, while the KBr and CsI windows were removed and repolished. Normally this was not required between runs, and the whole system was kept connected to the vacuum pump under a constant 5×10^{-3} torr vacuum to minimize contamination from outside air and remove volatile contaminations from inside the vacuum systems. Several hours before a run the diffusion pump was turned on, the liquid nitrogen cold trap filled, and the system allowed to evacuate to approximately a 3×10^{-4} torr vacuum. Next the cryostat was cooled to 170 K for an initial 1.5 minute deposit of H_2O vapor at a flow reading of 3.0 to 3.5 on the Fisher-Porter flowmeter scale. Subsequently the cryostat was cooled to 130 K for the main deposit. Since the main deposit was made at the amorphous to cubic ice transition temperature, an initial deposit of cubic ice at 170 K was needed to induce the main deposit to form cubic rather than amorphous ice. The crystallinity of the main D_2O/H_2O deposit was checked by examining the infrared spectrum in the 2800-2000

cm^{-1} OD stretch region for features indicative of a crystalline or
amorphous sample as shown in Figure 13. The main deposit of the
D_2O/H_2O vapor mixture was made at 130 K for 20 minutes with the H_2O
and D_2O flow rates adjusted to a 5% to 95% ratio of D_2O to H_2O vapors.
The flow rate of H_2O on the Fisher-Porter flowmeter scale was held at
approximately 7.4 while the D_2O flow rate was adjusted by trial and
error to give the proper ratio using a micro needle valve. Both the
D_2O and H_2O water reservoirs were immersed in a mixture of ice and
water for temperature control.

Once the deposit was completed the cryostat was sealed off and
removed from the vacuum line. Next it was moved to the FTIR spectro-
photometer and suspended in the FTIR sample cavity so that the IR beam
would pass through the sample but yet was mechanically isolated from
the interferometer to minimize vibrations from the operating displacer/
expander module. Then a 2 cm^{-1} resolution spectrum from 4000-500 cm^{-1}
was collected to examine the nature of the deposit. Figure 14 shows
a typical D_2O/H_2O ice FTIR spectrum. In all the deposits some HOD was
found initially. The HOD OD stretch would fall between the ν_3 and ν_1
of D_2O. If the HOD to D_2O ratio was sufficiently small, the D_2O to
H_2O ratio sufficiently close to an isolation ratio with little sign of
dimer formation, and the sample crystalline, then a kinetic analysis
was made. If not, the sample was prepared again.

To perform a kinetic analysis the cryostat was quickly warmed to
the desired temperature (135, 140, 145, or 150 K) to initiate isotopic
exchange, and then maintained there throughout the kinetic run with an
accuracy of ± .5 K. Interferograms were then collected and filed at
timed intervals at a 2 cm^{-1} resolution until exchange was complete or
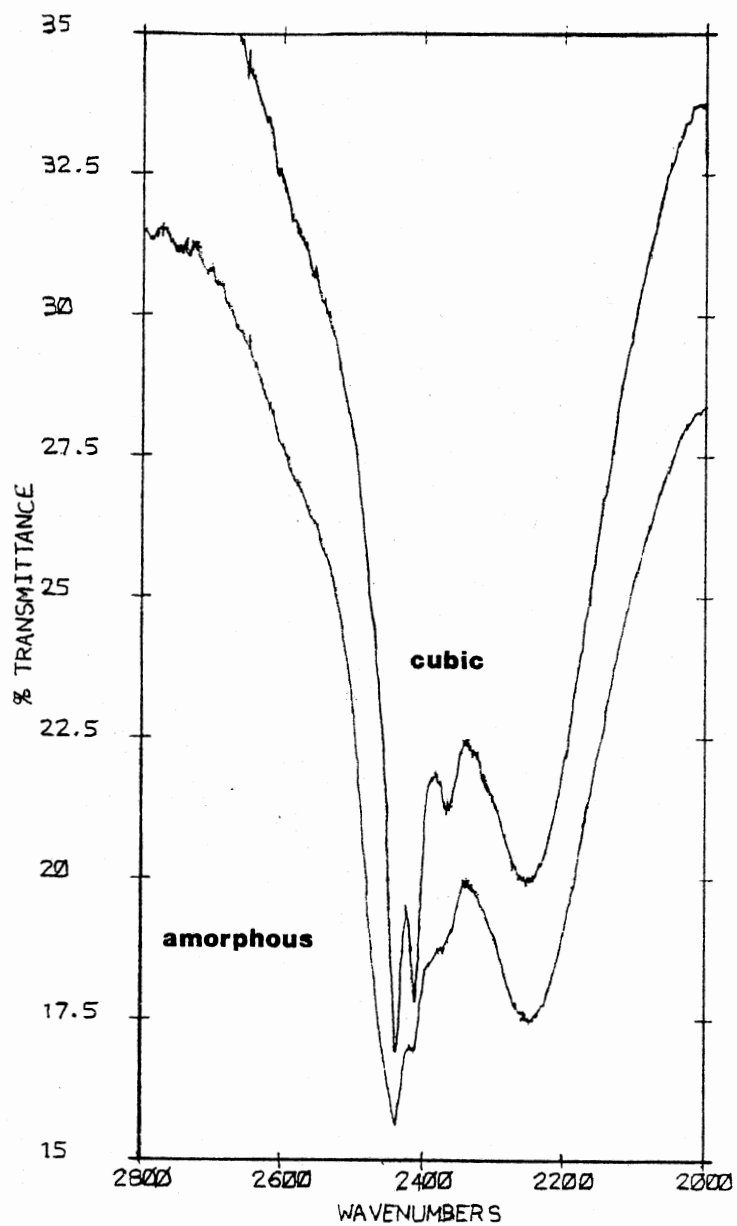
Figure 13.   Spectral Changes Occurring between
             Amorphous and Cubic Decoupled
             D_2O Ice
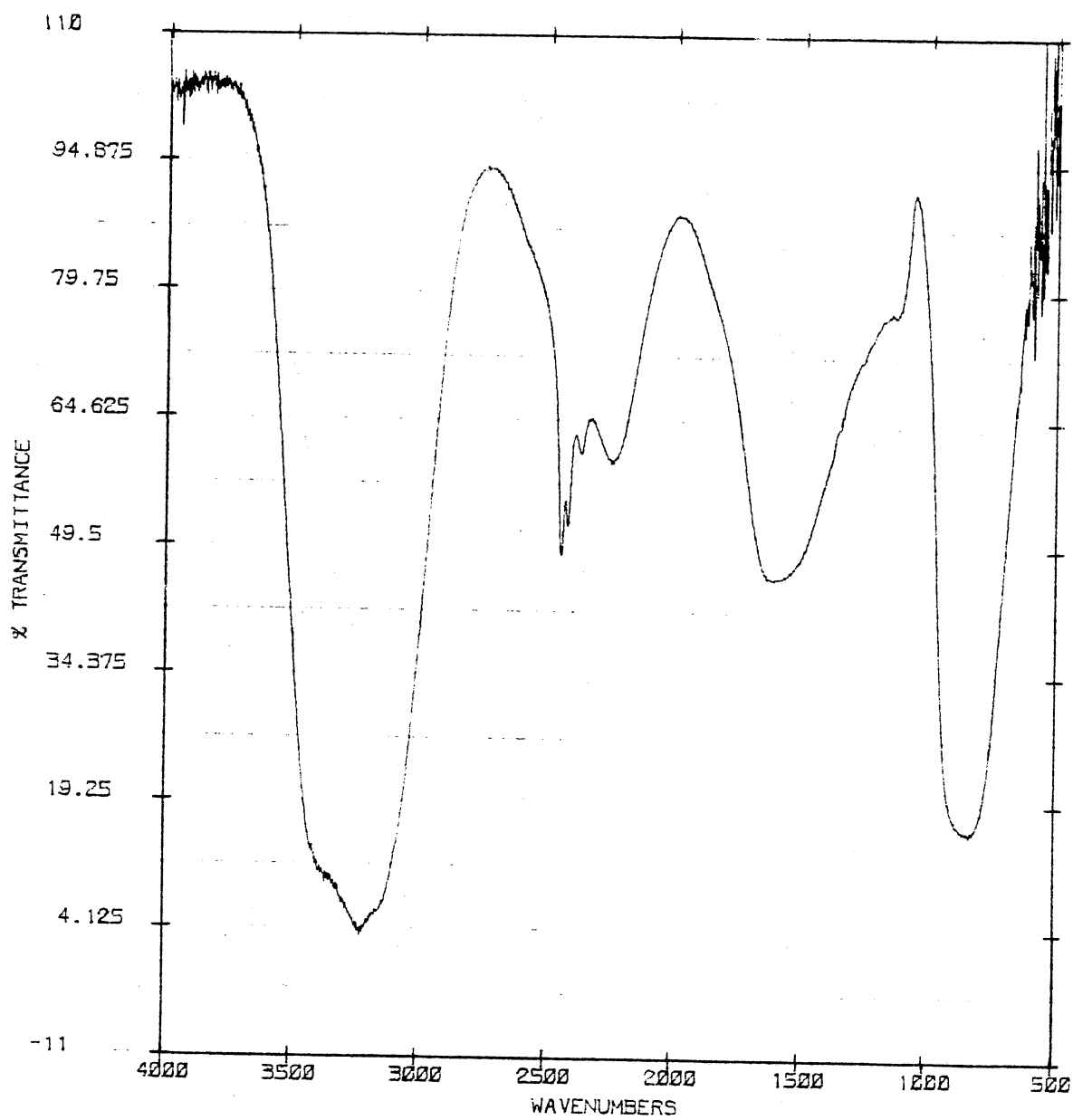
Figure 14. D_2O Decoupled in H_2O Cubic Ice Infrared Spectrum

sufficiently slow to warrant stopping. The collected interferograms were stored for later transformation to frequency spectra. The sample was then warmed to approximately 170 K for 10-20 minutes to completely convert the sample to HOD decoupled in H_2O. Next the sample was cooled to the kinetic exchange temperature and a spectrum of HOD in H_2O collected and stored. Lastly, the cryostat was reconnected to the vacuum and allowed to warm up to room temperature to vaporize and pump off the ice deposit. Thus with each sample a 130 K pre-kinetic run FTIR spectrum was made, a series of time correlated D_2O/H_2O exchange spectra at a chosen temperature, and a final converted HOD/H_2O product spectra at the chosen reaction temperature.

The glass-cell 7-azaindole doped D_2O in H_2O deposits were prepared in a similar manner except that the deposit temperature was raised to 155 K to ensure crystallinity. This modification was used because doping inhibited any significant exchange at 155 K and affected the formation of a crystalline deposit at 130 K.

The collected glass-cell spectra were used to produce totally resolved D_2O ν_1 and ν_3 bandshapes with no coupled HOD or isolated HOD band interference. These D_2O bandshapes were made at 2 and 3 K intervals between 135 and 165 K. Subsequently they were used to resolve the $D_2O/HOD/H_2O$ spectra collected with the metal cell.

Table I shows the collection parameters used for obtaining the kinetic data from the metal cell. The sampling time shows how long it took to collect the data for an interferogram, depending on the number of scans collected. Single beam spectra of the glass and metal cells cooled to approximately 150 K were used as background

TABLE I

COLLECTION PARAMETERS USED FOR COLLECTING KINETIC DATA

Sample	Main Deposit Temp. (^{O}K)	Kinetic Temp. (^{O}K)	Resolution (cm^{-1})	Scans Coadded	Sampling Time (sec)
2/2/82	130	150	2	20	50
6/7/82	130	150	2	10-20	25-50
6/9/82	125	150	2	10-20	25-50
1/29/82	130	145	2	20	50
5/10/82	130	145	2	20	50
5/24/82	130	145	2	10-20	25-50
6/3/82	130	145	2	20	50
5/11/82	130	140	2	20	50
5/25/82	130	140	2	20-50	50-120
5/15/82	130	135	2	20	50
5/26/82	130	135	2	20-50-100	50-120-240
6/11/82	125	135	2	20	50

references. Also spectra of these cells at 150 K with 20 minute H_2O deposits were used later in data manipulation.

The H_2O used was triply distilled and degassed under vacuum with several freeze-thaw cycles. The D_2O utilized was Merck and Co., Inc. deuterium oxide "100%" with a minimum isotopic purity of 99.96% deuterium. It was degassed under vacuum like H_2O. All chemical transfers were made with oven baked glassware under a dry nitrogen atmosphere. The 7-azaindole was obtained from Aldrich with a melting point of 105-107°, and IR and elemental analysis checks.

CHAPTER III

DATA TREATMENT AND THEORY DEVELOPMENT

Resolution of the Kinetic Spectral Data

The initial spectroscopic work on proton transfer in cubic ice deposits was reported by Devlin et al. (46, 47). As a result identification of the various vibrational bands in a typical $D_2O/HOD/H_2O$ deposit spectrum was readily made. Figure 15 shows the 2600 to 2250 cm^{-1} region of Figure 14 converted to absorbance units and expanded. Band for four distinct isotopic species are identifiable in the multiplet shown. The bands at 2444 cm^{-1} and 2367 cm^{-1} belong to ν_3 and ν_1 of D_2O. The strong band at 2418 cm^{-1} is assigned to the OD stretch of uncoupled HOD. The weak shoulder at 2396 cm^{-1} mentioned earlier is assigned to the in-phase coupled OD oscillator of coupled dimer HOD. Its companion out-of-phase OD stretch at 2442 cm^{-1} is obscured beneath the D_2O ν_3 band at 2444 cm^{-1}. The baseline slant is due to the shoulder of the 2250 cm^{-1} H_2O combination band.

If the $D_2O/HOD/H_2O$ deposit is warmed up and allowed to exchange the changes shown in Figure 16 occur. There the 2444 and 2367 cm^{-1} D_2O bands decrease in intensity and finally disappear, the 2396 cm^{-1} coupled dimer HOD band remains steady or increases to subsequently disappear, and the decoupled or isolated HOD band at 2418 cm^{-1} grows in intensity until eventually it becomes the sole spectral feature.

To follow the kinetics of the exchange process the multiplet
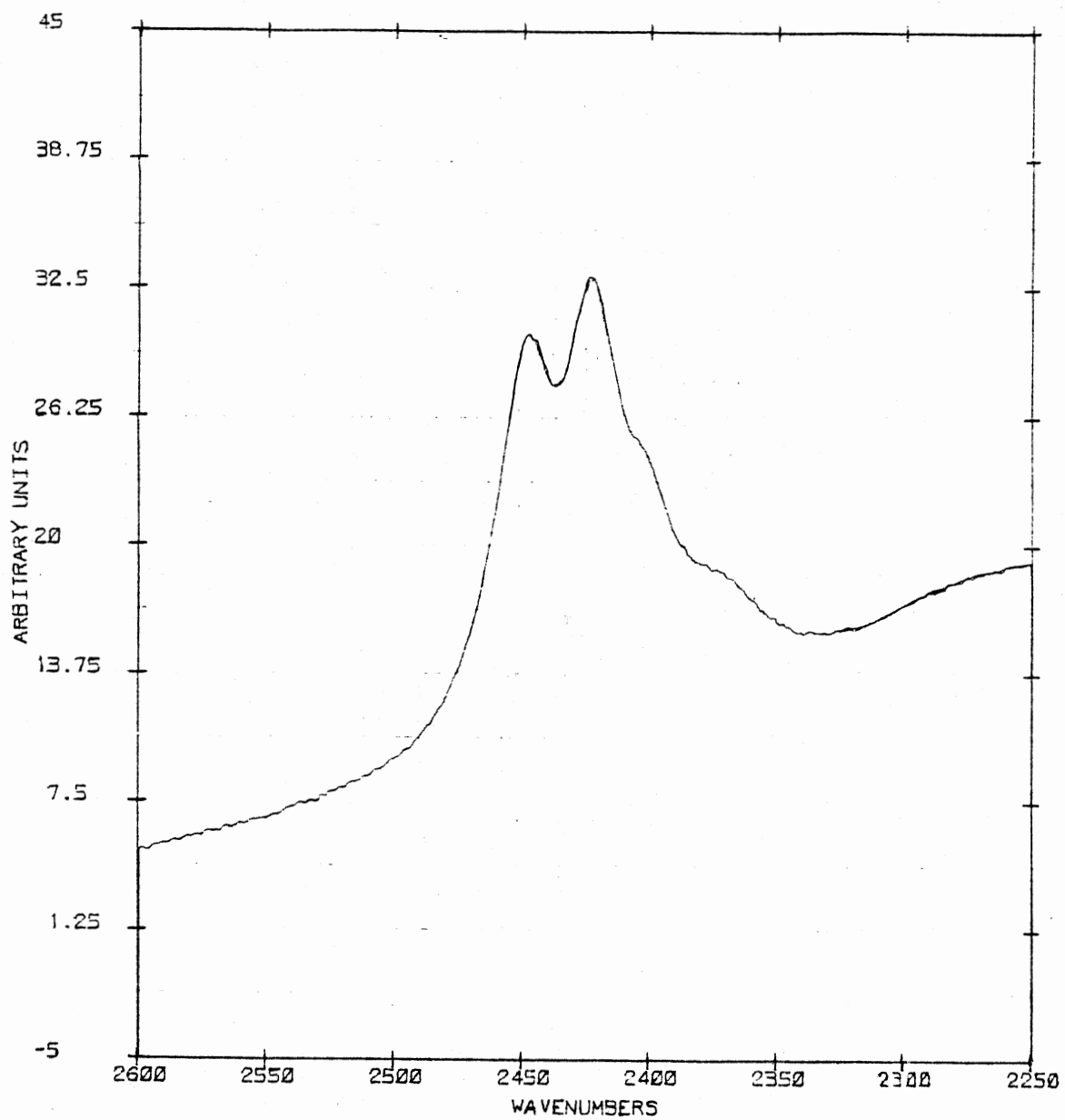
Figure 15. OD Stretch Multiplet of D_2O Decoupled in H_2O Ice

51
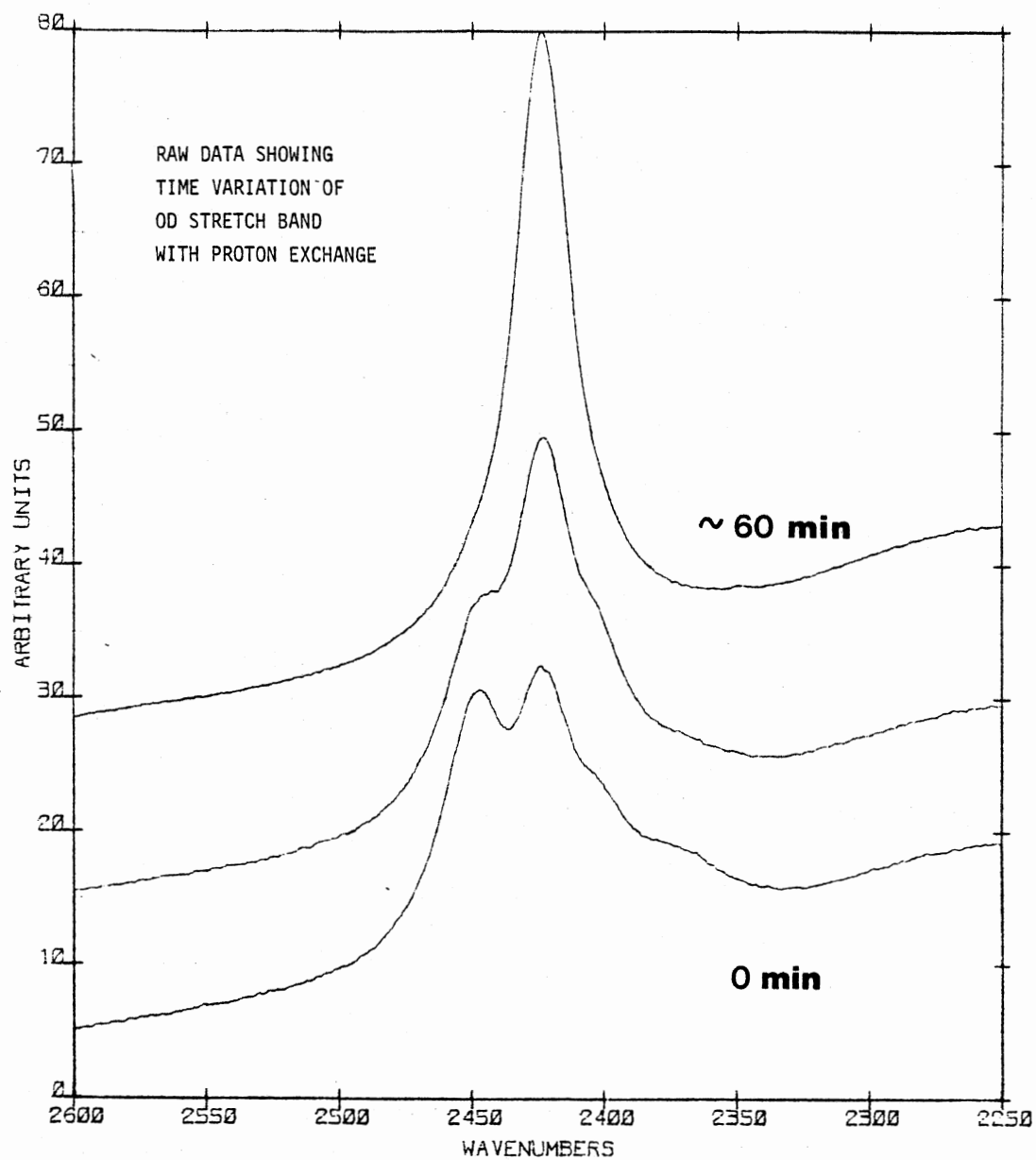
Figure 16.   Time Variation of OD Stretch Multiplet with Proton
            Exchange

must be resolved into the bands for the individual kinetic species for absorbance measurement. For a mixed multiplet of four distinct species this can be done if three pure component species spectra are available. There each component spectra may be scaled appropriately and subtracted from the multiplet to leave a multiplet with one less component. The process may be repeated until only the unknown component is left.

If all four pure component spectra are available, a standard least square type fitting program can be used to determine the best fit scaling constants for each component spectrum. However, in resolving the OD stretch multiplet only three pure component spectra were available. The best route to extracting the component absorbances was to extract the absorbance for three available pure components and check to see if the remaining pure component bandshape agreed with predictions. Fortunately for the $D_2O/HOD/H_2O$ deposit spectra, pure component spectra are obtainable for all except the coupled dimer HOD spectrum. In addition, from Haas and Hornig (22) some information is known about the coupled HOD bandshape. There should be two bands at about 2393 cm^{-1} (in-phase stretch) and 2442 cm^{-1} (out-of-phase stretch) with approximately a 2 to 1 (in-phase to out-of-phase) intensity ratio.

The 2250 cm^{-1} H_2O combination band pure component spectrum was obtained by making a deposit of H_2O only. The 2418 cm^{-1} uncoupled HOD band was obtained by allowing the $D_2O/HOD/H_2O$ deposit to convert completely to uncoupled HOD at the end of each kinetic run. Obtaining pure component D_2O ν_3 and ν_1 bands at each of the temperatures used for kinetics was considerably more involved.

From Devlin et al. (46), it is known that by introducing a dopant

such as 7-azaindole into the ice samples the transfer rate k_1 is slowed significantly relative to the k_2 rotational rate, thus causing a very small steady state concentration of coupled HOD that is spectroscopically unobservable. Using the glass deposition cell with the glass cell procedure outlined in Chapter II, 7-azaindole doped D_2O/H_2O ice deposits were made. Curve A Figure 17 shows a typical spectrum of the 2600-2250 cm^{-1} OD stretch region. Except for the absence of the 2396 and 2442 cm^{-1} coupled HOD bands the features are identical to Figure 15. By warming the deposit sufficiently, the sample could be made to convert enough to uncoupled HOD, that (see Figure 17 curve B) the converted HOD spectrum could be scaled appropriately and subtracted from the D_2O/HOD multiplet shown in curve A. This left the pure component D_2O ν_3 and ν_1 bands at the appropriate temperature (curve C). Several doped D_2O/H_2O deposit spectra were collected at 2 and 3 K intervals from 135 to 160 K, then warmed and converted to uncoupled HOD. After cooling the resulting spectra were collected at the same temperature as the pre-converted D_2O/H_2O spectra. Thus at each temperature a D_2O/H_2O multiplet and uncoupled HOD spectra were available for producing a pure component D_2O ν_3 and ν_1 spectrum. Figure 18 shows these pure D_2O ν_3 and ν_1 spectra.

Now with three pure component spectra at the same temperature as the metal cell OD stretch multiplet it is possible to subtract out each component and find its respective absorbance until only the pure coupled HOD spectrum remained. The following procedure was used.

The 2250 cm^{-1} combination band (Figure 19 curve B) is scaled and subtracted from the metal cell ice OD stretch multiplet (curve A) to
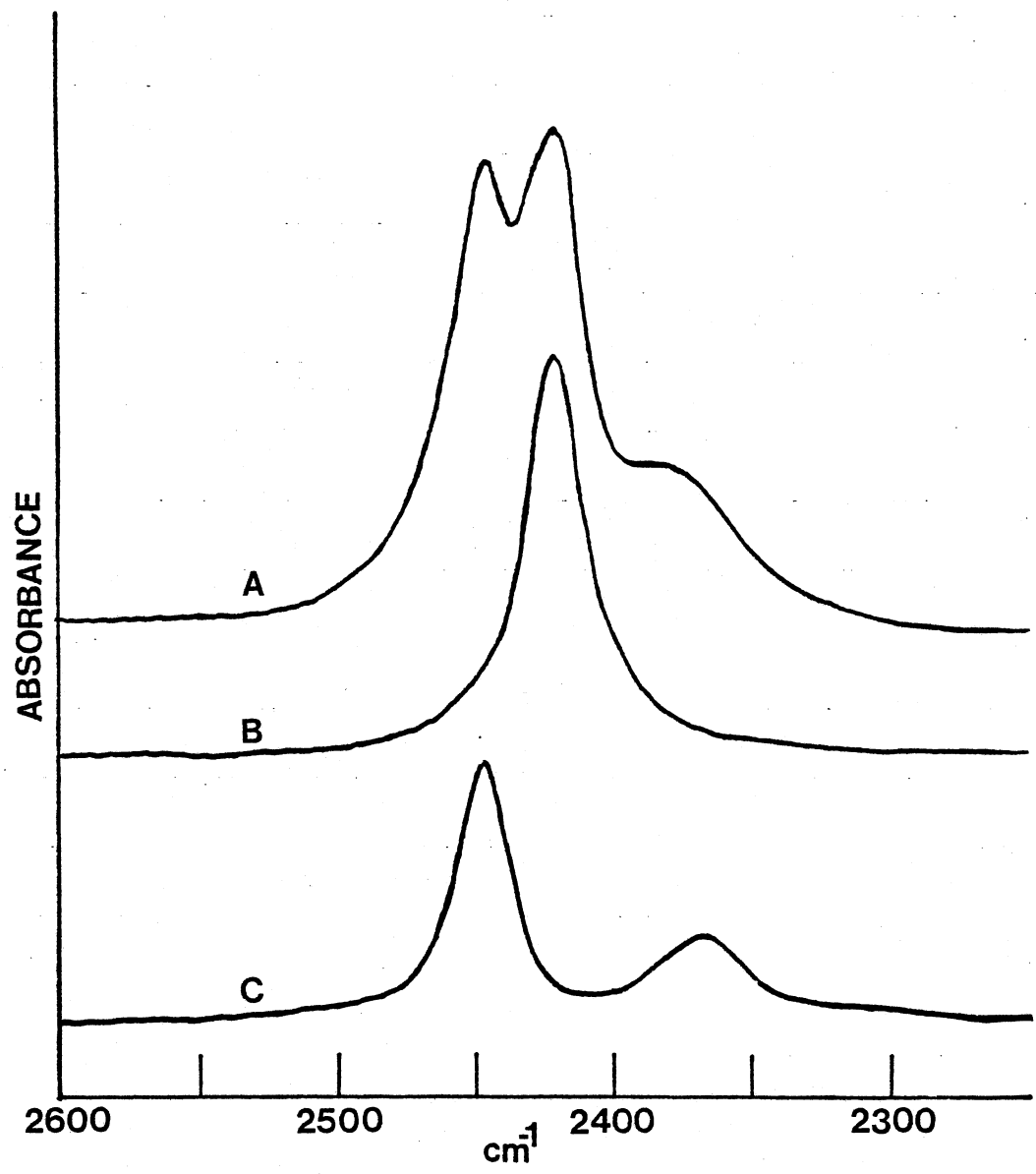
Figure 17. 7-Azaindole Doped D_2O/H_2O Ice Deposit Spectral Resolution
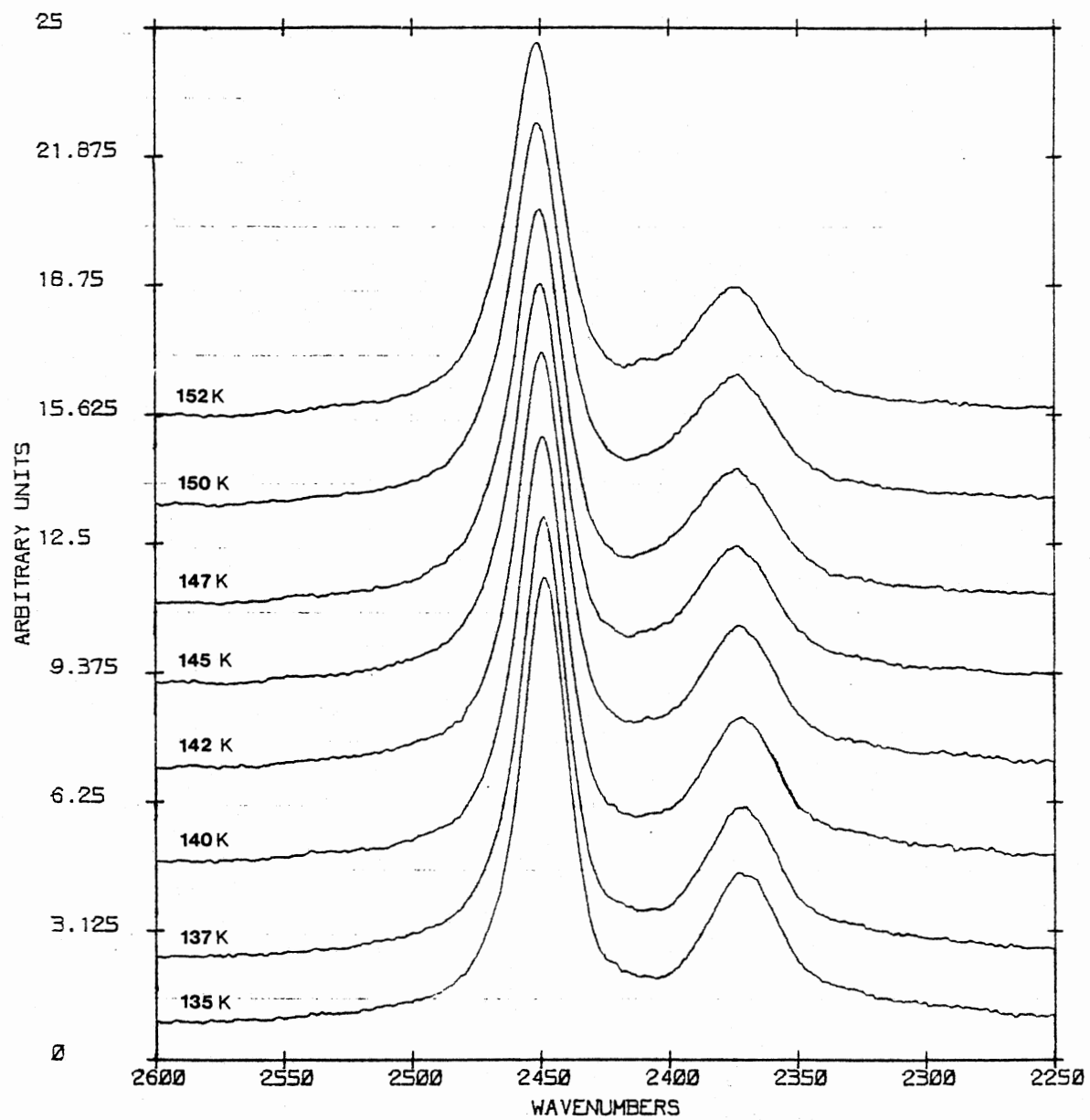
Figure 18. Pure Component D_2O ν_3 Bandshapes from Glass Cell
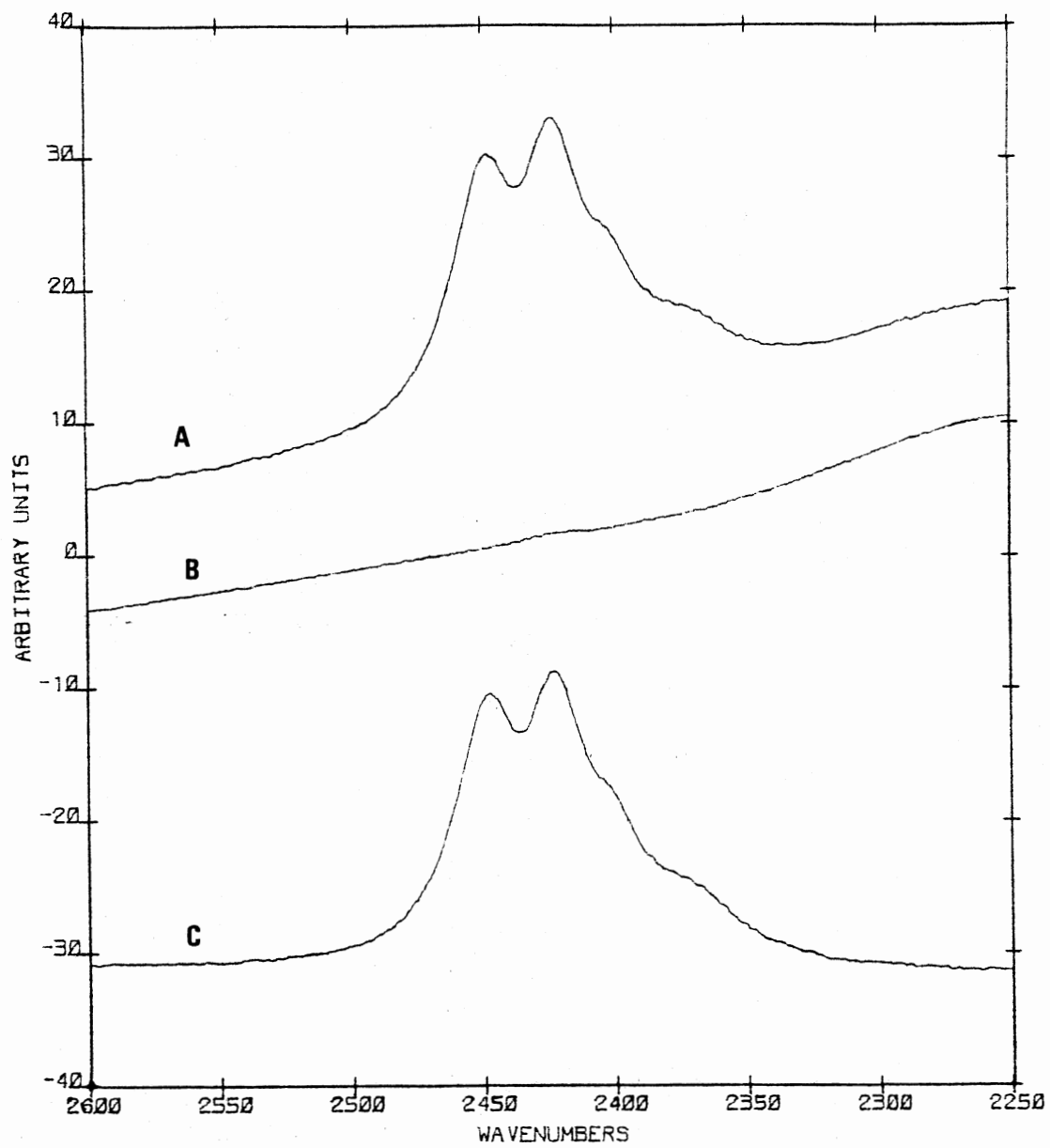
Figure 19.   Subtraction of H_2O Combination Shoulder from OD Multiplet

yield the multiplet on a flat background (curve C).

Next the pure D_2O spectrum (Figure 20 curve B), collected by the glass cell procedure at the same temperature as the OD stretch multiplet, was scaled and subtracted from the OD stretch multiplet (curve A) to yield the coupled and uncoupled HOD spectrum (curve C). Any significant over or under subtraction of the pure component D_2O (curve B) spectrum left small humps or dips at 2444 and 2367 cm^{-1}. By multiplying the particular pure component D_2O absorbance by the scaling factor used, the absorbance of the D_2O concentration in the ice deposition sample was found. The absorbance of the pure component D_2O band was taken from the more intense ν_3 band.

The uncoupled 2418 cm^{-1} HOD band (Figure 21 curve B) obtained at the end of each kinetic run was then scaled and subtracted from the previously found uncoupled and coupled HOD spectrum (Figure 21 curve A) to yield the pure component coupled HOD spectrum (curve C). The scaling factor used in the subtraction times the absorbance of the uncoupled HOD spectrum used (curve B) yielded the uncoupled HOD absorbance for that particular OD stretch multiplet. The absorbance of the coupled HOD was extracted from direct measurement of the in-phase 2396 cm^{-1} band. Any over subtraction of uncoupled HOD (curve B) would reveal itself as too steep and negative a dip between the coupled HOD in and out-of-phase bands. Too little subtraction would show as insufficient dip or even a small residual hump between the two coupled HOD bands.

As a further check, the coupled and uncoupled spectrum (Figure 22 curve B) can be subtracted from the starting OD stretch multiplet (curve A) to yield a replica of the pure D_2O component bands used in the Figure 20
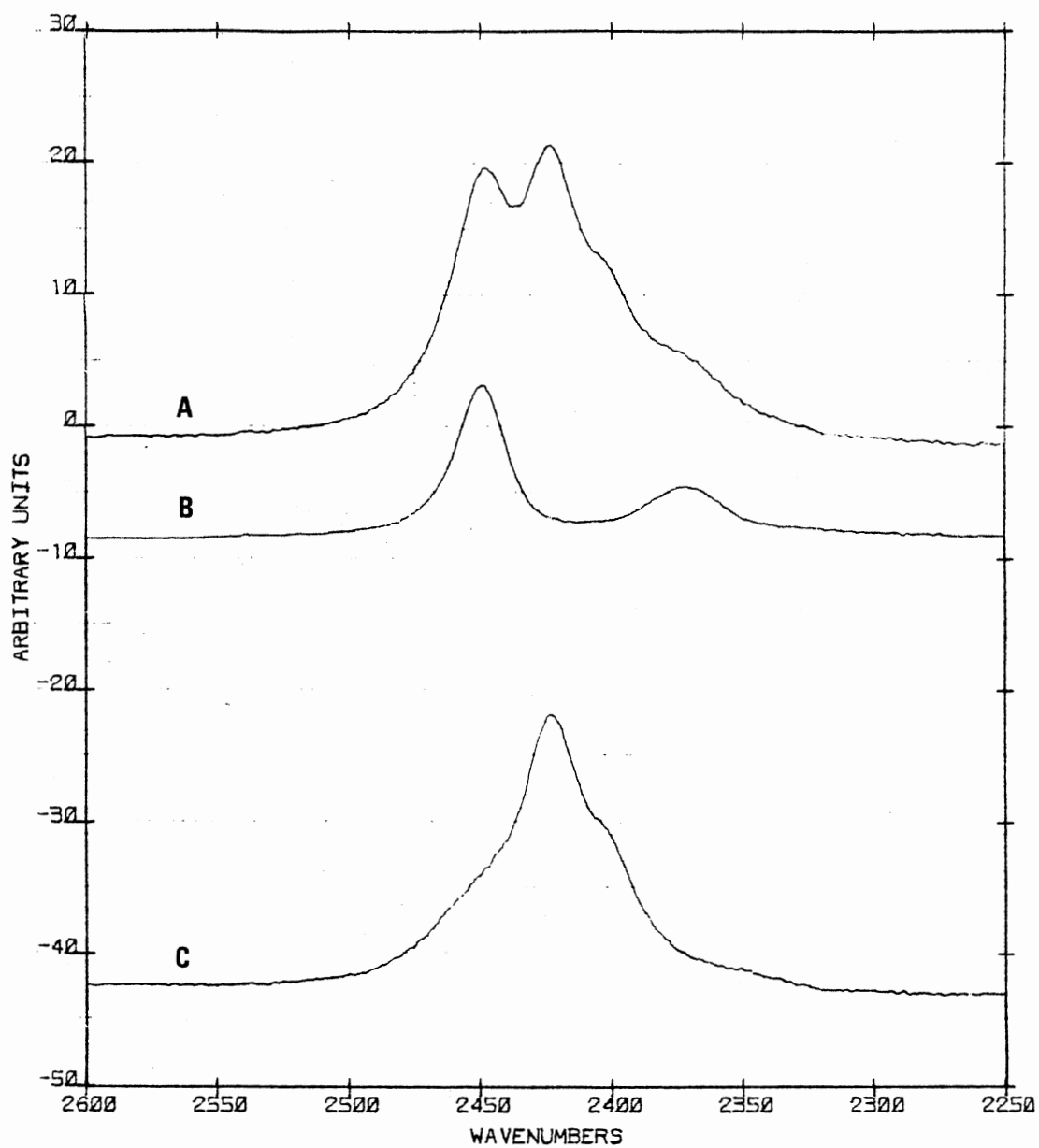
Figure 20. Subtraction of D_2O Component from OD Multiplet
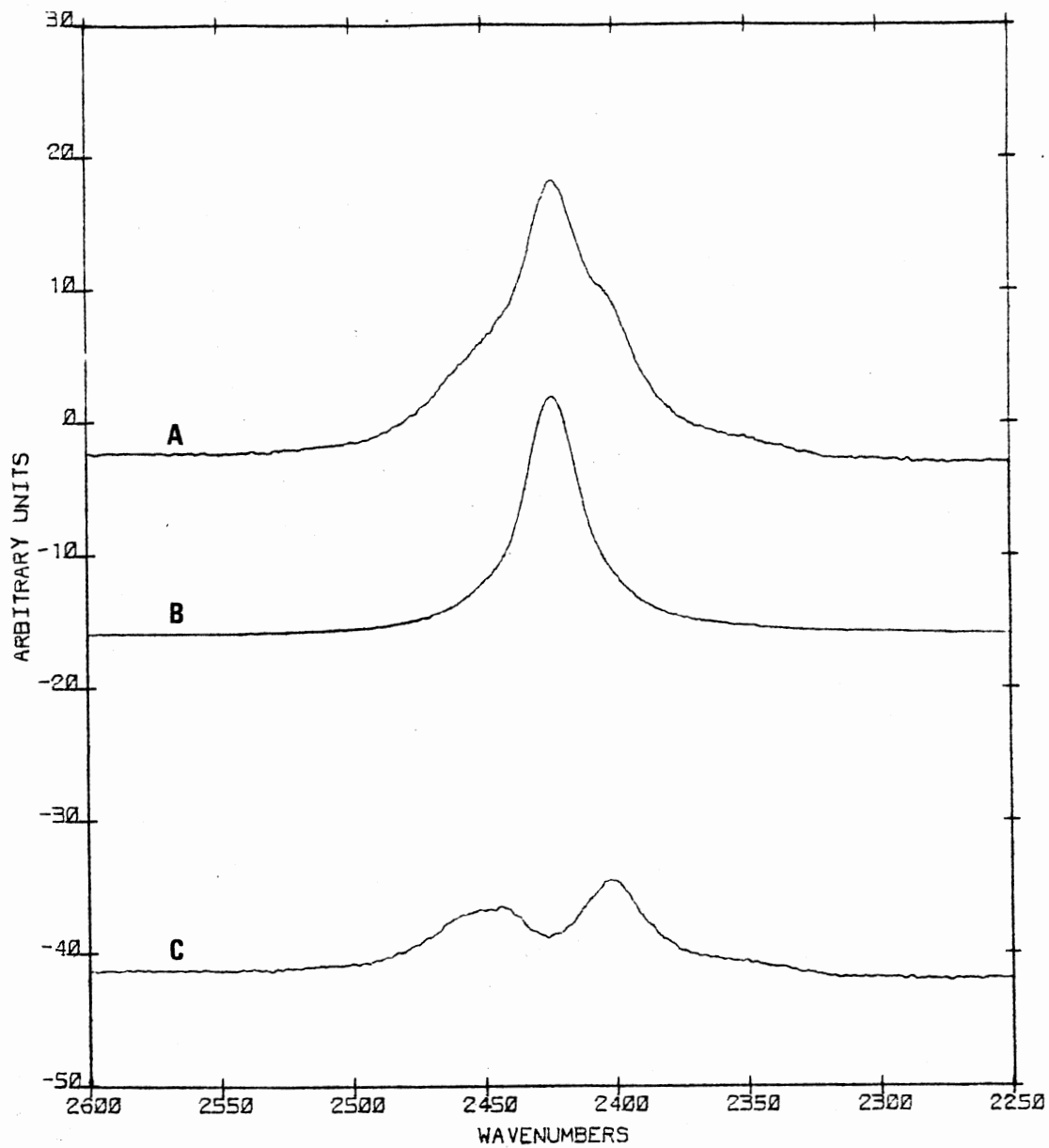
Figure 21. Subtraction of Uncoupled HOD Component from HOD Multiplet

subtraction, except that it has been scaled by the subtraction scaling

factor used in the Figure 20 subtraction. This process was repeated

for all multiplet resolutions at all data collection temperatures.

Usually two or three adjustments of the subtraction scaling factors

were necessary before the best resolution of the pure spectral compo-

nents was achieved.

Since the D_2O ν_3 band at 2444 cm^{-1} and the coupled HOD out-of-

phase band at 2442 cm^{-1} overlap so completely the D_2O component scaling

factor was not as correctly determined as the uncoupled HOD scaling

factor. Figure 23 illustrates the effects of deviations of the D_2O

pure component scaling factor from the correct scaling factor, on the

coupled HOD bandshapes. Additionally, when the concentration and hence

intensity of the coupled HOD was small, these deviations were difficult

to detect. To circumvent this problem the following reasoning was

used.

Both the in and out-of-phase bands arise from the same isotopic

chemical species. Thus assuming Beer's law of absorption holds over

the intensity range in question, there should be a constant ratio

between the in-phase band and out-of-phase band irrespective of concen-

tration or band intensity. To experimentally find this ratio, a series

of the best most intense pure coupled HOD spectra were measured to find

the best absorbance ratio. The best average ratio was 0.70 for the in-

phase absorbance to out-of-phase absorbance. Multiplying the better

determined in-phase coupled HOD band absorbance at 2396 cm^{-1} by 0.70

should yield a better out-of-phase 2442 cm^{-1} band absorbance. By

subtracting this ratio determined absorbance from the spectrally

measured coupled HOD out-of-phase absorbance the amount of over or
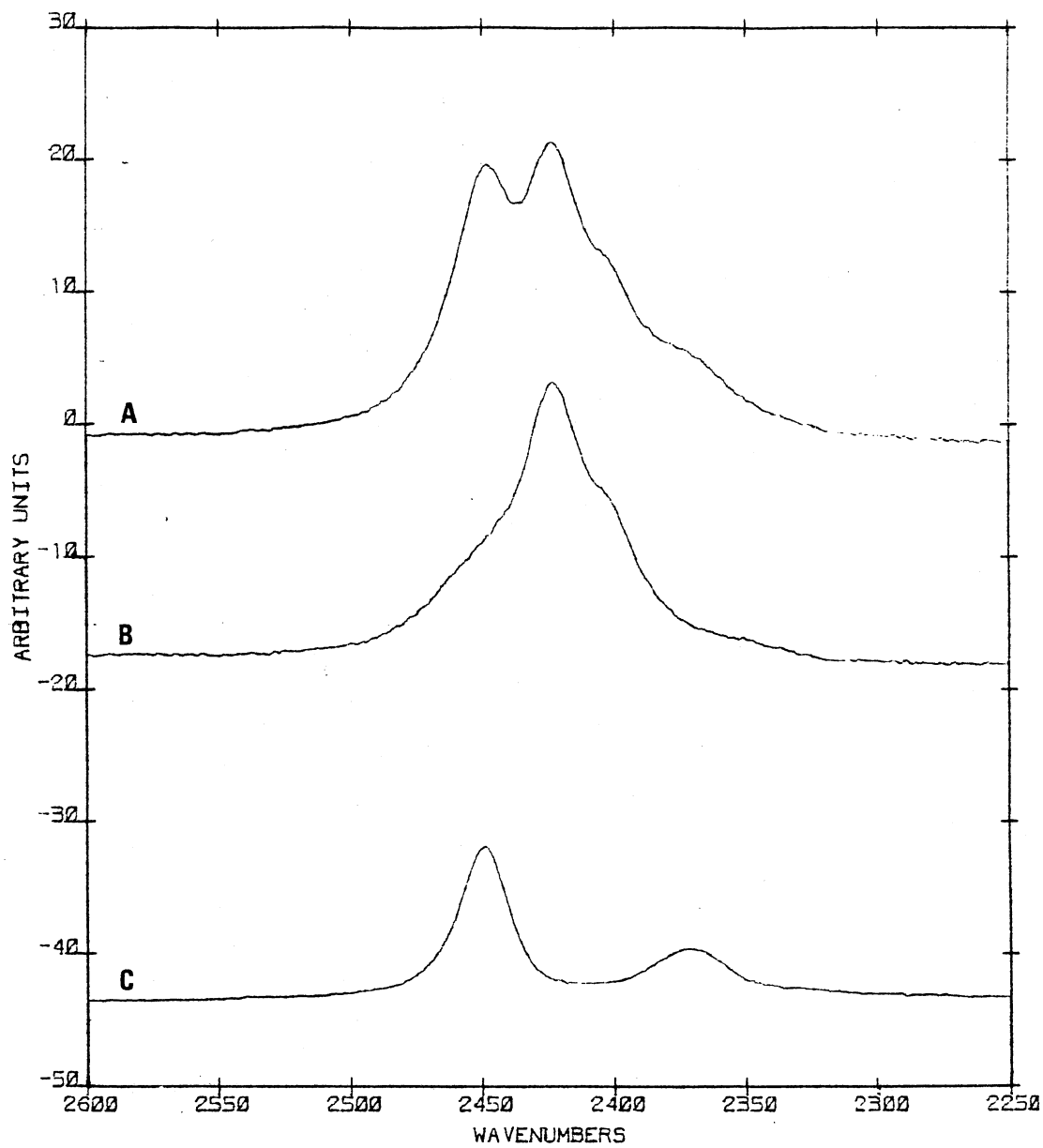
Figure 22. Subtraction of HOD Multiplet from OD Multiplet
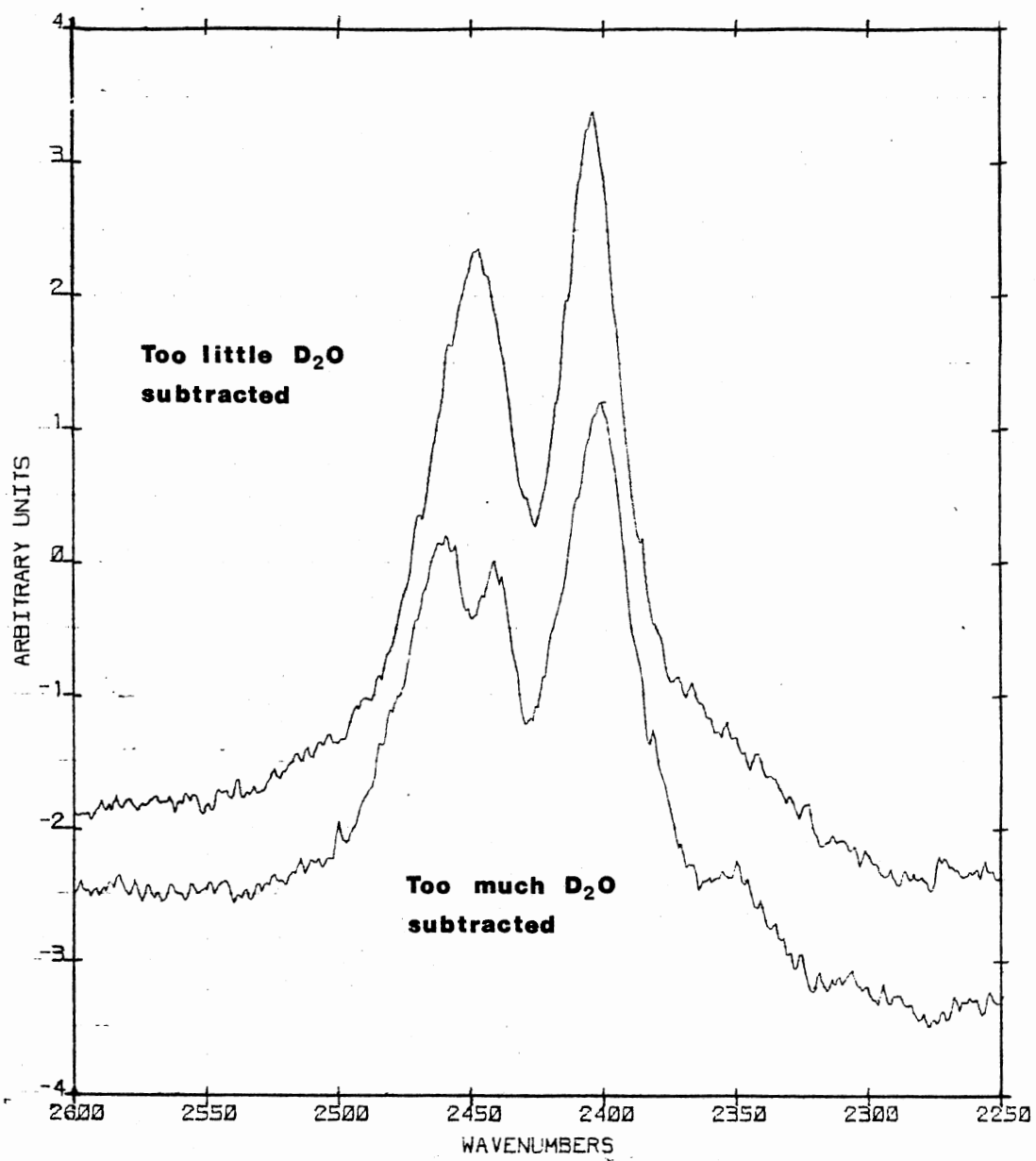
Figure 23. D_2O Scaling Factor Deviation Effects on Coupled HOD Bandshapes

under subtraction of the pure component D_2O band from the OD stretch multiplet could be determined. This positive or negative deviation was added to the previously determined D_2O component absorbance for the OD stretch multiplet being resolved. The resulting D_2O absorbances are called corrected D_2O absorbances. Most deviations calculated were small and served to smooth out the data of the corrected D_2O absorbance values as compared to the uncorrected D_2O absorbance values. Table II lists the scaling factors, corrected D_2O absorbance, coupled HOD absorbance, uncoupled HOD absorbances for the kinetic data found at 135, 140, 145, and 150 K. Also listed are the unscaled absorbances of the fully converted uncoupled HOD bands used in subtracting out the uncoupled HOD (see Figure 21) and glass cell doped ice deposit determined pure D_2O ν_3 bands (see Figure 20). All absorbance measurements determined from spectral plots were found by subtracting from the band peak absorbance the peak frequency absorbance of a baseline drawn tangest to the background absorption. All absorbance measurements are in Digilab's arbitrary absorbance units.

Table I shows the sampling times for the Table II data. The sampling or collection time for the interferogram is dependent on the resolution required, and number of interferometer scans coadded to form the final interferogram. For most data points the period of collection is small compared to the time interval between data points. The exceptions are the initial 150 K collected data. If the 2 to 4 minute interval of the 6/7/82 dataset is examined, it is found that the greatest change occurring with the D_2O absorbances are 12.639 at 2 minutes and 10.155 at 4 minutes. The Digilab FTIR takes 25 seconds to collect a 10 scan 2 cm^{-1} resolution interferogram. Thus one quarter

TABLE II

ABSORBANCES AND SCALING FACTORS FOR RESOLVED OD STRETCH MULTIPLETS

Dataset	Time (minutes)	D_2O		$(HOD)_2$	HOD	
		Scaling Factor	Absorbance[a,b]	Absorbance[a]	Scaling Factor	Absorbance[a]

150 K

Dataset	Time (minutes)	Scaling Factor	Absorbance	Absorbance	Scaling Factor	Absorbance
2/2/82		Doped D_2O absorbance = 9.20[c]		Fully converted HOD absorbance = 36.60[d]		
	0.0	1.27	11.869[e]	3.56[e]	0.31	11.346[e]
	2.0	0.98	9.281	5.05	0.35	12.81
	4.0	0.80	7.24	5.6	0.42	15.372
	6.0	0.65	5.665	5.45	0.49	17.934
	9.5	0.45	3.885	4.65	0.60	21.96
	12.5	0.33	3.041	3.85	0.67	24.522
	15.5	0.27	2.379	3.15	0.73	26.718
	20.5	0.19	1.873	2.25	0.79	28.914
6/7/82		Doped D_2O absorbance = 9.20		Fully converted HOD absorbance = 38.30		
	0.0	1.5	14.295	3.15	0.29	11.107
	2.0	1.35	12.639	3.83	0.335	12.831
	4.0	1.1	10.155	5.15	0.37	14.171
	6.0	0.88	8.131	5.55	0.43	16.469
	8.0	0.72	6.646	5.74	0.49	18.767
	10.0	0.62	5.809	5.35	0.54	20.682
	12.0	0.56	5.121	4.83	0.59	22.597
	15.0	0.49	4.253	4.15	0.655	25.087
	20.0	0.40	3.415	3.45	0.72	27.576
	25.0	0.32	2.714	2.9	0.72	29.491

TABLE II (Continued)

Dataset	Time (minutes)	D_2O		$(HOD)_2$	HOD	
		Scaling Factor	Absorbance[a,b]	Absorbance[a]	Scaling Factor	Absorbance[a]
6/9/82		Doped D_2O absorbance = 9.20		Fully converted HOD absorbance = 34.50		
	0.0	1.45	13.69	2.1	0.315	12.065
	1.0	1.41	12.832	2.2	0.335	12.831
	2.0	1.37	12.404	2.6	0.34	13.022
	3.0	1.30	11.79	2.8	0.35	13.405
	4.0	1.2	11.07	3.2	0.36	13.788
	5.0	1.08	10.081	3.65	0.39	14.937
	6.0	0.99	9.388	4.1	0.41	15.703
	8.0	0.90	8.59	4.1	0.45	17.235
	10.0	0.83	7.723	3.99	0.49	18.767
	12.0	0.77	6.834	4.0	0.53	20.299
	15.0	0.67	5.914	3.4	0.605	23.172
	20.0	0.53	4.718	2.94	0.675	25.853

<u>145 K</u>

Dataset	Time (minutes)	Scaling Factor	Absorbance	Absorbance	Scaling Factor	Absorbance
1/29/82		Doped D_2O absorbance = 9.50		Fully converted HOD absorbance = 38.00		
	0.0	1.4	13.73	3.1	0.30	11.4
	3.0	1.2	11.55	4.5	0.33	12.54
	6.0	0.98	9.53	5.4	0.37	14.06
	9.0	0.85	8.41	5.95	0.40	15.2
	12.0	0.76	7.415	6.15	0.43	16.34
	17.0	0.63	6.155	5.9	0.48	18.24
	21.7	0.50	5.165	5.55	0.54	20.52
	27.0	0.43	4.38	5.15	0.59	22.42
	32.0	0.38	3.82	4.7	0.63	23.94

TABLE II (Continued)

Dataset	Time (minutes)	D$_2$O		(HOD)$_2$	HOD	
		Scaling Factor	Absorbance[a,b]	Absorbance[a]	Scaling Factor	Absorbance[a]
	43	0.30	3.07	3.9	0.69	26.22
	52	0.26	2.59	3.4	0.73	27.74
	62	0.22	2.23	2.8	0.77	29.26
	72	0.18	2.125	2.55	0.79	30.02
5/10/82	Doped D$_2$O absorbance = 9.50			Fully converted HOD absorbance = 35.80		
	0.0	1.1	10.367	3.69	0.36	12.888
	3.0	1.0	9.537	4.09	0.38	13.604
	6.0	0.93	8.805	4.4	0.40	14.32
	9.0	0.85	7.95	4.65	0.43	15.394
	12.0	0.79	7.675	4.5	0.445	15.931
	17.0	0.70	6.609	4.63	0.485	17.363
	22.0	0.63	5.947	4.54	0.52	18.616
	27.0	0.58	5.435	4.25	0.555	19.869
	32.0	0.54	4.821	4.07	0.59	21.122
	47.0	0.41	3.561	3.32	0.67	23.986
	62.0	0.29	2.895	2.8	0.72	25.776
	77.0	0.22	2.245	2.35	0.77	27.566
5/24/82	Doped D$_2$O absorbance = 9.5			Fully converted HOD absorbance = 33.25		
	0.0	1.0	9.25	3.5	0.32	10.64
	3.0	0.88	8.117	3.89	0.34	11.305
	6.0	0.76	6.771	4.57	0.37	12.303
	9.0	0.64	5.925	4.65	0.40	13.3
	12.0	0.55	5.038	4.81	0.44	14.63
	17.0	0.40	3.809	4.83	0.50	10.625

TABLE II (Continued)

Dataset	Time (minutes)	D$_2$O		(HOD)$_2$	HOD	
		Scaling Factor	Absorbance[a,b]	Absorbance[a]	Scaling Factor	Absorbance[a]
	22.0	0.32	3.141	4.57	0.54	17.955
	27.0	0.29	2.997	4.14	0.57	18.953
	37.0	0.25	2.276	3.47	0.64	21.28
	47.0	0.22	1.935	3.05	0.685	22.776
6/3/82		Doped D$_2$O absorbance = 9.50		Fully converted HOD absorbance = 34.00		
	0.0	1.25	12.13	1.85	0.365	12.41
	3.0	1.1	10.481	2.67	0.385	13.09
	6.0	1.0	9.456	3.52	0.405	13.77
	9.0	0.915	8.737	3.68	0.425	14.45
	12.0	0.85	8.139	3.98	0.445	15.13
	17.0	0.75	7.325	4.1	0.475	16.15
	22.0	0.68	6.646	4.02	0.51	17.34
	27.0	0.63	5.764	4.03	0.55	18.7
	32.0	0.59	5.315	3.7	0.585	19.89
	42.0	0.50	4.459	3.43	0.64	21.76
	52.0	0.41	3.755	3.1	0.69	23.46
	62.0	0.32	3.18	2.8	0.72	24.48

<u>140 K</u>

Dataset	Time (minutes)	D$_2$O		(HOD)$_2$	HOD	
5/11/82		Doped D$_2$O absorbance = 10.20		Fully converted HOD absorbance = 33.50		
	0.0	1.2	11.788	2.26	0.37	12.395
	3.0	1.05	10.843	2.81	0.39	13.065
	6.0	0.97	10.195	3.17	0.40	13.4
	9.0	0.93	9.636	3.5	0.405	13.568

TABLE II (Continued)

Dataset	Time (minutes)	D_2O		$(HOD)_2$	HOD	
		Scaling Factor	Absorbance[a,b]	Absorbance[a]	Scaling Factor	Absorbance[a]
	12.0	0.90	9.44	3.7	0.41	13.735
	17.0	0.85	8.921	3.97	0.42	14.07
	22.0	0.81	8.396	4.28	0.43	14.405
	27.0	0.775	7.969	4.38	0.445	14.908
	32.0	0.745	7.756	4.39	0.455	15.243
	42.0	0.69	7.008	4.4	0.48	16.08
	60.0	0.59	6.025	4.49	0.53	17.755
	80.0	0.50	5.205	4.05	0.58	19.43
	100.0	0.42	4.554	3.8	0.62	20.77
	119.8	0.35	4.03	3.6	0.65	21.775
5/25/82		Doped D_2O absorbance = 10.20		Fully converted HOD absorbance = 37.60		
	0.0	1.41	14.384	2.54	0.31	11.656
	3.0	1.37	14.324	2.50	0.33	12.408
	6.0	1.33	13.951	2.85	0.33	12.408
	9.0	1.29	13.288	3.4	0.33	12.408
	12.0	1.25	12.937	3.59	0.34	12.784
	17.0	1.17	12.269	3.95	0.355	13.348
	27.0	1.1	11.306	4.52	0.37	13.912
	37.0	1.0	10.311	4.77	0.40	15.04
	47.0	0.92	9.797	4.91	0.42	15.792
	62.0	0.80	8.72	5.1	0.45	16.92
	82.0	0.71	7.587	5.15	0.49	18.424
	102.25	0.63	6.826	5.0	0.53	19.928
	132.0	0.54	5.839	4.77	0.57	21.432

TABLE II (Continued)

Dataset	Time (minutes)	D$_2$O		(HOD)$_2$	HOD	
		Scaling Factor	Absorbance[a,b]	Absorbance[a]	Scaling Factor	Absorbance[a]

135 K

5/15/82   Doped D$_2$O absorbance = 10.70   Fully converted HOD absorbance = 38.00

	Time	Scaling Factor	Absorbance	Absorbance	Scaling Factor	Absorbance
	0.1	1.29	14.148	2.65	0.327	12.426
	3.0	1.27	13.806	2.79	0.329	12.502
	6.0	1.25	13.681	2.92	0.331	12.578
	9.0	1.23	13.356	3.15	0.733	12.654
	14.3	1.20	13.152	3.34	0.335	12.73
	24.0	1.15	12.635	3.7	0.34	12.92
	34.0	1.09	12.093	4.1	0.345	13.11
	49.1	1.04	11.571	4.51	0.35	13.3
	64.0	0.98	10.886	4.8	0.36	13.68
	84.0	0.91	10.397	5.1	0.37	14.06
	104.0	0.88	9.906	5.3	0.38	14.44
	124.0	0.85	9.573	5.46	0.39	14.82
	144.0	0.82	9.134	5.7	0.40	15.2
	174.0	0.78	8.721	5.65	0.42	15.96

5/26/82   Doped D$_2$O absorbance = 10.70   Fully converted HOD absorbance = 23.65

	Time	Scaling Factor	Absorbance	Absorbance	Scaling Factor	Absorbance
	0.0	0.74	8.155	1.49	0.356	8.419
	6.0	0.725	7.918	1.6	0.359	8.490
	11.0	0.71	7.714	1.69	0.362	8.561
	16.0	0.695	7.471	1.88	0.365	8.632
	25.0	0.68	7.265	2.13	0.368	8.703
	35.0	0.65	7.049	2.18	0.375	8.869
	55.0	0.60	6.536	2.42	0.39	9.224

TABLE II (Continued)

Dataset	Time (minutes)	D$_2$O		(HOD)$_2$	HOD	
		Scaling Factor	Absorbance[a,b]	Absorbance[a]	Scaling Factor	Absorbance[a]
	85.0	0.55	6.061	2.72	0.405	9.578
	115.0	0.51	5.68	2.91	0.42	9.933
	145.0	0.48	5.391	3.05	0.435	10.288
	185.0	0.45	4.981	3.12	0.45	10.643
	225.0	0.435	4.685	3.2	0.465	10.997
	285.0	0.405	4.208	3.18	0.49	11.589
6/11/82		Doped D$_2$O absorbance = 10.7		Fully converted HOD absorbance = 35.50		
	0.0	1.28	14.053	2.09	0.320	11.36
	5.0	1.22	13.556	2.14	0.324	11.502
	10.0	1.20	12.99	2.5	0.326	11.573
	20.0	1.15	12.675	2.8	0.328	11.644
	30.0	1.10	12.368	3.26	0.33	11.715
	40.0	1.03	11.781	3.6	0.335	11.893
	60.0	0.98	11.166	4.0	0.35	12.425
	80.0	0.95	10.785	4.3	0.365	12.958
	100.0	0.93	10.266	4.55	0.37	13.135
	130.0	0.89	9.528	4.85	0.39	13.845
	160.0	0.85	9.011	5.12	0.41	14.555
	190.0	0.80	8.265	5.15	0.43	15.265
	220.0	0.75	7.815	5.3	0.45	15.975

[a] Digilab arbitrary absorbance units.
[b] Corrected D$_2$O concentrations as described in text.
[c] D$_2$O spectra obtained from glass cell ice deposits.
[d] Final converted HOD spectrum obtained at the end of each kinetic run.
[e] Data is accurate to 2 to 3 significant figures.

of the time interval was spent collecting data during which the D_2O

absorbance was decreasing slightly. Since the ten scans are averaged,

the interferometer would obtain a measured absorbance slightly lower

for the 2 minute mark where the data collection began, than the true

absorbance one would obtain for an instantaneous measurement at the

2 minute mark. If a linear decrease for the absorbance is assumed

over the 25 second time interval, then an approximate average intefero-

meter measured absorbance would be measured at about 13 seconds into

the time interval, or at 2.23 minutes instead of 2 minutes. Since

the absorbance changes by 2.484 (Digilab arbitrary absorbance units)

over the 2 minute interval, then over 13 seconds the absorbance should

change by approximately 0.31 absorbance units. This gives rise to

approximately a 2.5% relative error in the two minute absorbance

measurement of 12.639. In view of this small error, that decreases

dramatically as the time intervals increase and rate of absorbance

change decreases, the sampling error was ignored.

<div align="center">

Determination of Relative Molar

Absorptivities

</div>

Kinetic analysis is based on concentrations changes of chemical

species. Therefore some method must be found for converting the absorbance

measurements into concentration units before a kinetic mechanism may be

proposed for isotopic exchange in cubic ice. To accomplish this,

Beer's law is assumed to hold over the dynamic range of all kinetic

absorbance measurements. All absorbance measurements, though recorded

in arbitrary absorbance units, fell between 0.10 and 0.5 absorbance on

a true absorbance scale; a range where Beer's law deviations are not

severe.

Due to the thin layer nature of the ice deposits and the method used in their preparation it is very difficult if not impossible to determine thickness, thickness uniformity, and absolute concentrations of the various isotopic species. Thus there was no means available for preparing standard Beer's law plots of each isotopic specie isolated in H_2O cubic ice. Neither does the chemical literature contain reports of absorptivities of D_2O, HOD, or $(HOD)_2$ isolated in a cubic ice lattice at the necessary frequencies. But fortunately since first order rate constants are dependent on the change in concentrations rather than absolute concentrations, relative concentrations and hence relative molar absorptivities are sufficient. If the relative magnitudes of the absorptivities are found, then the relative concentrations can be found from the absorbance data.

The kinetic expression of the isotopic exchange is

$$[D_2O] \;\; \underset{k_{-1}}{\overset{k_1}{\rightleftharpoons}} \;\; [(HOD)_2] \;\; \underset{k_{-2}}{\overset{k_2}{\rightleftharpoons}} \;\; 2[HOD] \tag{3.1}$$
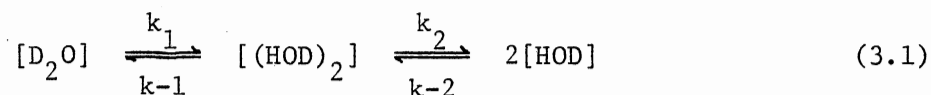
where $[D_2O]$ is the D_2O concentration in moles/liter of the ice deposit, $[(HOD)_2]$ the coupled HOD dimer concentration, and $[HOD]$ the uncoupled HOD concentration. From experimental data, (46, 47) it is known that the uncoupled HOD units in the cubic ice lattice eventually migrate apart. Therefore the equilibrium situation proposed in equation (3.1) is constantly perturbed until after an infinite period of time, essentially all the D_2O and $(HOD)_2$ have converted to HOD. Thus at any time a material balance yields

$$[D_2O] + [(HOD)_2] = \frac{1}{2}[HOD_\infty] - \frac{1}{2}[HOD] \tag{3.2}$$

where [HOD∞] is the uncoupled HOD concentration after an infinite amount of time and the other concentrations at some lesser time. Rearranging equation (3.2) gives

$$2[D_2O] + 2[(HOD)_2] + [HOD] - [HOD_\infty] \ = \ 0 \tag{3.3}$$

assuming Beer's law holds where [X] = peak absorbance of $X/\epsilon_x b$, ϵ_x is the molar absorptivity of component X and b the pathlength traversed in penetrating the sample medium then

$$\frac{2A_{D_2O}}{\epsilon_{D_2O}b} + \frac{2A_{(HOD)_2}}{\epsilon_{(HOD)_2}b} + \frac{A_{HOD}}{\epsilon_{HOD}b} - \frac{A_{HOD_\infty}}{\epsilon_{HOD}b} \ = \ 0 \tag{3.4}$$

$$\frac{2A_{D_2O}}{\epsilon_{D_2O}} + \frac{2A_{(HOD)_2}}{\epsilon_{(HOD)_2}} + \frac{A_{HOD} - A_{HOD_\infty}}{\epsilon_{HOD}} \ = \ 0 \tag{3.5}$$

By inserting absorbance data from three different time intervals three different equations may be constructed to solve for the three molar absorptivities. However these equations would form a homogeneous set of equations for which no unique solution exists; only a relational one. Thus to find the relational solution it is assumed that ϵ_{HOD} = 1.0, and a = $\dfrac{2}{\epsilon_{D_2O}}$, and b = $\dfrac{2}{\epsilon_{(HOD)_2}}$. Rewriting, we obtain

$$aA_{D_2O} + bA_{(HOD)_2} \ = \ A_{HOD_\infty} - A_{HOD} \tag{3.6}$$

Then with absorbance data from two different time intervals of a particular kinetic run the relative molar absorptivities of D_2O, $(HOD)_2$, and HOD may be found. Alternatively $\epsilon_{(HOD)_2}$ or ϵ_{D_2O} could be set equal to some constant and the relational solution then found.

REMOLE is a fortran program written to ascertain the relative molar absorptivities of cubic ice-isolated D_2O, $(HOD)_2$, and HOD. The program uses equation 3.6 and the equivalent equation found by setting ϵ_{HOD} =

1.0 plus inputted absorbance data for D_2O, $(HOD)_2$, and HOD to determine the best average relative molar absorptivities for each. A program listing with sample data and output is included in Appendix A.

Figure 24 shows a 150 K set of kinetic observations. REMOLE required that the observations of a dataset be numbered consecutively with integers starting from one. For example, observation 1 would contain the absorbances (Digilab arbitrary absorbance units) of D_2O, $(HOD)_2$, and HOD at time = 0 and observation 2 the absorbances at time = 2 minutes. Then by inputting the starting and ending observation numbers REMOLE would calculate the average relative molar absorptivities for all unique binary combinations of observations between and including the starting and ending observations using simultaneous equations from equation (3.6). As a check, equation (3.6) was solved with both ε_{HOD} = 1.0; and its appropriate variant equation where $\varepsilon_{(HOD)_2}$ = 1.0. The relative molar absorptivities obtained from setting $\varepsilon_{(HOD)_2}$ = 1.0 could be multiplied by a scaling factor for direct comparison with the molar absorptivities obtained from equation (3.6) with ε_{HOD} = 1.0. As illustrated in Figure 24 observation 10 is at the end of the dataset where the arbitrary absorbance values of HOD are high and the values of D_2O and $(HOD)_2$ quite low. Thus a 0.5 arbitrary absorbance error would be about a 15-20% error at observation 10 for D_2O and $(HOD)_2$ but only about a 5% error for D_2O at lower observations. Therefore it is expected that binary combinations of lower numbered observations should give more reliable consistent absorptivities. REMOLE prints out the relative absorptivities for each binary combination of absorbances used in the simultaneous equation solution so that visual
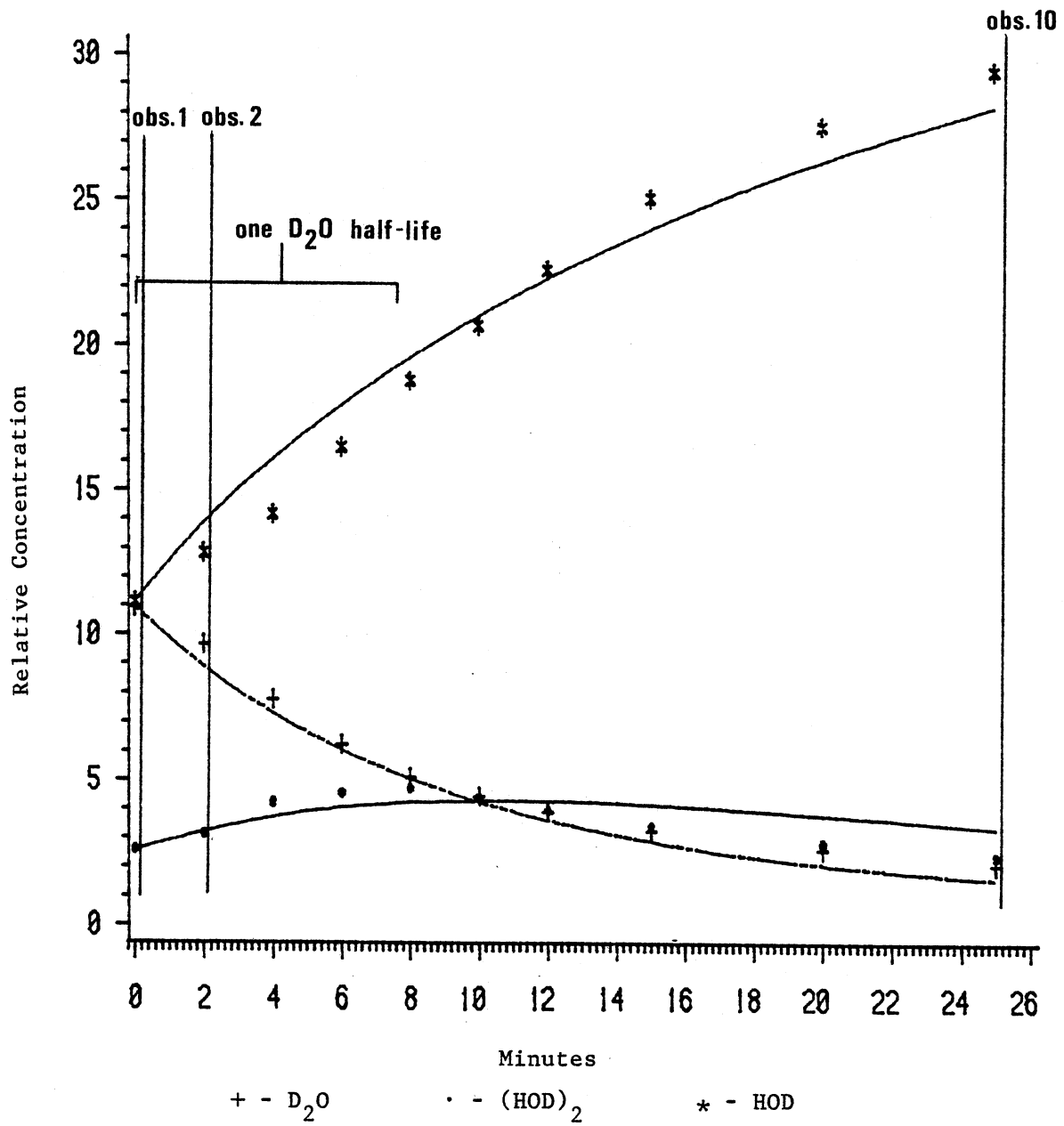
Figure 24. REMOLE Dataset Coverage and Analysis

inspection of the individual computed absorptivities was possible. An additional feature of REMOLE was to decrement the stopping observation by one and then recompute the average relative molar absorptivities. This process was repeated until only the starting and starting plus one observation absorbances were left for finding the relative molar absorptivities. By appropriate selection of starting and stopping observation numbers it is possible to confine the calculation to the most reliable part of the dataset. From calculations using REMOLE the best absorbances to use for relative-molar-absorptivity calculations were those within the first 1.5 half-lives of the D_2O absorbance.

Table III shows the results of these calculations for each dataset at each temperature. Included are the relative molar absorptivities for each dataset for calculations with ε_{HOD} set equal to 1.0 and also for $\varepsilon'_{(HOD)_2}$ set equal to 1.0. Unless the ε' values are multiplied by a ε_{HOD} scaling factor, the two calculations cannot be directly compared. The average relative molar absorptivities for datasets and temperatures with their associated sigmas is shown at the bottom of Table III. The primed average absorptivities have been scaled by $\varepsilon_{(HOD)_2} = 1.222$ so that the different calculations may be compared for the extent of data induced error. No noticeable temperature dependent trend is observed in the relative molar absorptivities. This should be no problem since the calculated first order rate constants are not dependent on the magnitude of the concentrations just their rate of change. Table IV lists the relative concentration values calculated for each temperature and run-time using Beer's law and the final calculated average relative molar absorptivities of Table III.

TABLE III

RELATIVE MOLAR ABSORPTIVITIES

Dataset	Relative Absorptivities $\varepsilon_{HOD} = 1.0$			Relative Absorptivities $\varepsilon_{(HOD)_2} = 1.0$		
	ε_{D_2O}	$\varepsilon_{(HOD)_2}$	ε_{HOD}	ε'_{D_2O}	$\varepsilon'_{(HOD)_2}$	ε'_{HOD}
150 K						
2/2/82	1.292	1.113	1.0	1.172	1.0	0.9027
6/7/82	1.289	1.247	1.0	1.042	1.0	0.8063
6/9/82	1.422	1.338	1.0	1.148	1.0	0.7942
145 K						
1/29/82	1.327	1.171	1.0	1.152	1.0	0.8603
5/10/82	1.214	1.141	1.0	.9669	1.0	1.101
5/24/82	1.277	0.9053	1.0	1.434	1.0	1.111
6/3/82	1.277	1.295	1.0	1.003	1.0	0.7817
140 K						
5/11/82	1.377	1.303	1.0	1.097	1.0	0.7803
5/25/82	-----omitted due to inconsistent first data points-----					
135 K						
5/15/82	1.307	1.285	1.0	1.032	1.0	0.7863
5/26/82	1.284	1.202	1.0	1.099	1.0	0.8481
6/11/82	1.311	1.441	1.0	1.021	1.0	0.7469
Average Value	1.307	1.222	1.0	1.106	1.0	0.8653
σ	0.05228	0.1347	0.0	0.1216	0.0	0.1209
90% Confidence Interval	± 0.026	± 0.067	—	± 0.060	—	± 0.060

$$\varepsilon'_{D_2O} \cdot \varepsilon_{(HOD)_2} = 1.352 \qquad \varepsilon_{D_2O} = 1.307$$

$$\varepsilon'_{(HOD)_2} \cdot \varepsilon_{(HOD)_2} = 1.222 \qquad \varepsilon_{(HOD)_2} = 1.222$$

$$\varepsilon'_{HOD} \cdot \varepsilon_{(HOD)_2} = 1.057 \qquad \varepsilon_{HOD} = 1.000$$

TABLE IV

RELATIVE CONCENTRATIONS DETERMINED FROM ABSORBANCE DATA

Dataset	Time (minutes)	$[D_2O]$	$[(HOD)_2]$	$[2HOD]$[a]
150 K				
2/2/82	0.0	9.08	2.82	5.67
	2.0	7.10	4.13	6.41
	4.0	5.54	4.58	7.69
	6.0	4.33	4.46	8.97
	9.5	2.97	3.81	10.98
	12.5	2.33	3.15	12.26
	15.5	1.82	2.58	13.36
	20.5	1.43	1.84	14.46
6/7/82	0.0	10.94	2.58	5.55
	2.0	9.67	3.13	6.42
	4.0	7.77	4.21	7.09
	6.0	6.22	4.54	8.24
	8.0	5.09	4.70	9.38
	10.0	4.45	4.38	10.34
	12.0	3.92	3.95	11.30
	15.0	3.25	3.40	12.54
	20.0	2.61	2.82	13.79
	25.0	2.08	2.37	14.75
6/9/82	0.0	10.47	1.72	6.03
	1.0	9.82	1.80	6.42
	2.0	9.49	2.13	6.51
	3.0	9.02	2.29	6.70
	4.0	8.47	2.62	6.89
	5.0	7.71	2.99	7.47
	6.0	7.18	3.36	7.85
	8.0	6.57	3.36	8.62
	10.0	5.91	3.27	9.38
	12.0	5.23	3.27	10.15
	15.0	4.53	2.78	11.59
	20.0	3.61	2.41	12.93
145 K				
1/29/82	0.0	10.50	2.54	5.70
	3.0	8.84	3.68	6.27
	6.0	7.29	4.42	7.03
	9.0	6.44	4.87	7.60
	12.0	5.67	5.03	8.17
	17.0	4.71	4.82	9.12
	21.7	3.95	4.54	10.26
	27.0	3.35	4.21	11.21
	32.0	2.92	3.85	11.97

TABLE IV (Continued)

Dataset	Time (minutes)	$[D_2O]$	$[(HOD)_2]$	$[2HOD]$[a]
	42.0	2.35	3.19	13.11
	52.0	1.98	2.78	13.87
	62.0	1.71	2.29	14.63
	72.0	1.63	2.09	15.01
5/10/82	0.0	7.93	3.02	6.44
	3.0	7.30	3.35	6.80
	6.0	6.74	3.60	7.16
	9.0	6.08	3.81	7.70
	12.0	5.87	3.68	7.97
	17.0	5.05	3.79	8.68
	22.0	4.55	3.71	9.31
	27.0	4.16	3.48	9.93
	32.0	3.69	3.33	10.56
	47.0	2.73	2.72	11.99
	62.0	2.22	2.29	12.89
	77.0	1.72	1.92	13.78
5/24/82	0.0	7.08	2.86	5.32
	3.0	6.21	3.18	5.65
	6.0	5.18	3.74	6.15
	9.0	4.53	3.81	6.65
	12.0	3.86	3.94	7.32
	17.0	2.91	3.95	8.31
	22.0	2.40	3.74	8.98
	27.0	2.29	3.39	9.48
	37.0	1.74	2.84	10.64
	47.0	1.48	2.50	11.39
6/3/82	0.0	9.28	1.51	6.21
	3.0	8.02	2.]9	6.55
	6.0	7.24	2.88	6.89
	9.0	6.69	3.01	7.23
	12.0	6.23	3.26	7.57
	17.0	5.60	3.36	8.08
	22.0	5.09	3.29	8.67
	27.0	4.41	3.30	9.35
	32.0	4.07	3.93	9.95
	37.0	7.93	3.90	7.52
	47.0	7.50	4.02	7.90
	62.0	6.67	4.17	8.46
	82.0	5.81	4.21	9.21
	102.25	5.22	4.09	9.96
	132.0	4.47	3.90	10.72

135 K

Dataset	Time (minutes)	$[D_2O]$	$[(HOD)_2]$	$[2HOD]$[a]
5/15/82	0.1	10.82	2.17	6.21
	3.0	10.56	2.28	6.25

TABLE IV (Continued)

Dataset	Time (minutes)	$[D_2O]$	$[(HOD)_2]$	$[2HOD]$[a]
	6.0	10.47	2.39	6.29
	9.0	10.22	2.58	6.33
	14.3	10.06	2.73	6.37
	24.0	9.67	3.03	6.46
	34.0	9.25	3.36	6.56
	49.1	8.55	3.69	6.65
	64.0	8.33	3.93	6.84
	84.0	7.96	4.17	7.03
	104.0	7.58	4.34	7.22
	124.0	7.32	4.47	7.41
	144.0	6.99	4.66	7.60
	174.0	6.67	4.62	7.98
5/26/82	0.0	6.24	1.22	4.21
	6.0	6.06	1.31	4.25
	11.0	5.90	1.38	4.28
	16.0	5.72	1.54	4.32
	25.0	5.56	1.74	4.35
	35.0	5.39	1.78	4.43
	55.0	5.00	1.98	4.61
	85.0	4.64	2.23	4.79
	115.0	4.35	2.38	4.97
	145.0	4.13	2.50	5.14
	185.0	3.81	2.55	5.32
	225.0	3.59	2.62	5.50
	285.0	3.22	2.60	5.79
6/11/82	0.0	10.75	1.71	5.68
	5.0	10.37	1.75	5.75
	10.0	9.94	2.05	5.79
	20.0	9.70	2.29	5.82
	30.0	9.46	2.67	5.86
	40.0	9.01	2.95	5.95
	60.0	8.54	3.27	6.21
	80.0	8.25	3.52	6.48
	100.0	7.86	3.72	6.57
	130.0	7.29	3.97	6.92
	160.0	6.89	4.19	7.28
	190.0	6.32	4.21	7.63
	220.0	5.98	4.34	7.99

[a]Concentration of two HOD units, thus $[2HOD] = \frac{1}{2} \cdot [HOD]$.

Model Development

One goal of this study was to find the proton transfer and
rotational rates and their respective activation energies.   To
accomplish this goal a model must be developed that relates k_t,
the rate constant for transfer of protons via an ionic defect migra-
tion, and k_r, the rate constant for migration via a D or L Bjerrum
defect migration, to the kinetics spectroscopically observed.

Since all the oxygens in a cubic ice lattice are tetrahedrally
linked one to another then any migration path of deuterons along
these linkages can be represented as a chain of OH groups as shown
in Figure 25a.

If the deuterons are examined in Figure 25a it can be seen that
with proton transfer alone, only 3 unique positions of the deuterons
in the OH chain are possible as shown and labeled in Figure 25b.   If
a Bjerrum D or L defect migrates through or along the chain then a
proton or deuterium rotation may follow that leaves the two deuterons
separated by two oxygen atoms instead of one.   However, this separation
of the deuterons will affect the positions of the deuterons relative
to each other only if they are in positions 2 or 3 (i.e. after a
transfer), and the defect approaches in such a manner that both defects
are not rotated together thus preserving their orientation and trans-
lating that particular deuteron configuration through the crystal
lattice.   So if the number of oxygens between the two deuterons are
counted and their position index as defined in Figure 25b noted, any
particular configuration of deuterons with respect to successive
rotations and transfers can be represented by using two subscripts
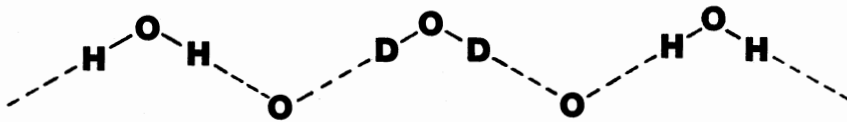
Figure 25a. Hydrogen Bonded Chain in Cubic Ice

Position 1

Position 2
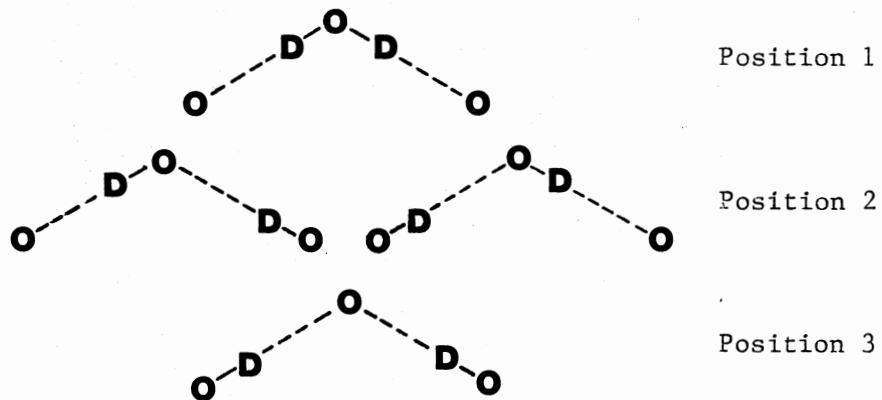
Position 3

Figure 25b. Possible Proton Transfer Positions

$(HOD)_2$ or $2HOD_{12}$

$2HOD_{13}$

$2HOD_{31}$
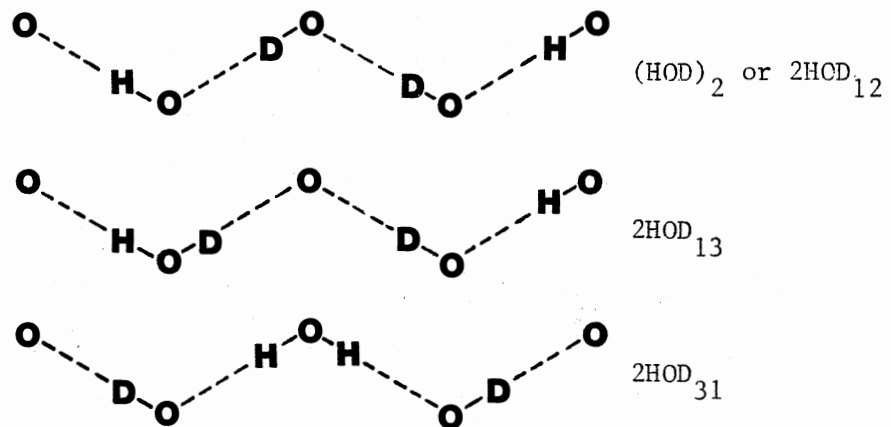
Figure 25c. Example $2HOD_{nm}$ Configurations

as shown in Figure 25c.

The next question presented is how does a D_2O unit in a crystal-
line ice lattice convert to two HODs which then migrate away from
each other. A D_2O unit can be represented by D_2O_{11} as shown in
Figure 26. If an ion defect encounters D_2O_{11} then a deuteron trans-
fer is possible leaving behind "coupled HOD" or $2HOD_{12}$. At this
point another ion pair defect could migrate through the $2HOD_{12}$ site
transferring or shifting the other deuteron to form $2HOD_{13}$ or "pseudo-
coupled HOD". Alternately a D or L Bjerrum defect could migrate
through the coupled HOD, or $2HOD_{12}$ site leaving behind a $2HOD_{21}$ or
"separated HOD". At this point "pseudo-coupled HOD", or $2HOD_{13}$, must
meet a D or L defect to proceed further to $2HOD_{22}$ or "fully separated
HOD". Likewise separated HOD or $2HOD_{21}$ cannot migrate further unless
an ion pair defect is encountered to leave $2HOD_{22}$ or fully separated
HOD behind. Thus the two divergent migration paths reunite back at
$2HOD_{22}$ where either a transfer or rotation can occur to the $2HOD_{31}$
"position 1 form" or $2HOD_{23}$ "position 3 form". These forms then
migrate to a "position 2 form" and the sequence can repeat continually.
But if deuterons can migrate apart from each other via a tunneling
transfer or thermally activated rotation they can also migrate together.
Figure 26 illustrates this aspect with double arrows and uses t or r
to indicate whether the step is a transfer or rotation. D_2O_{11} and
$2HOD_{12}$ are spectroscopically distinguishable. However according to
the experimental evidence to date, the other $2HOD_{nm}$ are perceived
spectroscopically as uncoupled HOD.

To relate this model to the measured D_2O, $(HOD)_2$, and HOD
absorbances some approximation must be incorporated to terminate the
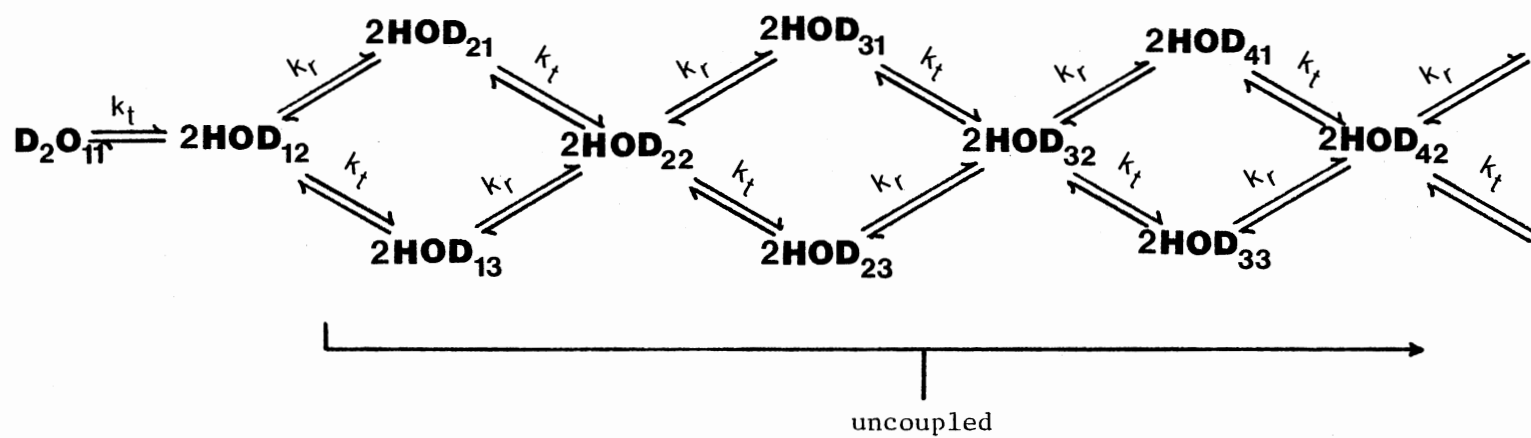
Figure 26. D_2O_{11} to $2HOD_{nm}$ Migration Mechanism

number of steps and make any least square fitting technique practical.

The first approximation suggested is that the exchange sequence ter-
minates at $2HOD_{21}$ and $2HOD_{13}$, the pseudo-coupled and separated forms
of HOD. In addition there is no back reaction of $2HOD_{21}$ or $2HOD_{13}$ to
$2HOD_{12}$. This would give

$$D_2O \underset{k_t{}'}{\overset{k_t}{\rightleftharpoons}} (HOD)_2 \xrightarrow{k_t{}'' + k_r} 2HOD_{uncoupled} \qquad (3.7)$$
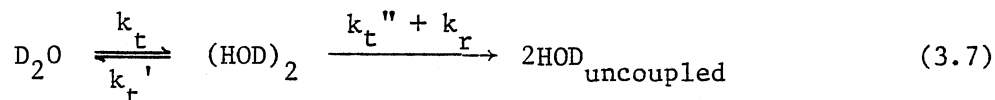
The lack of a back reaction from $2HOD_{uncoupled}$ to $(HOD)_2$ could be
justified by the probable small concentrations of $2HOD_{21}$ and $2HOD_{13}$
relative to $2HOD_{12}$ or $(HOD)_2$, due to the forward reactions of $2HOD_{21}$
and $2HOD_{13}$ that would tend to distribute the newly separated deuterons
further apart in the ice lattice. This single equilibrium approxi-
mation can be expanded to a double equilibrium model provided an
additional unknown parameter is introduced into the model, the $2HOD_{21}$
concentration. If the $2HOD_{12}$ to $2HOD_{13}$ to $2HOD_{22}$ forward and back
pathways are ignored on the basis of rate constant magnitudes, (to be
discussed later), then the following model approximation may be
written.

$$D_2O \underset{k_t{}'}{\overset{k_t}{\rightleftharpoons}} (HOD)_2 \underset{k_r{}'}{\overset{k_r}{\rightleftharpoons}} 2HOD_{separated} \xrightarrow{k_t{}''} 2HOD_{uncoupled} \qquad (3.8)$$
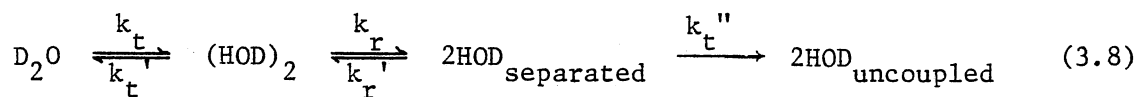
Here the back reaction of $2HOD_{uncoupled}$ or $2HOD_{22}$ to $2HOD_{separated}$
or $2HOD_{21}$ is ignored on the basis of the small concentration of $2HOD_{22}$
due to the $2HOD_{22}$ to $2HOD_{31}$ or $2HOD_{23}$ forward reactions and the position
of $2HOD_{22}$ configuration in the migration pathway. The latter is
suggested since the further two deuteriums migrate apart, the more
options there are for different migration paths leading to different
configurations. Hence the further two deuterons move apart the less

chance there is for the migration path to reverse to the original starting D_2O unit. The only remaining hurdle is to find the relationship between the various k_ts and k_rs before the models may be used.

Determining Rate Constant Relationships

In the gas or liquid phase, reaction rates are determined from collision frequencies, orientation factors, reaction cross sections, energy states populations, transition probabilities, and other factors. Mono and bi-molecular reactions can be expressed with first and second order kinetic rate equations. But reactions in the solid phase can be more complex and indeterminate. Orientations may be fixed, and two body collisions are almost nonexistent.

For a transfer or rotational movement of a deuteron to occur, a migrating ice defect must encounter a D_2O or HOD configuration. This suggests a second order process. But at a given temperature the concentration and rate of migration of the defects is constant. Furthermore, the defect is not consumed in the reaction so that its concentration still stays constant. Thus all the transfer rate constants (k_t) and rotational rate constants (k_r) expressed in Equation (3.7), (3.8), and Figure 26 are first order with respect to the D_2O or $2HOD_{nm}$ configuration concentrations. The transfer rates between configurations should be equal except for the effect that the different number of approaches and subsequent conversion possibilities arising from different configurations should produce on the transfer rates. A similar situation exists for the rotational rates. The next logical step is to determine what different defect approaches and reacting pathways are possible for different deuteron configurations.

Figure 27 and Table V show a brief representation and resulting mathematical formulation for the $D_2O_{11} \rightarrow 2HOD_{12}$ exchange reaction. Reaction I Figure 27 shows three sequential steps labeled the attack, transfer, and leaving factors. If the relative probability of occurrence for each step is determined for each reaction then a comparison between different k_ts may be made. For the attack step a hydronium ionic defect moves to the D_2O site. There are two different hydrogen bonds on which the attacking hydrogen can tunnel. Then the attack factor is written as $2\nu_H$ where ν_H is the tunneling frequency of the attacking proton (see Table V). On the transfer step either the proton can tunnel back to its original oxygen at a frequency of ν_H or one of the two deuterons may tunnel at a frequency of ν_D to another oxygen to yield $2HOD_{12}$ or coupled HOD. The total tunneling frequency would be $\nu_H + 2\nu_D$ and the tunneling frequency for the desired reaction would be $2\nu_D$. Then a probability of occurrence for the desired event could be defined as $2\nu_D/(\nu_H + 2\nu_D)$. To assure that the transfer step, which leaves a hydronium ion defect at the HOD_{12} site, does not back exchange to D_2O_{11} a leaving factor is included using the same logic as for the transfer step. Using these three factors a relative probability of reaction can be assigned to reaction I through VI by

$$P_{R_x} = (\text{attack factor } R_x)(\text{transfer factor } R_x)(\text{leaving factor } R_x) \quad (3.9)$$

The relationship between any given transfer reaction can be written as

$$k_t' = \frac{(\text{attack factor } k_t')(\text{transfer factor } k_t')(\text{leaving factor } k_t')}{(\text{attack factor } k_t)(\text{transfer factor } k_t)(\text{leaving factor } k_t)} k_t \quad (3.10)$$

Table V lists the transfer factors found for Figure 27 and 28 for the forward and back transfer exchange reactions between D_2O_{11}, $2HOD_{12}$,

I. $D_2O_{11} \longrightarrow 2HOD_{12}$

II. $2HOD_{12} \longrightarrow D_2O_{11}$

III. $2HOD_{12} \longrightarrow 2HOD_{13}$
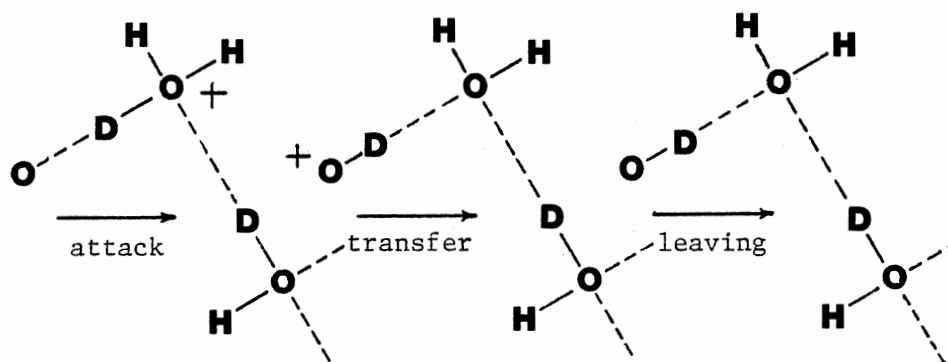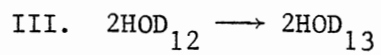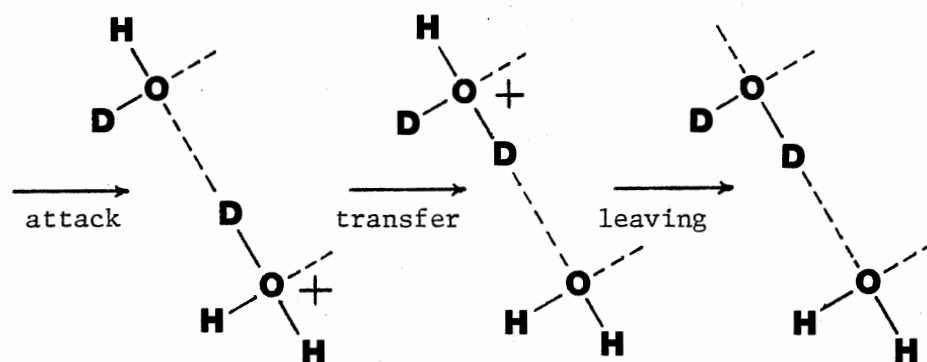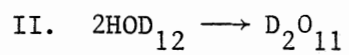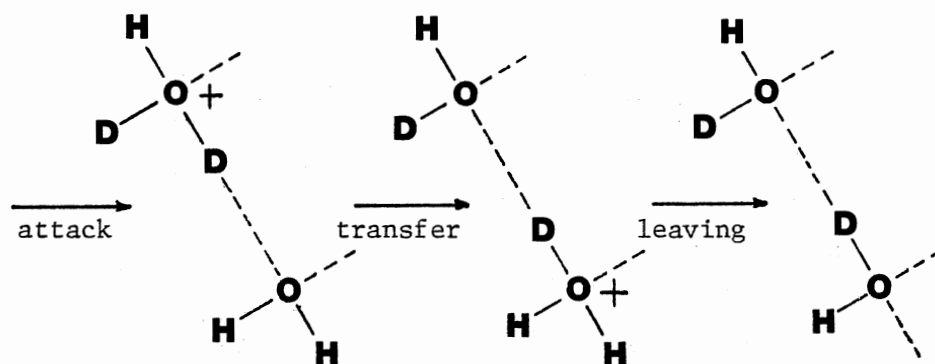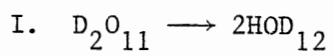
Figure 27.   Proton Transfer Steps for Deuterium Migration

TABLE V

RELATIVE PROBABILITY FACTORS FOR TRANSFER MIGRATION

Reaction	Attack Factor	Transfer Factor	Leaving Factor
$D_2O_{11} \rightarrow 2HOD_{12}$	$2\nu_H$	$\dfrac{2\nu_D}{\nu_H + \nu_H}$	$\dfrac{2\nu_H}{2\nu_H + \nu_D}$
$2HOD_{12} \rightarrow D_2O_{11}$	$2\nu_H$	$\dfrac{\nu_D}{2\nu_H + \nu_D}$	$\dfrac{2\nu_H}{\nu_H + 2\nu_D}$
$2HOD_{12} \rightarrow 2HOD_{13}$	$1\nu_H$	$\dfrac{\nu_D}{2\nu_H + \nu_D}$	$\dfrac{2\nu_H}{2\nu_H + \nu_D}$
$2HOD_{13} \rightarrow 2HOD_{12}$	$4\nu_H$	$\dfrac{\nu_D}{2\nu_H + \nu_D}$	$\dfrac{2\nu_H}{2\nu_H + \nu_D}$
$2HOD_{21} \rightarrow 2HOD_{22}$	$4\nu_H$	$\dfrac{\nu_D}{2\nu_H + \nu_D}$	$\dfrac{2\nu_H}{2\nu_H + \nu_D}$
$2HOD_{22} \rightarrow 2HOD_{21}$	$2\nu_H$	$\dfrac{\nu_D}{2\nu_H + \nu_D}$	$\dfrac{2\nu_H}{2\nu_H + \nu_D}$
$2HOD_{22} \rightarrow 2HOD_{23}$	$2\nu_H$	$\dfrac{\nu_D}{2\nu_H + \nu_D}$	$\dfrac{2\nu_H}{2\nu_H + \nu_D}$
$2HOD_{23} \rightarrow 2HOD_{22}$	$4\nu_H$	$\dfrac{\nu_D}{2\nu_H + \nu_D}$	$\dfrac{2\nu_H}{2\nu_H + \nu_D}$

For $n \geq 2$

Reaction	Attack Factor	Transfer Factor	Leaving Factor
$2HOD_{n1} \rightarrow 2HOD_{n2}$	$4\nu_H$	$\dfrac{\nu_D}{2\nu_H + \nu_D}$	$\dfrac{2\nu_H}{2\nu_H + \nu_D}$
$2HOD_{n2} \rightarrow 2HOD_{n1}$	$2\nu_H$	$\dfrac{\nu_D}{2\nu_H + \nu_D}$	$\dfrac{2\nu_H}{2\nu_H + \nu_D}$

TABLE V (Continued)

Reaction	Attack Factor	Transfer Factor	Leaving Factor
$2HOD_{n2} \rightarrow 2HOD_{n3}$	$2\nu_H$	$\dfrac{\nu_D}{2\nu_H + \nu_D}$	$\dfrac{2\nu_H}{2\nu_H + \nu_D}$
$2HOD_{n3} \rightarrow 2HOD_{n2}$	$4\nu_H$	$\dfrac{\nu_D}{2\nu_H + \nu_D}$	$\dfrac{2\nu_H}{2\nu_H + \nu_D}$

IV. $2HOD_{13} \longrightarrow 2HOD_{12}$

V. $2HOD_{21} \longrightarrow 2HOD_{22}$

VI. $2HOD_{22} \longrightarrow 2HOD_{21}$
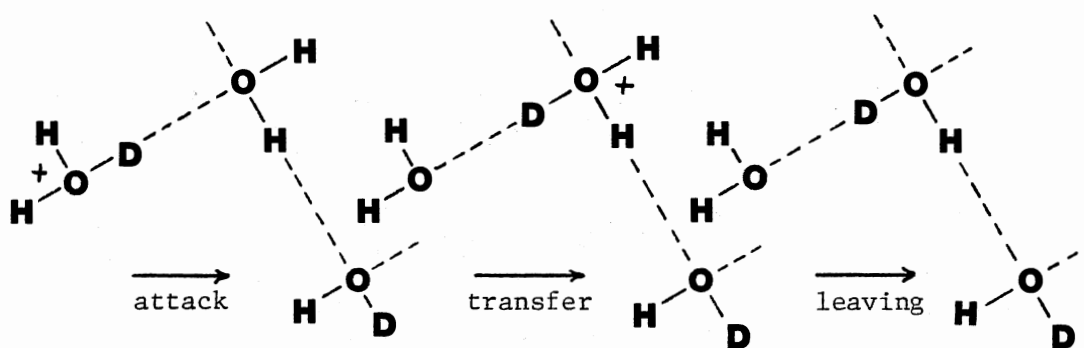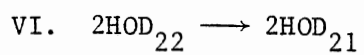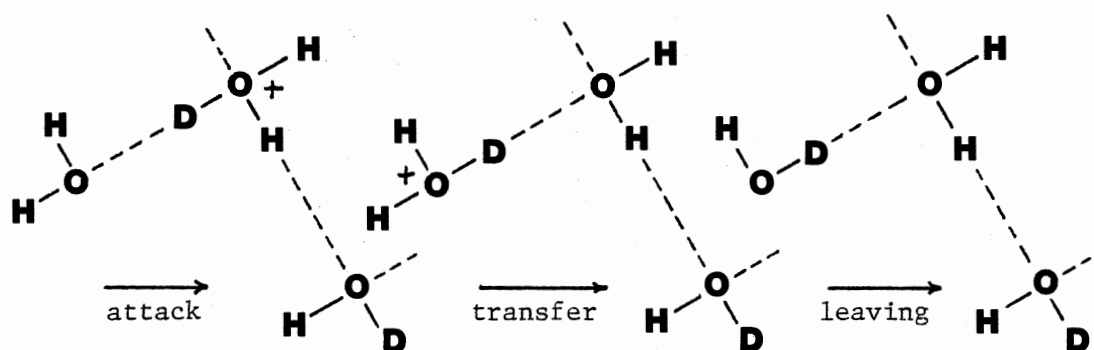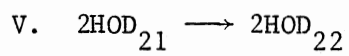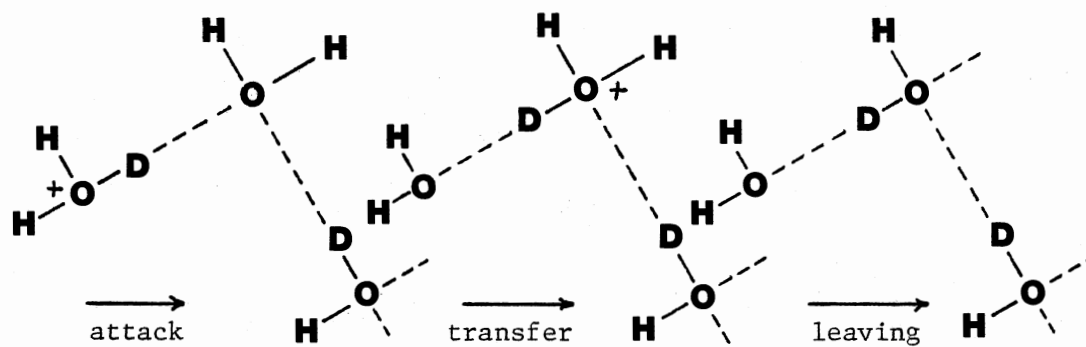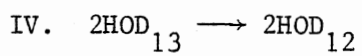
Figure 28.   Proton Transfer Steps for Deuterium Migration

$2HOD_{13}$, $2HOD_{21}$, and $2HOD_{22}$ the D_2O_1 coupled HOD, pseudo HOD, separated HOD, and fully separated HOD molecular units of cubic ice. It should be noted that the hydroxide ionic defect does not appear to play a significant part in the D_2O isotopic exchange reaction (46, 47).

Examining Table VI and Figures 29 and 30 reveals a similar formulation for the rotational step or a Bjerrum D or L defect migrating through a $2HOD_{nm}$ site. Reaction I the $2HOD_{12} \rightarrow 2HOD_{21}$ reaction in Figure 29 shows how an L defect can migrate through the $2HOD_{12}$ unit to change it to $2HOD_{21}$. The L defect may enter the $2HOD_{23}$ along 3 hydrogen bonded paths, shown by dotted lines. However, the top hydrogen bond pathway does not change the configuration. Thus there are only two attack paths. This gives an attack factor of 2 for the L defect (see Table VI). In the transfer step the L defect moves to the oxygen-oxygen linkage between the two HODs as a result of the deuteron rotating down to the lower O-O linkage. In the bottom O-O linkage, there are four different protons that can rotate into the L defect, as will always be the case of an L defect migrating through a perfect Bernard-Fowler ice crystal. If the bottom protons rotates in, the L defect will move backwards thus not initiating the transfer step. If the deuteron rotates in, the L defect moves up the hydroxyl chain to the middle position shown in the transfer step. However, if the proton on the bottom HOD unit rotated in, the L defect would simply shift to another attack position identical to the position shown in the attack step. Thus of four possible proton or deuteron rotations only three change the L defect with respect to the reaction pathway, and only one of these three, namely the deuteron rotation, initiates the transfer step. Therefore the relative probability for the transfer

TABLE VI

RELATIVE PROBABILITY FACTORS FOR ROTATIONAL MIGRATION

Reaction	Attach Factor	Transfer Factor	Leaving Factor	Total
		L Defect		
$2HOD_{12} \rightarrow 2HOD_{21}$	2	$\frac{1}{3}$	$\frac{1}{2}$	$\frac{1}{3}$
$2HOD_{21} \rightarrow 2HOD_{12}$	2	$\frac{1}{3}$	$\frac{1}{2}$	$\frac{1}{3}$
$2HOD_{13} \rightarrow 2HOD_{22}$	4	$\frac{1}{3}$	$\frac{3}{4}$	1
Sequence A				
$2HOD_{22} \rightarrow 2HOD_{13}$	2	$\frac{1}{3}$	$\frac{1}{4}$	$\frac{1}{6}$
Sequence B				
$2HOD_{22} \rightarrow 2HOD_{13}$	1	$\frac{1}{3}$	$\frac{1}{4}$	$\frac{1}{12}$
Total				
$2HOD_{22} \rightarrow 2HOD_{13}$	$\frac{1}{3}$ (Sequence A) $+ \frac{2}{3}$ (Sequence B) $= \frac{1}{9}$			
		D Defect		
$2HOD_{12} \rightarrow 2HOD_{21}$	1	$\frac{1}{3}$	$\frac{1}{2}$	$\frac{1}{6}$
$2HOD_{21} \rightarrow 2HOD_{12}$	1	$\frac{1}{3}$	$\frac{1}{2}$	$\frac{1}{6}$
$2HOD_{13} \rightarrow 2HOD_{22}$	2	$\frac{1}{2}$	$\frac{2}{3}$	$\frac{2}{3}$
$2HOD_{22} \rightarrow 2HOD_{13}$	1	$\frac{1}{3}$	$\frac{1}{3}$	$\frac{1}{9}$

I. $2HOD_{12} \longrightarrow 2\dot{H}OD_{21}$

II. $2HOD_{21} \longrightarrow 2HOD_{12}$

III. $2HOD_{13} \longrightarrow 2HOD_{22}$ sequence A
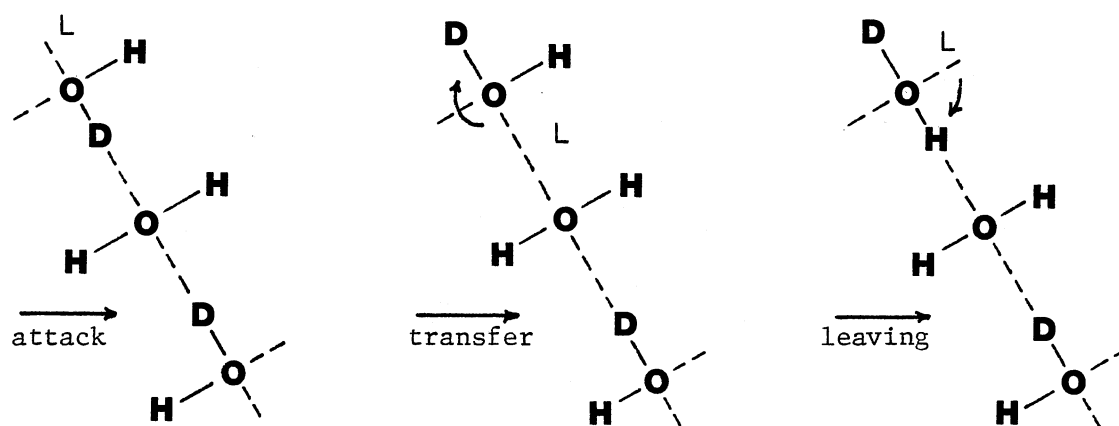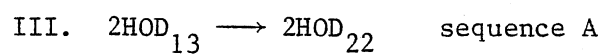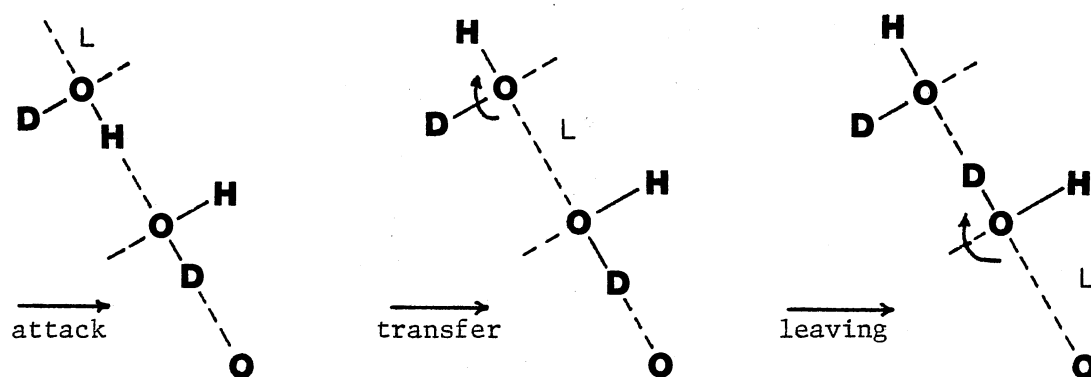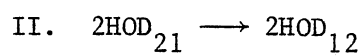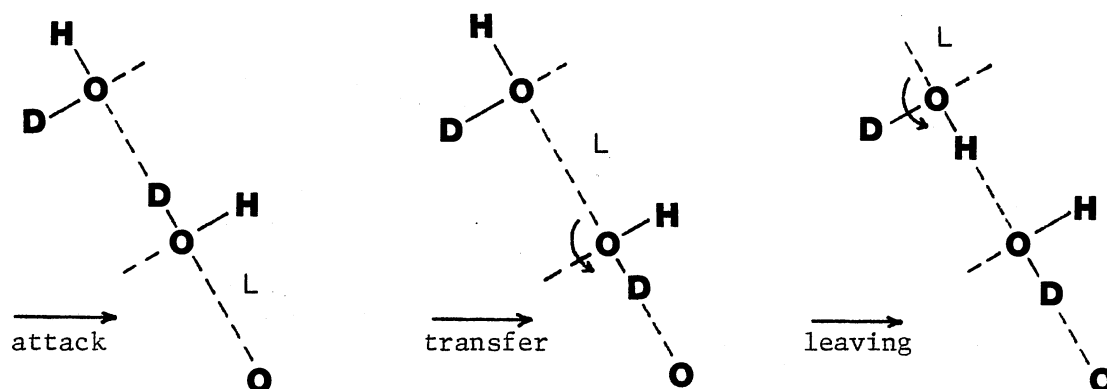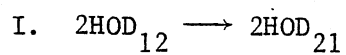
Figure 29. Proton Rotational Steps for Deuteron Migration

IV. 2HOD$_{13}$ $\longrightarrow$ 2HOD$_{22}$ sequence B

V. 2HOD$_{22}$ $\longrightarrow$ 2HOD$_{13}$ sequence A result
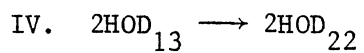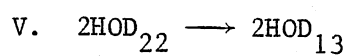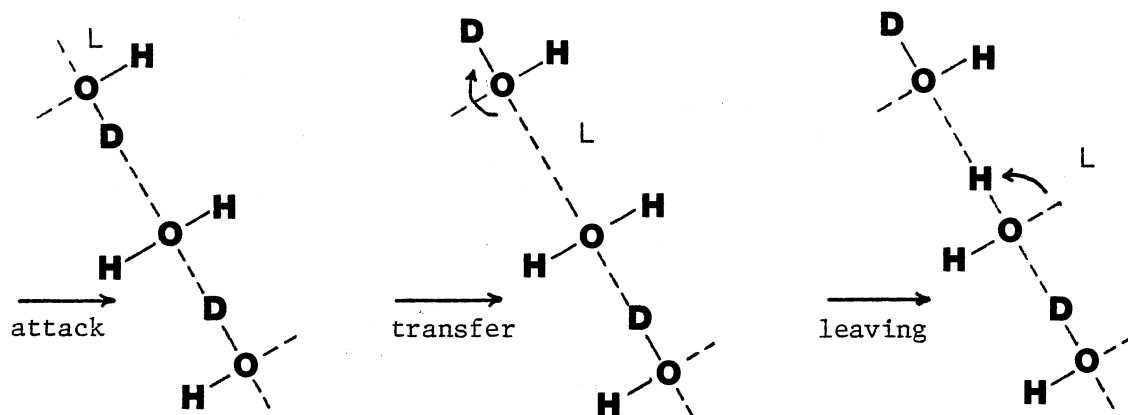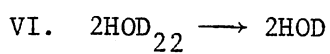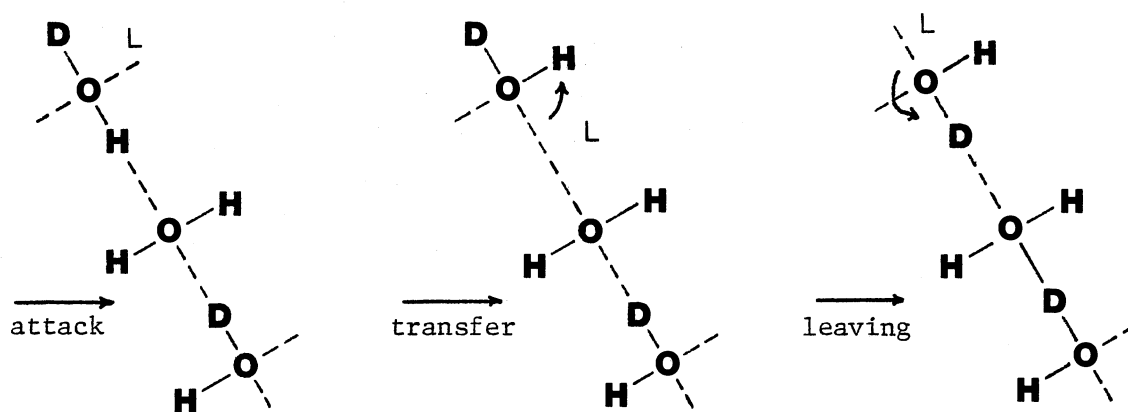
VI. 2HOD$_{22}$ $\longrightarrow$ 2HOD   sequence B result
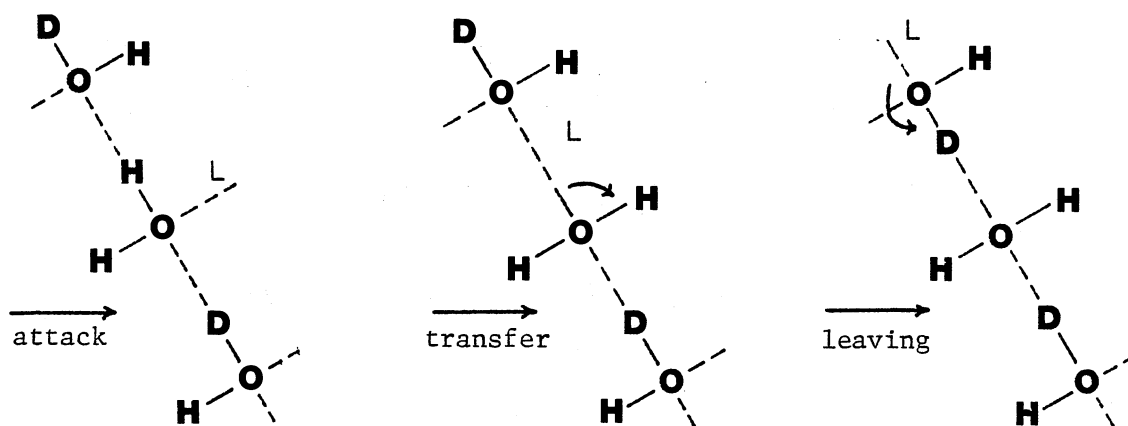
Figure 30. Proton Rotational Steps for Deuteron Migration

step is $\frac{1}{3}$. For the leaving step all four proton or deuterons will change the L defect with respect to the reaction pathway. Two of these (the protons rotating in) leave the $2HOD_{21}$ intact as the L defect moves on. But if either of the two deuterons rotates in then the L defect movement leaves a $2HOD_{12}$ configuration behind and a L defect position identical to the position shown in the attack step. Thus for the leaving step there is a $\frac{2}{4}$ or $\frac{1}{2}$ probability that the desired reaction or step occurs. The total relative probability is now found by multiplying these factors together to yield $\frac{1}{3}$ as shown in Table VI. The relative probability for the back reaction $2\ HOD_{21}$ $\rightarrow 2HOD_{12}$ is likewise determined.

The $2HOD_{13} \rightarrow 2HOD_{22}$ (pseudo to fully separated HOD) reaction is slightly more complex. As shown in reaction III Figure 29 and reaction IV Figure 30, there are two different sequences to convert $2HOD_{13}$ to $2HOD_{22}$, each leaving a different configured $2HOD_{22}$. Sequence A or reaction III leaves a $2HOD_{22}$ product with the end HOD group providing the rotated proton for the leaving step. Sequence B or reaction IV has the middle H_2O group providing the proton for the leaving step. Since the middle H_2O has two protons to rotate into the L defect but the end HOD group of sequence A has only one proton to rotate into the L defect on the transfer step then sequence B should occur twice as much as sequence A. For the forward $2HOD_{13} \rightarrow 2HOD_{22}$ reaction this should present no problem. But for the reverse $2HOD_{22} \rightarrow 2HOD_{13}$ reaction each sequence has different attack factors. So to account for this pathway splitting the sequence A total relative probability is weighted by $\frac{1}{3}$ to account for its share of the probability of $2HOD_{13} \rightarrow 2HOD_{22}$ occurring. Likewise sequence B is weighted by $\frac{2}{3}$.

The total reaction relative probability is given by the sum of the sequence relative probabilities.

Similar relative probability calculations for a D defect migration through a D_2O_{11} or $2HOD_{nm}$ site are also shown in Table VI. As with transfer rate constants the rotational rate constants can be related through

$$k_r' = \frac{(\text{total relative probability } k_r') \ k_r}{(\text{total relative probability } k_r)} \tag{3.11}$$

Using (3.10) and (3.11) the relationships between the various k_t's and k_r's (the transfer and rotational rate constants) of equation (3.7) and (3.8) are written in terms of one k_t and one k_r. Figure 26 may be rewritten in terms of the $D_2O_{11} \rightarrow 2HOD_{12}$ k_t and $2HOD_{12} \rightarrow 2HOD_{21}$ k_r as

$$\tag{3.12}$$
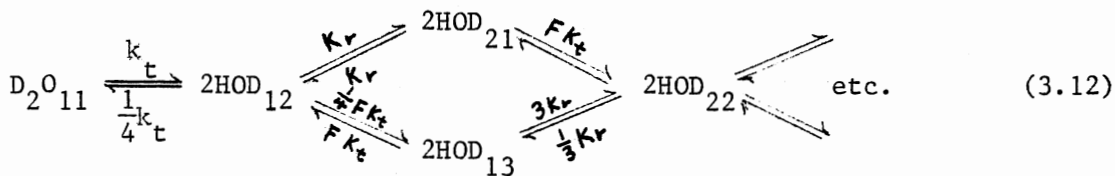
where $F = (\dfrac{\nu_H + 2\nu_D}{2\nu_H + \nu_D})$ and the k_r relationships are calculated using the L defect factors. If the D defect factors are used for k_r then Figure 26 may be written

$$\tag{3.13}$$
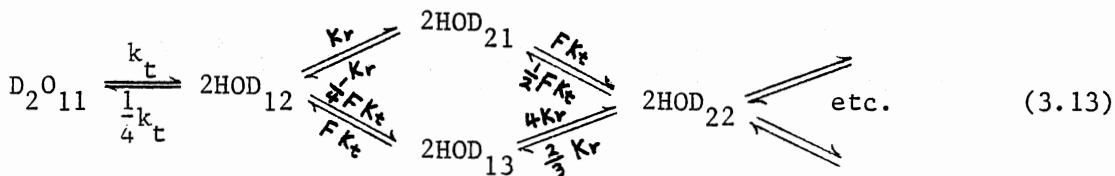
Equation (3.7) the single equilibrium model approximation may be written as

$$D_2O \underset{\frac{1}{4}k_t}{\overset{k_t}{\rightleftharpoons}} (HOD)_2 \xrightarrow{\frac{1}{4}Fk_t + k_r} 2HOD_{\text{uncoupled}} \tag{3.14}$$
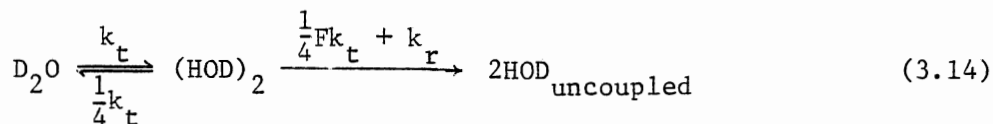
and the double equilibrium model given in Equation (3.7) using either D

or L rotational defects as

$$D_2O \underset{\frac{1}{4}k_t}{\overset{k_t}{\rightleftharpoons}} (HOD)_2 \underset{k_r}{\overset{k_r}{\rightleftharpoons}} 2HOD_{separated} \overset{Fk_t}{\longrightarrow} 2HOD_{fully\ separated} \qquad (3.15)$$
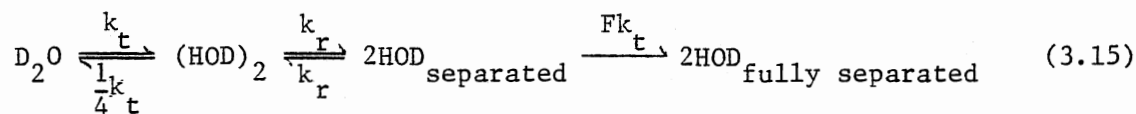
Since the rate constants depleting $2HOD_{13}$ in equations (3.12, 3.13) are significantly higher than the feeding rate constants, it is expected that the concentration of $2HOD_{13}$ in an exchange process would be small and steady state. Furthermore since the amount of $2HOD_{12}$ or coupled HOD being converted to $2HOD_{13}$ is small ($\frac{1}{4}k_t$) compared to the other decoupling rate constants, it is assumed that the deuterons primarily migrate apart through the $2HOD_{12}$, $2HOD_{21}$, $2HOD_{22}$ pathway, as suggested by the double equilibrium (3.15) model. The single equilibrium (3.14) model assumes that no back reaction of $2HOD_{21}$ or $2HOD_{13}$ to $2HOD_{12}$ occurs. Perusal of these rate constants shows that they are equal or greater in magnitude than the forward rate constants and hence the assumption may not be valid. The double equilibrium (3.15) has this same problem with the $2HOD_{21}$ to $2HOD_{22}$ forward and back rates. Here, however, the back reaction rate is significantly smaller than the forward (Fk_t forward to $\frac{1}{2}Fk_t$ back) and the concentration of $2HOD_{22}$ should be considerably smaller than $2HOD_{21}$. In summation the single equilibrium model (3.14) has three unknown parameters k_t, k_r, and F; and includes no provision for any back exchange into the coupled HOD or $2HOD_{12}$ configuration. The double equilibrium model (3.15) has four unknown parameters k_t, k_r, F, and an initial HOD separated or $2HOD_{21}$ concentration. It provides for a $2HOD_{21}$ back reaction to $2HOD_{12}$ or coupled HOD, but includes a spectroscopically unobservable species, $2HOD_{21}$. Fitting these two models to the experimental data should provide a measure of the importance of the $2HOD_{21}$ configuration in the

isotopic scrambling of D_2O in cubic ice.

Kunst and Warman (48) determined the virtual mobility of protons in ice at $-5^{\circ}C$ as 6.4×10^{-3} cm^{-2} V^{-1} sec^{-1} and deuterons in D_2O ice at $-5^{\circ}C$ as 2.4×10^{-3} cm^{-2} V^{-1} sec^{-1}. At $-30^{\circ}C$ they reported that the ratio remained the same though the magnitudes increased. Using these values F is calculated as .736842. This value was used throughout the calculations and any effects resulting from changing this value are noted.

Determining an initial $2HOD_{21}$ or separated HOD concentration was not straightforward. If an ice deposit of D_2O isolated in H_2O with no coupled or uncoupled HOD could be made, then the initial $2HOD_{21}$ concentration could be set equal to zero. However, all ice deposits made contained small amounts of coupled HOD initially and some uncoupled HOD in addition. So as a reasonable approximation the initial $2HOD_{21}$ concentration was taken as some function of the initial $(HOD)_2$ or $2HOD_{12}$ concentration. The idea being that whatever processes (limited pre-exchange or deposition contamination) created the initial $2HOD_{12}$ concentrations would also create the initial $2HOD_{21}$ concentration in the ice deposit. Fractional values of initial $2HOD_{12}$ between 0.0 and 1.0 were tried.

Thus with an initial guessed $2HOD_{21}$ concentration and the previously calculated F constant, both the single and double equilibrium models were used to fit the kinetic concentration data. These calculations served to determine the appropriate transfer (k_t) and rotational (k_r) rate constants, for isotopic exchange processes in cubic ice at temperatures ranging from 135-150 K.

Solution and Data Analysis of the Models

The differential rate equations for the single equilibrium (3.14) model are

$$\frac{d[D_2O]}{dt} = \frac{1}{4}k_t[(HOD)_2] - k_t[D_2O] \qquad (3.16)$$

$$\frac{d[(HOD)_2]}{dt} = k_t[D_2O] - \frac{1}{4}[(HOD)_2] - (\frac{1}{4}Fk_t + k_r)[(HOD)_2]$$

$$\frac{d[2HOD_{uncoupled}]}{dt} = (\frac{1}{4}Fk_t + k_r)[(HOD)_2]$$

Likewise for the two equilibrium model (3.15) the differential rate equations are

$$\frac{d[D_2O]}{dt} = \frac{1}{4}k_t[(HOD)_2] - k_t[D_2O] \qquad (3.17)$$

$$\frac{d[D_2O]}{dt} = k_t[D_2O] - \frac{1}{4}k_t[(HOD)_2] - k_r[(HOD)_2] + k_r[2HOD_{separated}]$$

$$\frac{d[2HOD_{separated}]}{dt} = k_r[(HOD)_2] - k_r[2HOD_{separated}] - Fk_t[2HOD_{separated}]$$

$$\frac{d[2HOD_{fully\ separated}]}{dt} = Fk_t[2HOD_{fully\ separated}]$$

and $[2HOD_{uncoupled}] = [2HOD_{separated}] + [2HOD_{fully\ separated}]$

Before any model fitting is accomplished these differential equations must be solved. For complex mechanisms two basic approaches are possible. One, find a way to solve the equations analytically, or, two numerically solve them using computer differential equation solvers. Matsen and Franklin (49) have published the general solution to the four component coupled set of first order reactions. The technique sets up the differential equations as a secular determinant similar to a standard eigenvalue problem. Solutions were then found

from the resulting eigenvalues and eigenvectors. Lewis and Johnson (50) recast the equations into a matrix formulation that is solved by matrix algebra. Unfortunately, these analytical solutions contain many of the problems often encountered in numerical solutions. Therefore, since the differential equations are not stiff; and fast, accurate, easy to use differential equation solvers are available, the numerical solution method was chosen to solve the equations.

A variable order Adams predictor-corrector differential equation solver written by the International Mathematical and Statistical Library group was used to solve all the differential equations of the model simultaneously. Among the features of this routine are variable step sizes, abilities to help handle mildly stiff differential equations, built in user determined relative error bounds, and internal error checking.

The subroutine is named DGEAR and was called from a main Fortran program whenever a solution to the model differential equations was required. DGEAR required that the user supply the differential equations in another subroutine named FCN. FCN required the initial time, D_2O, $(HOD)_2$, $HOD_{separated}$, $HOD_{fully \ separated}$ concentrations, final time at which the concentration solutions are desired, and various control parameters. DGEAR then outputs the various concentrations at the desired time of reaction along with an error flag indicating the reliability of the answers. Initial step-sizes of 0.00001 and relative error bounds of 0.0001 was found to give the best accuracy and speed. A description of DGEAR along with sample input and output is included in Appendix B. Due to copyright restrictions, a program listing is not included.

The next problem was to elucidate some method of varying the rate constants until the calculated concentration output is as identical to the experimental concentrations as possible. The method of nonlinear least squares was chosen. Though the methods of nonlinear least squares are legion they all attempt to minimize the square of the error residuals to find the best value of the minimizing parameters. The Marquardt strategy (5]) of nonlinear least squares is one of the most successful and efficient nonlinear routines used. Accordingly, it was used as a subroutine to find the best transfer and rotational rate constants for each dataset at each temperature. NLLSQ1 is a modified Fortran nonlinear least squares program based on the Marquardt strategy. It is composed of a main calling program which reads the data to be fitted, an initial parameter guess, and various control cards. After placing the needed information into array form, NLLSQ1 calls the Marquardt strategy subroutine NLLSQ. The NLLSQ subroutine also required that two additional subroutines DCALC and YCALC be written by the user. YCALC contains the function to be fitted such that at a given call with a chosen set of independent function variables the resulting dependent variables may be calculated and returned to NLLSQ. DCALC may optionally contain the function derivatives or be used as a dummy routine while the subroutine NLLSQ numerically calculated the derivatives. The latter option was used in this work. Once the data is least square fitted, the final optimized parameters (transfer and rotational rate constants), calculated dependent variables ($[D_2O]$, $[(HOD)_2]$, $[2HOD_{uncoupled}]$), and root mean square deviation of fit is printed.

Least squares analysis strives to fit an equation $Y = f(X_1, X_2, X_3, \ldots)$

to an observed set of Y, X_1, X_2, X_3... data. Y is called the dependent variable, and X_i the independent variable. For the single and double equilibrium models the dependent variables are the concentrations of D_2O, $(HOD)_2$, and uncoupled HOD. The uncoupled HOD is calculated from the sum of separated HOD and fully separated HOD for the double equilibrium models, and fully separated HOD for the single equilibrium model. The time of reaction t is the independent variable and k_t and k_r the minimizing parameters. The initial concentrations of D_2O, $(HOD)_2$, separated HOD, and fully separated HOD were function constants that changed with each dataset analyzed. But since NLLSQ operates on functions with one dependent variable, only one species concentration could be fitted per run, unless the three dependent concentrations are transformed into a single dependent variable. Thus to obtain a consistent fit of the models to all observed concentrations the three concentrations were transformed into a single dependent variable. This was accomplished by including the $(HOD)_2$ and uncoupled HOD values after the D_2O concentration values in the dependent variable array. Thus the first third of the array contained D_2O concentration values, the second third the $(HOD)_2$ values, and the last third the uncoupled HOD concentrations values. For the independent or time variable array the reaction time in minutes was repeated three times in the array therefore maintaining a one to one correspondence between the ith observations of the time and concentration arrays.

When NLLSQ called the subroutine YCALC, an index of observation requested, present calculated values of k_t and k_r, and concentration and time value arrays were inputted as arguments. YCALC would initialize the needed information required by DGEAR for solving the

differential kinetic rate equations. Using the time value found at the inputted index of observation DGEAR would solve the rate equations for the concentrations of D_2O, $(HOD)_2$, and uncoupled HOD for that observation time. YCALC then determined which third of the concentration and time arrays the observation index referred to and returned either the D_2O, $(HOD)_2$, or uncoupled HOD calculated concentration value to the NLLSQ calling subroutine. By calling YCALC for every observation a calculated array of concentrations values was determined for subsequent refinement of the transfer and rotational rate constants.

NLLSQ solved for k_t and k_r by iterative improvements of the initial guessed k_t and k_r rate constants. When the iteration failed to yield any significant improvement of k_t and k_r and specific internal convergence criteria were met, the iteration was stopped and the final computed concentration and time arrays along with the final k_t and k_r values were printed. By examining the root mean square deviation of fit and comparing the calculated versus observed values a judgement was made on the success of the least square fit for the model being tested. Most of the datasets were fit within 6-8 iterative cycles with good convergence criteria using the double equilibrium model. The single equilibrium model was less successful. To avoid the possibility of having converged on a local minima different initial k_t and k_r values were tried to see if the final results differed. A copy of NLLSQ with YCALC programmed for the double equilibrium model is included in Appendix C. Also included is sample input, output, and a written description of the NLLSQ nonlinear least square subroutine.

To determine the activation energies associated with the transfer
and rotational rate constants the Arrhenius expression for kinetic
rate constant temperature dependence was used.

$$\ln K = \frac{E_a}{RT} + \ln A \qquad (3.18)$$

Here, A, the pre-exponential factor, was assumed to be constant.
SAS, the Statistical Analysis System, marketed by the SAS Institute
is a system of computer software designed to perform complex or
simple statistical analysis of user data. It features a programming
language capability, several statistical procedures to perform linear
least square analysis, correlation calculations, and line printer or
plotter graphing capabilities.

An SAS program ACTIV was written to accomplish the least square
analysis of the rate constants versus temperature using equation
(3.18). Each least square analysis included the NLLSQ calculated
rate constants for all 12 kinetic datasets. A correlation analysis
was carried out on the calculated and observed values obtained from
the Arrhenius plots. The procedure was then repeated over all 12
kinetic datasets every time the model or a model functional constant
was changed. An examination of the Arrhenius plots and calculated
correlation values permitted an evaluation on which models gave the
best, most consistent activation energies, and what range of error
is expected in the activation energy values. A listing of ACTIV is
included in Appendix D.

CHAPTER IV

RESULTS AND CONCLUSIONS

Spectral and Concentration Data

One of the by-products of resolving the OD stretch multiplet at
2000-2800 cm^{-1} was an uncluttered look at the coupled HOD in and
out-of-phase modes. Figure 31 illustrates one of the better
(HOD)$_2$ spectrum collected. This particular spectrum was obtained
at 145 K at 17 min into the exchange reaction. The in-phase compo-
nent is located at 2404 cm^{-1} and the out-of-phase component at 2446
cm^{-1}, thus yielding a 42 cm^{-1} split. The peak absorbance ratio of the
two peaks is .70 but the intensity or band areas are almost equal.
This is due to the in-phase bandwidth measuring 32 cm^{-1} while the out-
of-phase component is 35 cm^{-1}.

This is in excellent agreement with Haas and Hornig's (22) coupled
HOD split of 49 cm^{-1} with frequencies of 2442 cm^{-1} and 2393 cm^{-1}.
However, Haas and Hornig's spectra were obtained at 190 K. Thus
allowing for temperature shifts, the agreement is excellent indeed.
The peak height ratios of the present work are comparable to those of
Haas and Hornig but their predicted 2 to 1 intensity ratio does not
agree with the present work. This is probably due to their inability
to resolve the HOD couplet and obtain a more quantitative measurement
of band areas.

One interesting feature of the (HOD)$_2$ doublet is the 35 and 32

106
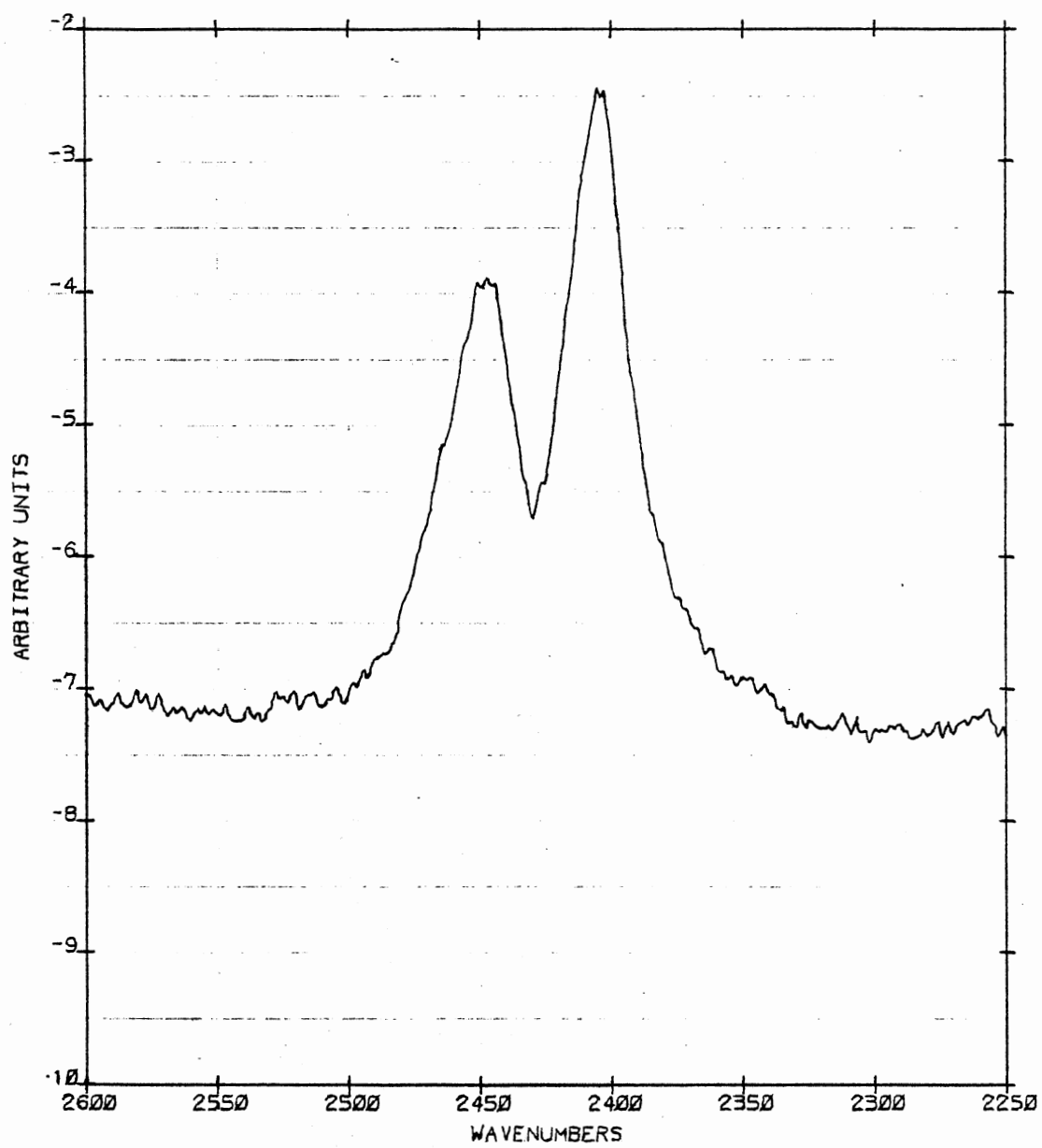
Figure 31.   Coupled HOD Absorbance Spectrum of 145 K

cm^{-1} bandwidths which are about 50% wider than the D_2O and uncoupled HOD bandwidths. Both the D_2O and uncoupled HOD oscillators have exactly one possible configuration if the surrounding H_2O network is ignored. However the $(HOD)_2$ oscillator has two possible configurations for the hydrogens valence bonded to the two coupled OD oscillators as shown in Figure 32a. This may explain the extra band breadth observed.

Occasionally in some $(HOD)_2$ spectra an extra wing or band was observed around 2460 cm^{-1}. The intensity would vary from a slight shoulder to an intense peak as shown in Figure 32b. Usually the shoulder would appear in initially collected spectra and quickly disappear as the exchange reaction occurred. A clue to the origin of this shoulder band was discovered when a few ice deposits made at 125 K instead of 130 K were more seriously affected by this band. A check of the lower 135 and 140 K runs revealed that when the band occurred at these temperatures it dissipated less rapidly than at the higher temperature kinetic runs. The ν_3 band of D_2O is the most intense feature of the initial ice deposit. If the deposit was slightly amorphous the ν_3 band would be slightly amorphous in character, and hence have a slightly greater bandwidth. But since the D_2O band being subtracted out was fully crystalline, in resolving the $(HOD)_2$ spectrum any residual amorphous character of ν_3 would not be subtracted and show up as a wing or band near the ν_3 frequency. As the deposit started to exchange at a higher temperature the ice deposit would quickly anneal and likewise any amorphous character of ν_3 would disappear. Therefore this wing was regarded as an amorphous residue and discounted as a spectrally significant feature when it occasionally
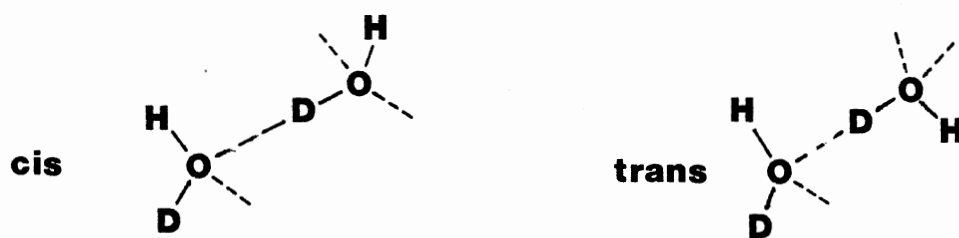
Figure 32a. Possible Coupled Configurations in Cubic Ice Lattice
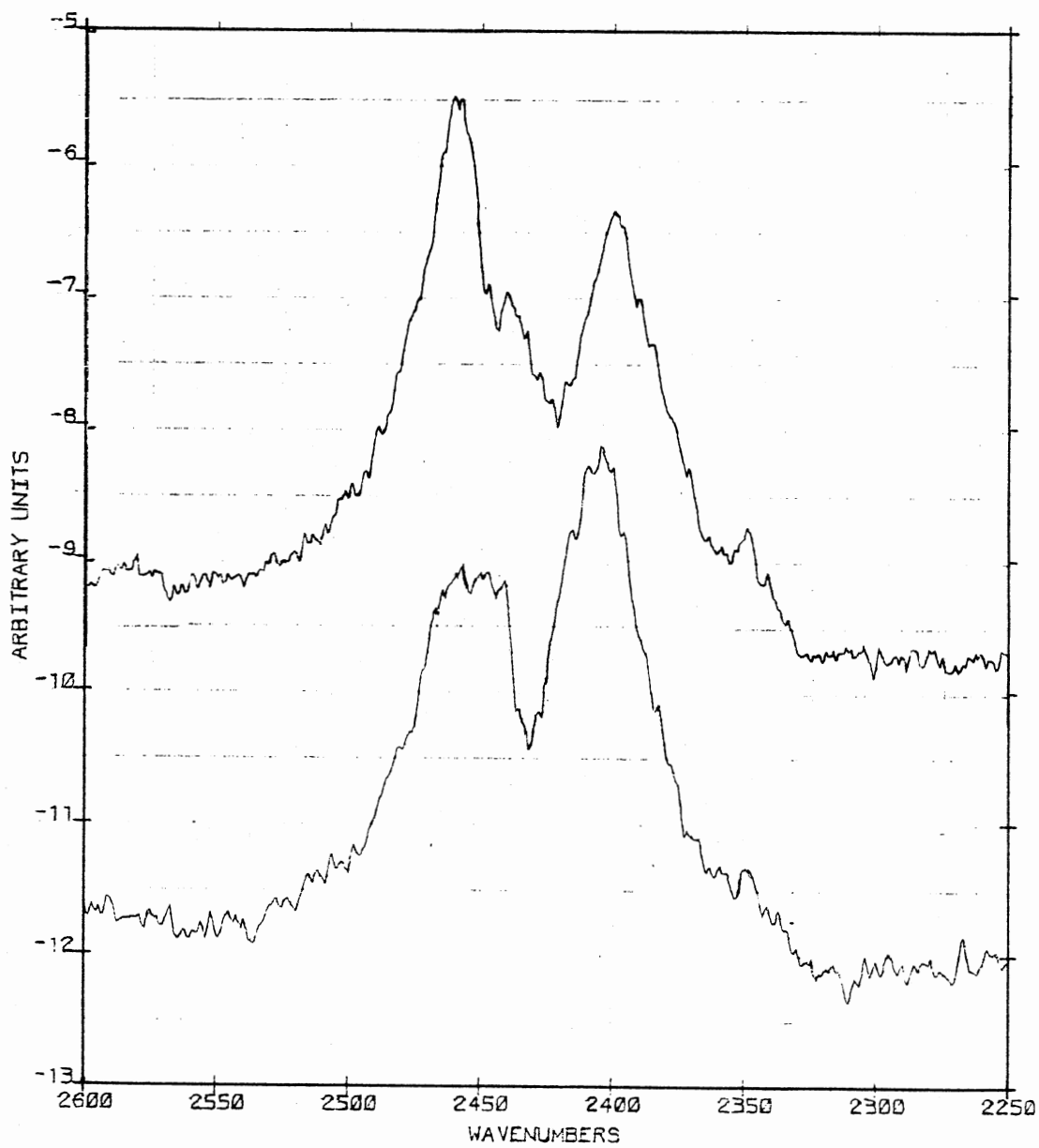
Figure 32b. Amorphous Induced Bands in Coupled HOD Bandshapes

appeared.

In Table IV the higher temperature (150 K, 145 K) deposits exchanged more completely. Likewise, the error for fitting the kinetic dataset was greatest for 150 K and 145 K and least for the 135 K temperature datasets. In the 150 K datasets and most of the 145 K datasets the reaction was followed through at least three half-lives of the D_2O concentrations. Thus they should provide a fairly rigorous test of the models proposed. The interesting facet of all the datasets is the extensive retardation of the reaction rates after about one to two D_2O half-lives. The reaction appears to follow an initial first order decay in D_2O concentration until the concentration level of all species is sufficiently low so that the feedback mechanisms present in the isotopic exchange mechanism becomes important. At that time large concentration changes appear to be stymied by the various back reactions.

Nonlinear Least Square Strategy

When fitting the one-equilibrium model to the kinetic data, the error became large near the completion of the data. Thus to improve the accuracy of the fit the latter data points of the 150, 145, and 140 K datasets were deleted. At least 1.5 D_2O concentration half-lives worth of data were retained in each dataset. Though a more acceptable fit was obtained, the accuracy of the fit is questionable. Table VII lists the rate constants obtained from this fit and Figure 33 displays the calculated and experimental relative concentration values for the 150 K 6/7/82 dataset.

As observed in Figure 33 there is difficulty in fitting the

TABLE VII

LEAST SQUARE CALCULATED RATE CONSTANTS FOR ONE AND TWO EQUILIBRIUM MODELS

Model F^a Initial HOD_{21}^b data Dataset	One equil. .73684 – shortened		Two equil. .73684 0.0 full		Two equil. .73684 0.25 full		Two equil. .73684 0.5 full	
	K_{trans}	K_{rot}	K_{trans}	K_{rot}	K_{trans}	K_{rot}	K_{trans}	K_{rot}
150 K								
2/2/82	.21300	.21830	.17495	.28568	.17496	.36879	.17430	.52666
$RMSD^c$	1.354		.5590		.5321		.5028	
6/7/82	.13660	.19843	.11100	.29613	.11115	.42103	.11099	.74646
RMSD	1.219		.5713		.5566		.5402	
6/9/82	.079542	.20734	.068384	.31804	.068654	.50200	.068748	1.4265
RMSD	.7247		.5357		.5345		.5310	
145 K								
1/29/82	.079151	.077733	.059852	.089019	.059440	.10920	.058936	.14205
RMSD	1.173		.3984		.38037		.3633	
5/10/82	.042268	.061057	.033598	.075077	.034035	.11292	.034340	.23085
RMSD	.7774		.4493		.4424		.4307	
5/24/82	.082043	.069061	.061907	.074030	.061634	.096254	.061115	.13880
RMSD	.7908		.2278		.2082		.1877	
6/3/83	.042662	.068473	.032988	.088568	.033011	.11470	.032995	.16417
RMSD	.6586		.4111		.4029		.3940	
140 K								
5/11/82	.018463	.023522	.014124	.023192	.014096	.028898	.014048	.038439
RMSD	.6210		.3752		.3678		.3605	
5/25/82	.011992	.017621	.0092350	.019506	.0092242	.025360	.0092230	.036234
RMSD	.6657		.2383		.23270		.2279	

TABLE VII (Continued)

Model F^a Initial HOD_{21}[b] data Dataset	One equil. ,73684 – shortened K_{trans}	K_{rot}	Two equil. .73684 0.0 full K_{trans}	K_{rot}	Two equil. .73684 0.25 full K_{trans}	K_{rot}	Two equil. .73684 0.5 full K_{trans}	K_{rot}
135 K								
5/15/82	.0042115	.0040228	.0037078	.0033044	.0037055	.0040094	.0037008	.0050681
RMSD	.3258		.1997		.1961		.1926	
5/26/82	.0037345	.0043476	.0031359	.0037833	.0031316	.0046006	.0031249	.0058465
RMSD	.3059		.1491		.1489		.1484	
6/11/82	.0038900	.0047298	.0033464	.0039339	.0033437	.0046827	.0033392	.0057573
RMSD	.4305		.2068		.2022		.1979	

[a] Frequency factor; $F = (\dfrac{\nu_H + 2\nu_D}{\nu_D + 2\nu_H})$.

[b] Initial HOD_{21} determined by $[HOD_{21}]_{initial}$ = (table value shown)$\cdot[HOD_{12}]_{Initial}$.

[c] Root mean square deviation of nonlinear least square fit.
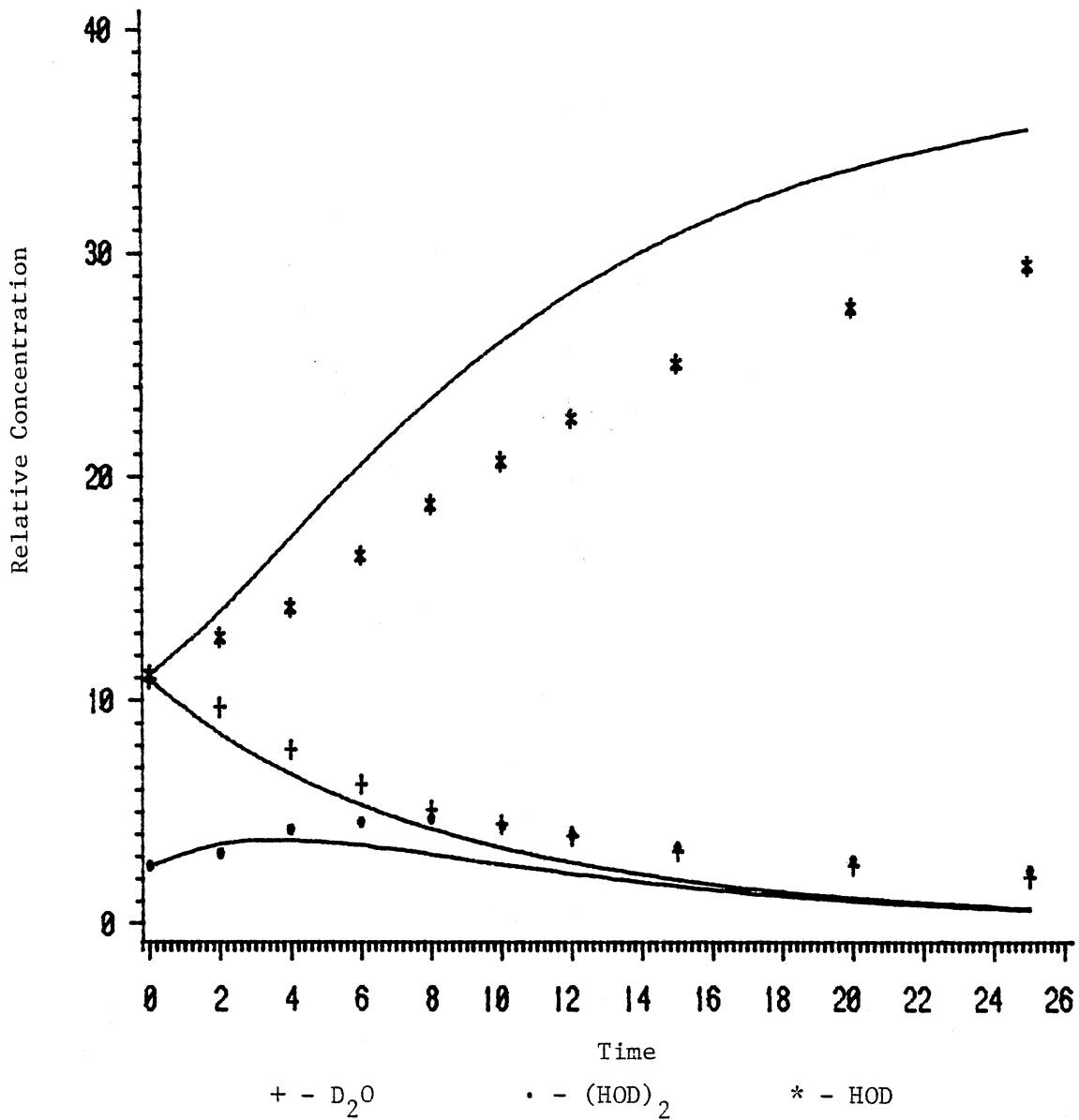
Figure 33. Experimental and One Equilibrium Model Calculated Relative
Concentration Curves for 6/7/82 150 K Data

(HOD_2) concentration at the longer time intervals. The lack of
back exchange to $(HOD)_2$ favors a more rapid depletion of $(HOD)_2$,
thus more quickly eliminating any feedback from $(HOD)_2$ to D_2O.
As a result both the $(HOD)_2$ and D_2O concentrations fall off too
rapidly.

For the two-equilibrium model both the above described shortened
datasets and the full datasets were fitted. The full datasets yielded
the most consistent results and hence were used for the remainder of
the calculations. Several fits were made, each with different initial
separated HOD concentrations. Table VII lists the transfer and rota-
tional rate constants found for the three best runs. They are initial
separated HOD values of 0.0, 0.25 x $(HOD)_2$ initial, and 0.5 x $(HOD)_2$
initial. The root mean square deviation of the fit for each dataset
is included beneath each rate constant entry. The 150 K and 145 K
determined transfer rate constants show the greatest error spread,
while the rotational rate constants seem to be more consistent. This
is not entirely unexpected. The concentration of hydronium ions in
water at $25^{o}C$ is about 1.0 x 10^{-7} moles/liter. So the concentration
of ionic defects in ice at 145 K should be even less. This concen-
tration of defects is less than two parts per billion. It is very
difficult to obtain water of this purity. Accordingly the transfer
rate constant variance at fixed temperatures is attributed to the
ionic defect's sensitivity to small changes in the concentration of
impurities in the ice such as arises from normal operation of a
vacuum system. So the transfer rate constants listed are assumed
to arise from a pure ice deposition situation perturbed by minute
contaminations. The fact that the transfer rate constants are so

sensitive to small contamination changes provides evidence that the ice deposition is pure enough that contamination concentrations are of the same order as the hydronium ion defect concentration. If the contamination was greater, the trapping would be large enough to significantly lower the transfer rates and suppress $(HOD)_2$ formation as illustrated by Devlin et al. (46, 47).

Not surprisingly the rotational rates appear to be more consistent. This may reflect their insensitivity to impurity doping as suggested by Devlin et al. (47).

The transfer rate constants are largely insensitive to the initial separated HOD concentration and corresponding differing rotational rate constants. The rotational rates are affected by the initial separated HOD concentrations as Table VII illustrates. The .5 x $(HOD)_2$ initial concentration data has the smallest RMSD of fit but yet this is misleading. The least square analysis showed the .5 calculation to be the least correlated with respect to activation energy plots. In addition for some rate constants the standard error associated with the rotational rate constant was 50% greater than for the 0.0, and .25 calculations.

Figures 34-45 show calculated and experimental concentration versus time curves for each dataset. All three two-equilibrium calculations gave practically identical calculated concentration values so the .25 initial HOD_{21}, F = .7368 rate constant calculated concentration values were used. For each graph the symbols represent the experimental data and the lines the corresponding calculated values. Representative extimated error bars are shown for Figure 34 but are omitted from the rest for clarity.
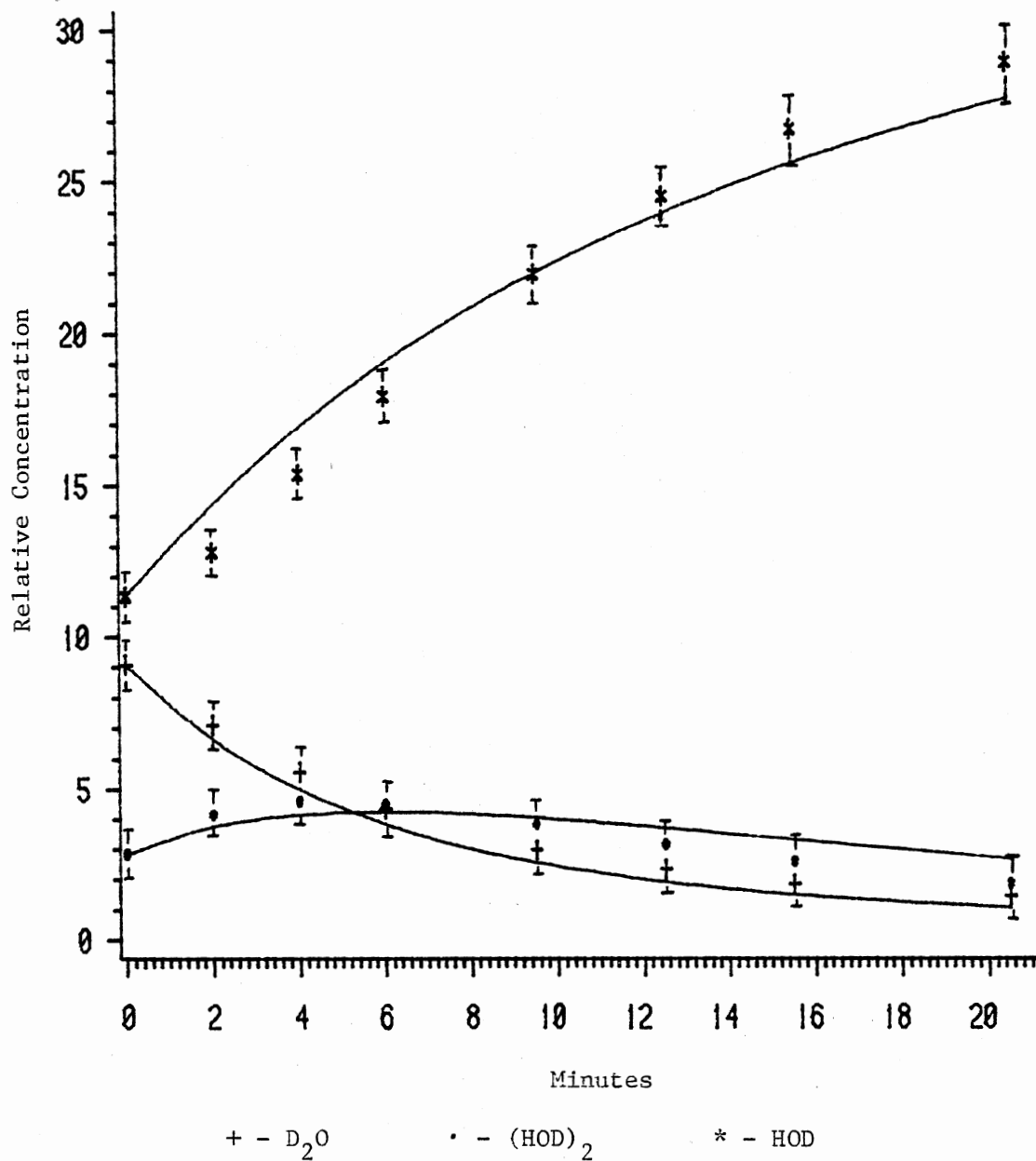
Figure 34. Experimental and Two Equilibrium Model Calculated Relative Concentration Curves for 2/2/82 150 K Data
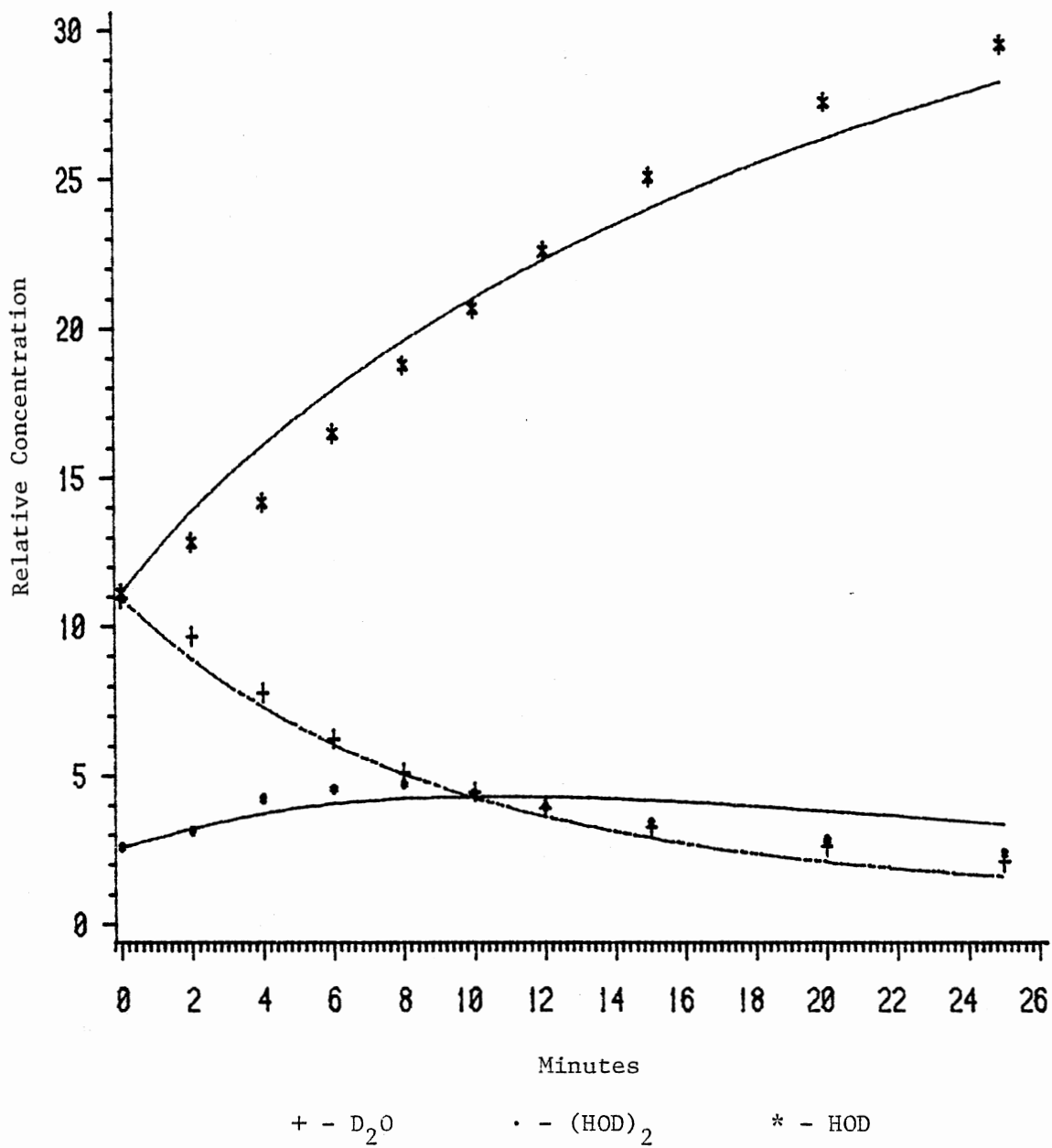
Figure 35. Experimental and Two Equilibrium Model Calculated Relative Concentration Curves for 6/7/82 150 K Data
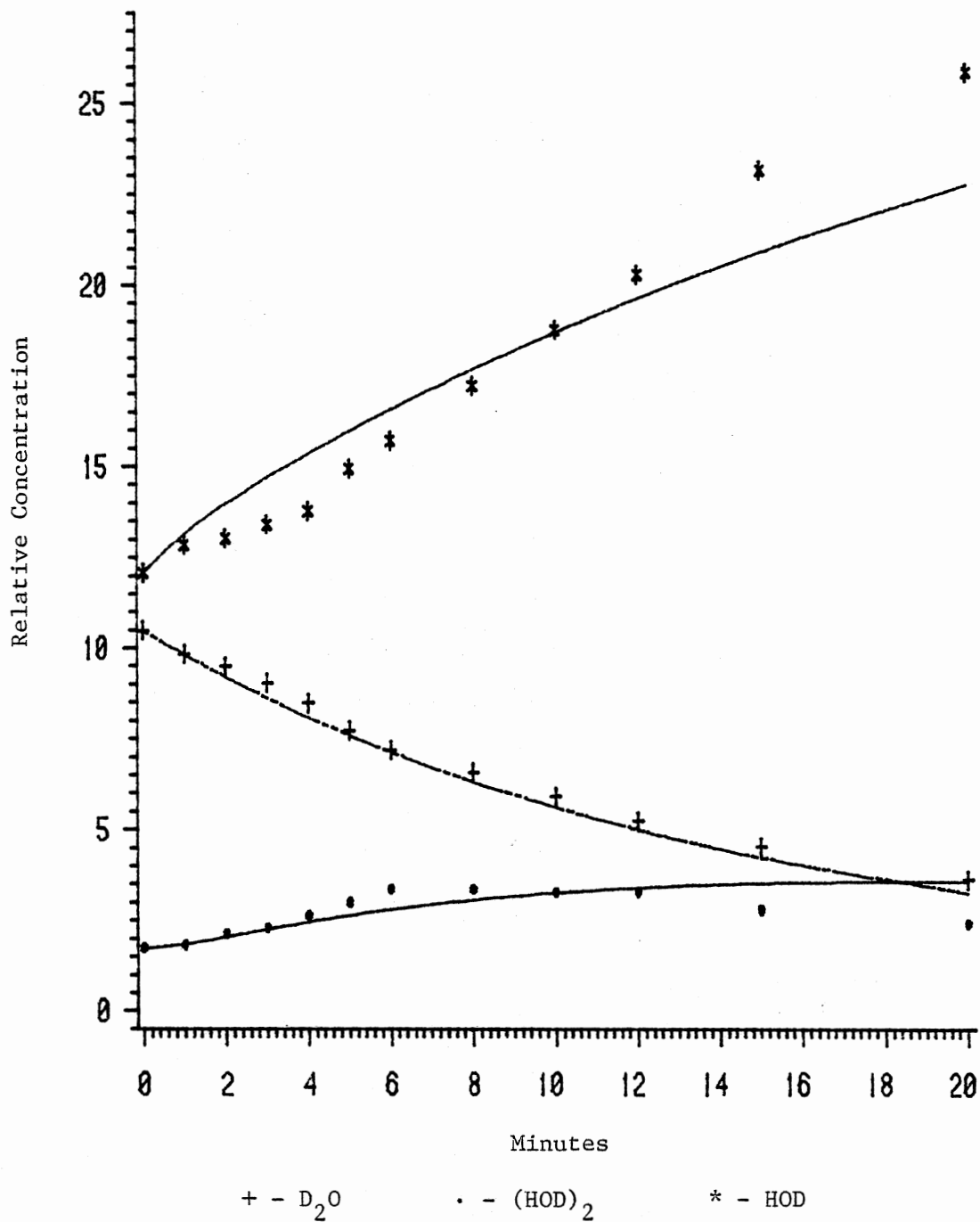
Figure 36. Experimental and Two Equilibrium Model Calculated Relative Concentration Curves for 6/9/82 150 K Data
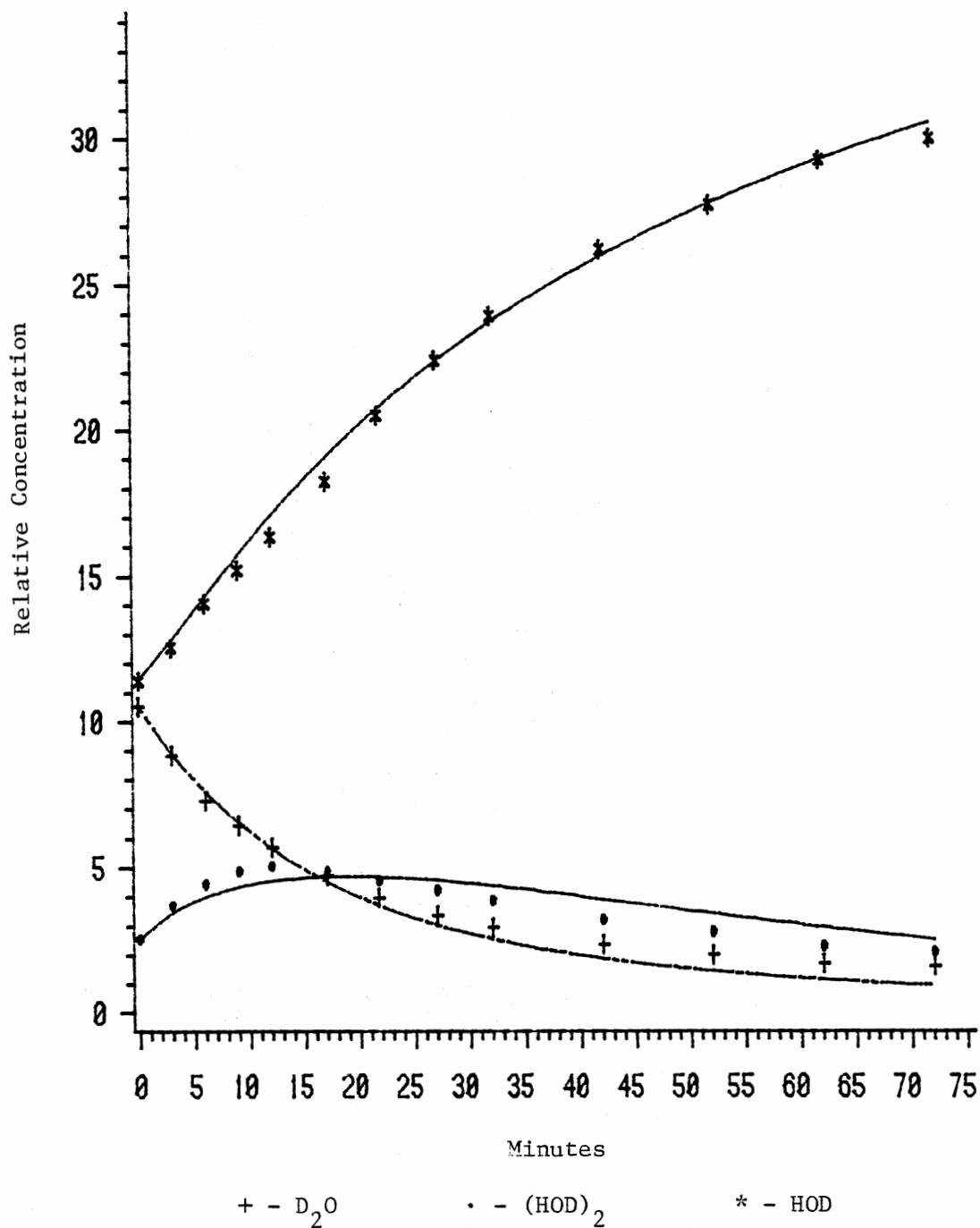
Figure 37. Experimental and Two Equilibrium Model Calculated Relative
Concentration Curves for 1/29/82 145 K Data
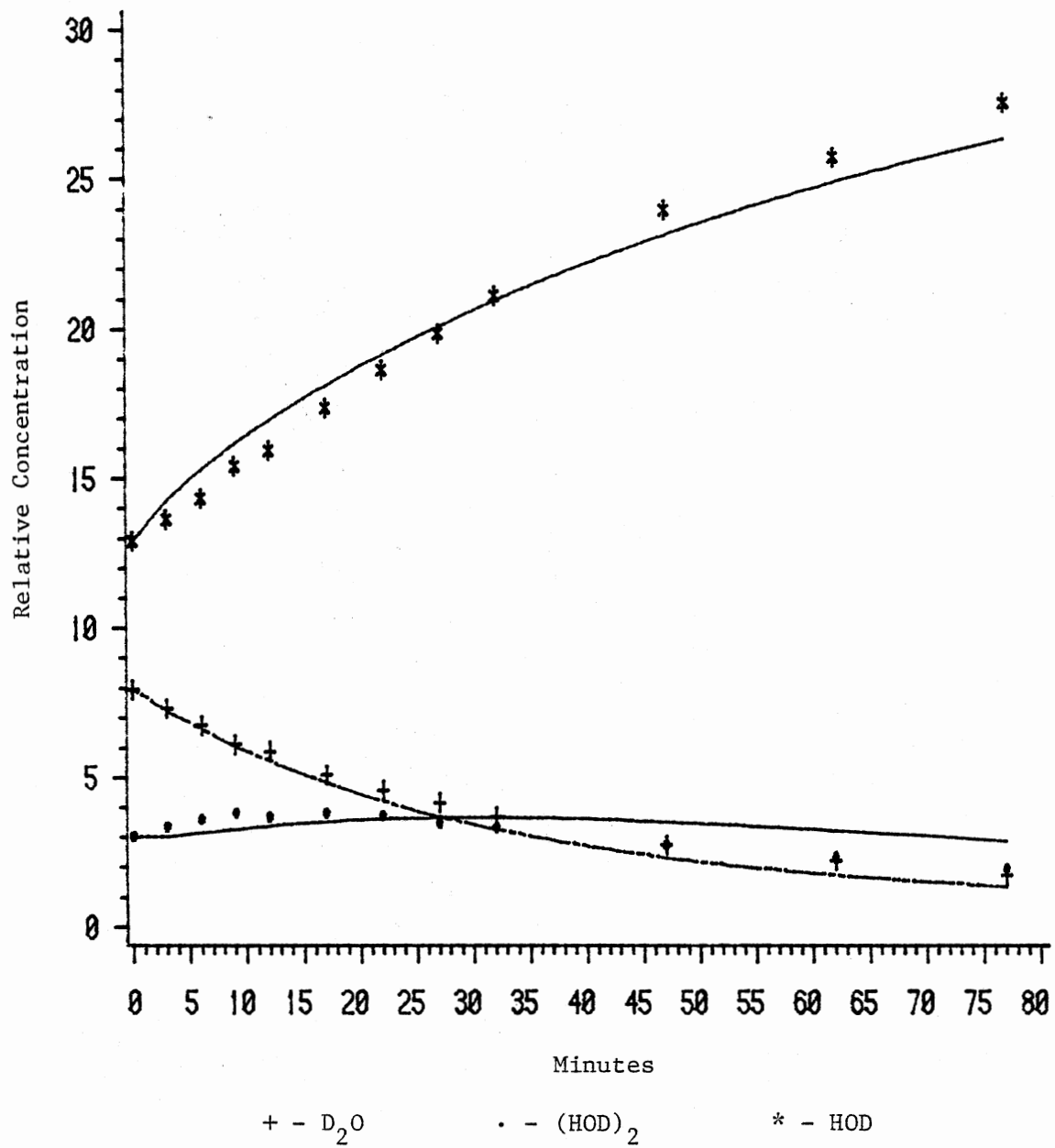
Figure 38.   Experimental and Two Equilibrium Model Calculated Relative
Concentration Curves for 5/10/82 145 K Data
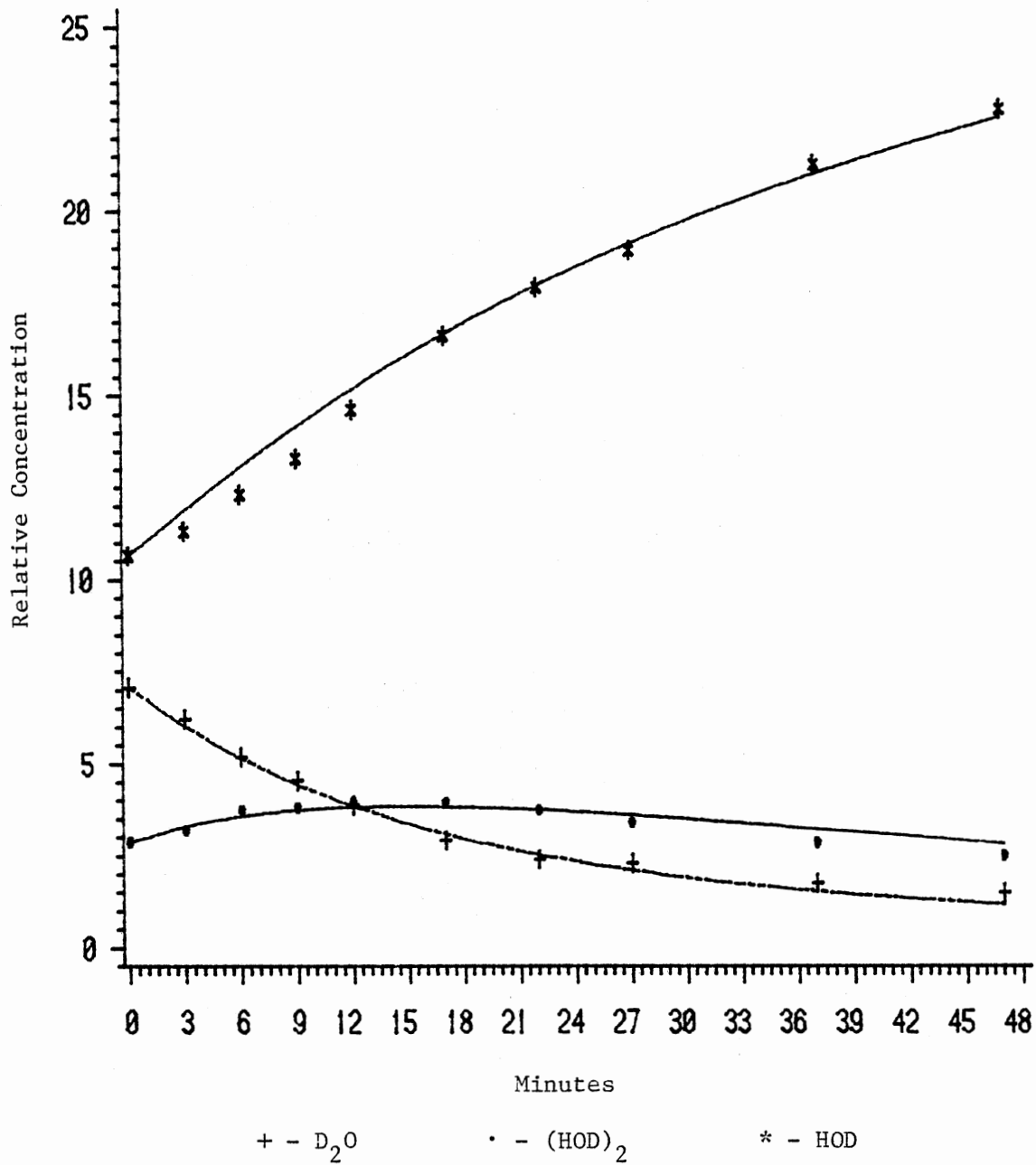
Figure 39. Experimental and Two Equilibrium Model Calculated Relative
Concentration Curves for 5/24/82 145 K Data
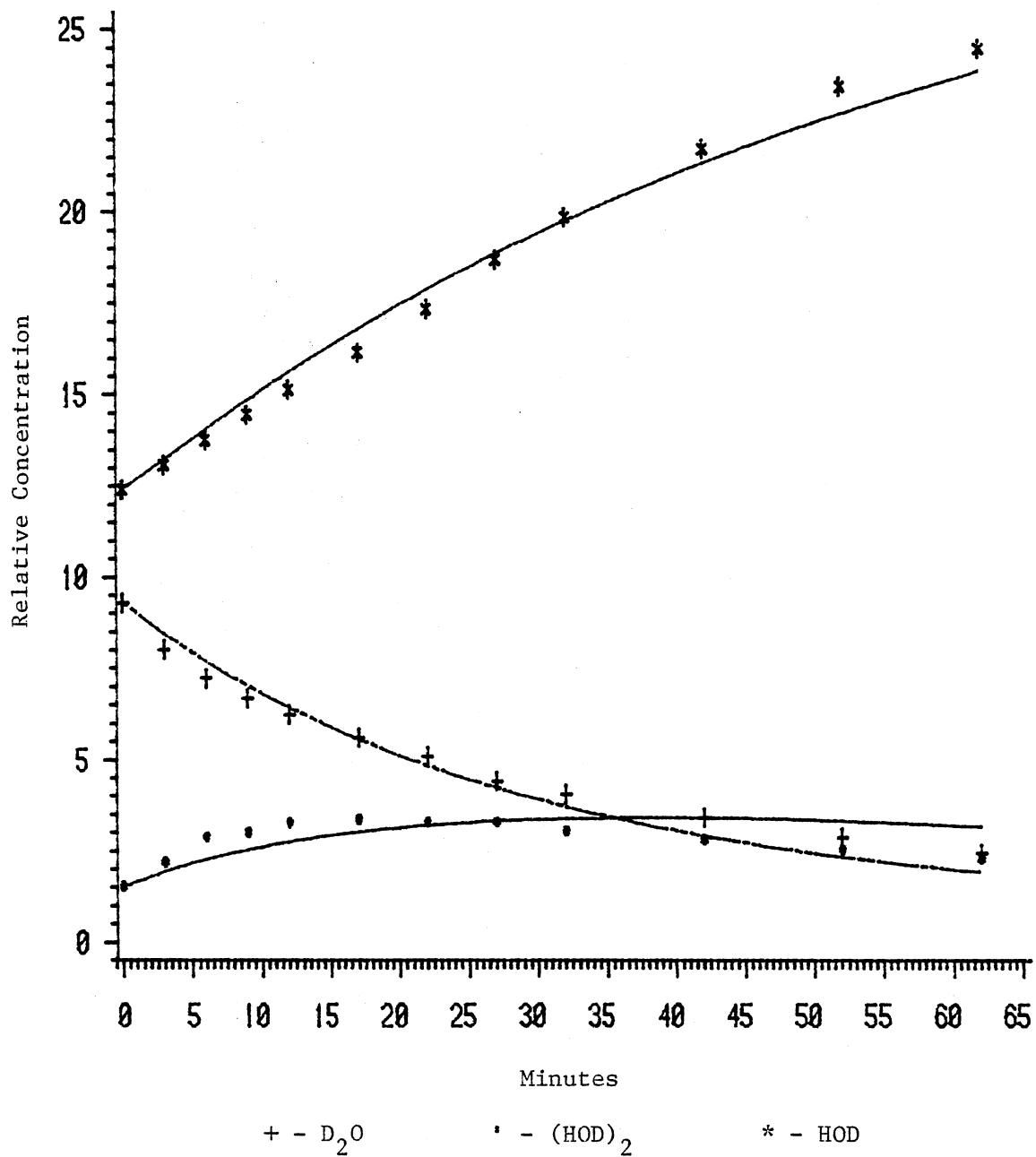
Figure 40. Experimental and Two Equilibrium Model Calculated Relative
Concentration Curves for 6/3/82 145 K Data
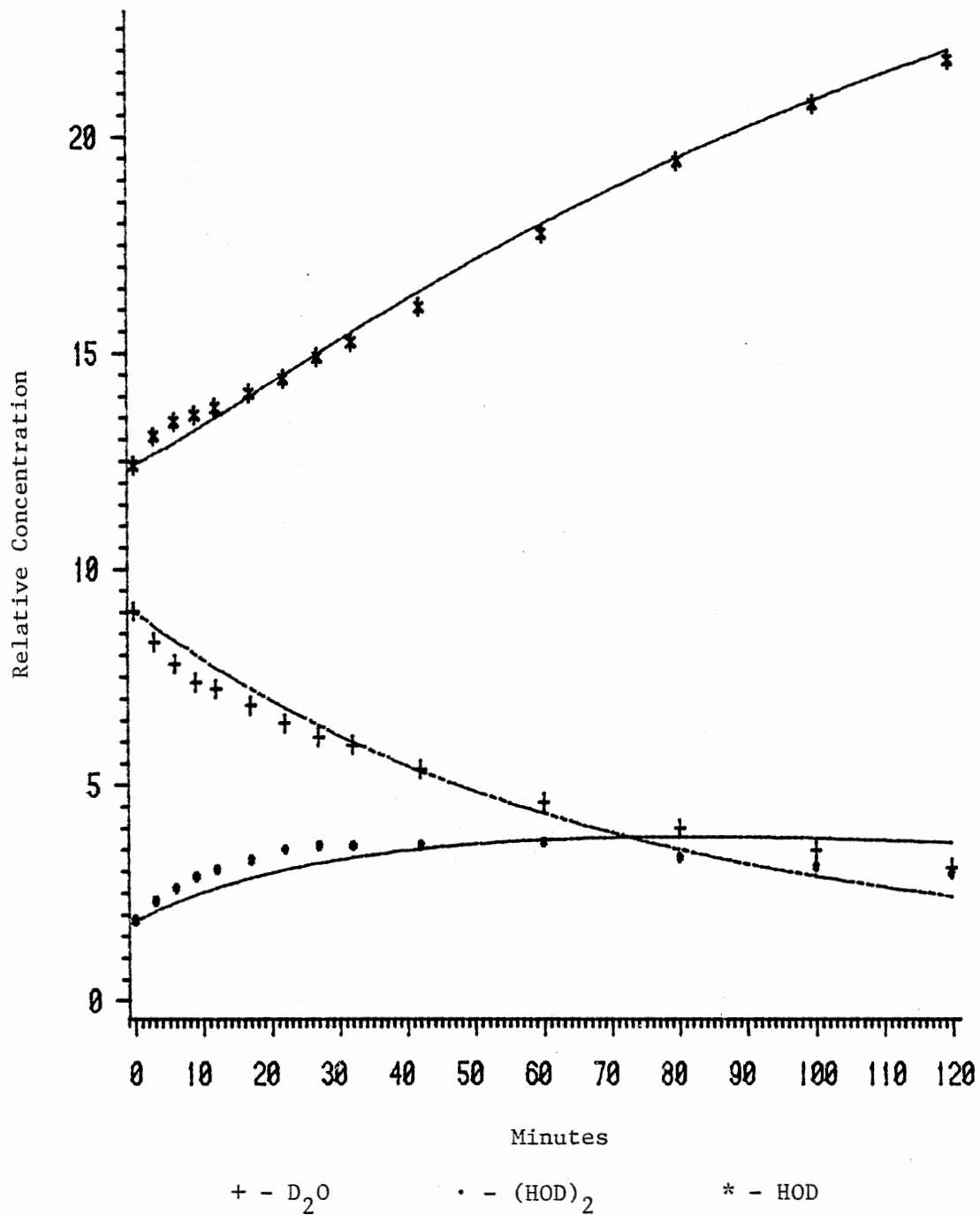
Figure 41. Experimental and Two Equilibrium Model Calculated Relative Concentration Curves for 5/4/82 140 K Data
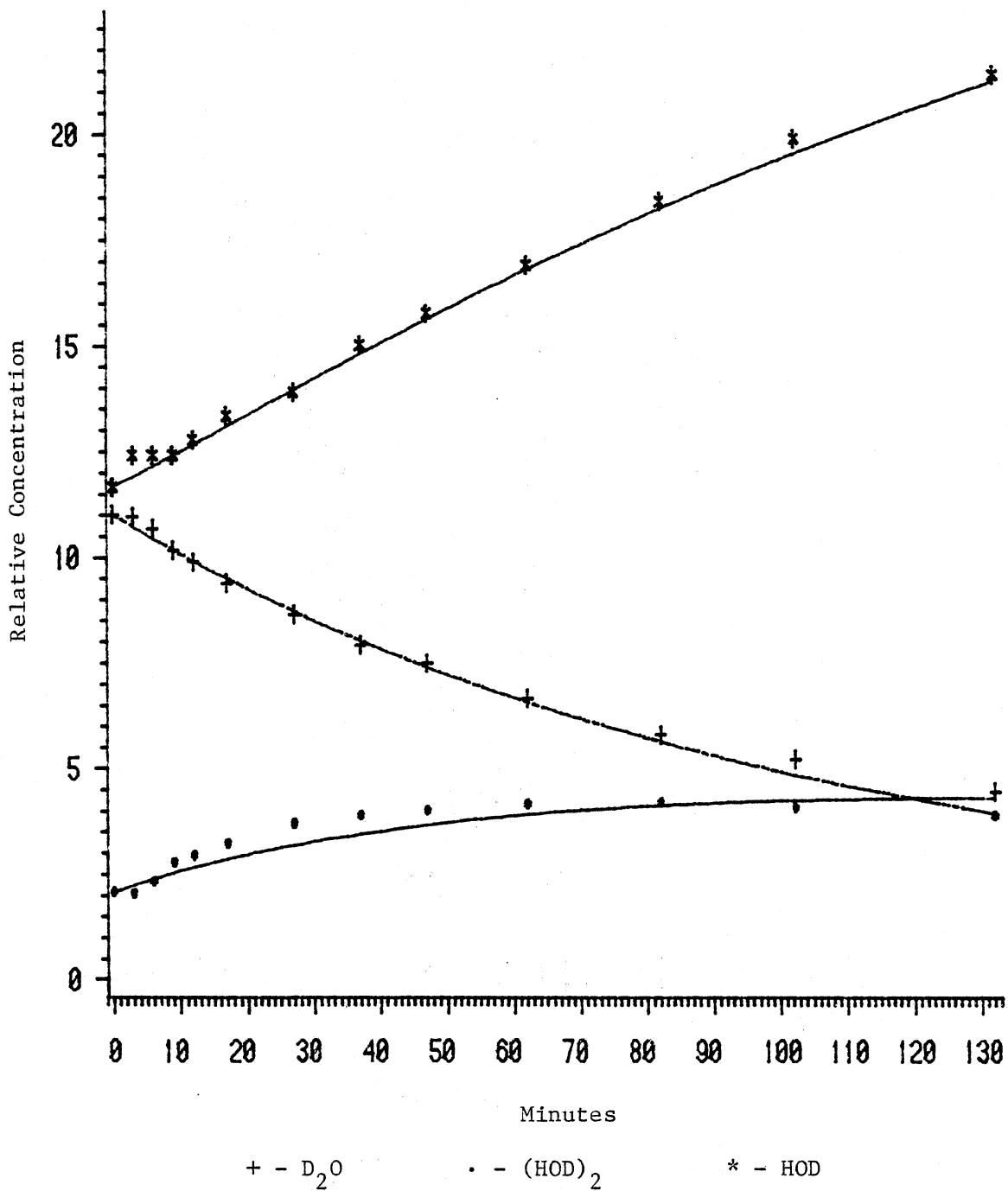
Figure 42. Experimental and Two Equilibrium Model Calculated Relative Concentration Curves for 5/25/82 140 K Data
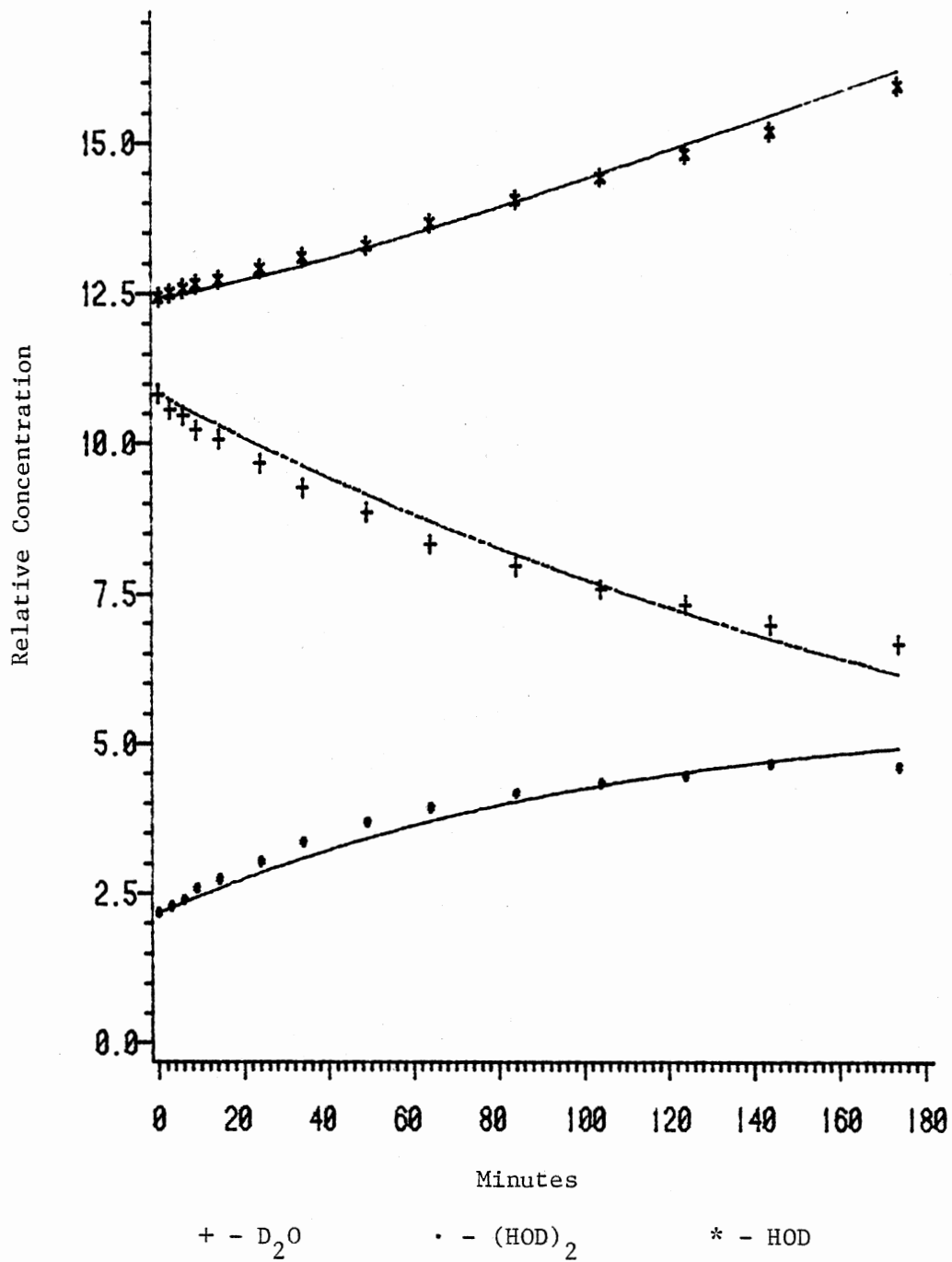
Figure 43. Experimental and Two Equilibrium Model Calculated Relative Concentration Curves for 5/15/83 135 K Data
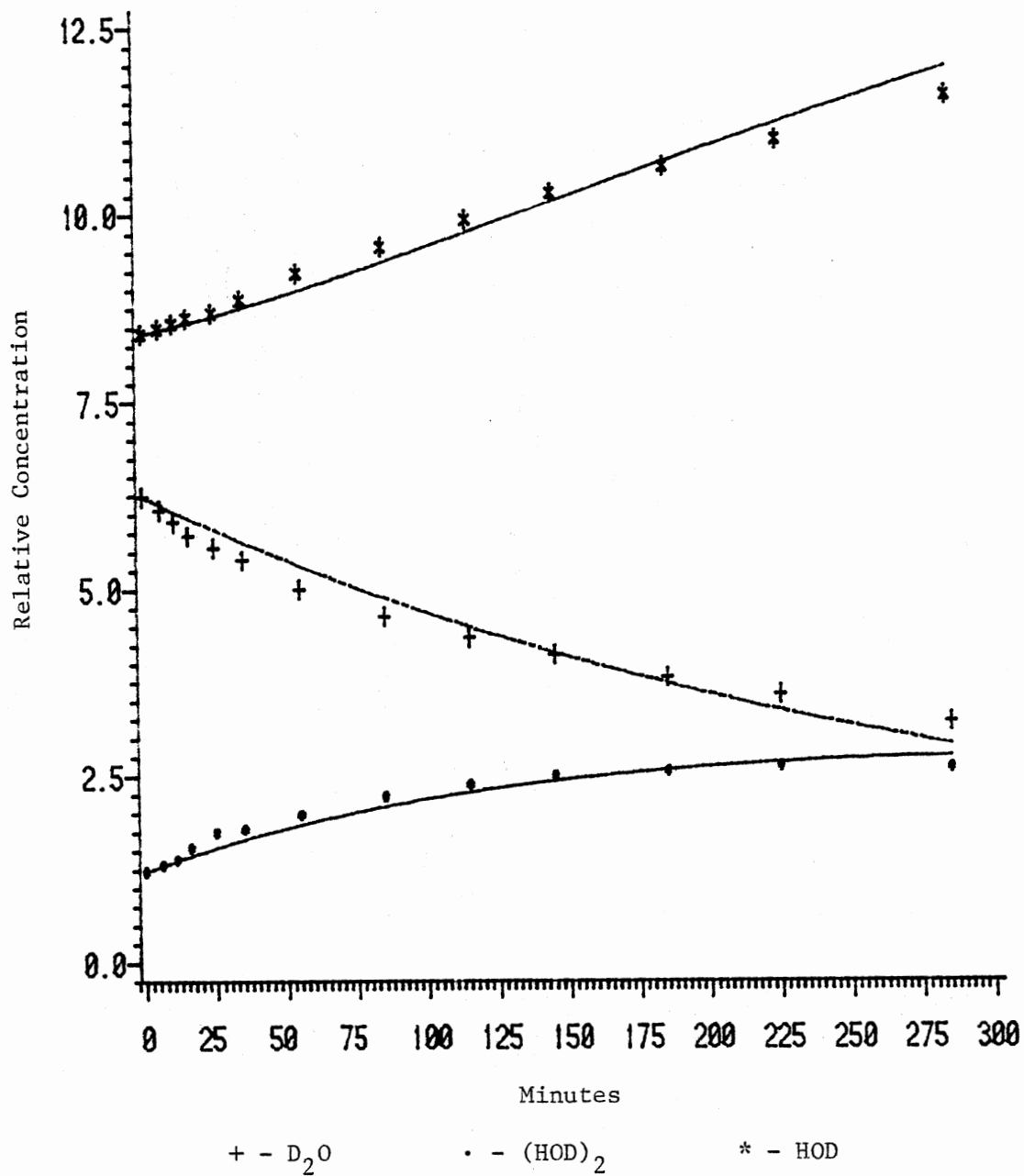
Figure 44. Experimental and Two Equilibrium Model Calculated Relative Concentration Curves for 5/26/82 135 K Data
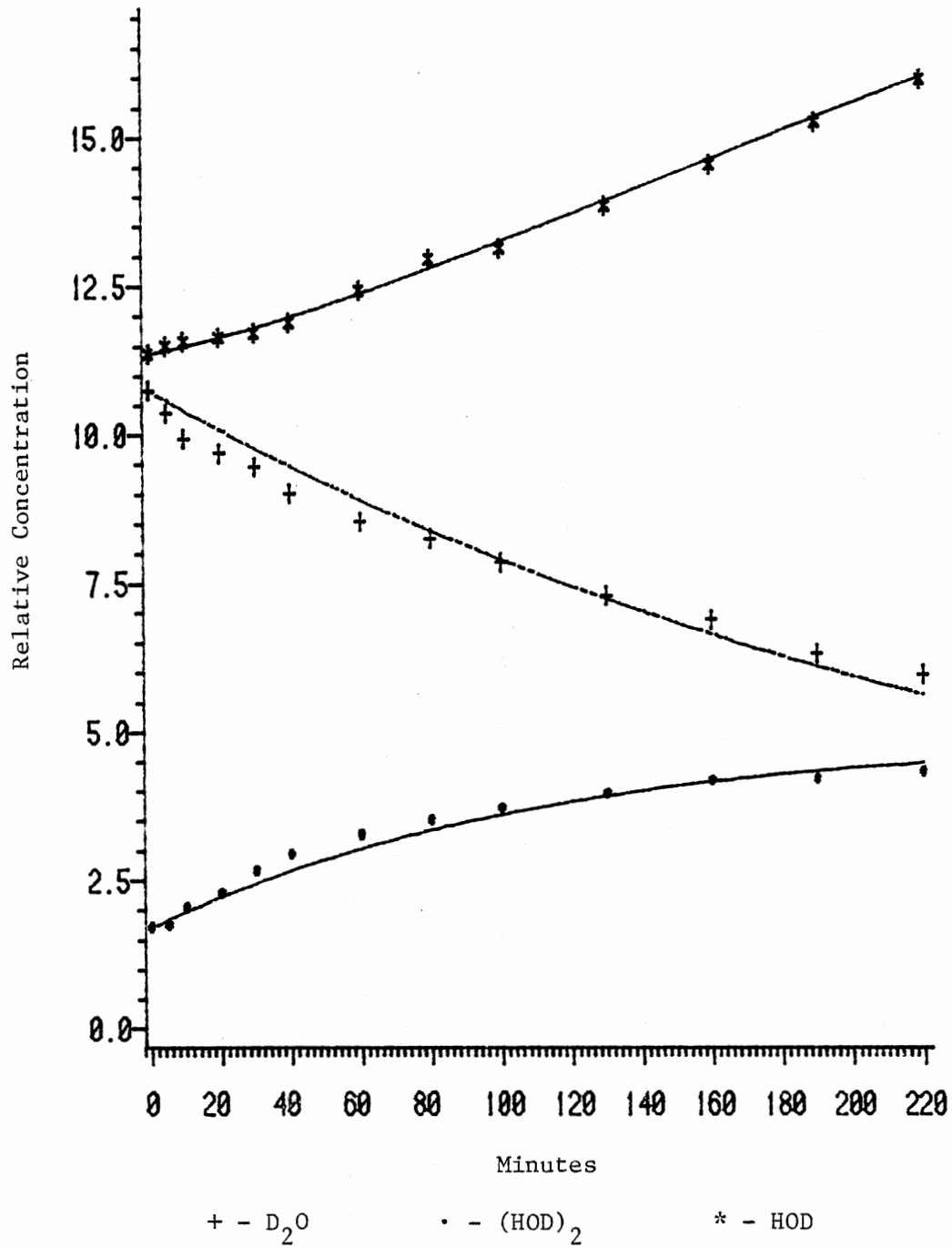
Figure 45. Experimental and Two Equilibrium Model Calculated Relative
Concentration Curves for 6/11/82 135 K Data

Figures 46-57 show the calculated D_2O_{11} and $2HOD_{nm}$ configuration concentrations determined from the two-equilibrium model used for Figures 34-45. The top decaying curve is the D_2O configuration relative concentration. The increasing curve just below D_2O_{11} corresponds to the $2HOD_{22}$ and higher (fully separated) configuration concentration. Note that the concentration is less than one half the corresponding uncoupled HOD concentrations seen in Figures 34-45. This is because the $2HOD_{22}$ concentration includes both HOD units rather than a single HOD unit. Also, the $2HOD_{21}$ configuration concentration (separated HOD) is shown separately, rather than added into the $2HOD_{22}$ concentration to form the uncoupled HOD shown in Figures 34-45. The lowest intermediary curve in Figures 46-57 is the $2HOD_{21}$ configuration relative concentration (separated HOD). The intermediary curve just above it is the $2HOD_{12}$ configuration concentration (coupled HOD). The initial value of $2HOD_{21}$ is always one quarter the $2HOD_{12}$ concentration as defined in the model. It is interesting to note that the $2HOD_{21}$ concentration never exceeds the $2HOD_{12}$ concentration in the data shown, but quickly establishes a slightly lower concentration. This is probably due to the equal magnitude of the forward and reverse rotational rate constants between these two configurations.

Compared with the one-equilibrium model, the two-equilibrium model is a significantly better fit, especially at the completion of the exchange reaction. The fit of $(HOD)_2$ is improved with deviations occurring at two to three D_2O half-lives instead of one half-life as in the one-equilibrium model. The two-equilibrium model tends to overestimate the $(HOD)_2$ concentration and underestimate the
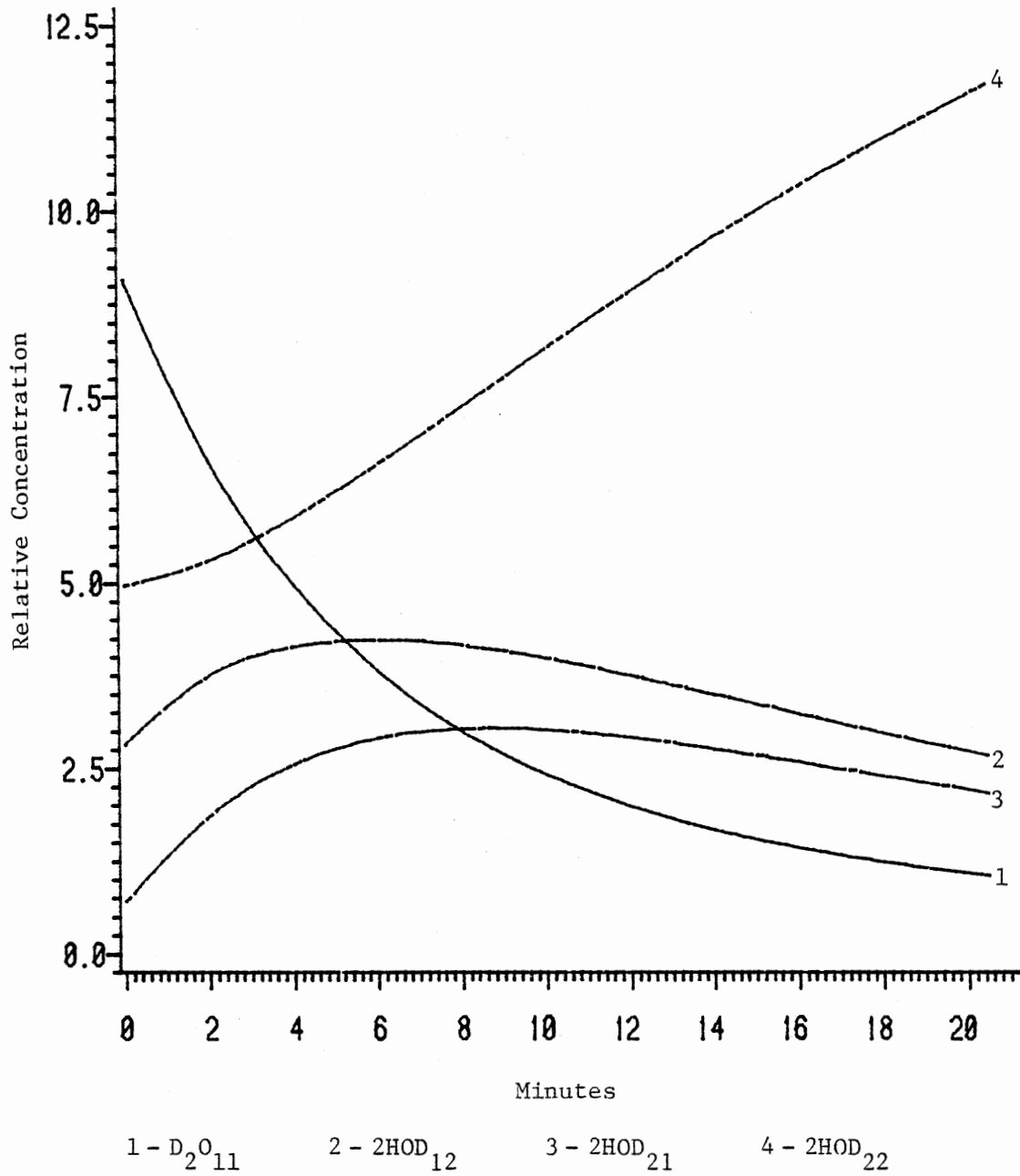
Figure 46. Calculated D_2O_{11} and $2HOD_{nm}$ Configuration Concentration Curves for 2/2/82 150 K Data
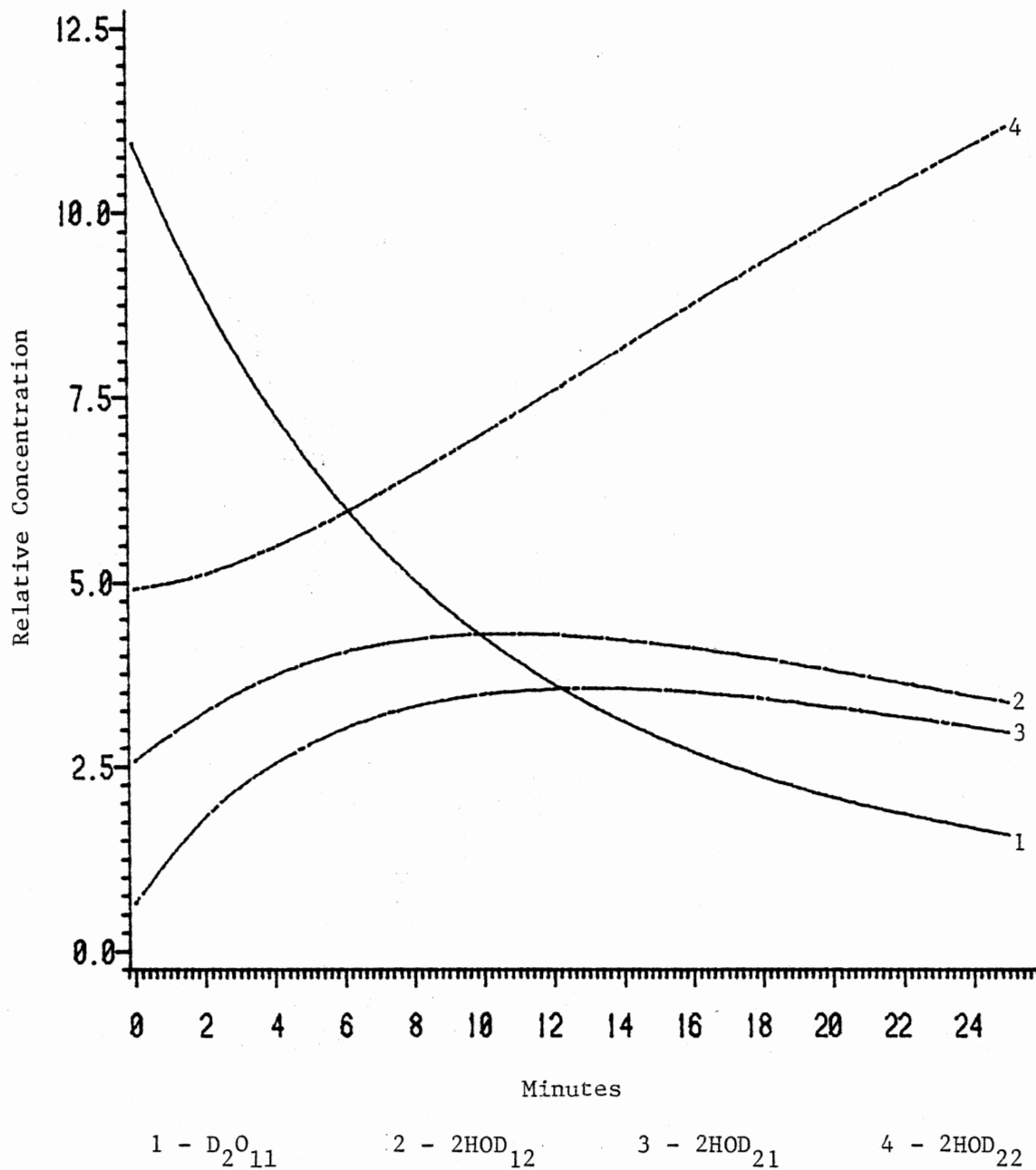
Figure 47. Calculated D_2O_{11} and $2HOD_{nm}$ Configuration Concentration Curves for 6/7/82 150 K Data

$1 - D_2O_{11}$ $2 - 2HOD_{12}$ $3 - 2HOD_{21}$ $4 - 2HOD_{22}$

1 - D_2O_{11}　　　　2 - $2HOD_{12}$　　　　3 - $2HOD_{21}$　　　　4 - $2HOD_{22}$
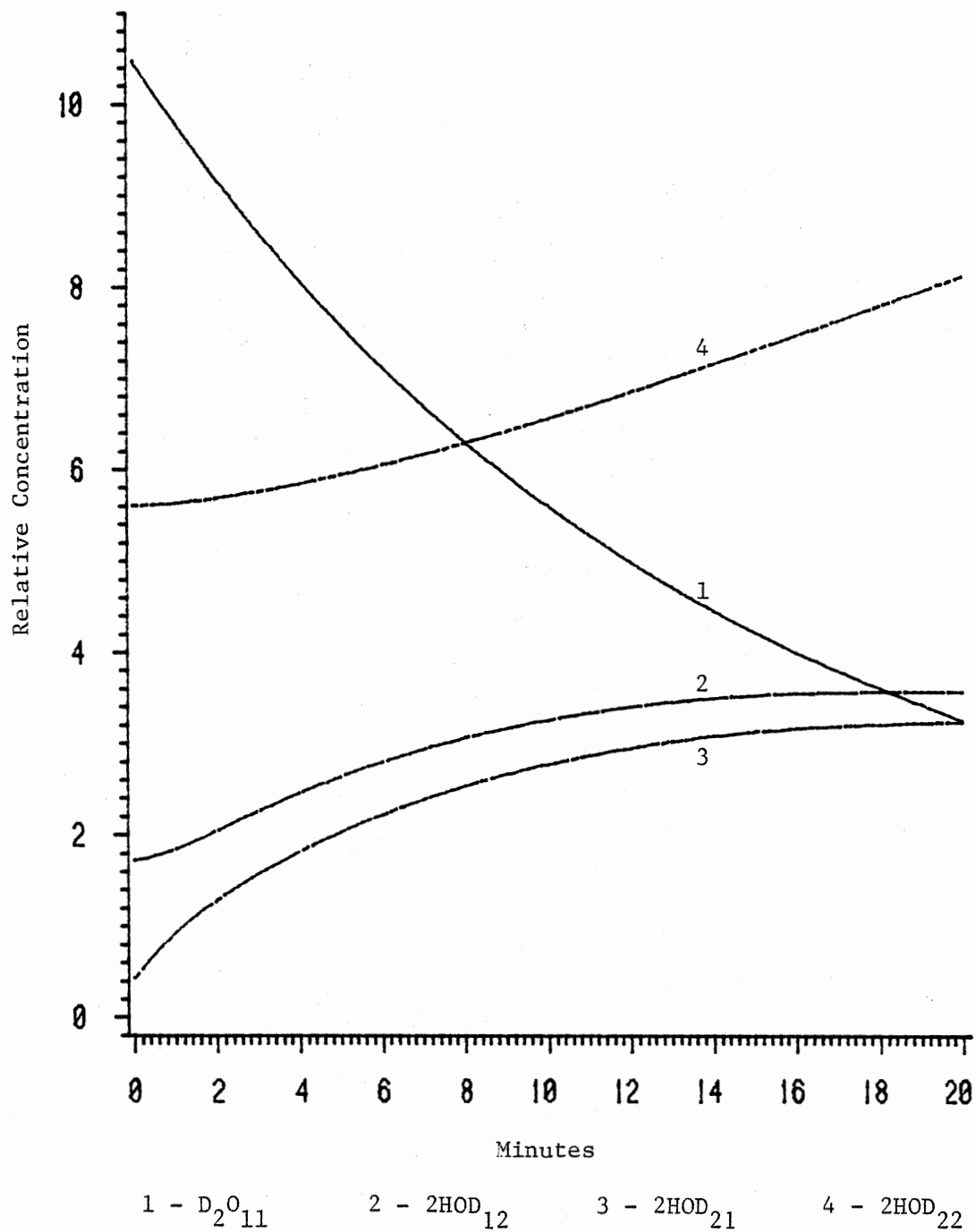
Figure 48.　Calculated D_2O_{11} and $2HOD_{nm}$ Configuration Concentration Curves for 6/9/82 150 K Data
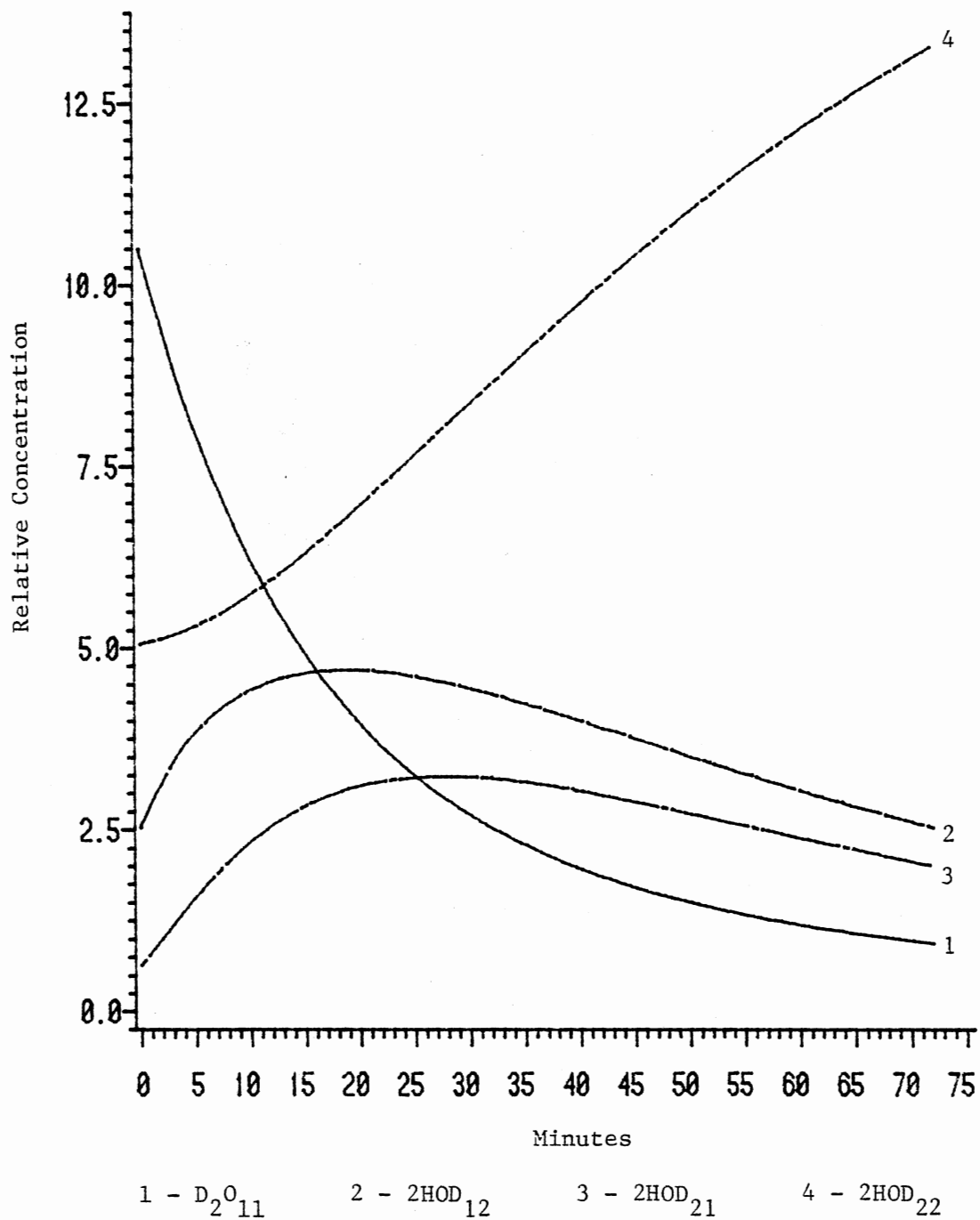
Figure 49. Calculated D_2O_{11} and $2HOD_{nm}$ Configuration Concentration Curves for 1/29/82 145 K Data
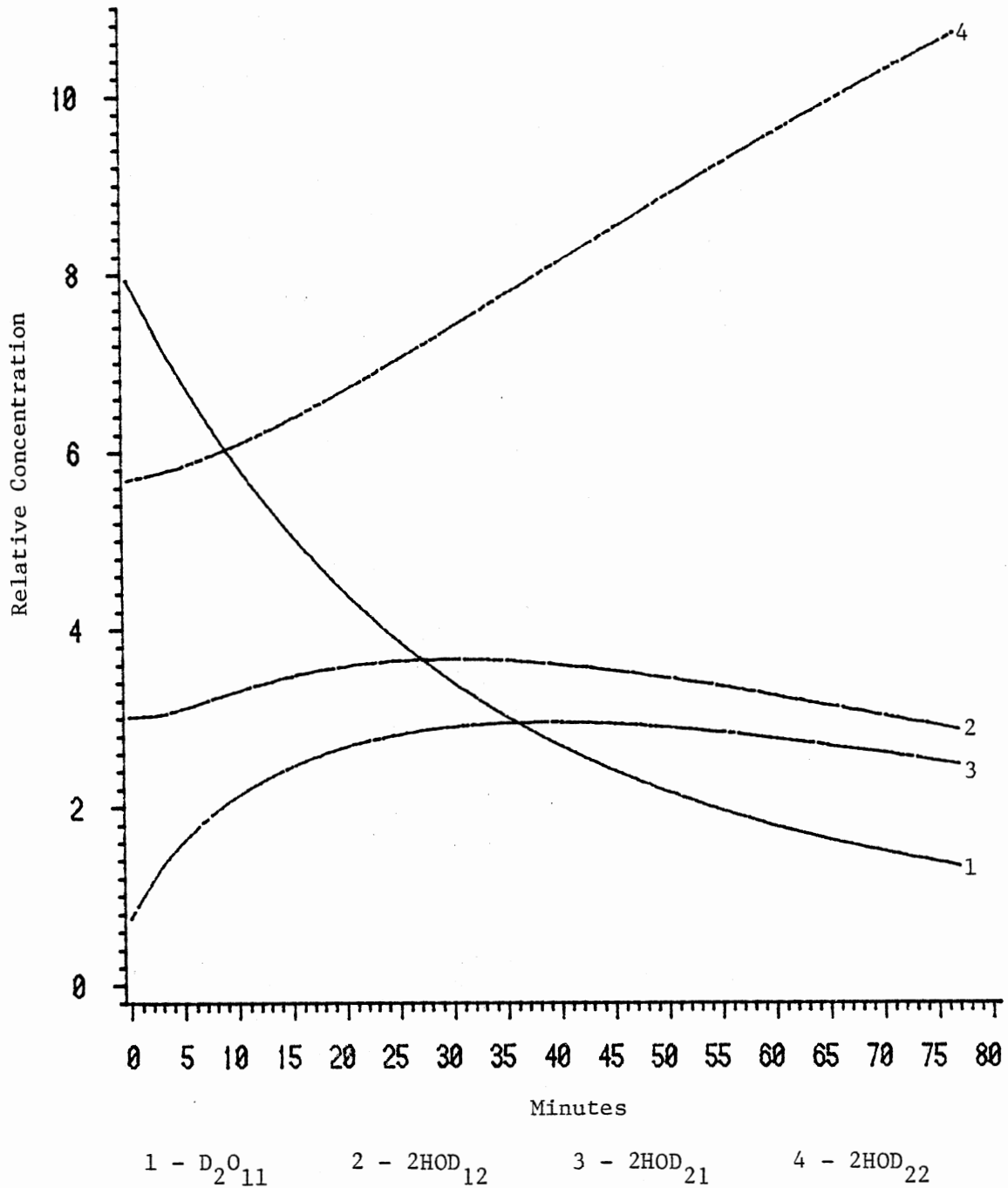
Figure 50. Calculated D_2O_{11} and $2HOD_{nm}$ Configuration Concentration Curves for 5/10/82 145 K Data

1 - D_2O_{11} 2 - $2HOD_{12}$ 3 - $2HOD_{21}$ 4 - $2HOD_{22}$
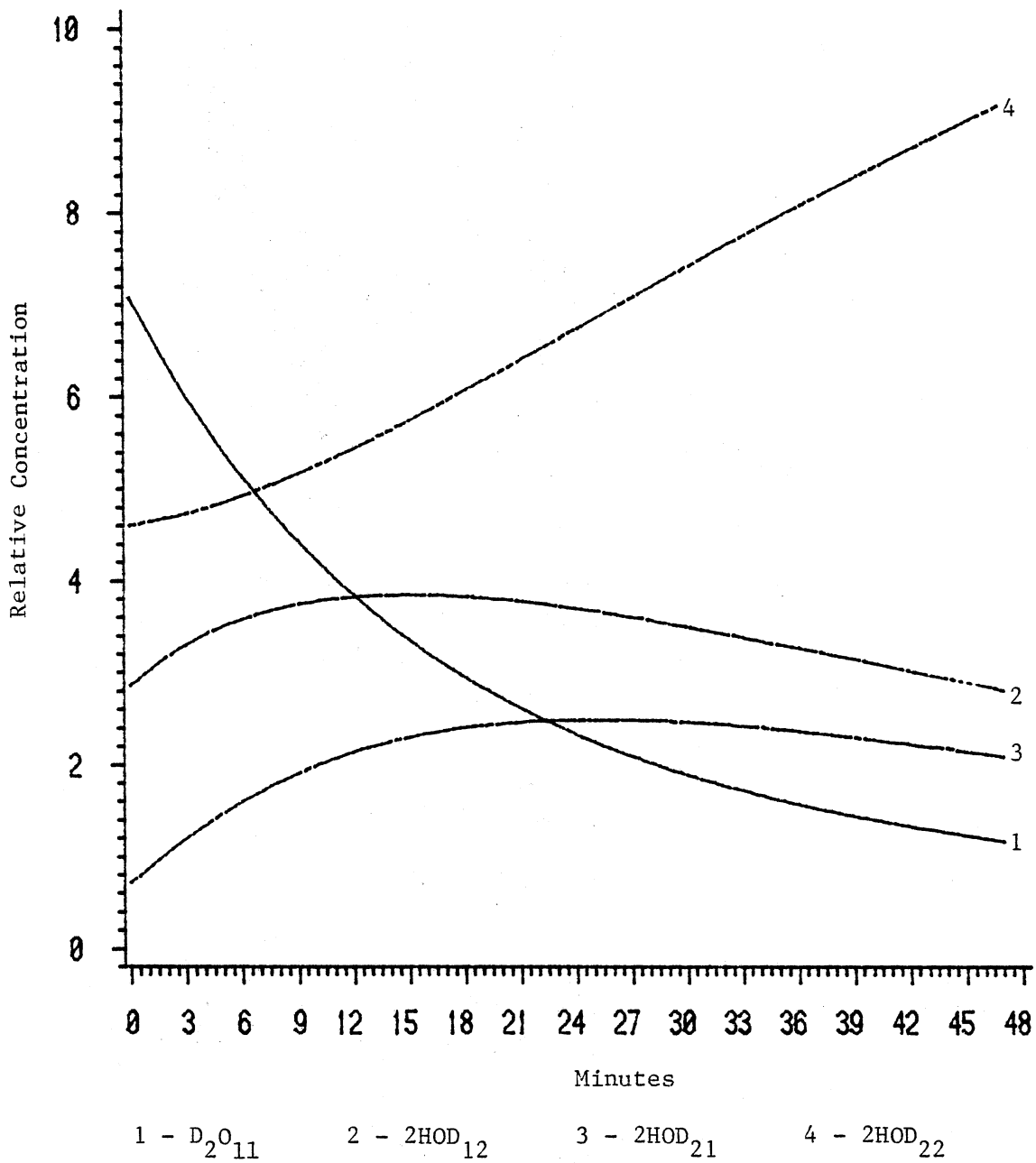
Figure 51.   Calculated D_2O_{11} and $2HOD_{nm}$ Configuration Concentration
Curves for 5/24/82 145 K Data
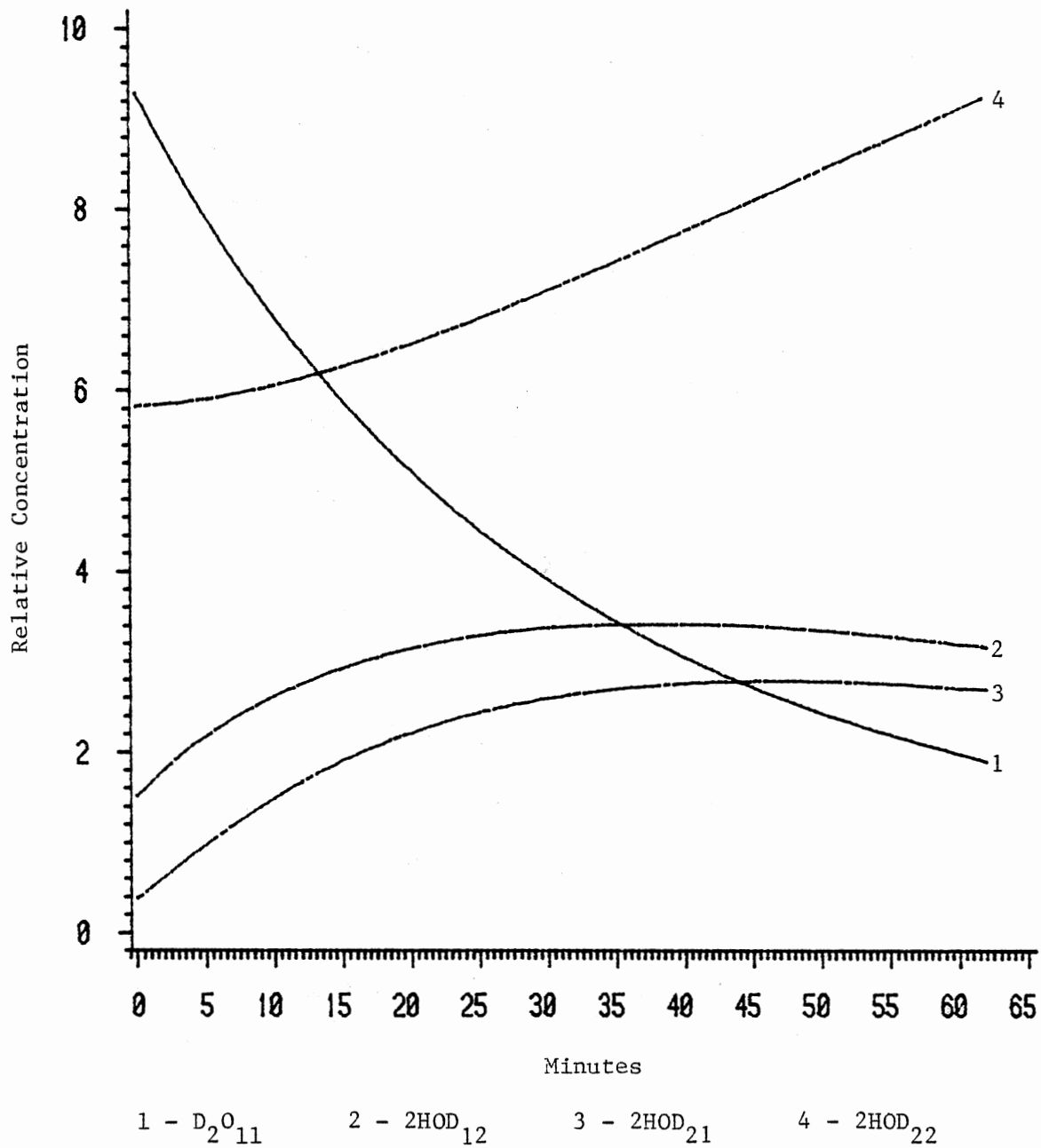
Figure 52. Calculated D_2O_{11} and $2HOD_{nm}$ Configuration Concentration Curves for 6/3/82 145 K Data

$1 - D_2O_{11}$ $2 - 2HOD_{12}$ $3 - 2HOD_{21}$ $4 - 2HOD_{22}$

$$1 - D_2O_{11} \qquad 2 - 2HOD_{12} \qquad 3 - 2HOD_{21} \qquad 4 - 2HOD_{22}$$
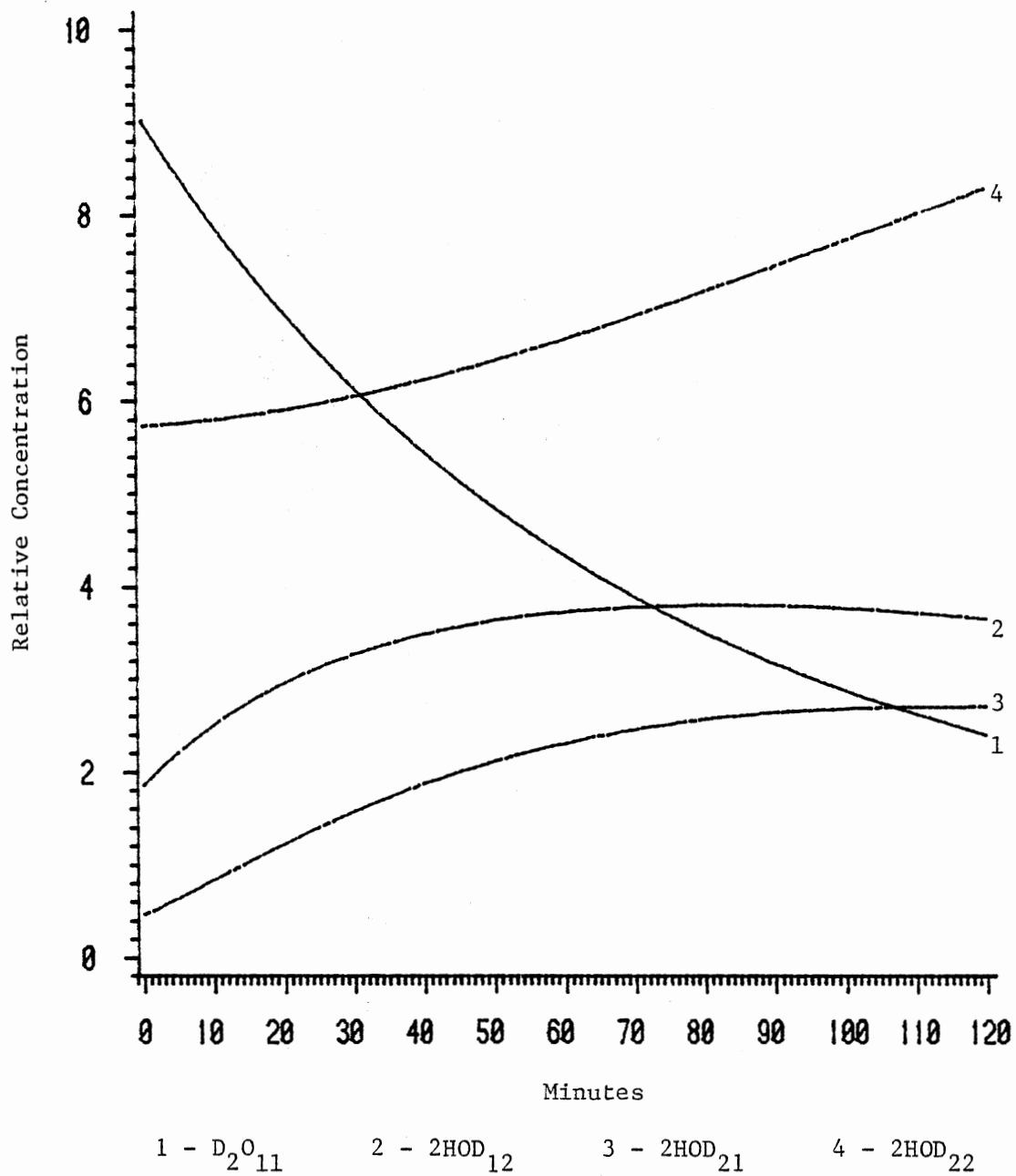
Figure 53.   Calculated D_2O_{11} and $2HOD_{nm}$ Configuration Concentration
Curves for 5/11/82 140 K Data
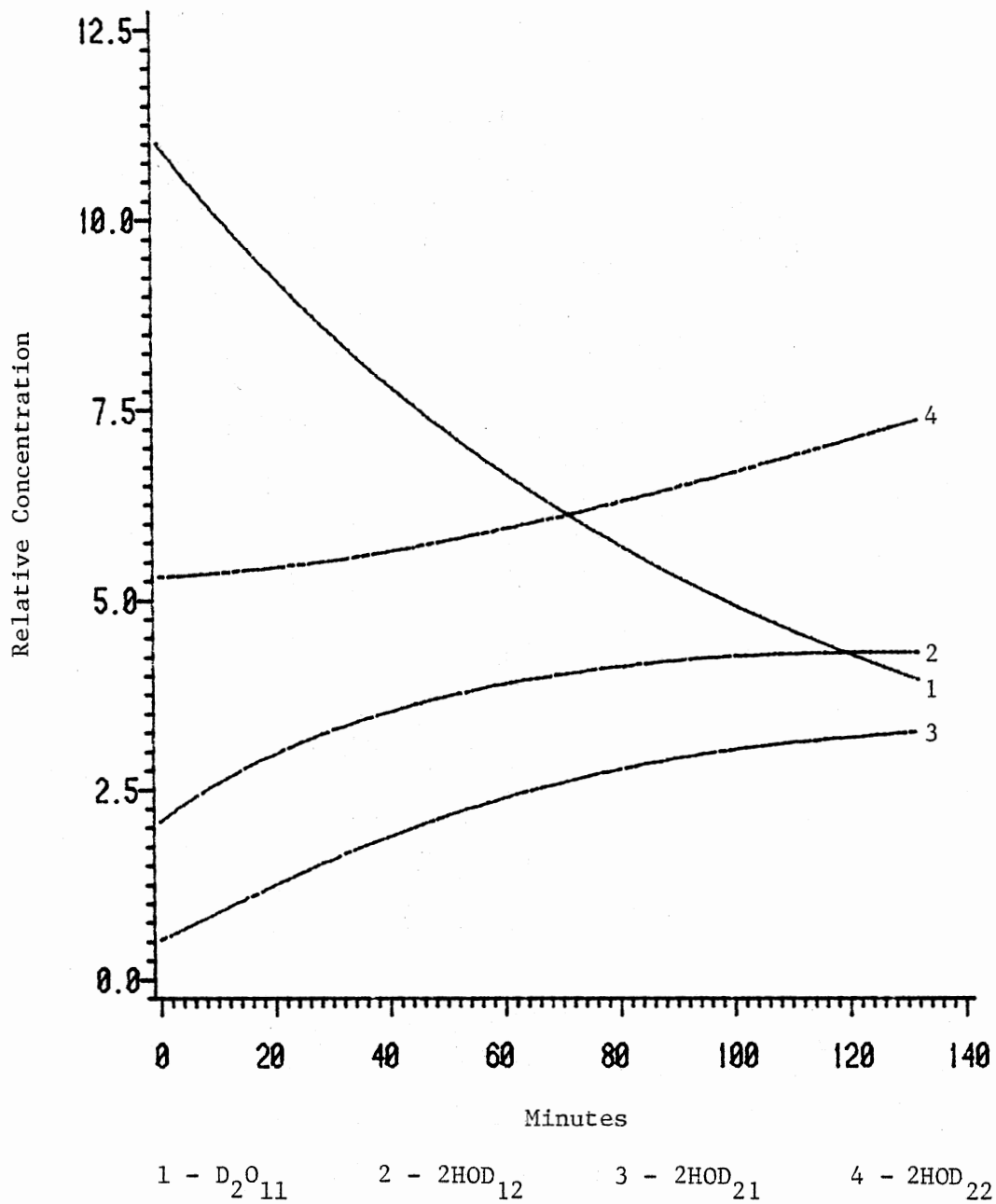
Figure 54. Calculated D_2O_{11} and $2HOD_{nm}$ Configuration Concentration Curves for 5/25/82 140 K Data

The legend below the figure reads:

$1 - D_2O_{11}$ $2 - 2HOD_{12}$ $3 - 2HOD_{21}$ $4 - 2HOD_{22}$
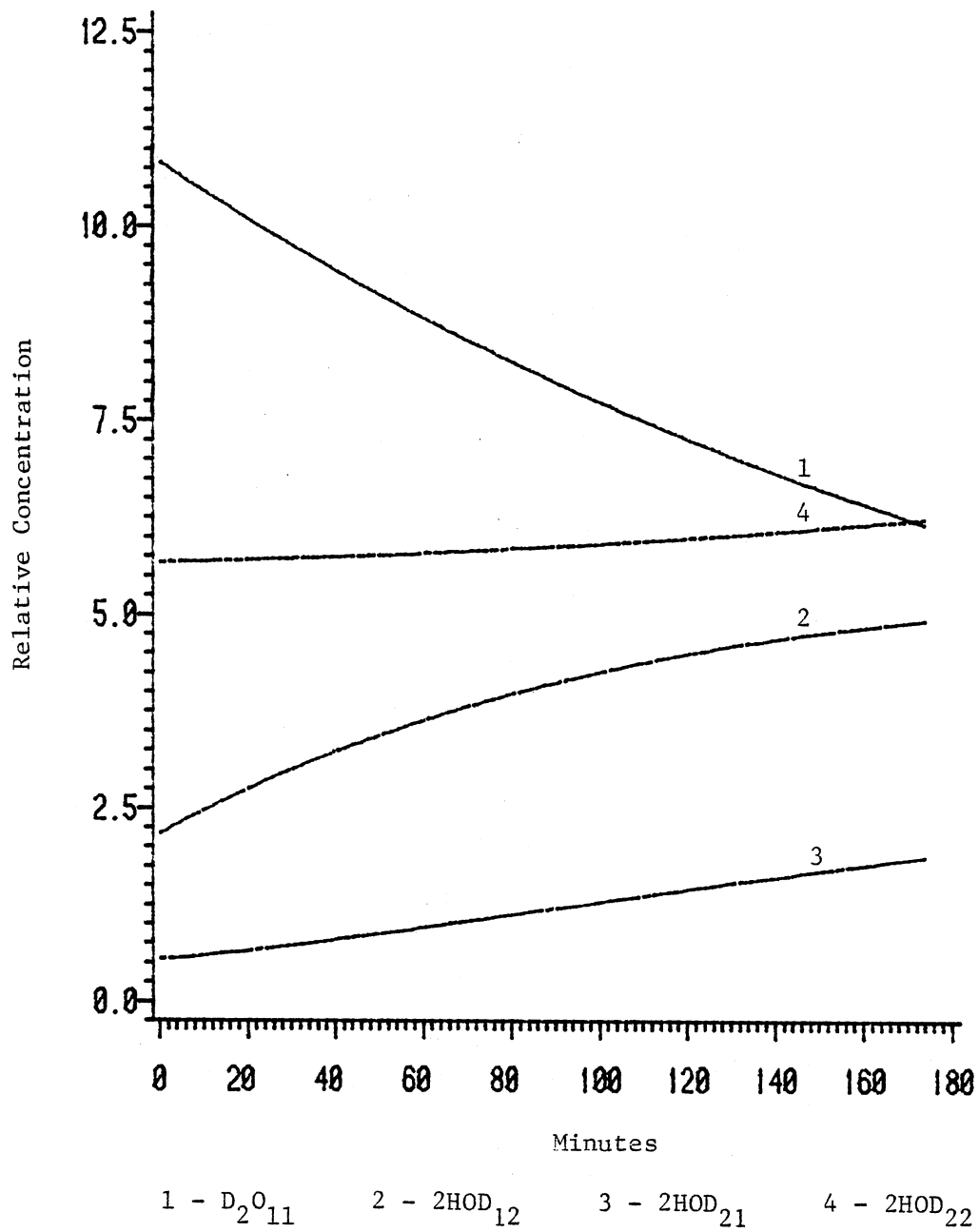
Figure 55. Calculated D_2O_{11} and $2HOD_{nm}$ Configuration Concentration Curves for 5/15/82 135 K Data
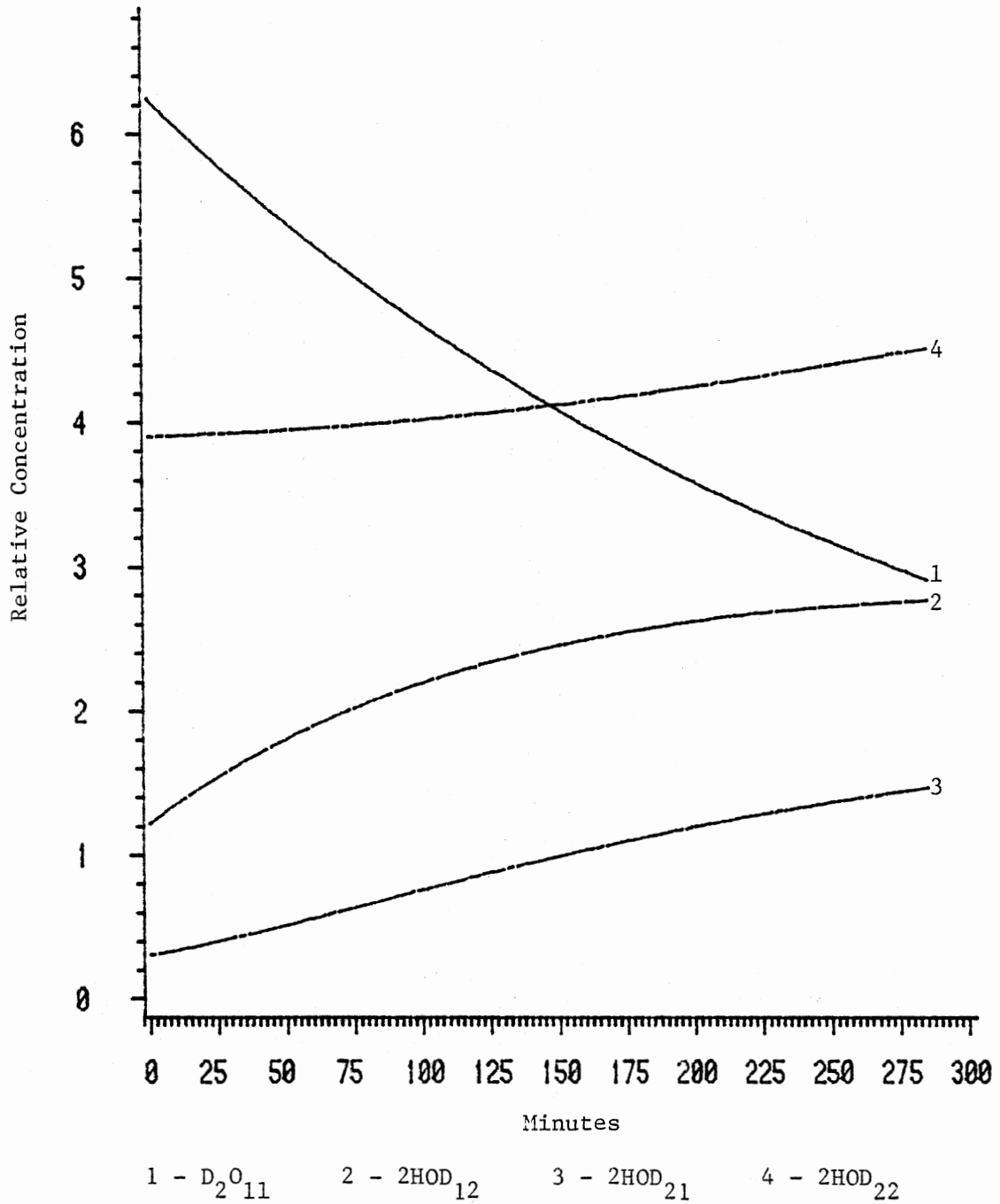
Figure 56. Calculated D_2O_{11} and $2HOD_{nm}$ Configuration Concentration Curves for 5/28/82 135 K Data
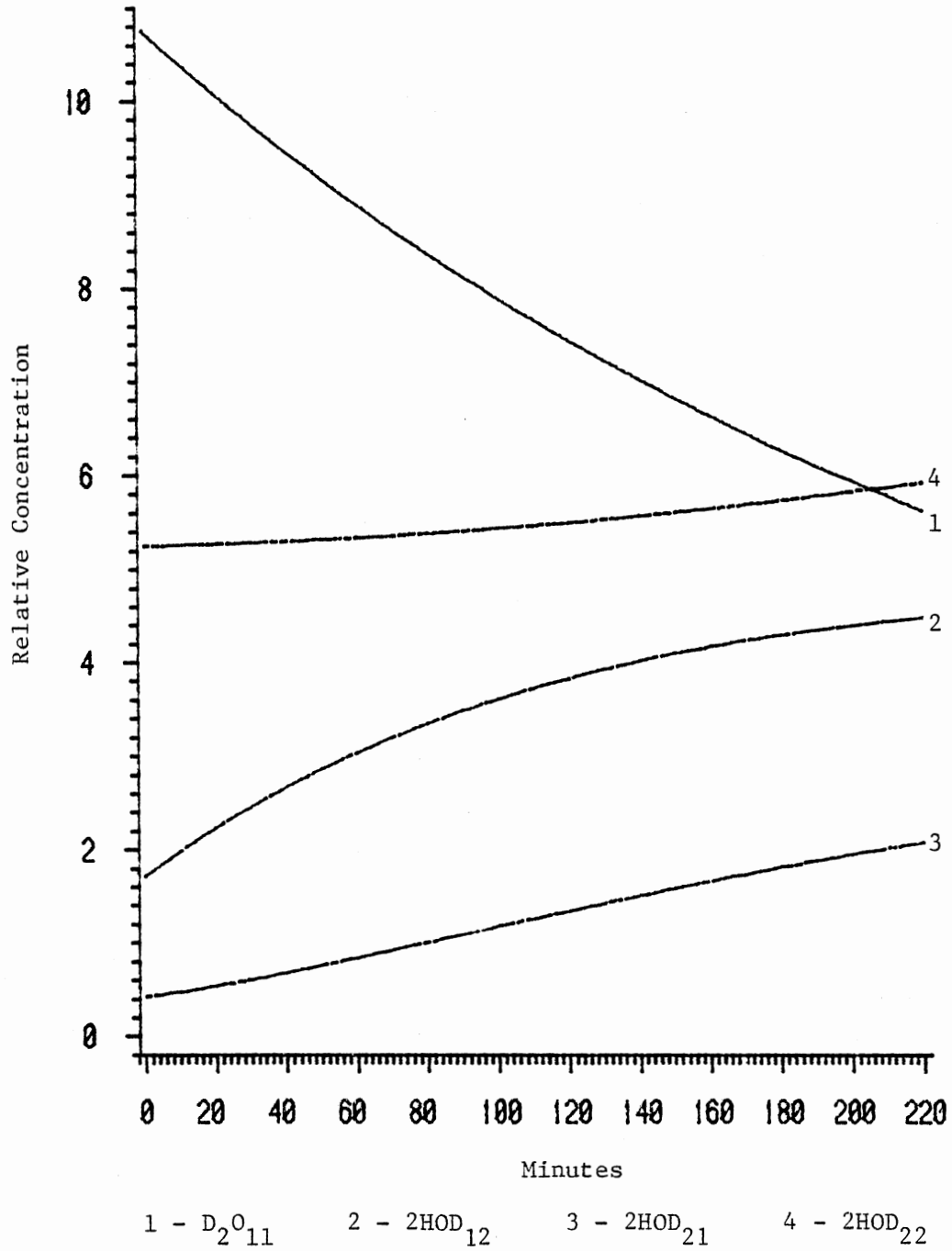
Figure 57.   Calculated D_2O_{11} and $2HOD_{nm}$ Configuration Concentration
Curves for 6/11/82 135 K Data

$1 - D_2O_{11}$ $2 - 2HOD_{12}$ $3 - 2HOD_{21}$ $4 - 2HOD_{22}$

D_2O concentration after several half-lives of the D_2O concentration. This may be due to the slightly fast depletion of D_2O which builds up the $(HOD)_2$ too fast. The exclusion of the $(HOD)_2$ to pseudo-HOD to separated HOD migration path (see Figure 26, $2HOD_{12} \leftrightarrow 2HOD_{13} \leftrightarrow 2HOD_{22}$) may account for some of the deviations. But attempts to include this pathway in the model failed due to too high a correlation in the rate constants and too many unknowns in the model equation.

Transfer and Rotational Activation Energies

The two-equilibrium model calculated rate constants shown in Table VII were least square fitted to standard Arrhenius plots to find the activation energies predicted for each calculation. Table VIII lists these results.

The correlation factors for the Arrhenius plots tend to support the contention that the 0.0 and .25 calculations are the best fit. For the transfer rate constants the .25 calculation has the best correlation and for the rotational rate constants the 0.0 calculation. In contrast the .5 calculation has the lowest correlation for both the transfer and rotational rate constant plots. A further indication of the poorer fit of the .5 calculation is the .561 standard error which is twice the standard error of the 0.0 and .25 calculations. A .7 calculation not shown gave an even poorer fit. So in summarizing, the 0.0 and .25 calculations gave the best activation energies for the rotational and transfer rate constants. Both calculations give essentially the same rate constants and hence the same activation energies. The upper plot of Figure 58 shows the Arrhenius plot for the transfer rate constants. From this a transfer

TABLE VIII

TRANSFER AND ROTATIONAL ACTIVATION ENERGIES

Model initial HOD_{21}	Two-equilibrium 0.0	Two-equilibrium 0.25	Two-equilibrium 0.5
Transfer Activation Energy (kcal/mole)	9.531	9.537	9.513
Standard Error	0.658	0.653	0.661
Least Square Correlation	0.97697	0.97736	0.97667
Rotational Activation Energy (kcal/mole)	11.767	12.199	13.296
Standard Error	0.228	0.244	0.561
Least Square Correlation	0.99813	0.99801	0.99123
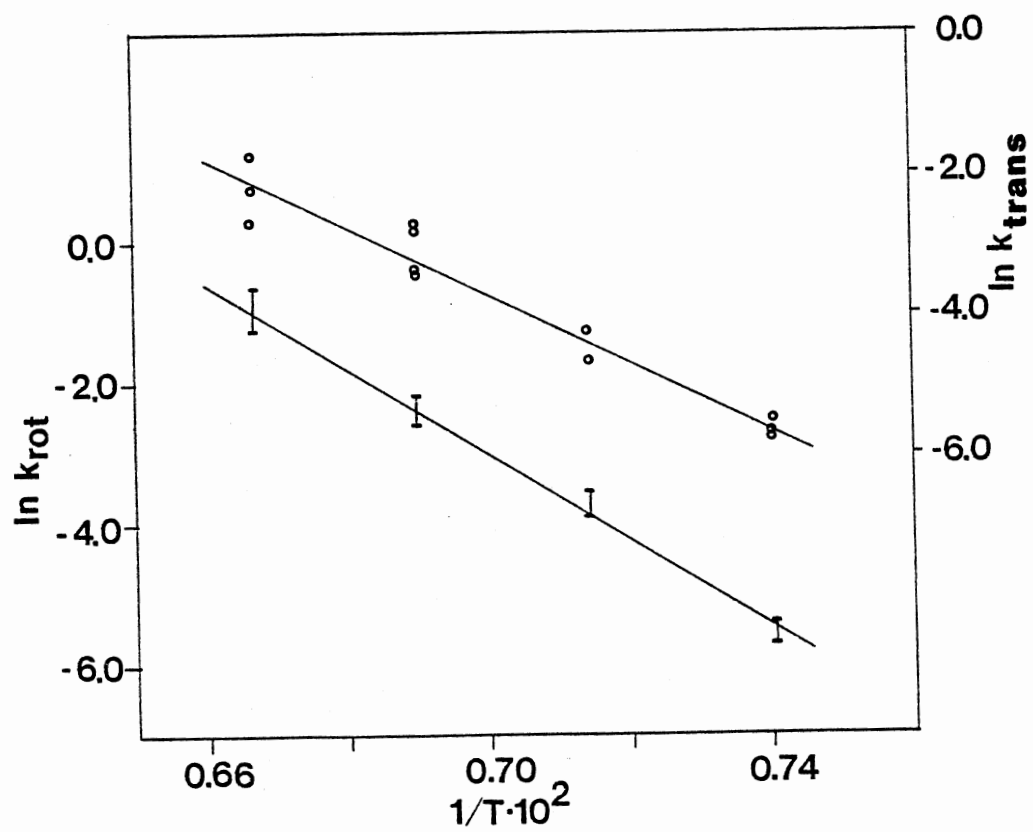
Figure 58.   Transfer and Rotational Rate Constants Arrhenius Plots

rate constant activation energy of 9.5 ± .7 kcal/mole with a pre-exponential factor of $(9.4 \pm .7) \times 10^{12}$ is determined.

The rotational activation energy is not as well determined. Though the standard errors are smaller than those of the transfer rate constant activation energy the 0.0 and .25 calculations still give different activation energies. Unfortunately there is no suitable criteria to determine which value is correct. Thus since the initial separated HOD concentration cannot be determined closer than 0.0 to .25 times the initial $(HOD)_2$ concentration the 0.0 and .25 calculations should represent acceptable bounds to the rotational rate constant activation energy.

The lower Arrhenius plot of Figure 58 shows the error bars determined from the lowest and highest rate constant from either the 0.0 or .25 calculations for a given temperature. Thus the upper error bar of the 150 K data point was determined from the natural log of .5020 the 150 K 6/9/82 dataset .25 calculated rotational rate constant, and the lower error bar from the log of .2857 the 150 K 2/2/82 dataset 0.0 claculated rotational rate constant. Then taking the average of the 0.0 calculation 11.8 and .25 calculation 12.2 activation energies and drawing in the resulting straight line plot gives the lower plot shown in Figure 58. So in spute of the initial separated HOD indeterminacy, the rotational activation energy can still be error bounded to an accuracy equal or better than the transfer activation energy. Interestingly, unlike the transfer plot, the rotational plot errors are fairly consistent over the 150 to 135 K temperature range. This may reflect the possibility that the $(HOD)_2$ concentrations are less affected by sampling and spectral resolution

errors in obtaining the coupled HOD absorbances. From the lower plot a rotational rate constant activation energy of $12.0 \pm .5$ kcal/mole with a pre-exponential factor of $(1.1 \pm 1.1) \times 10^{17}$ is determined. The error limits were calculated by adding the calculated standard errors to one half the difference between the 0.0 and .25 least square determined activation energies and pre-exponential factors.

Discussion of Activation Energies

The calculated $9.5 \pm .7$ kcal/mole transfer activation energy is quite close to the 9.3 kcal/mole value found by Ritzhaupt and Devlin (46) on their studies of doped ice systems. The transfer activation energy reflects an independence of the dopants that drastically affect the transfer rates. This gives further credence to the suggestion that the dopants affect the concentration of ionic defects and hence the rate. Accordingly the activation energy measured represents the ion pair defect formation energy. This ionization is dependent on the temperature, but independent of defect concentration or dopants present in the ice lattice.

A. von Hippel (42) suggested that D and L Bjerrum defects were the only charge carriers in bulk ice conductivity measurements. In view of the magnitudes of the transfer and rotational rate constants and the magnitudes of the D_2O and $(HOD)_2$ concentrations, this view is hard to support at 135-150 K temperatures. Both the ionic and Bjerrum defects appear to be equally active in isotopic scrambling for pure ice systems. But the $12.0 \pm .5$ kcal/mole rotational activation energy does imply that the rotational step may become more

predominant and the transfer step more rate determining at higher temperatures. Thus conductivity activation energies of pure ice in the 135 to 180 K region may be hard to relate to a particular defect activation energy. The 9 and 13 kcal/mole conductivity activation energies at 240-200 K and 180-170 K, reported by Durand et al. (40) may be a reflection of this problem.

Nagle and Tristram-Nagle (52) have reviewed various models for proton transport in biological membranes. In particular the hydrogen bonded chain mechanisms in which various amino acid hydroxyl and amine groups hydrogen bond to form a chain capable of transmitting protons via a hop/turn mechanism. For a particular hydrogen bonded chain (HBC) to transmit a proton more than once each hopping or ionic defect migration must be followed by a turn or D,L defect migration through the chain. The model presented in Figure 26 presents a similar situation. Here a particular deuteron cannot move through the ice lattice unless an alternating sequence of transfer and rotational steps is followed. Thus if D_2O completely scrambles to uncoupled HOD both transfer and rotational defects should be present. But if proton transfer could be induced without a rotational decoupling then a statistical 1:2:1 ratio of D_2O, coupled HOD, and uncoupled HOD should be produced. This should be identifiable spectroscopically provided the $2HOD_{13}$ configuration contributes to the uncoupled HOD band intensity. Laser photoexcitation of the D_2O OD stretch modes and overtones in a D_2O/H_2O deposit cooled below 120 K may be one method of accomplishing this via a photoionization pathway.

Summary

The primary goal of this study was to elucidate the kinetics and resulting activation energies for isotopic scrambling in pure cubic ice. Pertinent to this goal was the identification and quantification of mixed isotope vapor deposited ice spectra and development of an experimentally consistent kinetic model to explain the observed spectral changes.

Twelve D_2O/H_2O vapor deposited ice samples were made at 130 K and 125 K where no isotopic exchange would occur. After warming these samples to 135, 140, 145, or 150 K to initiate exchange, FTIR spectra were collected at various time intervals to monitor the respective spectral changes. To help resolve these spectra into their various components for absorbance and concentration measurements, additional D_2O/H_2O ice samples lightly doped with 7-azaindole were made. The IR spectra collected from these ice samples were used to produce pure component D_2O spectra at the required kinetic temperatures. Using the pure component uncoupled HOD spectra collected at the completion of isotopic exchange, and previously determined pure component D_2O spectra, the FTIR spectra collected for each ice sample could be resolved into the individual D_2O, and uncoupled HOD spectra. Accordingly absorbances were extracted from these spectra.

Relative concentrations were ascertained from calculated relative molar absorptivities. Using a material balance equation a system of simultaneous equations utilizing the kinetic absorbance data was solved repetitively for the relative molar absorptivities of D_2O, coupled HOD, and uncoupled HOD.

With the kinetic concentration data in hand, a model was developed relating the various component concentration changes to the migration of ionic and Bjerrum D,L defects. By breaking the interaction of an ionic or Bjerrum D,L defect with a D_2O or HOD unit in an ice crystal into three steps, the attack factor, the transfer factor, and the leaving factor, it was possible to relate the individual transfer and rotational steps necessary in isotopic scrambling to a common set of transfer and rotation rate constants reflecting the rate of ionic defect migration and D,L defect migration. Approximations yielded both a one- or two-equilibrium model suitable for nonlinear least square fit in the experimental concentration data.

Using an iterative nonlinear least square routine both the one- and two-equilibrium models were fit to the data. The two-equilibrium model with feedback from separated HOD to coupled HOD gave a superior fit. From the rate constants determined with the two equilibrium model Arrhenius plots were constructed and analyzed for the respective transfer and rotational rate activation energies.

As with most investigations, more questions are raised than are answered. One of the interesting prospects raised in this study is what would be the effect of NH_3 or HF doping on the transfer or rotation rates? If rate suppression or enhancement is observed, then possibly the degree of suppression or enhancement could be used as a probe of the proton donicity or affinity of the dopant. A modification of the simultaneous deposit of sample and dopant would be a layered deposit where each layer is a different isotopic or chemical species. Two isotopes could be separated by a third sandwiched

layer which would have to transport protons for isotopic scrambling to occur. Proton transport across a specifically prepared molecular film could be monitored by this method. Thus there are numerous prospects for further study of proton trnasport in vapor deposited ice samples.

REFERENCES

(1) Rinne, F., Math.-Phys. Kl, 69, 57, (1917). St. John, A., Proc.
       Natn. Acad. Sci. U.S.A., 4, (1918).

(2) Bragg, W. H., Proc. Phys. Soc., 34, 98, (1922).

(3) Brill, R., and Tippe, A., Acta Cryst., 23, 343, (1967).

(4) Barnes, W. H., Proc. R. Soc., A125, 670, (1929).

(5) Bernal, J. D., and Fowler, R. H., J. Chem. Phys., 1, 515, (1933).

(6) Pauling, L., J. Am. Chem. Soc., 57, 2680, (1935).

(7) Bjerrum, W., K. Danshe Vidensk., 27, 1, (1951).

(8) Honjo, G., Kitamura, N., Shimaoka, K., and Mihama, K., J. Phys.
       Soc. Japan, 11, 527, (1956).

(9) Honjo, G., and Shimaoka, K., Acta Cryst., 10, 710, (1957).

(10) Bertie, J. E., Labbe', H. J., and Whalley, E., J. Chem. Phys.,
        50, 4501, (1969).

(11) Hardin, A. H., and Harvey, K. B., Spec. Acta, 29A, 1139, (1973).

(12) Li, P. C., and Devlin, J. P., J. Chem. Phys., 59, 547, (1973).

(13) Narten, A. H., Venkatesh, C. G., and Rice, S. A., J. Chem. Phys.,
        64, 1106, (1976).

(14) Whalley, E., Can. J. Chem., 55, 3429, (1977).

(15) Scherer, J. R., and Snyder, R. G., J. Chem. Phys., 67, 4794,
        (1977).

(16) Bergren, M. S., Schuh, D., Sceats, M. G., and Rice, S. A., J.
        Chem. Phys., 69, 3468, (1978).

(17) Sivakumar, T. C., Rice, S. A., and Sceats, M. G., J. Chem. Phys.,
        69, 3468, (1978).

(18) Scherer, J. R., Advances in Infrared and Raman Spectroscopy,
        (R. J. H. Clark and R. E. Hester, eds.), Vol. 5, Heyden,
        London, 1978, p. 149.

(19) Rhim, W. K., Burum, D. P., and Elleman, D. D., J. Chem. Phys., 71, 3139, (1979).

(20) Hagen, W., Tielens, A. G. G. M., and Greenberg, J. M., Chem. Phys., 56, 367, (1981).

(21) Theil, M. V., Becker, E. D., and Pimentel, G. C., J. Chem. Phys., 27, 486, (1957).

(22) Haas, C., and Hornig, D. F., J. Chem. Phys., 32, 1763, (1960).

(23) Tursi, A. J., and Nixon, E. R., J. Chem. Phys., 52, 1521, (1970).

(24) Ritzhaupt, G., and Devlin, J. P., J. Chem. Phys., 67, 4779, (1977).

(25) Ritzhaupt, G., Thornton, C., and Devlin, J. P., Chem. Phys. Lett., 59, 420, (1978).

(26) Ritzhaupt, G., Collier, W. B., Thornton, C., and Devlin, J. P., Chem. Phys. Lett., 70, 294, (1980).

(27) Sceats, M. G., Stavola, M., and Rice, S. A., J. Chem. Phys., 71, 983, (1979).

(28) Murby, E. J., and Pullin, A. D. E., Aust. J. Chem., 32, 1167, (1979).

(29) Bentwood, R. M., Barnes, A. J., and Orville-Thomas, W. J., J. Mole. Spec., 84, 391, (1980).

(30) Barnes, A. J., and Suzuki, S., J. Mole. Struct., 70, 301, (1981).

(31) McGraw, R., Madden, W. G., Bergren, M. S., Rice, S. A., and Sceats, M. G., J. Chem. Phys., 69, 3483, (1978).

(32) Madden, W. G., Bergren, M. S., McGraw, W. G., Rice, S. A., and Sceats, M. G., J. Chem. Phys., 69, 3497, (1978).

(33) Sceats, M. G., and Rice, S. A., J. Chem. Phys., 71, 973, (1979).

(34) Sceats, M. G., Stavola, M., and Rice, S. A., J. Chem. Phys., 71, 983, (1979).

(35) Morse, M. D., and Rice, S. A., J. Chem. Phys., 76, 650, (1981).

(36) Matsuoka, O., Clementi, E., and Yoshimine, M., J. Chem. Phys., 64, 1351, (1976).

(37) Conway, B. E., Bockris, J. O'M., Linton, H., J. Chem. Phys., 24, 834, (1956).

(38) Conway, B. E., Bockris, J. O'M., J. Chem. Phys., 28, 354, (1958).

(39) Kim, D., and Schmidt, V. H., Can. J. Phys., 45, 1507, (1967).

(40) Durand, M., Deleplanque, M., and Kahane, A., Sol. State Comm., 5, 759, (1967).

(41) Bullemer, B., Eisle, I., Engelhardt, H., Riehl, N., and Seige, P., Sol. State Comm., 6, 663, (1968).

(42) Hippel, A. von, Knoll, D. B., Westphal, W. B., J. Chem. Phys., 54, 134, (1971). Hippel, A. von, J. Chem. Phys., 54, 145, (1971). Maidique, M. A., Hippel, A. von, Westphal, W. B., J. Chem. Phys., 54, 150, (1971).

(43) Jaccard, C., Helv. Phys. Acta, 32, 89, (1959).

(44) Hubmann, M., Z. Physik B, 32, 127, (1979).

(45) Lumpkin, O., and Dixon, W. T., Chem. Phys. Lett., 62, 139, (1979).

(46) Ritzhaupt, G., and Devlin, J. P., Chem. Phys. Lett., 65, 592, (1979).

(47) Ritzhaupt, G., and Devlin, J. P., J. Chem. Phys., 72, 6807, (1980).

(48) Kunst, M., and Warman, J. M., Nature, 288, 465, (1980).

(49) Matsen, S. A., and Franklin, J. L., J. Am. Chem. Soc., 72, 3337, (1950).

(50) Lewis, E. S., and Johnson, M. D., J. Am. Chem. Soc., 82, 5399, (1960).

(51) Marquardt, D. W., J. Soc. Ind. Appl. Math., 11(2), 431, (1963).

(52) Nagle, J. F., and Tristram-Nagle, S., J. Mem. Biol., to be published.

APPENDIX A

FORTRAN PROGRAM REMOLE

```
          C   OSU BILL COLLIER CHEMISTRY PS203 4/27/82
          C   MAIN PROGRAM TO FIND D2O, (HOD)2, HOD RELATIVE MOLAR ABSORBTIVITIES
          C   FROM ABSORBANCE DATA AND MATERIAL BALANCE
          C   DOUBLE PRECISION USED
          C
          C                                      INITIALIZE PROGRAM AND READ CONTROL
          C                                      CARDS.   TIME DATA LISTED NEXT
          C                                      WITH TWO CARDS FOR GRAPHING
          C                                      ROUTINE LABELS IN FRONT OF EACH
          C                                      DATA SET
          C
0001            IMPLICIT REAL*8 (A-H,O-Z)
0002            DIMENSION ICARD(100),T(50),A(50),B(50),C(50),ITITLE(144),
               1IMAG4(5151),RANGE(4),ICHAR(10),OUT(50,3),AA(2,2),BB(2),WKAREA(20)
0003            DATA IN/5/,IOUT/6/,RANGE/4*0.0D00/
0004            DATA ICHAR/1HA,1HB,1HC,1H ,1H ,1H ,1H ,1H ,1H ,1H /
          C
          C                                      START DATA SETS LOOP, READ GRAPH
          C                                      TITLE, READ HOD AT T=INFINITY
          C                                      AB UNITS (CINF), ISTART, ISTOP
          C                                      LIMITS AND THEN EACH DATA SET
          C
0005            I = 0
0006      10    CONTINUE
0007            READ (IN,515) ISTART,ISTOP,NNCARD,CINF
0008            IF (ISTART.EQ.9999) STOP
0009            IF (ISTOP.LE.ISTART) GOTO 50
0010            IF (ISTART.GT.0) GOTO 15
0011            ISTART = IABS(ISTART)
0012            GOTO 35
0013      15    READ (IN,510) (ITITLE(M),M=1,144)
0014            I = I+1
0015            WRITE (IOUT,600)
0016            WRITE (IOUT,605) I
0017            DO 20 J=1,NNCARD
0018              READ (IN,520) T(J),A(J),B(J),C(J)
0019              C(J) = C(J)*CINF
0020              WRITE (IOUT,610) T(J),A(J),B(J),C(J)
0021      20    CONTINUE
          C
          C                                      PLOT INPUTTED DATA ON LINE
          C                                      PRINTER ROUTINE.   ALIGN DATA FILES
          C
0022            DO 30 J=1,NNCARD
0023              OUT(J,1) = A(J)
0024              OUT(J,2) = B(J)
0025              OUT(J,3) = C(J)
0026      30    CONTINUE
0027            INC = 1
0028            NP = NNCARD
0029            M = 3
0030            IOPT = 1
0031            IY = 50
0032            CALL USPLTD (T,OUT,IY,NP,M,INC,ITITLE,RANGE,ICHAR,IOPT,IMAG4,
               1  IER)
          C
          C                                      SOLVE FOR RELATIVE MOLAR ABSORBTION
          C                                      COEFFICIENTS FOR ALL UNIQUE BINARY
```

```
                  C                              COMBINATIONS OF OBSERVATIONS (TIMES)
                  C                              ISTART TO ISTOP
                  C
0033        35    WRITE (IOUT,615)
0034              SUME1 = 0.0D00
0035              SUME2 = 0.0D00
0036              SUME3 = 0.0D00
0037              SUMEE1 = 0.0D00
0038              SUMEE2 = 0.0D00
0039              SUMEE3 = 0.0D00
0040              NMIN1 = ISTOP-1
0041              ICOUNT = 0
0042              DO 40 J=ISTART,NMIN1
0043                NPLUS1 = J+1
0044                DO 45 K=NPLUS1,ISTOP
                  C
                  C                              SET UP AA MATRIX AND BB VECTOR
                  C                              FOR E1, E2, E3 SOLUTIONS, SET E3
                  C                              EQUAL TO 1.0 AND SOLVE TWO MATERIAL
                  C                              BALANCE EQUATIONS FOR E1 AND E2 WHERE
                  C                              2A/E1+2B/E2 = CINF-C
                  C
0045                AA(1,1) = A(J)
0046                AA(1,2) = B(J)
0047                AA(2,1) = A(K)
0048                AA(2,2) = B(K)
0049                BB(1) = CINF-C(J)
0050                BB(2) = CINF-C(K)
0051                CALL LEQT1F (AA,1,2,2,BB,2,WKAREA,IER)
0052                E1 = 2.0D00/BB(1)
0053                E2 = 2.0D00/BB(2)
0054                E3 = 1.0D00
0055                SUME1 = SUME1+E1
0056                SUME2 = SUME2+E2
0057                SUME3 = SUME3+E3
                  C
                  C                              SET UP AA MATRIX AND BB VECTOR
                  C                              FOR E1, E2, E3 SOLUTIONS, SET E2
                  C                              EQUAL TO 1.0 AND SOLVE TWO MATERIAL
                  C                              BALANCE EQUATIONS FOR E1 AND E3 WHERE
                  C                              CINF-C/2E3-A/E1 = B
                  C
0058                AA(1,1) = CINF-C(J)
0059                AA(1,2) = -A(J)
0060                AA(2,1) = CINF-C(K)
0061                AA(2,2) = -A(K)
0062                BB(1) = B(J)
0063                BB(2) = B(K)
0064                CALL LEQT1F (AA,1,2,2,BB,2,WKAREA,IER)
0065                EE1 = 1.0D00/BB(2)
0066                EE2 = 1.0D00
0067                EE3 = 0.5D00/BB(1)
0068                SUMEE1 = SUMEE1+EE1
0069                SUMEE2 = SUMEE2+EE2
0070                SUMEE3 = SUMEE3+EE3
0071                ICOUNT = ICOUNT+1
0072                WRITE (IOUT,620) J,K,T(J),T(K),E1,E2,E3,EE1,EE2,EE3
0073        45    CONTINUE
```

```
0074              40   CONTINUE
            C
            C                              FIND AVERAGE E'S AND PRINT RESULTS
            C
0075                 COUNTS = DFLOAT(ICOUNT)
0076                 AVEE1 = SUME1/COUNTS
0077                 AVEE2 = SUME2/COUNTS
0078                 AVEE3 = SUME3/COUNTS
0079                 AVEEE1 = SUMEE1/COUNTS
0080                 AVEEE2 = SUMEE2/COUNTS
0081                 AVEEE3 = SUMEE3/COUNTS
0082                 WRITE (IOUT,625) AVEE1,AVEE2,AVEE3,AVEEE1,AVEEE2,AVEEE3
0083                 GOTO 10
0084            50   WRITE (IOUT,630) ISTART,ISTOP
0085                 STOP
0086           510   FORMAT (72A1)
0087           515   FORMAT (3I5,F10.4)
0088           520   FORMAT (4F10.4)
0089           600   FORMAT ('1','PS203 BILL COLLIER CHEMISTRY',/,'0','RELATIVE MOLAR A
                    1BSORBTIVITIES BY SIMULTANEOUS EQUATIONS',//)
0090           605   FORMAT ('0','DATASET # ',I2,/,'0',6X,'MIN',7X,'D20',5X,'(HOD)2',
                    16X,'HOD',/)
0091           610   FORMAT (' ',4F10.4)
0092           615   FORMAT ('1','CALCULATED MOLAR ABSORBTIVITIES AT EACH STEP',/,'0',
                    1'OBS. #',3X,'OBS. #',3X,'TIME',3X,'TIME',6X,'E1',11X,'E2',11X,'E3'
                    2,11X,'EE1',10X,'EE2',10X,'EE3',/,' ')
0093           620   FORMAT (' ',I4,5X,I4,4X,F5.1,2X,F5.1,6D13.5)
0094           625   FORMAT ('0',3X,'AVERAGE E1',3X,'AVERAGE E2',3X,'AVERAGE E3',2X,'AV
                    1ERAGE EE1',2X,'AVERAGE EE2',2X,'AVERAGE EE3',//,' ',6D13.5)
0095           630   FORMAT ('0','ERROR ISTART = ',I3,' IS GREATER THAN ISTOP = ',I3)
0096                 END
```

PS203 BILL COLLIER CHEMISTRY

RELATIVE MOLAR ABSORBTIVITIES BY SIMULTANEOUS EQUATIONS

DATASET # 1

MIN	D20	(HOD)2	HOD
0.0	13.5000	3.1000	11.4000
3.0000	11.4000	4.5000	12.5400
6.0000	9.4000	5.4000	14.0600
9.0000	8.1500	5.9500	15.2000
12.0000	7.2500	6.1500	16.3400
17.0000	6.1500	5.9000	18.2400
21.7000	4.8000	5.5500	20.5200
27.0000	4.1000	5.1500	22.4200
32.0000	3.5000	4.7000	23.9400
42.0000	2.8500	3.9000	26.2200
52.0000	2.5000	3.4000	27.7400
62.0000	2.1000	2.8000	29.2600
72.0000	1.7000	2.5500	30.0200

D2O ISOLATED IN H2O 1/29/82 RUN 145K UNCORRECTED D2O VALUES

```
  0.30D+02  +*****************+*****************+*****************+*****************+*****************+*****************C
            *                                                                                              C        *
            *                                                                                                       *
            *                                                                                                       *
            *                                                                                     C                 *
  0.27D+02  +                                                                                                       +
            *                                                                                                       *
            *                                                                          C                            *
            *                                                                                                       *
  0.24D+02  +                                                                                                       +
            *                                                                 C                                     *
            *                                                          C                                            *
  0.22D+02  +                                                                                                       +
            *                                                                                                       *
            *                                             C                                                         *
A           *                                                                                                       *
R  0.19D+02 +                                                                                                       +
B           *                                    C                                                                  *
I           *                                                                                                       *
T           *                             C                                                                         *
R  0.16D+02 +                                                                                                       +
A           *                         C                                                                             *
R           *                   C                                                                                   *
Y           A                                                                                                       *
  0.13D+02  +                                                                                                       +
U           *      C                                                                                                *
N           C   A                                                                                                   *
I  0.10D+02 +                                                                                                       +
T           *       A                                                                                               *
S           *          A                                                                                            *
  0.74D+01  +        A                                                                                              +
            *                                                                                                       *
            *     B     B       A                                                                                   *
            *  B              B       B                                                                             *
  0.45D+01  + B                               B                                                                     +
            *                     A                 B                                                               *
            *                      A            A              B                                                    *
            B                                              A             B                          B              B*
  0.17D+01  +*****************+*****************+*****************+*****************+*****A***********+*****************A
          0.0              0.14D+02          0.29D+02          0.43D+02          0.58D+02          0.72D+02
```

                              T I M E   M I N U T E S

CALCULATED MOLAR ABSORBTIVITIES AT EACH STEP

OBS. #	OBS. #	TIME	TIME	E1	E2	E3	EE1	EE2	EE3
1	2	0.0	3.0	0.12464D+01	0.12557D+01	0.10000D+01	0.99254D+00	0.10000D+01	0.79634D+00
1	3	0.0	6.0	0.12606D+01	0.11964D+01	0.10000D+01	0.10536D+01	0.10000D+01	0.83581D+00
1	4	0.0	9.0	0.12572D+01	0.12100D+01	0.10000D+01	0.10390D+01	0.10000D+01	0.82646D+00
1	5	0.0	12.0	0.12557D+01	0.12164D+01	0.10000D+01	0.10323D+01	0.10000D+01	0.82213D+00
1	6	0.0	17.0	0.12664D+01	0.11745D+01	0.10000D+01	0.10782D+01	0.10000D+01	0.85145D+00
1	7	0.0	21.7	0.12852D+01	0.11089D+01	0.10000D+01	0.11590D+01	0.10000D+01	0.90182D+00
1	8	0.0	27.0	0.12812D+01	0.11220D+01	0.10000D+01	0.11418D+01	0.10000D+01	0.89123D+00
1	9	0.0	32.0	0.12918D+01	0.10878D+01	0.10000D+01	0.11876D+01	0.10000D+01	0.91930D+00
1	10	0.0	42.0	0.13036D+01	0.10530D+01	0.10000D+01	0.12380D+01	0.10000D+01	0.94967D+00
1	11	0.0	52.0	0.13013D+01	0.10596D+01	0.10000D+01	0.12281D+01	0.10000D+01	0.94377D+00
1	12	0.0	62.0	0.13206D+01	0.10072D+01	0.10000D+01	0.13111D+01	0.10000D+01	0.99281D+00
1	13	0.0	72.0	0.13532D+01	0.93281D+00	0.10000D+01	0.14506D+01	0.10000D+01	0.10720D+01
2	3	3.0	6.0	0.12946D+01	0.11467D+01	0.10000D+01	0.11290D+01	0.10000D+01	0.87207D+00
2	4	3.0	9.0	0.12746D+01	0.11886D+01	0.10000D+01	0.10723D+01	0.10000D+01	0.84129D+00
2	5	3.0	12.0	0.12683D+01	0.12026D+01	0.10000D+01	0.10546D+01	0.10000D+01	0.83152D+00
2	6	3.0	17.0	0.12916D+01	0.11527D+01	0.10000D+01	0.11206D+01	0.10000D+01	0.86756D+00
2	7	3.0	21.7	0.13304D+01	0.10814D+01	0.10000D+01	0.12302D+01	0.10000D+01	0.92469D+00
2	8	3.0	27.0	0.13198D+01	0.10996D+01	0.10000D+01	0.12002D+01	0.10000D+01	0.90941D+00
2	9	3.0	32.0	0.13417D+01	0.10630D+01	0.10000D+01	0.12621D+01	0.10000D+01	0.94071D+00
2	10	3.0	42.0	0.13670D+01	0.10249D+01	0.10000D+01	0.13337D+01	0.10000D+01	0.97568D+00
2	11	3.0	52.0	0.13621D+01	0.10320D+01	0.10000D+01	0.13198D+01	0.10000D+01	0.96899D+00
2	12	3.0	62.0	0.14062D+01	0.97336D+00	0.10000D+01	0.14447D+01	0.10000D+01	0.10274D+01
2	13	3.0	72.0	0.14766D+01	0.89830D+00	0.10000D+01	0.16437D+01	0.10000D+01	0.11132D+01
3	4	6.0	9.0	0.12338D+01	0.12411D+01	0.10000D+01	0.99410D+00	0.10000D+01	0.80575D+00
3	5	6.0	12.0	0.12330D+01	0.12424D+01	0.10000D+01	0.99247D+00	0.10000D+01	0.80490D+00
3	6	6.0	17.0	0.12883D+01	0.11555D+01	0.10000D+01	0.11150D+01	0.10000D+01	0.86546D+00
3	7	6.0	21.7	0.13645D+01	0.10628D+01	0.10000D+01	0.12840D+01	0.10000D+01	0.94095D+00
3	8	6.0	27.0	0.13417D+01	0.10878D+01	0.10000D+01	0.12334D+01	0.10000D+01	0.91926D+00
3	9	6.0	32.0	0.13816D+01	0.10452D+01	0.10000D+01	0.13219D+01	0.10000D+01	0.95676D+00
3	10	6.0	42.0	0.14297D+01	0.10009D+01	0.10000D+01	0.14285D+01	0.10000D+01	0.99913D+00
3	11	6.0	52.0	0.14204D+01	0.10089D+01	0.10000D+01	0.14079D+01	0.10000D+01	0.99117D+00
3	12	6.0	62.0	0.15104D+01	0.93972D+00	0.10000D+01	0.16073D+01	0.10000D+01	0.10642D+01
3	13	6.0	72.0	0.16475D+01	0.86204D+00	0.10000D+01	0.19111D+01	0.10000D+01	0.11600D+01
4	5	9.0	12.0	0.12316D+01	0.12441D+01	0.10000D+01	0.98995D+00	0.10000D+01	0.80379D+00
4	6	9.0	17.0	0.13562D+01	0.11038D+01	0.10000D+01	0.12287D+01	0.10000D+01	0.90598D+00
4	7	9.0	21.7	0.14798D+01	0.10098D+01	0.10000D+01	0.14654D+01	0.10000D+01	0.99031D+00
4	8	9.0	27.0	0.14222D+01	0.10495D+01	0.10000D+01	0.13551D+01	0.10000D+01	0.95284D+00
4	9	9.0	32.0	0.14875D+01	0.10049D+01	0.10000D+01	0.14802D+01	0.10000D+01	0.99511D+00
4	10	9.0	42.0	0.15750D+01	0.95578D+00	0.10000D+01	0.16478D+01	0.10000D+01	0.10463D+01
4	11	9.0	52.0	0.15583D+01	0.96435D+00	0.10000D+01	0.16159D+01	0.10000D+01	0.10370D+01
4	12	9.0	62.0	0.17445D+01	0.88433D+00	0.10000D+01	0.19727D+01	0.10000D+01	0.11308D+01
4	13	9.0	72.0	0.20016D+01	0.81193D+00	0.10000D+01	0.24652D+01	0.10000D+01	0.12316D+01
5	6	12.0	17.0	0.15797D+01	0.98547D+00	0.10000D+01	0.16030D+01	0.10000D+01	0.10147D+01
5	7	12.0	21.7	0.16863D+01	0.94170D+00	0.10000D+01	0.17907D+01	0.10000D+01	0.10619D+01
5	8	12.0	27.0	0.15411D+01	0.10040D+01	0.10000D+01	0.15350D+01	0.10000D+01	0.99604D+00
5	9	12.0	32.0	0.16370D+01	0.96077D+00	0.10000D+01	0.17038D+01	0.10000D+01	0.10408D+01
5	10	12.0	42.0	0.17872D+01	0.90796D+00	0.10000D+01	0.19684D+01	0.10000D+01	0.11014D+01
5	11	12.0	52.0	0.17591D+01	0.91673D+00	0.10000D+01	0.19189D+01	0.10000D+01	0.10908D+01
5	12	12.0	62.0	0.21415D+01	0.82611D+00	0.10000D+01	0.25923D+01	0.10000D+01	0.12105D+01
5	13	12.0	72.0	0.26096D+01	0.76380D+00	0.10000D+01	0.34167D+01	0.10000D+01	0.13092D+01
6	7	17.0	21.7	0.17786D+01	0.91868D+00	0.10000D+01	0.19360D+01	0.10000D+01	0.10885D+01
6	8	17.0	27.0	0.15205D+01	0.10111D+01	0.10000D+01	0.15039D+01	0.10000D+01	0.98904D+00
6	9	17.0	32.0	0.16647D+01	0.95384D+00	0.10000D+01	0.17452D+01	0.10000D+01	0.10484D+01
6	10	17.0	42.0	0.18963D+01	0.88897D+00	0.10000D+01	0.21332D+01	0.10000D+01	0.11249D+01
6	11	17.0	52.0	0.18526D+01	0.89934D+00	0.10000D+01	0.20600D+01	0.10000D+01	0.11119D+01
6	12	17.0	62.0	0.25678D+01	0.78825D+00	0.10000D+01	0.32576D+01	0.10000D+01	0.12686D+01
6	13	17.0	72.0	0.34195D+01	0.73006D+00	0.10000D+01	0.46839D+01	0.10000D+01	0.13697D+01
7	8	21.7	27.0	0.11061D+01	0.12612D+01	0.10000D+01	0.87701D+00	0.10000D+01	0.79288D+00
·	^	21.7	33.0	0.15807D+01	0.90998D+00	0.10000D+01	0.15300D+01	0.10000D+01	0.10061D+01

7	10	21.7	42.0	0.20784D+01	0.86307D+00	0.10000D+01	0.24082D+01	0.10000D+01	0.11387D+01
7	11	21.7	52.0	0.19646D+01	0.88140D+00	0.10000D+01	0.22290D+01	0.10000D+01	0.11346D+01
7	12	21.7	62.0	0.81693D+01	0.68078D+00	0.10000D+01	0.12000D+02	0.10000D+01	0.14689D+01
7	13	21.7	72.0	0.19684D+02	0.65324D+00	0.10000D+01	0.30133D+02	0.10000D+01	0.15308D+01
8	9	27.0	32.0	0.30477D+01	0.79910D+00	0.10000D+01	0.38140D+01	0.10000D+01	0.12514D+01
8	10	27.0	42.0	0.27632D+02	0.67394D+00	0.10000D+01	0.41000D+02	0.10000D+01	0.14838D+01
8	11	27.0	52.0	0.16015D+02	0.68357D+00	0.10000D+01	0.23429D+02	0.10000D+01	0.14629D+01
8	12	27.0	62.0	-0.95890D+00	0.42683D+00	0.10000D+01	-0.22466D+01	0.10000D+01	0.23429D+01
8	13	27.0	72.0	-0.24854D+01	0.54557D+00	0.10000D+01	-0.45556D+01	0.10000D+01	0.18329D+01
9	10	32.0	42.0	-0.95865D+00	0.44003D+00	0.10000D+01	-0.21786D+01	0.10000D+01	0.22725D+01
9	11	32.0	52.0	-0.71770D+00	0.39474D+00	0.10000D+01	-0.18182D+01	0.10000D+01	0.25333D+01
9	12	32.0	62.0	0.81871D-01	-0.13158D+00	0.10000D+01	-0.62222D+00	0.10000D+01	-0.76000D+01
9	13	32.0	72.0	-0.11313D+01	0.46425D+00	0.10000D+01	-0.24368D+01	0.10000D+01	0.21540D+01
10	11	42.0	52.0	-0.31579D+00	0.57416D+00	0.10000D+01	-0.55000D+01	0.10000D+01	0.17417D+01
10	12	42.0	62.0	0.38113D+00	-0.24561D+01	0.10000D+01	-0.15517D+00	0.10000D+01	-0.40714D+00
10	13	42.0	72.0	-0.11773D+01	0.46927D+00	0.10000D+01	-0.25088D+01	0.10000D+01	0.21310D+01
11	12	52.0	62.0	0.28340D+00	-0.92105D+00	0.10000D+01	-0.30769D+00	0.10000D+01	-0.10857D+01
11	13	52.0	72.0	-0.12281D+01	0.47448D+00	0.10000D+01	-0.25882D+01	0.10000D+01	0.21076D+01
12	13	62.0	72.0	-0.20877D+02	0.62632D+00	0.10000D+01	-0.33333D+02	0.10000D+01	0.15966D+01

AVERAGE E1	AVERAGE E2	AVERAGE E3	AVERAGE EE1	AVERAGE EE2	AVERAGE EE3
0.17510D+01	0.85713D+00	0.10000D+01	0.19007D+01	0.10000D+01	0.99247D+00

CALCULATED MOLAR ABSORBTIVITIES AT EACH STEP

OBS. #	OBS. #	TIME	TIME	E1	E2	E3	EE1	EE2	EE3
1	2	0.0	3.0	0.12464D+01	0.12557D+01	0.10000D+01	0.99254D+00	0.10000D+01	0.79634D+00
1	3	0.0	6.0	0.12606D+01	0.11964D+01	0.10000D+01	0.10536D+01	0.10000D+01	0.83581D+00
1	4	0.0	9.0	0.12572D+01	0.12100D+01	0.10000D+01	0.10390D+01	0.10000D+01	0.82646D+00
1	5	0.0	12.0	0.12557D+01	0.12164D+01	0.10000D+01	0.10323D+01	0.10000D+01	0.82213D+00
1	6	0.0	17.0	0.12664D+01	0.11745D+01	0.10000D+01	0.10782D+01	0.10000D+01	0.85145D+00
1	7	0.0	21.7	0.12852D+01	0.11089D+01	0.10000D+01	0.11590D+01	0.10000D+01	0.90182D+00
1	8	0.0	27.0	0.12812D+01	0.11220D+01	0.10000D+01	0.11418D+01	0.10000D+01	0.89123D+00
1	9	0.0	32.0	0.12918D+01	0.10878D+01	0.10000D+01	0.11876D+01	0.10000D+01	0.91930D+00
1	10	0.0	42.0	0.13036D+01	0.10530D+01	0.10000D+01	0.12380D+01	0.10000D+01	0.94967D+00
1	11	0.0	52.0	0.13013D+01	0.10596D+01	0.10000D+01	0.12281D+01	0.10000D+01	0.94377D+00
2	3	3.0	6.0	0.12946D+01	0.11467D+01	0.10000D+01	0.11290D+01	0.10000D+01	0.87207D+00
2	4	3.0	9.0	0.12746D+01	0.11886D+01	0.10000D+01	0.10723D+01	0.10000D+01	0.84129D+00
2	5	3.0	12.0	0.12683D+01	0.12026D+01	0.10000D+01	0.10546D+01	0.10000D+01	0.83152D+00
2	6	3.0	17.0	0.12916D+01	0.11527D+01	0.10000D+01	0.11206D+01	0.10000D+01	0.86756D+00
2	7	3.0	21.7	0.13304D+01	0.10814D+01	0.10000D+01	0.12302D+01	0.10000D+01	0.92469D+00
2	8	3.0	27.0	0.13198D+01	0.10996D+01	0.10000D+01	0.12002D+01	0.10000D+01	0.90941D+00
2	9	3.0	32.0	0.13417D+01	0.10630D+01	0.10000D+01	0.12621D+01	0.10000D+01	0.94071D+00
2	10	3.0	42.0	0.13670D+01	0.10249D+01	0.10000D+01	0.13337D+01	0.10000D+01	0.97568D+00
2	11	3.0	52.0	0.13621D+01	0.10320D+01	0.10000D+01	0.13198D+01	0.10000D+01	0.96899D+00
3	4	6.0	9.0	0.12338D+01	0.12411D+01	0.10000D+01	0.99410D+00	0.10000D+01	0.80575D+00
3	5	6.0	12.0	0.12330D+01	0.12424D+01	0.10000D+01	0.99247D+00	0.10000D+01	0.80490D+00
3	6	6.0	17.0	0.12883D+01	0.11555D+01	0.10000D+01	0.11150D+01	0.10000D+01	0.86546D+00
3	7	6.0	21.7	0.13645D+01	0.10628D+01	0.10000D+01	0.12840D+01	0.10000D+01	0.94095D+00
3	8	6.0	27.0	0.13417D+01	0.10878D+01	0.10000D+01	0.12334D+01	0.10000D+01	0.91926D+00
3	9	6.0	32.0	0.13816D+01	0.10452D+01	0.10000D+01	0.13219D+01	0.10000D+01	0.95676D+00
3	10	6.0	42.0	0.14297D+01	0.10009D+01	0.10000D+01	0.14285D+01	0.10000D+01	0.99913D+00
3	11	6.0	52.0	0.14204D+01	0.10089D+01	0.10000D+01	0.14079D+01	0.10000D+01	0.99117D+00
4	5	9.0	12.0	0.12316D+01	0.12441D+01	0.10000D+01	0.98995D+00	0.10000D+01	0.80379D+00
4	6	9.0	17.0	0.13562D+01	0.11038D+01	0.10000D+01	0.12287D+01	0.10000D+01	0.90598D+00
4	7	9.0	21.7	0.14798D+01	0.10098D+01	0.10000D+01	0.14654D+01	0.10000D+01	0.99031D+00
4	8	9.0	27.0	0.14222D+01	0.10495D+01	0.10000D+01	0.13551D+01	0.10000D+01	0.95284D+00
4	9	9.0	32.0	0.14875D+01	0.10049D+01	0.10000D+01	0.14802D+01	0.10000D+01	0.99511D+00
4	10	9.0	42.0	0.15750D+01	0.95578D+00	0.10000D+01	0.16478D+01	0.10000D+01	0.10463D+01
4	11	9.0	52.0	0.15583D+01	0.96435D+00	0.10000D+01	0.16159D+01	0.10000D+01	0.10370D+01
5	6	12.0	17.0	0.15797D+01	0.98547D+00	0.10000D+01	0.16030D+01	0.10000D+01	0.10147D+01
5	7	12.0	21.7	0.16863D+01	0.94170D+00	0.10000D+01	0.17907D+01	0.10000D+01	0.10619D+01
5	8	12.0	27.0	0.15411D+01	0.10040D+01	0.10000D+01	0.15350D+01	0.10000D+01	0.99604D+00
5	9	12.0	32.0	0.16370D+01	0.96077D+00	0.10000D+01	0.17038D+01	0.10000D+01	0.10408D+01
5	10	12.0	42.0	0.17872D+01	0.90796D+00	0.10000D+01	0.19684D+01	0.10000D+01	0.11014D+01
5	11	12.0	52.0	0.17591D+01	0.91673D+00	0.10000D+01	0.19189D+01	0.10000D+01	0.10908D+01
6	7	17.0	21.7	0.17786D+01	0.91868D+00	0.10000D+01	0.19360D+01	0.10000D+01	0.10885D+01
6	8	17.0	27.0	0.15205D+01	0.10111D+01	0.10000D+01	0.15039D+01	0.10000D+01	0.98904D+00
6	9	17.0	32.0	0.16647D+01	0.95384D+00	0.10000D+01	0.17452D+01	0.10000D+01	0.10484D+01
6	10	17.0	42.0	0.18963D+01	0.88897D+00	0.10000D+01	0.21332D+01	0.10000D+01	0.11249D+01
6	11	17.0	52.0	0.18526D+01	0.89934D+00	0.10000D+01	0.20600D+01	0.10000D+01	0.11119D+01
7	8	21.7	27.0	0.11061D+01	0.12612D+01	0.10000D+01	0.87701D+00	0.10000D+01	0.79288D+00
7	9	21.7	32.0	0.15207D+01	0.99398D+00	0.10000D+01	0.15300D+01	0.10000D+01	0.10061D+01
7	10	21.7	42.0	0.20784D+01	0.86307D+00	0.10000D+01	0.24082D+01	0.10000D+01	0.11587D+01
7	11	21.7	52.0	0.19646D+01	0.88140D+00	0.10000D+01	0.22290D+01	0.10000D+01	0.11346D+01
8	9	27.0	32.0	0.30477D+01	0.79910D+00	0.10000D+01	0.38140D+01	0.10000D+01	0.12514D+01
8	10	27.0	42.0	0.27632D+02	0.67394D+00	0.10000D+01	0.41000D+02	0.10000D+01	0.14838D+01
8	11	27.0	52.0	0.16015D+02	0.68357D+00	0.10000D+01	0.23429D+02	0.10000D+01	0.14629D+01
9	10	32.0	42.0	-0.95865D+00	0.44003D+00	0.10000D+01	-0.21786D+01	0.10000D+01	0.22725D+01
9	11	32.0	52.0	-0.71770D+00	0.39474D+00	0.10000D+01	-0.18182D+01	0.10000D+01	0.25333D+01
10	11	42.0	52.0	-0.31579D+01	0.57416D+00	0.10000D+01	-0.55000D+01	0.10000D+01	0.17417D+01

AVERAGE E1   AVERAGE E2   AVERAGE E3   AVERAGE EE1   AVERAGE EE2   AVERAGE EE3

CALCULATED MOLAR ABSORBTIVITIES AT EACH STEP

OBS. #	OBS. #	TIME	TIME	E1	E2	E3	EE1	EE2	EE3
1	2	0.0	3.0	0.12464D+01	0.12557D+01	0.10000D+01	0.99254D+00	0.10000D+01	0.79634D+00
1	3	0.0	6.0	0.12606D+01	0.11964D+01	0.10000D+01	0.10536D+01	0.10000D+01	0.83581D+00
1	4	0.0	9.0	0.12572D+01	0.12100D+01	0.10000D+01	0.10390D+01	0.10000D+01	0.82646D+00
1	5	0.0	12.0	0.12557D+01	0.12164D+01	0.10000D+01	0.10323D+01	0.10000D+01	0.82213D+00
1	6	0.0	17.0	0.12664D+01	0.11745D+01	0.10000D+01	0.10782D+01	0.10000D+01	0.85145D+00
1	7	0.0	21.7	0.12852D+01	0.11089D+01	0.10000D+01	0.11590D+01	0.10000D+01	0.90182D+00
1	8	0.0	27.0	0.12812D+01	0.11220D+01	0.10000D+01	0.11418D+01	0.10000D+01	0.89123D+00
2	3	3.0	6.0	0.12946D+01	0.11467D+01	0.10000D+01	0.11290D+01	0.10000D+01	0.87207D+00
2	4	3.0	9.0	0.12746D+01	0.11886D+01	0.10000D+01	0.10723D+01	0.10000D+01	0.84129D+00
2	5	3.0	12.0	0.12683D+01	0.12026D+01	0.10000D+01	0.10546D+01	0.10000D+01	0.83152D+00
2	6	3.0	17.0	0.12916D+01	0.11527D+01	0.10000D+01	0.11206D+01	0.10000D+01	0.86756D+00
2	7	3.0	21.7	0.13304D+01	0.10814D+01	0.10000D+01	0.12302D+01	0.10000D+01	0.92469D+00
2	8	3.0	27.0	0.13198D+01	0.10996D+01	0.10000D+01	0.12002D+01	0.10000D+01	0.90941D+00
3	4	6.0	9.0	0.12338D+01	0.12411D+01	0.10000D+01	0.99410D+00	0.10000D+01	0.80575D+00
3	5	6.0	12.0	0.12330D+01	0.12424D+01	0.10000D+01	0.99247D+00	0.10000D+01	0.80490D+00
3	6	6.0	17.0	0.12883D+01	0.11555D+01	0.10000D+01	0.11150D+01	0.10000D+01	0.86546D+00
3	7	6.0	21.7	0.13645D+01	0.10628D+01	0.10000D+01	0.12840D+01	0.10000D+01	0.94095D+00
3	8	6.0	27.0	0.13417D+01	0.10878D+01	0.10000D+01	0.12334D+01	0.10000D+01	0.91926D+00
4	5	9.0	12.0	0.12316D+01	0.12441D+01	0.10000D+01	0.98995D+00	0.10000D+01	0.80379D+00
4	6	9.0	17.0	0.13562D+01	0.11038D+01	0.10000D+01	0.12287D+01	0.10000D+01	0.90598D+00
4	7	9.0	21.7	0.14798D+01	0.10098D+01	0.10000D+01	0.14654D+01	0.10000D+01	0.99031D+00
4	8	9.0	27.0	0.14222D+01	0.10495D+01	0.10000D+01	0.13551D+01	0.10000D+01	0.95284D+00
5	6	12.0	17.0	0.15797D+01	0.98547D+00	0.10000D+01	0.16030D+01	0.10000D+01	0.10147D+01
5	7	12.0	21.7	0.16863D+01	0.94170D+00	0.10000D+01	0.17907D+01	0.10000D+01	0.10619D+01
5	8	12.0	27.0	0.15411D+01	0.10040D+01	0.10000D+01	0.15350D+01	0.10000D+01	0.99604D+00
6	7	17.0	21.7	0.17786D+01	0.91868D+00	0.10000D+01	0.19360D+01	0.10000D+01	0.10885D+01
6	8	17.0	27.0	0.15205D+01	0.10111D+01	0.10000D+01	0.16039D+01	0.10000D+01	0.98904D+00
7	8	21.7	27.0	0.11061D+01	0.12612D+01	0.10000D+01	0.87701D+00	0.10000D+01	0.79288D+00

AVERAGE E1	AVERAGE E2	AVERAGE E3	AVERAGE EE1	AVERAGE EE2	AVERAGE EE3
0.13498D+01	0.11241D+01	0.10000D+01	0.12217D+01	0.10000D+01	0.89658D+00

CALCULATED MOLAR ABSORBTIVITIES AT EACH STEP

OBS. #	OBS. #	TIME	TIME	E1	E2	E3	EE1	EE2	EE3
1	2	0.0	3.0	0.12464D+01	0.12557D+01	0.10000D+01	0.99254D+00	0.10000D+01	0.79634D+00
1	3	0.0	6.0	0.12606D+01	0.11964D+01	0.10000D+01	0.10536D+01	0.10000D+01	0.83581D+00
1	4	0.0	9.0	0.12572D+01	0.12100D+01	0.10000D+01	0.10390D+01	0.10000D+01	0.82646D+00
1	5	0.0	12.0	0.12557D+01	0.12164D+01	0.10000D+01	0.10323D+01	0.10000D+01	0.82213D+00
1	6	0.0	17.0	0.12664D+01	0.11745D+01	0.10000D+01	0.10782D+01	0.10000D+01	0.85145D+00
1	7	0.0	21.7	0.12852D+01	0.11089D+01	0.10000D+01	0.11590D+01	0.10000D+01	0.90182D+00
2	3	3.0	6.0	0.12946D+01	0.11467D+01	0.10000D+01	0.11290D+01	0.10000D+01	0.87207D+00
2	4	3.0	9.0	0.12746D+01	0.11886D+01	0.10000D+01	0.10723D+01	0.10000D+01	0.84129D+00
2	5	3.0	12.0	0.12683D+01	0.12026D+01	0.10000D+01	0.10546D+01	0.10000D+01	0.83152D+00
2	6	3.0	17.0	0.12916D+01	0.11527D+01	0.10000D+01	0.11206D+01	0.10000D+01	0.86756D+00
2	7	3.0	21.7	0.13304D+01	0.10814D+01	0.10000D+01	0.12302D+01	0.10000D+01	0.92469D+00
3	4	6.0	9.0	0.12338D+01	0.12411D+01	0.10000D+01	0.99410D+00	0.10000D+01	0.80575D+00
3	5	6.0	12.0	0.12330D+01	0.12424D+01	0.10000D+01	0.99247D+00	0.10000D+01	0.80490D+00
3	6	6.0	17.0	0.12883D+01	0.11555D+01	0.10000D+01	0.11150D+01	0.10000D+01	0.86546D+00
3	7	6.0	21.7	0.13645D+01	0.10628D+01	0.10000D+01	0.12840D+01	0.10000D+01	0.94095D+00
4	5	9.0	12.0	0.12316D+01	0.12441D+01	0.10000D+01	0.98995D+00	0.10000D+01	0.80379D+00
4	6	9.0	17.0	0.13562D+01	0.11038D+01	0.10000D+01	0.12287D+01	0.10000D+01	0.90598D+00
4	7	9.0	21.7	0.14798D+01	0.10098D+01	0.10000D+01	0.14654D+01	0.10000D+01	0.99031D+00
5	6	12.0	17.0	0.15797D+01	0.98547D+00	0.10000D+01	0.16030D+01	0.10000D+01	0.10147D+01
5	7	12.0	21.7	0.16863D+01	0.94170D+00	0.10000D+01	0.17907D+01	0.10000D+01	0.10619D+01
6	7	17.0	21.7	0.17786D+01	0.91868D+00	0.10000D+01	0.19360D+01	0.10000D+01	0.10885D+01

AVERAGE E1	AVERAGE E2	AVERAGE E3	AVERAGE EE1	AVERAGE EE2	AVERAGE EE3
0.13458D+01	0.11352D+01	0.10000D+01	0.12077D+01	0.10000D+01	0.88826D+00

CALCULATED MOLAR ABSORBTIVITIES AT EACH STEP

OBS. #	OBS. #	TIME	TIME	E1	E2	E3	EE1	EE2	EE3
1	2	0.0	3.0	0.12464D+01	0.12557D+01	0.10000D+01	0.99254D+00	0.10000D+01	0.79634D+00
1	3	0.0	6.0	0.12606D+01	0.11964D+01	0.10000D+01	0.10536D+01	0.10000D+01	0.83581D+00
1	4	0.0	9.0	0.12572D+01	0.12100D+01	0.10000D+01	0.10390D+01	0.10000D+01	0.82646D+00
1	5	0.0	12.0	0.12557D+01	0.12164D+01	0.10000D+01	0.10323D+01	0.10000D+01	0.82213D+00
1	6	0.0	17.0	0.12664D+01	0.11745D+01	0.10000D+01	0.10782D+01	0.10000D+01	0.85145D+00
2	3	3.0	6.0	0.12946D+01	0.11467D+01	0.10000D+01	0.11290D+01	0.10000D+01	0.87207D+00
2	4	3.0	9.0	0.12746D+01	0.11886D+01	0.10000D+01	0.10723D+01	0.10000D+01	0.84129D+00
2	5	3.0	12.0	0.12683D+01	0.12026D+01	0.10000D+01	0.10546D+01	0.10000D+01	0.83152D+00
2	6	3.0	17.0	0.12916D+01	0.11527D+01	0.10000D+01	0.11206D+01	0.10000D+01	0.86756D+00
3	4	6.0	9.0	0.12338D+01	0.12411D+01	0.10000D+01	0.99410D+00	0.10000D+01	0.80575D+00
3	5	6.0	12.0	0.12330D+01	0.12424D+01	0.10000D+01	0.99247D+00	0.10000D+01	0.80490D+00
3	6	6.0	17.0	0.12883D+01	0.11555D+01	0.10000D+01	0.11150D+01	0.10000D+01	0.86546D+00
4	5	9.0	12.0	0.12316D+01	0.12441D+01	0.10000D+01	0.98995D+00	0.10000D+01	0.80379D+00
4	6	9.0	17.0	0.13562D+01	0.11038D+01	0.10000D+01	0.12287D+01	0.10000D+01	0.90598D+00
5	6	12.0	17.0	0.15797D+01	0.98547D+00	0.10000D+01	0.16030D+01	0.10000D+01	0.10147D+01

AVERAGE E1	AVERAGE E2	AVERAGE E3	AVERAGE EE1	AVERAGE EE2	AVERAGE EE3
0.12892D+01	0.11811D+01	0.10000D+01	0.10997D+01	0.10000D+01	0.84968D+00

APPENDIX B

INPUT INSTRUCTIONS TO FORTRAN SUBROUTINE DGEAR

PURPOSE   - DIFFERENTIAL EQUATION SOLVER - VARIABLE ORDER
                        ADAMS PREDICTOR CORRECTOR METHOD OR
                        GEARS METHOD

USAGE   - CALL DGEAR (N,FCN,FCNJ,X,H,Y,XEND,TOL,METH,
                        MITER,INDEX,IWK,WK,IER)

ARGUMENTS   N   - INPUT NUMBER OF FIRST-ORDER DIFFERENTIAL
                        EQUATIONS. N CAN BE REDUCED, BUT NEVER
                        INCREASED, DURING A PROBLEM. N MUST BE
                        GREATER THAN ZERO.
             FCN   - NAME OF SUBROUTINE FOR EVALUATING FUNCTIONS.
                        (INPUT)
                        THE SUBROUTINE ITSELF MUST ALSO BE PROVIDED
                          BY THE USER AND IT SHOULD BE OF THE
                          FOLLOWING FORM
                            SUBROUTINE FCN (N,X,Y,YPRIME)
                            REAL Y(N),YPRIME(N)
                                  .
                                  .
                                  .
                        FCN SHOULD EVALUATE YPRIME(1),...,YPRIME(N)
                          GIVEN N,X, AND Y(1),...,Y(N). YPRIME(I)
                          IS THE FIRST DERIVATIVE OF Y(I) WITH
                          RESPECT TO X.
                        FCN MUST APPEAR IN AN EXTERNAL STATEMENT IN
                          THE CALLING PROGRAM AND N,X,Y(1),...,Y(N)
                          MUST NOT BE ALTERED BY FCN.
             FCNJ   - NAME OF THE SUBROUTINE FOR COMPUTING THE N BY
                        N JACOBIAN MATRIX OF PARTIAL DERIVATIVES.
                        (INPUT)
                        THE SUBROUTINE ITSELF MUST ALSO BE PROVIDED
                          BY THE USER AND IT SHOULD BE OF THE
                          FOLLOWING FORM
                            SUBROUTINE FCNJ (N,X,Y,PD)
                            REAL Y(N),PD(N,N)
                                  .
                                  .
                                  .
                        FCNJ SHOULD COMPUTE PD(I,J) WHICH IS THE
                          PARTIAL DERIVATIVE OF YPRIME(I) WITH
                          RESPECT TO Y(J).
                        FCNJ MUST APPEAR IN AN EXTERNAL STATEMENT IN
                          THE CALLING PROGRAM AND N,X,Y(1),...,Y(N)
                          MUST NOT BE ALTERED BY FCNJ.
                        FCNJ IS CALLED ONLY IF MITER IS EQUAL TO
                          ONE. OTHERWISE A DUMMY ROUTINE CAN BE
                          SUBSTITUTED. SEE REMARKS.
             X   - INDEPENDENT VARIABLE. (INPUT AND OUTPUT)
                        ON INPUT, X SUPPLIES THE INITIAL VALUE AND
                          AND IS USED ONLY ON THE FIRST CALL.
                        ON OUTPUT, X IS REPLACED WITH THE CURRENT
                          VALUE OF THE INDEPENDENT VARIABLE AT WHICH
                          INTEGRATION HAS BEEN COMPLETED.

H   - INPUT/OUTPUT.
          ON INPUT, H CONTAINS THE NEXT STEP SIZE IN
            X. H IS USED ONLY ON THE FIRST CALL.
          ON OUTPUT, H CONTAINS THE STEP SIZE USED
            LAST, WHETHER SUCCESSFULLY OR NOT.

Y   - DEPENDENT VARIABLES, VECTOR OF LENGTH N.
          (INPUT AND OUTPUT)
          ON INPUT, Y(1),...,Y(N) SUPPLY INITIAL
            VALUES.
          ON OUTPUT, Y(1),...,Y(N) ARE REPLACED WITH
            A COMPUTED VALUE AT XEND.

XEND   - INPUT VALUE OF X AT WHICH SOLUTION IS DESIRED
          NEXT. INTEGRATION WILL NORMALLY GO SLIGHTLY
          BEYOND XEND AND THE ROUTINE WILL INTERPOLATE
          TO X = XEND.
          NOTE THAT (X-XEND)*H MUST BE LESS THAN
          ZERO (X AND H AS SPECIFIED ON INPUT).

TOL   - INPUT RELATIVE ERROR BOUND. TOL MUST BE
          GREATER THAN ZERO. TOL IS USED ONLY ON THE
          FIRST CALL UNLESS INDEX IS EQUAL TO -1.
          TOL SHOULD BE AT LEAST AN ORDER OF
          MAGNITUDE LARGER THAN THE UNIT ROUNDOFF
          BUT GENERALLY NOT LARGER THAN .001.
          SINGLE STEP ERROR ESTIMATES DIVIDED BY
          YMAX(I) WILL BE KEPT LESS THAN TOL IN
          ROOT-MEAN-SQUARE NORM (EUCLIDEAN NORM
          DIVIDED BY SQRT(N)). THE VECTOR YMAX OF
          WEIGHTS IS COMPUTED INTERNALLY AND STORED
          IN WORK VECTOR WK. INITIALLY YMAX(I) IS
          THE ABSOLUTE VALUE OF Y(I), WITH A DEFAULT
          VALUE OF ONE IF Y(I) IS EQUAL TO ZERO.
          THEREAFTER, YMAX(I) IS THE LARGEST VALUE
          OF THE ABSOLUTE VALUE OF Y(I) SEEN SO FAR,
          OR THE INITIAL VALUE OF YMAX(I) IF THAT IS
          LARGER.

METH   - INPUT BASIC METHOD INDICATOR.
          USED ONLY ON THE FIRST CALL UNLESS INDEX IS
          EQUAL TO -1.
         METH = 1, IMPLIES THAT THE ADAMS METHOD IS
           TO BE USED.
         METH = 2, IMPLIES THAT THE STIFF METHODS OF
           GEAR, OR THE BACKWARD DIFFERENTIATION
           FORMULAE ARE TO BE USED.

MITER - INPUT ITERATION METHOD INDICATOR.
         MITER = 0, IMPLIES THAT FUNCTIONAL
           ITERATION IS USED. NO PARTIAL
           DERIVATIVES ARE NEEDED. A DUMMY FCNJ
           CAN BE USED.
         MITER = 1, IMPLIES THAT THE CHORD METHOD
           IS USED WITH AN ANALYTIC JACOBIAN. FOR
           THIS METHOD, THE USER SUPPLIES
           SUBROUTINE FCNJ.
         MITER = 2, IMPLIES THAT THE CHORD METHOD
           IS USED WITH THE JACOBIAN CALCULATED
           INTERNALLY BY FINITE DIFFERENCES.
           A DUMMY FCNJ CAN BE USED.

```
        MITER = 3, IMPLIES THAT THE CHORD METHOD
          IS USED WITH THE JACOBIAN REPLACED BY
          A DIAGONAL APPROXIMATION BASED ON A
          DIRECTIONAL DERIVATIVE.
          A DUMMY FCNJ CAN BE USED.
INDEX   - INPUT AND OUTPUT PARAMETER USED TO INDICATE
          THE TYPE OF CALL TO THE SUBROUTINE.
          ON INPUT, INDEX = 1, IMPLIES THAT THIS IS THE
          FIRST CALL FOR THIS PROBLEM. ON OUTPUT INDEX
          IS RESET TO 0 IF INTEGRATION WAS SUCCESSFUL.
          OTHERWISE, THE VALUE OF INDEX IS UNCHANGED.
          ON INPUT, INDEX = 0, IMPLIES THAT THIS IS NOT
          THE FIRST CALL FOR THIS PROBLEM. INDEX IS
          UNCHANGED ON OUTPUT.
          ON INPUT, INDEX = -1, IMPLIES THAT THIS IS NOT
          THE FIRST CALL FOR THIS PROBLEM, AND THE
          USER HAS RESET TOL. ON OUTPUT INDEX IS RESET
          TO 0 IF INTEGRATION WAS SUCCESSFUL.
          OTHERWISE THE VALUE OF INDEX IS UNCHANGED.
          ON INPUT, INDEX = 2, IMPLIES THAT THIS IS NOT
          THE FIRST CALL FOR THIS PROBLEM. INTEGRATION
          IS TO CONTINUE AND XEND IS TO BE HIT EXACTLY
          (NO INTERPOLATION IS DONE). THIS VALUE OF
          INDEX ASSUMES THAT XEND IS BEYOND THE
          CURRENT VALUE OF X. INDEX IS UNCHANGED ON
          OUTPUT.
          ON INPUT, INDEX = 3, IMPLIES THAT THIS IS NOT
          THE FIRST CALL FOR THIS PROBLEM. INTEGRATION
          IS TO CONTINUE AND CONTROL IS TO BE RETURNED
          TO THE CALLING PROGRAM AFTER ONE STEP. XEND
          IS IGNORED. INDEX IS UNCHANGED ON OUTPUT.
IWK     - INTEGER WORK VECTOR OF LENGTH N. USED ONLY IF
          MITER IS EQUAL TO 1 OR 2.
WK      - REAL WORK VECTOR OF LENGTH 4*N+NMETH+NMITER.
          THE VALUE OF NMETH DEPENDS ON THE VALUE OF
          METH.
          IF METH IS EQUAL TO 1,
            NMETH IS EQUAL TO N*13.
          IF METH IS EQUAL TO 2,
            NMETH IS EQUAL TO N*6.
          THE VALUE OF NMITER DEPENDS ON THE VALUE OF
          MITER.
          IF MITER IS EQUAL TO 1 OR 2,
            NMITER IS EQUAL TO N*(N+1).
          IF MITER IS EQUAL TO 3,
            NMITER IS EQUAL TO N.
          IF MITER IS EQUAL TO 0,
            NMITER IS EQUAL TO 1.
          WK MUST REMAIN UNCHANGED BETWEEN SUCCESSIVE
          CALLS DURING INTEGRATION.
IER     - ERROR PARAMETER. (OUTPUT)
          WARNING ERROR
          IER = 33, IMPLIES THAT X+H WILL EQUAL X ON
            THE NEXT STEP. THIS CONDITION DOES NOT
            FORCE THE ROUTINE TO HALT. HOWEVER, IT
            DOES INDICATE ONE OF TWO CONDITIONS.
```

THE USER MIGHT BE REQUIRING TOO MUCH
ACCURACY VIA THE INPUT PARAMETER TOL.
IN THIS CASE THE USER SHOULD CONSIDER
INCREASING THE VALUE OF TOL. THE OTHER
CONDITION WHICH MIGHT GIVE RISE TO THIS
ERROR MESSAGE IS THAT THE SYSTEM OF
DIFFERENTIAL EQUATIONS BEING SOLVED
IS STIFF (EITHER IN GENERAL OR OVER
THE SUBINTERVAL OF THE PROBLEM BEING
SOLVED AT THE TIME OF THE ERROR). IN
THIS CASE THE USER SHOULD CONSIDΓR
USING A NONZERO VALUE FOR THE INPUT
PARAMETER MITER.

WARNING WITH FIX ERROR

IER = 66, IMPLIES THAT THE ERROR TEST
FAILED. H WAS REDUCED BY .1 ONE OR MORE
TIMES AND THE STEP WAS TRIED AGAIN
SUCCESSFULLY.

IER = 67, IMPLIES THAT CORRECTOR
CONVERGENCE COULD NOT BE ACHIEVED.
H WAS REDUCED BY .1 ONE OR MORE TIMES AND
THE STEP WAS TRIED AGAIN SUCCESSFULLY.

TERMINAL ERROR

IER = 132, IMPLIES THE INTEGRATION WAS
HALTED AFTER FAILING TO PASS THE ERROR
TEST EVEN AFTER REDUCING H BY A FACTOR
OF 1.0E10 FROM ITS INITIAL VALUE.
SEE REMARKS.

IER = 133, IMPLIES THE INTEGRATION WAS
HALTED AFTER FAILING TO ACHIEVE
CORRECTOR CONVERGENCE EVEN AFTER
REDUCING H BY A FACTOR OF 1.0E10 FROM
ITS INITIAL VALUE. SEE REMARKS.

IER = 134, IMPLIES THAT AFTER SOME INITIAL
SUCCESS, THE INTEGRATION WAS HALTED EITHER
BY REPEATED ERROR TEST FAILURES OR BY
A TEST ON TOL. SEE REMARKS.

IER = 135, IMPLIES THAT ONE OF THE INPUT
PARAMETERS N,X,H,XEND,TOL,METH,MITER, OR
INDEX WAS SPECIFIED INCORRECTLY.

IER = 136, IMPLIES THAT INDEX HAD A VALUE
OF -1 ON INPUT, BUT THE DESIRED CHANGES
OF PARAMETERS WERE NOT IMPLEMENTED
BECAUSE XEND WAS NOT BEYOND X.
INTERPOLATION TO X = XEND WAS PERFORMED.
TO TRY AGAIN, SIMPLY CALL AGAIN WITH
INDEX EQUAL TO -1 AND A NEW VALUE FOR
XEND.

PRECISION/HARDWARE - SINGLE AND DOUBLE/H32
                       - SINGLE/H36,H48,H60

REQD. IMSL ROUTINES - DGRCS,DGRIN,DGRPS,DGRST,LUDATF,LUELMF,UERTST,
                       UGETIO

REMARKS   1.   THE EXTERNAL SUBROUTINE FCNJ IS USED ONLY WHEN
INPUT PARAMETER MITER IS EQUAL TO 1. OTHERWISE, A
DUMMY FUNCTION CAN BE USED. THE DUMMY SUBROUTINE
SHOULD BE OF THE FOLLOWING FORM

```
    SUBROUTINE FCNJ (N,X,Y,PD)
    INTEGER N
    REAL Y(N),PD(N,N),X
    RETURN
    END
```

       2.   AFTER THE INITIAL CALL, IF A NORMAL RETURN OCCURRED
(IER=0) AND A NORMAL CONTINUATION IS DESIRED, SIMPLY
RESET XEND AND CALL DGEAR AGAIN. ALL OTHER
PARAMETERS WILL BE READY FOR THE NEXT CALL. A CHANGE
OF PARAMETERS WITH INDEX EQUAL TO -1 CAN BE MADE
AFTER EITHER A SUCCESSFUL OR AN UNSUCCESSFUL RETURN.

       3.   THE COMMON BLOCK /GEAR/ USED IN DGEAR NEEDS TO BE
PRESERVED BETWEEN CALLS TO DGEAR. IF IT IS NECESSARY
FOR THE COMMON BLOCK TO EXIST IN THE CALLING PROGRAM
THE FOLLOWING STATEMENT SHOULD BE INCLUDED

```
    COMMON  /GEAR/ DUMMY(48),SDUMMY(4),IDUMMY(38)
```

WHERE DUMMY, SDUMMY, AND IDUMMY ARE VARIABLE NAMES NOT
USED ELSEWHERE IN THE CALLING PROGRAM.   (FOR DOUBLE
PRECISION DUMMY IS TYPE DOUBLE AND SDUMMY IS TYPE REAL)

       4.   THE CHOICE OF VALUES FOR METH AND MITER MAY REQUIRE
SOME EXPERIMENTATION, AND ALSO SOME CONSIDERATION OF
THE NATURE OF THE PROBLEM AND OF STORAGE REQUIREMENTS.
THE PRIME CONSIDERATION IS STIFFNESS. IF
THE PROBLEM IS NOT STIFF, THE BEST CHOICE IS PROBABLY
METH = 1 WITH MITER = 0. IF THE PROBLEM IS STIFF TO A
SIGNIFICANT DEGREE, THEN METH SHOULD BE 2 AND MITER
SHOULD BE 1, 2, OR 3. IF THE USER HAS NO KNOWLEDGE OF
THE INHERENT TIME CONSTANTS OF THE PROBLEM, WITH
WHICH TO PREDICT ITS STIFFNESS, ONE WAY TO DETERMINE
THIS IS TO TRY METH = 1 AND MITER = 0 FIRST, AND LOOK
AT THE BEHAVIOR OF THE SOLUTION COMPUTED AND THE STEP
SIZES USED. IF THE TYPICAL VALUES OF H ARE MUCH
SMALLER THAN THE SOLUTION BEHAVIOR WOULD SEEM TO
REQUIRE (THAT IS, MORE THAN 100 STEPS ARE TAKEN OVER
AN INTERVAL IN WHICH THE SOLUTIONS CHANGE BY LESS
THAN ONE PERCENT), THEN THE PROBLEM IS PROBABLY STIFF
AND THE DEGREE OF STIFFNESS CAN BE ESTIMATED FROM THE
VALUES OF H USED AND THE SMOOTHNESS OF THE SOLUTION.
IF THE DEGREE OF STIFFNESS IS ONLY SLIGHT, IT MAY BE
THAT METH = 1 IS MORE EFFICIENT THAN METH = 2.
EXPERIMENTATION WOULD BE REQUIRED TO DETERMINE THIS.
REGARDLESS OF METH, THE LEAST EFFECTIVE VALUE OF
MITER IS 0, AND THE MOST EFFECTIVE IS 1 OR 2.
MITER = 3 IS GENERALLY SOMEWHERE IN BETWEEN. SINCE
THE STORAGE REQUIREMENTS GO UP IN THE SAME ORDER AS
EFFECTIVENESS, TRADE-OFF CONSIDERATIONS ARE
NECESSARY. FOR REASONS OF ACCURACY AND SPEED, THE
CHOICE OF MITER = 1 IS GENERALLY PREFERRED TO
MITER = 2, UNLESS THE SYSTEM IS FAIRLY COMPLICATED

(AND FCNJ IS THUS NOT FEASIBLE TO CODE). THE
ACCURACY OF THE FCNJ CALCULATION CAN BE CHECKED BY
COMPARISON OF THE JACOBIAN WITH THAT GENERATED WITH
MITER = 2. IF THE JACOBIAN MATRIX IS SIGNIFICANTLY
DIAGONALLY DOMINANT, THEN THE OPTION MITER = 3 IS
LIKELY TO BE NEARLY AS EFFECTIVE AS MITER = 1 OR 2,
AND WILL SAVE CONSIDERABLE STORAGE AND RUN TIME.
IT IS POSSIBLE, AND POTENTIALLY QUITE DESIRABLE, TO
USE DIFFERENT VALUES OF METH AND MITER IN DIFFERENT
SUBINTERVALS OF THE PROBLEM. FOR EXAMPLE, IF THE
PROBLEM IS NON-STIFF INITIALLY AND STIFF LATER,
METH = 1 AND MITER = 0 MIGHT BE SET INITIALLY, AND
METH = 2 AND MITER = 1 LATER.

5.   THE INITIAL VALUE OF THE STEP SIZE, H, SHOULD BE
CHOSEN CONSIDERABLY SMALLER THAN THE AVERAGE VALUE
EXPECTED FOR THE PROBLEM, AS THE FIRST-ORDER METHOD
WITH WHICH DGEAR BEGINS IS NOT GENERALLY THE MOST
EFFICIENT ONE. HOWEVER, FOR THE FIRST STEP, AS FOR
EVERY STEP, DGEAR TESTS FOR THE POSSIBILITY THAT
THE STEP SIZE WAS TOO LARGE TO PASS THE ERROR TEST
(BASED ON TOL), AND IF SO ADJUSTS THE STEP SIZE
DOWN AUTOMATICALLY. THIS DOWNWARD ADJUSTMENT, IF
ANY, IS NOTED BY IER HAVING THE VALUES 66 OR 67,
AND SUBSEQUENT RUNS ON THE SAME OR SIMILAR PROBLEM
SHOULD BE STARTED WITH AN APPROPRIATELY SMALLER
VALUE OF H.

6.   SOME OF THE VALUES OF INTEREST LOCATED IN THE
COMMON BLOCK /GEAR/ ARE
A.   HUSED, THE STEP SIZE H LAST USED SUCCESSFULLY
(DUMMY(8))
B.   NQUSED, THE ORDER LAST USED SUCCESSFULLY
(IDUMMY(6))
C.   NSTEP, THE CUMULATIVE NUMBER OF STEPS TAKEN
(IDUMMY(7))
D.   NFE, THE CUMULATIVE NUMBER OF FCN EVALUATIONS
(IDUMMY(8))
E.   NJE, THE CUMULATIVE NUMBER OF JACOBIAN
EVALUATIONS, AND HENCE ALSE OF MATRIX LU
DECOMPOSITIONS (IDUMMY(9))

7.   THE NORMAL USAGE OF DGEAR MAY BE SUMMARIZED AS FOLLOWS
A.   SET THE INITIAL VALUES IN Y.
B.   SET N, X, H, TOL, METH, AND MITER.
C.   SET XEND TO THE FIRST OUTPUT POINT, AND INDEX TO 1.
D.   CALL DGEAR
E.   EXIT IF IER IS GREATER THAN 128.
F.   OTHERWISE, DO DESIRED OUTPUT OF Y.
G.   EXIT IF THE PROBLEM IS FINISHED.
H.   OTHERWISE, RESET XEND TO THE NEXT OUTPUT POINT, AND
RETURN TO STEP D.

8.   THE ERROR WHICH IS CONTROLLED BY WAY OF THE PARAMETER
TOL IS AN ESTIMATE OF THE LOCAL TRUNCATION ERROR, THAT
IS, THE ERROR COMMITTED ON TAKING A SINGLE STEP WITH
THE METHOD, STARTING WITH DATA REGARDED AS EXACT. THIS
IS TO BE DISTINGUISHED FROM THE GLOBAL TRUNCATION
ERROR, WHICH IS THE ERROR IN ANY GIVEN COMPUTED VALUE
OF Y(X) AS A RESULT OF THE LOCAL TRUNCATION ERRORS
FROM ALL STEPS TAKEN TO OBTAIN Y(X). THE LATTER ERROR

ACCUMULATES IN A NON-TRIVIAL WAY FROM THE LOCAL
ERRORS, AND IS NEITHER ESTIMATED NOR CONTROLLED BY 172
THE ROUTINE. SINCE IT IS USUALLY THE GLOBAL ERROR THAT
A USER WANTS TO HAVE UNDER CONTROL, SOME
EXPERIMENTATION MAY BE NECESSARY TO GET THE RIGHT
VALUE OF TOL TO ACHIEVE THE USERS NEEDS. IF THE
PROBLEM IS MATHEMATICALLY STABLE, AND THE METHOD USED
IS APPROPRIATELY STABLE, THEN THE GLOBAL ERROR AT A
GIVEN X SHOULD VARY SMOOTHLY WITH TOL IN A MONOTONE
INCREASING MANNER.

9. IF THE ROUTINE RETURNS WITH IER VALUES OF 132. 133,
OR 134, THE USER SHOULD CHECK TO SEE IF TOO MUCH
ACCURACY IS BEING REQUIRED. THE USER MAY WISH TO
SET TOL TO A LARGER VALUE AND CONTINUE. ANOTHER
POSSIBLE CAUSE OF THESE ERROR CONDITIONS IS AN
ERROR IN THE CODING OF THE EXTERNAL FUNCTIONS FCN
OR FCNJ. IF NO ERRORS ARE FOUND, IT MAY BE NECESSARY
TO MONITOR INTERMEDIATE QUANTITIES GENERATED BY THE
ROUTINE. THESE QUANTITIES ARE STORED IN THE WORK VECTOR
WK AND INDEXED BY SPECIFIC ELEMENTS IN THE COMMON BLOCK
/GEAR/. IF IER IS 132 OR 134, THE COMPONENTS CAUSING
THE ERROR TEST FAILURE CAN BE IDENTIFIED FROM LARGE
VALUES OF THE QUANTITY
      WK(IDUMMY(11)+I)/WK(I), FOR I=1,...,N.
ONE CAUSE OF THIS MAY BE A VERY SMALL BUT NONZERO
INITIAL VALUE OF ABS(Y(I)).
IF IER IS 133, SEVERAL POSSIBILITIES EXIST.
IT MAY BE INSTRUCTIVE TO TRY DIFFERENT VALUES OF MITER.
ALTERNATIVELY, THE USER MIGHT MONITOR SUCCESSIVE
CORRECTOR ITERATES CONTAINED IN WK(IDUMMY(12)+I), FOR
I=1,...,N. ANOTHER POSSIBILITY MIGHT BE TO MONITOR
THE JACOBIAN MATRIX, IF ONE IS USED, STORED, BY
COLUMN, IN WK(IDUMMY(10)+I), FOR I=1,...,N*N IF
MITER IS EQUAL TO 1 OR 2, OR FOR I=1,...,N IF
MITER IS EQUAL TO 3.

Algorithm

DGEAR finds approximations to the solution of a system of first order
ordinary differential equations of the form y'=f(x,y) with initial
conditions. The basic methods used for the solution are of implicit
linear multistep type. There are two classes of such methods avail-
able to the user. The first is the implicit Adams methods (up to
order twelve), and the second is the backward differentiation formula
(BDF) methods (up to order five), also called Gear's stiff methods.
In either case the implicitness of the basic formula requires that an
algebraic system of equations be solved at each step. A variety of
corrector iteration methods is available for this.

DGEAR and the associated nuclei are adaptations of a package designed
by A. C. Hindmarsh based on C. W. Gear's subroutine DIFSUB.

See references:

1. Hindmarsh, A.C., "GEAR: Ordinary Differential Equation System
    Solver", Lawrence Livermore Laboratory, Report UCID-30001,
    Revision 3, December, 1974.

2.   Gear, C.W., <u>Numerical Initial Value Problems in Ordinary Differential Equations</u>, Prentice-Hall, Englewood Cliffs, New Jersey, 1971.

<u>Example</u>

This example illustrates the basic usage of DGEAR. A table of solution values for x = 1.0,2.0,...,10.0 is obtained for the predator-prey problem:

$$y_1' = 2y_1(1-y_2) \qquad y_1 = 1$$
$$y_2' = y_2(y_1-1) \qquad y_2 = 3 \qquad \text{at } x = 0$$

Input:

```
      INTEGER    N,METH,MITER,INDEX,IWK(2),IER,K
      REAL       Y(2),WK(35),X,TOL,XEND,H
      EXTERNAL   FCN,FCNJ
      N     = 2
      X     = 0.0
      Y(1) = 1.0
      Y(2) = 3.0
      TOL   = .00001
      H     = .00001
      METH =  1
      MITER=  0
      INDEX=  1
      DO 10 K=1,10
         XEND=FLOAT(K)
         CALL DGEAR (N,FCN,FCNJ,X,H,Y,XEND,TOL,METH,MITER,INDEX,IWK,WK,IER)
         IF(IER.GT.128) GO TO 20
C                   Y(1) and Y(2) are current solution values at X.
C                   Insert write statement here.
   10 CONTINUE
      STOP
   20 CONTINUE
C                   Handle IER.GT.128
C                   Items that may help diagnose the problem should be
C                   output here.
C                   TOL,N,Y(1),...,Y(N),XEND,H,X,METH,MITER, AND INDEX.
      STOP
      END
      SUBROUTINE    FCN(N,X,Y,YPRIME)
      INTEGER       N
      REAL          Y(N),YPRIME(N),X
      YPRIME(1) = 2.0*Y(1)*(1.0-Y(2))
      YPRIME(2) = Y(2)*(Y(1)-1.0)
      RETURN
      END

      SUBROUTINE FCNJ(N,X,Y,PD)
      INTEGER    N
      REAL       Y(N),PD(N,N),X
      RETURN
      END
```

Output:

IER = 0

X	Y(1)	Y(2)
1.	0.08	1.46
2.	0.035	0.58
3.	0.29	.25
4.	1.45	0.19
5.	4.05	1.44
6.	0.18	2.26
7.	0.07	0.91
8.	0.15	0.37
9.	0.65	0.19
10.	3.15	0.35

APPENDIX C

FORTRAN PROGRAM NLLSQ1

OPTIONS IN EFFECT:　NOLIST NOMAP NOXREF NOGOSTMT NODECK　SOURCE　TERM　OBJECT FIXED　NOTEST NOTRMFLG　SRCFLG NOSYM
　　　　　　　　　　OPT(0) LANGLVL(77) NOFIPS　FLAG(I)　NAME(MAIN)　LINECOUNT(60)　　　　　　CHARLEN(500)　　SDUMP

```
                    *....*....1.........2.........3.........4.........5.........6.........7.*.......8

ISN        1            IMPLICIT REAL *8 (A-H,O-Z)                          00000010
          C            SAMPLE MAINLINE FOR NLLSQ                            00000020
          C            UNIVERSITY OF OKLAHOMA  1975    E.L.ENWALL           00000030
ISN        2            DIMENSION X(100,10),Y(100), B(10), IB(10), TITLE(10), JJ(10)   00000040
ISN        3            COMMON /ABYC/ NNOB                                  00000050
ISN        4            COMMON /CDYC/ XSTRT,YASTRT,YBSTRT,YCSTRT            00000060
ISN        5          1 CONTINUE                                           00000070
          C            BLANK IB                                            00000080
ISN        6            DO 2 K=1,10                                        00000090
ISN        7          2 IB(K)=0                                            00000100
ISN        8            READ (6,12,END=9) TITLE                            00000110
ISN        9            WRITE (6,13) TITLE                                 00000120
          C            READ INTEGERS                                       00000130
ISN       10            READ (5,10) NO,NP,NOM,M,ID,IP                      00000140
ISN       11            WRITE (6,15) NO,NP,NOM,M,ID,IP                     00000150
ISN       12            IF (NO.EQ.0) STOP                                  00000160
ISN       14            NNP=IABS(NP)                                       00000170
ISN       15            NNO=IABS(NO)                                       00000180
ISN       16            MM=IABS(M)                                         00000190
          C            IF NOM.NE.0 READ AND SET FLAGS FOR OMITTED  PARAMETERS   00000200
ISN       17            IF (NOM.LE.0) GO TO 4                              00000210
ISN       18            READ (5,10) (JJ(K),K=1,NOM)                        00000220
ISN       19            WRITE (6,14) (JJ(K),K=1,NOM)                       00000230
ISN       20            DO 3 K=1,NOM                                       00000240
ISN       21            KK=JJ(K)                                           00000250
ISN       22          3 IB(KK)=1                                          00000260
          C            IF IP.EQ.0 READ NEW PARAMETERS                      00000270
ISN       23          4 IF (IP.EQ.0) READ (5,11) (B(K),K=1,NNP)           00000280
ISN       25            IF (IP.EQ.0) WRITE (6,16) (B(K),K=1,NNP)          00000290
          C            IF NO.LT.0 DO NOT READ NEW DATA                     00000300
ISN       27            IF (NO.LT.0) GO TO 8                               00000310
ISN       28            READ (5,11) XSTRT,YASTRT,YBSTRT,YCSTRT             00000320
ISN       29            DO 5 I=1,NNO                                       00000330
ISN       30            READ (5,11) Y(I),(X(I,K),K=1,MM)                   00000340
ISN       31          5 CONTINUE                                          00000350
          C            MASSAGE RAW DATA--------USER ROUTINE                00000360
ISN       32            DO 50 II=1,NNO                                     00000370
ISN       33               TEMP = Y(II)                                   00000380
ISN       34               Y(II) = X(II,1)/1.307D00                       00000390
ISN       35               X(II,1) = TEMP                                 00000400
ISN       36               Y(NNO+II) = X(II,2)/1.222D00                   00000410
ISN       37               X(NNO+II,1) = X(II,1)                          00000420
ISN       38               X(NNO+II,2) = X(II,2)                          00000430
ISN       39               X(NNO+II,3) = X(II,3)                          00000440
ISN       40               Y(2*NNO+II) = X(II,3)/2.0D00                   00000450
ISN       41               X(2*NNO+II,1) = X(II,1)                        00000460
ISN       42               X(2*NNO+II,2) = X(II,2)                        00000470
ISN       43               X(2*NNO+II,3) = X(II,3)                        00000480
ISN       44         50 CONTINUE                                          00000490
          C            END MASSAGE                                         00000500
ISN       45          8 CONTINUE                                          00000510
```

```
                 *....*....1.........2.........3.........4.........5.........6.........7.*.......8
 ISN      46          NNOB= NNO                                                          00000520
 ISN      47          NNO = 3*NNO                                                        00000530
 ISN      48          NCYCLS=20                                                          00000540
 ISN      49          CALL NLLSQ (X,Y,B,IB,NP,NNO,M,IRET,NCYCLS)                         00000550
 ISN      50          IF (IRET.NE.5) WRITE (6,17) IRET                                   00000560
 ISN      52          GO TO 1                                                            00000570
 ISN      53        9 STOP                                                               00000580
          C                                                                              00000590
          C                                                                              00000600
 ISN      54       10 FORMAT (25I3)                                                      00000610
 ISN      55       11 FORMAT (8F10.0)                                                    00000620
 ISN      56       12 FORMAT (10A8)                                                      00000630
 ISN      57       13 FORMAT ('1',10A8)                                                  00000640
 ISN      58       14 FORMAT (' INVARIANT PARAMETER SUBSCRIPTS   ',10I3)                 00000650
 ISN      59       15 FORMAT (' NO=',I3,' NP=',I3,' NOM=',I3,' M=',I3,' D=',I3,' IP=',I300000660
          1)                                                                             00000670
 ISN      60       16 FORMAT (' INITIAL PARAMETER VALUES',/,2(5X,5(1PD15.7)))            00000680
 ISN      61       17 FORMAT ('0','PROBLEM IN SUBROUTINE NLLSQ CALCULATIONS IRET= ',I5)  00000690
 ISN      62          END                                                               00000700
```

*** VS FORTRAN ERROR MESSAGES ***

IFX0030I   CNTL   0(I)   TRMFLG HAS BEEN SPECIFIED BUT SYSTERM IS NOT A TERMINAL. TRMFLG CANCELED.

STATISTICS   SOURCE STATEMENTS = 58, PROGRAM SIZE = 13062 BYTES, PROGRAM NAME = MAIN   PAGE: 1.

STATISTICS 1 DIAGNOSTIC GENERATED, SEVERITY CODE IS 0.

****** END OF COMPILATION 1 ******

OPTIONS IN EFFECT: NOLIST NOMAP NOXREF NOGOSTMT NODECK   SOURCE   TERM   OBJECT FIXED   NOTEST NOTRMFLG   SRCFLG NOSYM
                     OPT(0) LANGLVL(77) NOFIPS   FLAG(I)   NAME(MAIN)   LINECOUNT(60)   CHARLEN(500)   SDUMP

```
                    *....*...1.........2.........3.........4.........5.........6.........7.*.......8
ISN     1           SUBROUTINE DCALC (X,Y,B,D,NP,I)                                              00000710
ISN     2           IMPLICIT REAL *8 (A-H,O-Z)                                                   00000720
ISN     3           DIMENSION X(100,10),Y(100),B(10),D(10)                                       00000730
        C           D CALC ROUTINE SPECIFIC TO RUN OR DUMMY                                      00000740
ISN     4           RETURN                                                                       00000750
ISN     5           END                                                                          00000760
```

STATISTICS   SOURCE STATEMENTS = 5, PROGRAM SIZE = 432 BYTES, PROGRAM NAME = DCALC   PAGE: 3.

STATISTICS   NO DIAGNOSTICS GENERATED.

****** END OF COMPILATION 2 ******

```
                       *....*...1.........2.........3.........4.........5.........6.........7.*......8

ISN         1          SUBROUTINE YCALC (X,Y,B,YC,WDEL,I)                              00000770
ISN         2          IMPLICIT REAL*8 (A-H,O-Z)                                       00000780
ISN         3          DIMENSION X(100,10),Y(100),B(10),YY(4),WK(400)                  00000790
ISN         4          COMMON XKT,XKR,F                                                00000800
ISN         5          COMMON /ABYC/ NNOB                                              00000810
ISN         6          COMMON /CDYC/ XSTRT,YASTRT,YBSTRT,YCSTRT                         00000820
ISN         7          EXTERNAL FCN,FCNJ                                               00000830
ISN         8          N = 4                                                           00000840
ISN         9          METH = 1                                                        00000850
ISN        10          MITER = 0                                                       00000860
ISN        11          INDEX = 1                                                       00000870
ISN        12          F = 0.5D00                                                      00000880
ISN        13          XKT = B(1)                                                      00000890
ISN        14          XKR = B(2)                                                      00000900
ISN        15          XX = XSTRT                                                      00000910
ISN        16          YY(1) = YASTRT/1.307D00                                         00000920
ISN        17          YY(2) = YBSTRT/1.22D00                                          00000930
ISN        18          YY(3) = YBSTRT*0.0D00                                           00000940
ISN        19          YY(4) = YCSTRT/2.0D00-YY(3)                                     00000945
ISN        20          H = 1.0D-05                                                     00000950
ISN        21          TOL = 1.0D-04                                                   00000960
ISN        22          XEND = X(I,1)                                                   00000970
ISN        23          IF (I.GT.(2*NNOB)) GOTO 20                                      00000980
ISN        24          IF (I.GT.NNOB) GOTO 10                                          00000990
ISN        25          CALL DGEAR (N,FCN,FCNJ,XX,H,YY,XEND,TOL,METH,MITER,INDEX,IWK,WK, 00001000
                      1IER)                                                            00001010
ISN        26          YC = YY(1)                                                      00001020
ISN        27          X(I,4) = YY(1)                                                  00001030
ISN        28          X(I,5) = YY(3)                                                  00001040
ISN        29          WDEL = Y(I)-YC                                                  00001050
ISN        30          RETURN                                                          00001060
ISN        31       10 CALL DGEAR (N,FCN,FCNJ,XX,H,YY,XEND,TOL,METH,MITER,INDEX,IWK,WK, 00001070
                      1IER)                                                            00001080
ISN        32          YC = YY(2)                                                      00001090
ISN        33          X(I,4) = YY(2)                                                  00001100
ISN        34          X(I,5) = YY(3)                                                  00001110
ISN        35          WDEL = Y(I)-YC                                                  00001120
ISN        36          RETURN                                                          00001130
ISN        37       20 CALL DGEAR (N,FCN,FCNJ,XX,H,YY,XEND,TOL,METH,MITER,INDEX,IWK,WK, 00001140
                      1IER)                                                            00001150
ISN        38          YC = YY(3)+YY(4)                                                00001160
ISN        39          X(I,4) = YY(1)                                                  00001170
ISN        40          X(I,5) = YY(4)                                                  00001180
ISN        41          WDEL = Y(I)-YC                                                  00001190
ISN        42          RETURN                                                          00001200
ISN        43          END                                                            00001210
```

STATISTICS   SOURCE STATEMENTS = 43, PROGRAM SIZE = 5752 BYTES, PROGRAM NAME = YCALC   PAGE: 4.

STATISTICS   NO DIAGNOSTICS GENERATED.

****** END OF COMPILATION 3 ******

OPTIONS IN EFFECT: NOLIST NOMAP NOXREF NOGOSTMT NODECK   SOURCE   TERM   OBJECT FIXED   NOTEST NOTRMFLG   SRCFLG NOSYM
                     OPT(0) LANGLVL(77) NOFIPS   FLAG(I)   NAME(MAIN) LINECOUNT(60)   CHARLEN(500)   SDUMP

```
                    *....*...1.........2.........3.........4.........5.........6.........7.*......8
ISN        1            SUBROUTINE FCN (N,X,Y,YPRIME)                                   00001220
ISN        2            IMPLICIT REAL*8 (A-H,O-Z)                                       00001230
ISN        3            DIMENSION Y(N),YPRIME(N),B(10)                                  00001240
ISN        4            COMMON XKT,XKR,F                                                00001250
ISN        5            YPRIME(1) = 0.25D00*XKT*Y(2)-XKT*Y(1)                           00001260
ISN        6            YPRIME(2) = XKT*Y(1)-0.25D00*XKT*Y(2)-XKR*Y(2)+XKR*Y(3)         00001270
ISN        7            YPRIME(3) = XKR*Y(2)-XKR*Y(3)-F*XKT*Y(3)                        00001280
ISN        8            YPRIME(4) = F*XKT*Y(3)                                          00001285
ISN        9            RETURN                                                          00001290
ISN       10            END                                                            00001300
```

STATISTICS   SOURCE STATEMENTS = 10, PROGRAM SIZE = 1038 BYTES, PROGRAM NAME = FCN   PAGE: 5.

STATISTICS   NO DIAGNOSTICS GENERATED.

****** END OF COMPILATION 4 ******

OPTIONS IN EFFECT: NOLIST NOMAP NOXREF NOGOSTMT NODECK   SOURCE   TERM   OBJECT FIXED   NOTEST NOTRMFLG   SRCFLG NOSYM
                    OPT(0) LANGLVL(77) NOFIPS   FLAG(I)   NAME(MAIN) LINECOUNT(60)   CHARLEN(500)   SDUMP

                     ....1.........2.........3.........4.........5.........6.........7.*......8

ISN   1   SUBROUTINE FCNJ (N,X,Y,PD)   00001310
ISN   2   IMPLICIT REAL*8 (A-H,O-Z)   00001320
ISN   3   DIMENSION Y(N),PD(N,N)   00001330
ISN   4   RETURN   00001340
ISN   5   END   00001350

STATISTICS   SOURCE STATEMENTS = 5, PROGRAM SIZE = 556 BYTES, PROGRAM NAME = FCNJ   PAGE: 6.

STATISTICS   NO DIAGNOSTICS GENERATED.

****** END OF COMPILATION 5 ******

```
                      *....*...1.........2.........3.........4.........5.......6.........7.*......8

ISN        1              SUBROUTINE NLLSQ (X,Y,B,IB,NP,NO,MM,IRET,NCYCLS)                00001360
           C          NON LINEAR LEAST SQUARES ROUTINE USING MARQUARDT CONVERG STRATEGY 00001370
           C          J.SOC.INDUST.APPL.MATH.VOL.11.NO.2.JUNE 1963--D.W.MARQUARDT        00001380
           C          DIMENSIONED FOR 10 VARIABLES, 100 OBSERVATIONS, 5 IND. VARIABLES   00001390
           C          NP NEGATIVE CALCULATES ESTIMATED DERIVATIVES                       00001400
           C          MM NEGATIVE PRINTS B VALUES ON EVERY CYCLE                         00001410
           C          WRITTEN    U OF OKLA   MARCH 1975 E.L.ENWALL                       00001420
ISN        2              IMPLICIT REAL *8 (A-H,O-Z)                                     00001430
ISN        3              REAL*8 PHIR,PHI,PHIL10,PHILB10,DEN,DARCOS,SUMA                 00001440
ISN        4              DIMENSION X(100,10), Y(100), B(10), D(10), IB(10)              00001450
ISN        5              DIMENSION A(10,10), AS(10,10), S(100), BS(10), DB(10), DDB(10), DG 00001460
                        1(10), V(10), AAS(10,10), AM(100)                               00001470
ISN        6              REAL GAMZRO/4.5E01/,DDEL/5.E-5/,EPS/2.5E-09/,FEPS/1.E-6/,LAMBDA 00001480
ISN        7              COMMON XK1,XK4,XK2                                             00001490
ISN        8              DATA IO1/'B('/,IO2/')='/,NIP/0/                                00001500
***ERROR 1755(W)***          A CHARACTER CONSTANT HAS BEEN ASSIGNED TO A NON-CHARACTER VARIABLE OR ARRAY. INITIALIZE WITH CONSTANT OF
                             LIKE TYPE TO AVOID ERROR MESSAGE.
***ERROR 1755(W)***          A CHARACTER CONSTANT HAS BEEN ASSIGNED TO A NON-CHARACTER VARIABLE OR ARRAY. INITIALIZE WITH CONSTANT OF
                             LIKE TYPE TO AVOID ERROR MESSAGE.
ISN        9              IF (NCYCLS.LT.1.OR.NCYCLS.GT.100) NCYCLS=20                    00001510
ISN       11              LAMBDA=0.01000001                                             00001520
ISN       12              ND=1                                                          00001530
ISN       13              NPRT=1                                                        00001540
ISN       14              IRET=0                                                        00001550
ISN       15              IF (NP.LE.0) ND=-1                                            00001560
ISN       17              IF (MM.LE.0) NPRT=-1                                          00001570
ISN       19              NP=IABS(NP)                                                   00001580
ISN       20              IF (NP.NE.0) GO TO 101                                        00001590
ISN       21              WRITE (6,189)                                                 00001600
ISN       22              RETURN                                                        00001610
ISN       23          101 MM=IABS(MM)                                                   00001620
ISN       24              WRITE (6,176)                                                 00001630
ISN       25              NCYC=0                                                        00001640
ISN       26          102 CONTINUE                                                      00001650
           C          TEST FOR TOO MANY CYCLES                                          00001660
ISN       27              IF (NCYC.GT.NCYCLS) GO TO 147                                 00001670
ISN       28              NCYC=NCYC+1                                                   00001680
           C          BUILD MATRIX                                                      00001690
ISN       29              NIP=0                                                         00001700
ISN       30              DO 103 K=1,NP                                                 00001710
ISN       31              IF (IB(K).NE.0) NIP=NIP+1                                     00001720
ISN       33              D(K)=0.0                                                      00001730
ISN       34              V(K)=0.0                                                      00001740
ISN       35              DO 103 L=1,NP                                                 00001750
ISN       36              A(K,L)=0.0                                                    00001760
ISN       37          103 CONTINUE                                                      00001770
ISN       38              PHI=0.0                                                       00001780
ISN       39              DO 109 I=1,NO                                                 00001790
ISN       40              CALL YCALC (X,Y,B,YC,WDEL,I)                                  00001800
ISN       41              IF (ND.GT.0) GO TO 105                                        00001810
ISN       42              SDEL=WDEL                                                      00001820
ISN       43              DO 104 K=1,NP                                                 00001830
ISN       44              IF (IB(K).NE.0) GO TO 104                                     00001840
```

```
                   *....*....1.........2.........3.........4.........5.........6.........7.*.......8
 ISN      45          BZ=B(K)                                                              00001850
 ISN      46          DD=BZ*DDEL                                                            00001860
 ISN      47          B(K)=BZ+DD                                                            00001870
 ISN      48          CALL YCALC (X,Y,B,YC,WDEL,I)                                          00001880
 ISN      49          D(K)=(SDEL-WDEL)/DD                                                   00001890
 ISN      50          B(K)=BZ                                                               00001900
 ISN      51      104 CONTINUE                                                              00001910
 ISN      52          WDEL=SDEL                                                             00001920
 ISN      53          GO TO 106                                                             00001930
 ISN      54      105 CALL DCALC (X,Y,B,D,NP,I)                                             00001940
 ISN      55      106 PHI=PHI+WDEL*WDEL                                                     00001950
 ISN      56          DO 108 K=1,NP                                                         00001960
 ISN      57          IF (IB(K).NE.0) GO TO 108                                             00001970
 ISN      58          V(K)=V(K)+D(K)*WDEL                                                   00001980
 ISN      59          DO 107 L=1,NP                                                         00001990
 ISN      60          IF (IB(L).NE.0) GO TO 107                                             00002000
 ISN      61          A(K,L)=A(K,L)+D(K)*D(L)                                               00002010
 ISN      62      107 CONTINUE                                                              00002020
 ISN      63      108 CONTINUE                                                              00002030
 ISN      64      109 CONTINUE                                                              00002040
 ISN      65          PHIR=PHI                                                              00002050
          C           CALC RMSD                                                             00002060
 ISN      66          RMSD=(PHIR/(NO-NP+NIP))**.5                                           00002070
 ISN      67          IF (NPRT.LE.0.OR.NCYC.EQ.1) WRITE (6,182) NCYC,RMSD,LAMBDA            00002080
 ISN      69          IF (NPRT.LE.0.OR.NCYC.EQ.1) WRITE (6,187) (IO1,K,IO2,B(K),K=1,NP)     00002090
 ISN      71          M=0                                                                   00002100
          C           SAVE DIAGONAL ELEMENTS                                                00002110
 ISN      72          DO 110 K=1,NP                                                         00002120
 ISN      73          IF (IB(K).NE.0) A(K,K)=1.0                                            00002130
 ISN      75          IF (A(K,K).LE.0.0) GO TO 169                                          00002140
 ISN      76      110 DG(K)=A(K,K)**.5                                                      00002150
 ISN      77          DO 111 K=1,NP                                                         00002160
 ISN      78          V(K)=V(K)/DG(K)                                                       00002170
 ISN      79          DO 111 L=1,NP                                                         00002180
          C           SAVE ORIGINAL MATRIX                                                  00002190
 ISN      80          AAS(K,L)=A(K,L)                                                       00002200
          C           SCALE MATRIX                                                          00002210
 ISN      81      111 A(K,L)=A(K,L)/(DG(K)*DG(L))                                           00002220
          C           SAVE MATRIX, ORIG PARAMS                                              00002230
 ISN      82          DO 112 K=1,NP                                                         00002240
 ISN      83          BS(K)=B(K)                                                            00002250
 ISN      84          DO 112 L=1,NP                                                         00002260
 ISN      85          AS(K,L)=A(K,L)                                                        00002270
 ISN      86      112 IF (K.EQ.L) A(K,L)=A(K,L)+LAMBDA                                      00002280
 ISN      88          IRET=1                                                                00002290
 ISN      89          GO TO 149                                                             00002300
 ISN      90      113 CONTINUE                                                              00002310
 ISN      91          DO 114 K=1,NP                                                         00002320
 ISN      92      114 DDB(K)=DB(K)                                                          00002330
          C           CHECK FOR CONVERGENCE                                                 00002340
 ISN      93          DO 115 K=1,NP                                                         00002350
 ISN      94          Z=DDB(K)**2/(FEPS+B(K)**2)                                            00002360
 ISN      95          IF (Z.GT.EPS) GO TO 116                                               00002370
 ISN      96      115 CONTINUE                                                              00002380
 ISN      97          WRITE (6,179)                                                         00002390
 ISN      98          GO TO 134                                                             00002400
```

```
                    *....*...1.........2.........3.........4.........5.........6.........7.*.......8

              C       CALC PHI (LAMBDA)                                                  00002410
ISN    99       116 PHIL=0.0                                                             00002420
ISN   100           DO 117 I=1,NO                                                        00002430
ISN   101           CALL YCALC (X,Y,B,YC,WDEL,I)                                         00002440
ISN   102       117 PHIL=PHIL+WDEL*WDEL                                                  00002450
              C       TEST PHIL                                                          00002460
ISN   103           IF (PHIL.LE.PHIR) GO TO 128                                          00002470
ISN   104       118 CONTINUE                                                             00002480
ISN   105           IF (LAMBDA.GE.1.0) GO TO 123                                         00002490
              C       DO FOR LAMBDA*10                                                   00002500
ISN   106           LAMBDA=LAMBDA*10                                                     00002510
ISN   107           DO 119 K=1,NP                                                        00002520
ISN   108           DO 119 L=1,NP                                                        00002530
ISN   109           A(K,L)=AS(K,L)                                                       00002540
ISN   110       119 IF (K.EQ.L) A(K,L)=A(K,L)+LAMBDA                                     00002550
ISN   112           IRET=2                                                               00002560
ISN   113           GO TO 149                                                            00002570
ISN   114       120 CONTINUE                                                             00002580
              C       CALC PHI (LAMBDA*10)                                               00002590
ISN   115       121 PHIL10=0.0                                                           00002600
ISN   116           DO 122 I=1,NO                                                        00002610
ISN   117           CALL YCALC (X,Y,B,YC,WDEL,I)                                         00002620
ISN   118       122 PHIL10=PHIL10+WDEL*WDEL                                              00002630
ISN   119           IF (PHIL10.GE.PHIR.AND.LAMBDA.GE.1.0) GO TO 123                      00002640
ISN   120           IF (PHIL10.GE.PHIR) GO TO 118                                        00002650
              C       NEW LAMBDA, NEW CYCLE                                              00002660
ISN   121           GO TO 102                                                            00002670
              C       LARGE  LAMBDA, GAMMA TEST                                          00002680
ISN   122       123 CONTINUE                                                             00002690
ISN   123           DTG=0.0                                                             00002700
ISN   124           GTG=0.0                                                             00002710
ISN   125           BTB=0.0                                                             00002720
ISN   126           DO 124 K=1,NP                                                        00002730
ISN   127           DTG=DTG+DB(K)*DG(K)                                                 00002740
ISN   128           GTG=GTG+DG(K)*DG(K)                                                 00002750
ISN   129       124 BTB=BTB+DB(K)*DB(K)                                                 00002760
ISN   130           DEN=DTG/((BTB*GTG)**.5)                                             00002770
ISN   131           GAM=(180./3.141592)*DARCOS(DEN)                                     00002780
ISN   132           IF (NPRT.LE.0.OR.NCYC.EQ.1) WRITE (6,177) GAM,LAMBDA                00002790
ISN   134           IF (GAM.GE.90.0) GO TO 148                                          00002800
ISN   135           IF (GAM.GE.GAMZRO) GO TO 102                                        00002810
ISN   136           DO 125 K=1,NP                                                        00002820
ISN   137           DB(K)=DB(K)/2.                                                      00002830
ISN   138       125 B(K)=BS(K)+DB(K)                                                    00002840
ISN   139           DO 126 K=1,NP                                                        00002850
ISN   140           Z=DB(K)**2/(FEPS+B(K)**2)                                           00002860
ISN   141           IF (Z.GT.EPS) GO TO 127                                             00002870
ISN   142       126 CONTINUE                                                             00002880
ISN   143           GO TO 146                                                            00002890
ISN   144       127 GO TO 121                                                            00002900
              C       CALC PHI (LAMBDA/10)                                               00002910
ISN   145       128 LAMBDA=LAMBDA/10.                                                   00002920
ISN   146           PHLB10=0.0                                                          00002930
ISN   147           DO 129 K=1,NP                                                        00002940
ISN   148           DO 129 L=1,NP                                                        00002950
ISN   149           A(K,L)=AS(K,L)                                                      00002960
```

```
         *...*...1.........2.........3.........4.........5.........6.........7.*.......8

ISN      150          129 IF (K.EQ.L) A(K,L)=A(K,L)+LAMBDA                        00002970
ISN      152              IRET=3                                                  00002980
ISN      153              GO TO 149                                               00002990
ISN      154          130 CONTINUE                                                00003000
ISN      155              DO 131 I=1,NO                                           00003010
ISN      156              CALL YCALC (X,Y,B,YC,WDEL,I)                            00003020
ISN      157          131 PHLB1O=PHLB1O+WDEL*WDEL                                 00003030
ISN      158              IF (PHLB1O.GT.PHIR) GO TO 132                           00003040
ISN      159              GO TO 102                                               00003050
         C        RESTORE STARTING VALUE OF LAMBDA                                00003060
ISN      160          132 LAMBDA=LAMBDA*10.                                       00003070
ISN      161              DO 133 K=1,NP                                           00003080
ISN      162          133 B(K)=BS(K)+DDB(K)                                       00003090
ISN      163              GO TO 102                                               00003100
         C           CONVERGENCE                                                  00003110
ISN      164          134 CONTINUE                                                00003120
ISN      165              WRITE (6,178) NCYC,PHIR,RMSD                            00003130
         C        SET UP FOR FINAL MATRIX INVERSION, CALC EST CONDITION NUMBER    00003140
         C        SAVE SCALED MATRIX IN AS                                        00003150
ISN      166              AMIN=1.E25                                              00003160
ISN      167              AMAX=0.0                                                00003170
ISN      168              DO 135 K=1,NP                                           00003180
ISN      169              IF (AAS(K,K).GT.AMAX) AMAX=AAS(K,K)                     00003190
ISN      171              IF (AAS(K,K).LT.AMIN) AMIN=AAS(K,K)                     00003200
ISN      173              DO 135 L=1,NP                                           00003210
ISN      174              A(K,L)=AAS(K,L)/(DG(K)*DG(L))                           00003220
ISN      175          135 AS(K,L)=A(K,L)                                          00003230
ISN      176              CONDNO=AMAX/AMIN                                        00003240
ISN      177              WRITE (6,185) CONDNO                                    00003250
ISN      178              IRET=4                                                  00003260
ISN      179              GO TO 149                                               00003270
ISN      180          136 CONTINUE                                                00003280
         C        SCALED INVERSE IN A                                             00003290
ISN      181              DO 137 K=1,NP                                           00003300
ISN      182              DO 137 L=1,NP                                           00003310
ISN      183          137 AAS(K,L)=A(K,L)/(DG(K)*DG(L))                           00003320
         C        TRUE INVERSE IN AAS                                             00003330
ISN      184              DO 138 K=1,NP                                           00003340
ISN      185          138 B(K)=BS(K)                                              00003350
ISN      186              DO 139 K=1,NP                                           00003360
ISN      187          139 DG(K)=AAS(K,K)**.5                                      00003370
ISN      188              DO 140 K=1,NP                                           00003380
ISN      189              DO 140 L=1,NP                                           00003390
ISN      190          140 AAS(K,L)=AAS(K,L)/(DG(K)*DG(L))                         00003400
         C        AAS NOW CORRELATION MATRIX                                      00003410
         C        CALC STD ERRORS IN EACH PARAMETER                              00003420
ISN      191              DO 141 K=1,NP                                           00003430
ISN      192              DB(K)=DG(K)*RMSD                                        00003440
ISN      193              IF (IB(K).NE.0) DB(K)=0.0                               00003450
ISN      195          141 CONTINUE                                                00003460
ISN      196              WRITE (6,170)                                           00003470
ISN      197              WRITE (6,171) (K,BS(K),DB(K),K=1,NP)                    00003480
ISN      198              WRITE (6,173)                                           00003490
ISN      199              DO 142 I=1,NO                                           00003500
ISN      200              CALL YCALC (X,Y,B,YC,WDEL,I)                            00003510
ISN      201              WRITE (6,172) Y(I),YC,WDEL,(X(I,K),K=1,MM)              00003520
```

```
*....*...1.........2.........3.........4.........5........6.........7.*.......8

ISN    202       142 CONTINUE                                              00003530
ISN    203           WRITE (6,175)                                         00003540
ISN    204           DO 143 K=1,NP                                         00003550
ISN    205       143 WRITE (6,174) K,(AAS(K,L),L=1,NP)                     00003560
ISN    206           DO 144 K=1,NP                                         00003570
ISN    207           DO 144 L=1,NP                                         00003580
ISN    208           AAS(K,L)=0.0                                          00003590
ISN    209           DO 144 J=1,NP                                         00003600
ISN    210       144 AAS(K,L)=AAS(K,L)+A(K,J)*AS(J,L)                      00003610
       C             WRITE OUT PRODUCT OF INVERSE AND STARTING MATRICES    00003620
ISN    211           WRITE (6,184)                                         00003630
ISN    212           DO 145 K=1,NP                                         00003640
ISN    213       145 WRITE (6,183) K,(AAS(K,L),L=1,NP)                     00003650
ISN    214           IRET=5                                                00003660
ISN    215           RETURN                                                00003670
       C         G L TEST                                                  00003680
ISN    216       146 WRITE (6,180)                                         00003690
ISN    217           GO TO 134                                             00003700
       C         TOO MANY CYCLES                                           00003710
ISN    218       147 CONTINUE                                              00003720
ISN    219           WRITE (6,181)                                         00003730
ISN    220           GO TO 134                                             00003740
ISN    221       148 WRITE (6,186) GAM                                     00003750
ISN    222           GO TO 134                                             00003760
ISN    223       149 CONTINUE                                              00003770
       C             INTERNAL SUBROUTINE TO INVERT MATRIX  CHOLESKI METHOD 00003780
ISN    224           M=1                                                   00003790
ISN    225           DO 150 K=1,NP                                         00003800
ISN    226           DO 150 L=K,NP                                         00003810
ISN    227           AM(M)=A(K,L)                                          00003820
ISN    228       150 M=M+1                                                 00003830
ISN    229           K=1                                                   00003840
ISN    230           IF (NP.GT.1) GO TO 151                                00003850
ISN    231           AM(1)=1.0/AM(1)                                       00003860
ISN    232           GO TO 165                                             00003870
ISN    233       151 DO 158 M=1,NP                                         00003880
ISN    234           IMAX=M-1                                              00003890
ISN    235           DO 157 L=M,NP                                         00003900
ISN    236           SUMA=0.0                                              00003910
ISN    237           KLI=L                                                 00003920
ISN    238           KMI=M                                                 00003930
ISN    239           IF (IMAX) 154,154,152                                00003940
ISN    240       152 DO 153 I=1,IMAX                                       00003950
ISN    241           SUMA=SUMA+AM(KLI)*AM(KMI)                             00003960
ISN    242           J=NP-I                                                00003970
ISN    243           KLI=KLI+J                                             00003980
ISN    244       153 KMI=KMI+J                                             00003990
ISN    245       154 TERM=AM(K)-SUMA                                       00004000
ISN    246           IF (L-M) 155,155,156                                  00004010
ISN    247       155 IF (TERM.LE.0.0) GO TO 169                            00004020
ISN    248           DENOM=TERM**.5                                        00004030
ISN    249           AM(K)=DENOM                                           00004040
ISN    250           GO TO 157                                             00004050
ISN    251       156 AM(K)=TERM/DENOM                                      00004060
ISN    252       157 K=K+1                                                 00004070
ISN    253       158 CONTINUE                                              00004080
```

```
                     *....*....1....:....2....:....3....:....4....:....5....:....6....:....7.*......8

ISN      254            AM(1)=1.0/AM(1)                                              00004090
ISN      255            KDM=1                                                        00004100
ISN      256            DO 161 L=2,NP                                                00004110
ISN      257            KDM=KDM+NP-L+2                                               00004120
ISN      258            TERM=1.0/AM(KDM)                                             00004130
ISN      259            AM(KDM)=TERM                                                 00004140
ISN      260            KMI=0                                                        00004150
ISN      261            KLI=L                                                        00004160
ISN      262            IMAX=L-1                                                     00004170
ISN      263            DO 160 M=1,IMAX                                              00004180
ISN      264            K=KLI                                                        00004190
ISN      265            SUMA=0.0                                                     00004200
ISN      266            DO 159 I=M,IMAX                                              00004210
ISN      267            II=KMI+I                                                     00004220
ISN      268            SUMA=SUMA-AM(KLI)*AM(II)                                     00004230
ISN      269        159 KLI=KLI+NP-I                                                 00004240
ISN      270            AM(K)=SUMA*TERM                                              00004250
ISN      271            J=NP-M                                                       00004260
ISN      272            KLI=K+J                                                      00004270
ISN      273        160 KMI=KMI+J                                                    00004280
ISN      274        161 CONTINUE                                                     00004290
ISN      275            K=1                                                          00004300
ISN      276            DO 164 M=1,NP                                                00004310
ISN      277            KLI=K                                                        00004320
ISN      278            DO 163 L=M,NP                                                00004330
ISN      279            KMI=K                                                        00004340
ISN      280            IMAX=NP-L+1                                                  00004350
ISN      281            SUMA=0.0                                                     00004360
ISN      282            DO 162 I=1,IMAX                                              00004370
ISN      283            SUMA=SUMA+AM(KLI)*AM(KMI)                                    00004380
ISN      284            KLI=KLI+1                                                    00004390
ISN      285        162 KMI=KMI+1                                                    00004400
ISN      286            AM(K)=SUMA                                                   00004410
ISN      287        163 K=K+1                                                        00004420
ISN      288        164 CONTINUE                                                     00004430
ISN      289        165 CONTINUE                                                     00004440
ISN      290            M=1                                                          00004450
ISN      291            DO 166 K=1,NP                                                00004460
ISN      292            DO 166 L=K,NP                                                00004470
ISN      293            A(K,L)=AM(M)                                                 00004480
ISN      294            A(L,K)=AM(M)                                                 00004490
ISN      295        166 M=M+1                                                        00004500
ISN      296            DO 168 K=1,NP                                                00004510
ISN      297            DB(K)=0.0                                                    00004520
ISN      298            IF (IB(K).NE.0) GO TO 168                                    00004530
ISN      299            DO 167 L=1,NP                                                00004540
ISN      300        167 DB(K)=DB(K)+A(K,L)*V(L)                                      00004550
ISN      301            DB(K)=DB(K)/DG(K)                                            00004560
ISN      302        168 B(K)=BS(K)+DB(K)                                             00004570
ISN      303            GO TO (113,120,130,136), IRET                               00004580
ISN      304        169 WRITE (6,188) M,NCYC,IRET                                    00004590
ISN      305            IRET=IRET+1000*NCYC+M*1000**2                               00004600
ISN      306            RETURN                                                       00004610
                     C                                                              00004620
                     C                                                              00004630
ISN      307        170 FORMAT ('0PARAMETERS AND SIGMAS')                          00004640
```

```
          *....*....1.........2.........3.........4.........5.........6.........7.*.......8
ISN    308     171 FORMAT ('OB(',I2,')=',1PE13.5,' +-',E13.5)                  00004650
ISN    309     172 FORMAT (1X,1P3E11.3,(T35,5E10.3))                           00004660
***ERROR 1264(W)***     SLASH, COLON, OR COMMA EXPECTED AFTER DELIMITER GROUP "2".  COMMA ASSUMED.
ISN    310     173 FORMAT ('O',5X,'Y',10X,'YC',10X,'DEL',8X,'X-1-M')           00004670
ISN    311     174 FORMAT (I5,5X,10F7.3)                                       00004680
ISN    312     175 FORMAT (' CORRELATION MATRIX')                             00004690
ISN    313     176 FORMAT ('ONON LINEAR LSQ ROUTINE WITH MARQUARDT STRATEGY') 00004700
ISN    314     177 FORMAT (' GAMMA LAMBDA TEST GAMMA=',F4.0,'; LAMBDA=',1PE7.0) 00004710
ISN    315     178 FORMAT (' IN',I3,' CYCLES; SUM WDEL SQ=',1PE12.5,';   RMSD=',E12.6)00004720
ISN    316     179 FORMAT (' CONVERGENCE')                                    00004730
ISN    317     180 FORMAT (' GAMMA EPSILON TEST -- CONVERGENCE')              00004740
ISN    318     181 FORMAT (' NCYCLES EXCEEDED')                               00004750
ISN    319     182 FORMAT (' CYCLE',I2,'; RMSD=',1PE12.5,';   LAMBDA=',E7.1)  00004760
ISN    320     183 FORMAT (I5,5X,5(1PE13.4),/,12X,5E13.4)                     00004770
ISN    321     184 FORMAT ('     B*B INVERSE')                                00004780
ISN    322     185 FORMAT (' MATRIX CONDITION NUMBER=',1PE7.1)                00004790
ISN    323     186 FORMAT (' GAMMA TEST   NO CONVERGENCE GAMMA=',F4.0)        00004800
ISN    324     187 FORMAT (5X,5(A3,I2,A2,1PE10.3))                           00004810
ISN    325     188 FORMAT (' MATRIX INVERSION ERROR M=',I5,' NCYC=',I5,' IRET=',I5) 00004820
ISN    326     189 FORMAT (' NUM OF PARAMETERS = O')                         00004830
ISN    327         END                                                       00004840
```

*** VS FORTRAN ERROR MESSAGES ***

IFX1755I   DATA   4(W)   8   A CHARACTER CONSTANT HAS BEEN ASSIGNED TO A NON-CHARACTER VARIABLE OR ARRAY. INITIALIZE WITH
                                  CONSTANT OF LIKE TYPE TO AVOID ERROR MESSAGE.

IFX1755I   DATA   4(W)   8   A CHARACTER CONSTANT HAS BEEN ASSIGNED TO A NON-CHARACTER VARIABLE OR ARRAY. INITIALIZE WITH
                                  CONSTANT OF LIKE TYPE TO AVOID ERROR MESSAGE.

IFX1264I   FORM   4(W)   309   SLASH, COLON, OR COMMA EXPECTED AFTER DELIMITER GROUP "2". COMMA ASSUMED.

STATISTICS   SOURCE STATEMENTS = 313, PROGRAM SIZE = 22746 BYTES, PROGRAM NAME = NLLSQ   PAGE: 7.

STATISTICS 3 DIAGNOSTICS GENERATED. HIGHEST SEVERITY CODE IS 4.

****** END OF COMPILATION 6 ******

APPENDIX D

SAS PROGRAM ACTIV

SAS PROGRAM ACTIV TO FIND ACTIVATION ENERGIES
FROM RATE CONSTANT DATA

```
//ACTIV     JOB (13530,240-94-9716),'COLLIER',TIME=(00,40),CLASS=A,
//  MSGCLASS=A
/*ROUTE PRINT LOCAL
/*PASSWORD ?
//  EXEC SAS
//SYSIN DD *
MACRO SOLVE
PROC GLM DATA=SUBDATA;
   TITLE HEADING;
   MODEL LKT=RETEMP;
   OUTPUT OUT=SUBDATA P=LPKT;
PROC CORR DATA=SUBDATA;
   VAR LPKT LKT;
PROC PLOT DATA=SUBDATA;
   PLOT LKT*RETEMP LPKT*RETEMP='P' / OVERLAY;
PROC PRINT DATA=SUBDATA;
   VAR TEMP KT RETEMP LKT LPKT;
PROC GLM DATA=SUBDATA;
   MODEL LKR=RETEMP;
   OUTPUT OUT=SUBDATA P=LPKR;
PROC CORR DATA=SUBDATA;
   VAR LPKR LKR;
PROC PLOT DATA=SUBDATA;
   PLOT LKR*RETEMP LPKR*RETEMP='P' / OVERLAY;
PROC PRINT DATA=SUBDATA;
   VAR TEMP KR RETEMP LKR LPKR%
MACRO INDATA
DATA SUBDATA;
   INPUT TEMP KT KR;
   LKT=LOG(KT);
   LKR=LOG(KR);
   RETEMP=1.0/TEMP;
   CARD%
MACRO HEADING LEAST SQUARES ANALYSIS DATASET HOD=0.0 AND F=.5%
MACRO SUBDATA HOD0F5%
INDATA;
150.      .1558      .2250
150.      .1046      .2079
150.      .06363     .1974
145.      .06018     .08179
145.      .03102     .05578
145.      .06154     .06897
145.      .03442     .06602
140.      .01501     .02201
140.      .009688    .01621
135.      .003708    .003328
135.      .003138    .003862
135.      .003346    .003985
SOLVE;
```

```
MACRO HEADING LEAST SQUARES ANALYSIS DATASET HOD=0.0 AND F=.7368%
MACRO SUBDATA HOD0F73%
INDATA;
150.      .1556      .2143
150.      .1046      .1974
150.      .06366     .1924
145.      .05999     .07713
145.      .03105     .05444
145.      .06144     .06632
145.      .03442     .06388
140.      .01500     .02135
140.      .009688    .01578
135.      .003707    .003304
135.      .003136    .003783
135.      .003346    .003934
SOLVE;
MACRO HEADING LEAST SQUARES ANALYSIS DATASET HOD=0.0 AND F=1.0%
MACRO SUBDATA HOD0F1%
INDATA;
150.      .1551      .2041
150.      .1045      .1878
150.      .06367     .1873
145.      .05977     .07297
145.      .03105     .05307
145.      .06131     .06386
145.      .03441     .06178
140.      .01498     .02068
140.      .009684    .01535
135.      .003708    .003280
135.      .003134    .003706
135.      .003346    .003882
SOLVE;
MACRO HEADING LEAST SQUARES ANALYSIS DATASET HOD=.25 AND F=.5%
MACRO SUBDATA HOD25F5%
INDATA;
150.      .1567      .3059
150.      .1047      .2927
150.      .06367     .2841
145.      .06024     .1050
145.      .03121     .08420
145.      .06168     .09504
145.      .03442     .08425
140.      .01501     .02809
140.      .009691    .02076
135.      .003706    .004098
135.      .003134    .004810
135.      .003344    .004823
SOLVE;
MACRO HEADING LEAST SQUARES ANALYSIS DATASET HOD=.25 AND F=.7368%
MACRO SUBDATA HOD25F73%
INDATA;
150.      .1559      .2760
150.      .1046      .2617
150.      .06367     .2674
```

VITA 2

William Bridgman Collier

Candidate for the Degree of

Doctor of Philosophy

Thesis: SPECTROSCOPICALLY EVALUATED RATES AND ENERGIES FOR PROTON TRANSFER AND BJERRUM DEFECT MIGRATION IN CUBIC ICE

Major Field: Chemistry

Biographical:

Personal Data: Born in Rocky Mount, North Carolina on October 30, 1954, one of four children of John R. and Carrie M. Collier.

Education: Graduated from Roanoke Rapids High School, Roanoke Rapids, North Carolina, in 1973; received Bachelor of Science degree from Oral Roberts University, Tulsa, Oklahoma with a major in Chemistry in May 1977; received Master of Science degree from Oklahoma State University, Stillwater, Oklahoma with a major in Physical Chemistry in December 1981; and completed requirements for the Doctor of Philosophy degree at Oklahoma State University, December, 1983.

Professional Experience: Undergraduate Research Program Participant, University of Oklahoma, Summer, 1976; Graduate Teaching Assistant, 1977-1978, 1980-1983; Graduate Research Assistant, 1978-1983; Member of American Chemical Society; Member of Phi Lambda Upsilon, Honorary Chemical Society.